List of Poster Presentations
(Author: S-V)

ECT P-65

ALKALINE SALT BASED DELIMING: A NEW HOLISTIC PARADIGM TOWARD A NEW ARENA IN LEATHER PROCESSING

S. Das*, A. Biswas, S. Chakraborty,I. Kanungo

Department of Leather Technology, Biotechnology Laboratory, Government of Engineering and Leather Technology, LB Block, Sector III, Salt Lake, Kolkata-700106, West Bengal, India

**Email:sanjoy85@hotmail.com*

Conventional leather processing, a chemically and energetically intensive multistage process, engages various biological, inorganic, and organic materials. Viable white methodology for leather processing is intended to overcome environmental and economic constraints. Growing environmental regulations dictate the prerequisite for the substitutes in the conventional leather manufacturing process. Deliming, one of the unit pre-tanning operations among them, is acknowledged for generation and release of ammoniacal nitrogen gas, resulting negative impact on the environment. In this approach, usage of an alkaline based salt has been explored for performing the above process in order to achieve cleaner leather processing. Lime liquor has been neutralized using $NaHCO_3$. The amount of sodium bicarbonate required for neutralization process is standardized to optimize the deliming process. It has been found that the extent of neutralization of lime liquor is comparable to that of conventionally processed leathers. This direct the way for using alkaline based salt as an alternative in conventional leather making. Further, this newly developed recipe seems to be economically viable.

Key words: Deliming, Ammoniacal nitrogen, Ammonia gas.

1. Introduction

Leather processing is one of the chemically and energetically intensive process which converts the putrefiable collagen matrices into nonputrescible one (Saravanabhavan et al. 2006). Wide variation in pH during conventional leather processing results unfavorable consequences to the environment due to the generation of extensive amount of liquid, solid and gaseous waste. During pretanning operations, a number of unit operations such as liming-deliming are initiated which alone contribute

to maximum pollution load and (Saravanabhavan et al. 2008), leading to deleterious health hazards for human life and aquatic biota.

Deliming process using ammonium salts is aimed to reduce pH from 12.5 to 8 by the removal of lime. This reduces swelling and prepares the matrices for enzymatic treatment. Usage of ammonium salt becomes a biggest environmental trepidation due to ammoniacal nitrogen generation in the effluent (Covington) and release of ammonia gas. This compels the alternative green approaches by revamping this individual processing step. Although a great deal of research has been initiated into overhauling the whole or part of leather processing steps, but very few attempts have been made to replace ammonium salt in a techno commercial-economic viable manner.

In the current study, an ammonium salts free deliming process has been attempted in order to develop a greener leather processing. Sodium bicarbonate has been selected to neutralize the alkaline lime liquor. It is an alkaline salt. The extent of neutralization of lime liquor has been assessed from both the control and experimental processes by pH meter and chromatographically. Techno-economic feasibility of the developed recipe has also been discussed.

2. Materials and methods

Ammonium chloride, Sodium bicarbonate ($NaHCO_3$) and calcium hydroxide ($Ca(OH)_2$) GR grade have been procured from Merck, India. All chemicals used for this experiment were of analytical grade. Millipore grade water (resistance 18.2 Ω) was used for this study. Whattman filter paper was used for filtration process.

Neutralization of 0.1 g of lime mixed with 50 mL of millipore water was achieved with the addition of Sodium bicarbonate salt at 30° C. Three beakers each containing required amount of lime and water were kept at 30° C. Variable amount of sodium bicarbonate salt (1g, 2 g, 3 g) was added in each beaker for neutralization of lime solution. After completion of the neutralization process, pH of the solution was measured through pH meter. Subsequently, each solution was filtered for chromatographic analysis.

Ammonium chloride was used as a standard. Average value has been reported from triplicate measurement of each experiment.

3. Result and discussion

Involvement of lime and sodium sulfide in the conventional unhairing and fiber opening processes with the removal of interfibrillary unwanted cementing protein contributes towards depletion of water resources, leading to increase of pH up to 12-12.5. Increase in pH induces osmotic swelling and plumping of hide and skin, which in turn causes a hydrostatic pressure inside the matrix. The practice of liming claims to follow deliming process where ammonium salts are used for neutralization of lime. This is aimed in order to avoid the deposition of insoluble calcium salt on the skin matrix and

loss of tanning materials. The challenges of unhairing process such as liberation of toxic ammonia gas, generation of huge solid waste, resource depletion and threats to aquatic biodiversity, energy securities require a paradigm shift in leather production. This study explores the possible usage of an alkaline based salt $NaHCO_3$ as a substituent of acidic ammonium chloride or ammonium sulphate in order to prevent the generation of ammoniacal nitrogen and ammonia gas. $NaHCO_3$ alters the pH of the solution due to neutralization of lime. A comprehensive input-output analysis of the neutralization process using ammonium chloride and $NaHCO_3$ was carried out for the conventional and experimental deliming process. The input-output assessment in deliming process evaluates the environmental impact of the developed process as against the existing process.

The proposed neutralization scheme by $NaHCO_3$ is given by equation (1)- equation (5)

$Ca(OH)_2 + NaHCO_3 = CaCO_3 + H_2O$ (1)

$Ca(OH)_2 = Ca^{2+} + 2\ (OH^-)$ (2)

$NaHCO_3 = Na^+ + (HCO_3^-)$ (3)

$(HCO_3^-) + (OH)^- = (CO_3^{2-}) + H_2O$ (4)

$(HCO_3^-) + H_2O = H_2CO_3 + (OH)^-$ (5)

The comprehensive calculated values of input-output analysis for neutralizing 0.012 M of are tabulated in Table 1.

Molar concentration of lime in the solution is calculated by equation (6)

$$[M_{Lime}] = \frac{Solubilty\ of\ lime}{MW\ of\ Lime} \quad (6)$$

Now, solubility and molecular weight of lime is 0.9 g / L and 74, respectively (Vogel et al 1978).

So, $[M_{Lime}] = 0.9/74 = 0.012\ M$

From equation (2), it is evident that $[Ca(OH)_2)] \equiv 2[OH^-]$

Molar concentration of hydroxyl ion in the solution is calculated as

$$[M_{OH^-}] = 2 * [M_{Lime}] = 2 *\ 0.012 \frac{moles}{L} = 0.024\ moles/L$$

Equation (4) reflects that1 mole of OH^- reacts with 1 mole of HCO_3^- to give 1 mole of CO_3^{2-}. So, concentration of $[CO_3^{2-}]$ is 0.024 M.

Molar concentration of HCO_3^- is calculated using equation (7)

$$[HCO_3^-] = \left({}^{W/MW}/_{V} \right) * 1000 \quad (7)$$

Where, W is amount of $NaHCO_3$, MW is the molecular weight of $NaHCO_3$, V is the volume of the sample solution, respectively.

Concentration of HCO_3^- in the solution is denoted as $[HCO_3^-]$ = y M (8)

Amount of unreacted HCO_3^- is calculated as followsType equation here.

$[HCO_3^-]=(y - [CO_3^{2-}])$ M (9)

The alteration in pH of the solution is calculated usingHenderson–Hasselbalch equation (equation (10))

$$pH = pK_{a2} + log\left[\frac{[CO_3^{=}]}{[unreacted\ HCO_3^-]}\right] \quad (10)$$

TABLE 1. Neutralization process-c omprehensive input-output analysis of the

Amount of Salt added (g)	**NH_4Cl**		**$NaHCO_3$**					
	pH	TSS (g)	Molar concentration of HCO_3^- (y) M	$[CO_3^{2-}]$	Remaining unreacted $[HCO_3^-]$ (M)	Calculated pH	Observed pH	TSS (g)
1	9	0.048	0.23	0.024	0.206	9.36	9.18	0.1869
2	8.5	0.103	0.4761		0.4521	9.0	8.77	0.258
3	8.2	0.134	0.7142		0.6902	8.84	8.63	0.285

pH reduction profile of the conventional as well as experimental neutralization process is shown in Fig. 1. It is clearly evident that sodium bicarbonate mediated neutralization process follows similar trend of pH reduction as compared to the conventional process i.e. ammonium chloride mediated neutralization process. The observed pH of the neutralized solution mediated by $NaHCO_3$ is in good accordance with the theoretical pH. Generation of TSS in the experimental process and the conventional process as tabulated in table 1. It has been manifested that there is a significant increase in the experimental process compared to the conventional process. The postulated mechanism of this process is similar to that of an alkali-mild alkali neutralization process.

Fig. 1. pH reduction profile of neutralization process at temperature 30ºC.

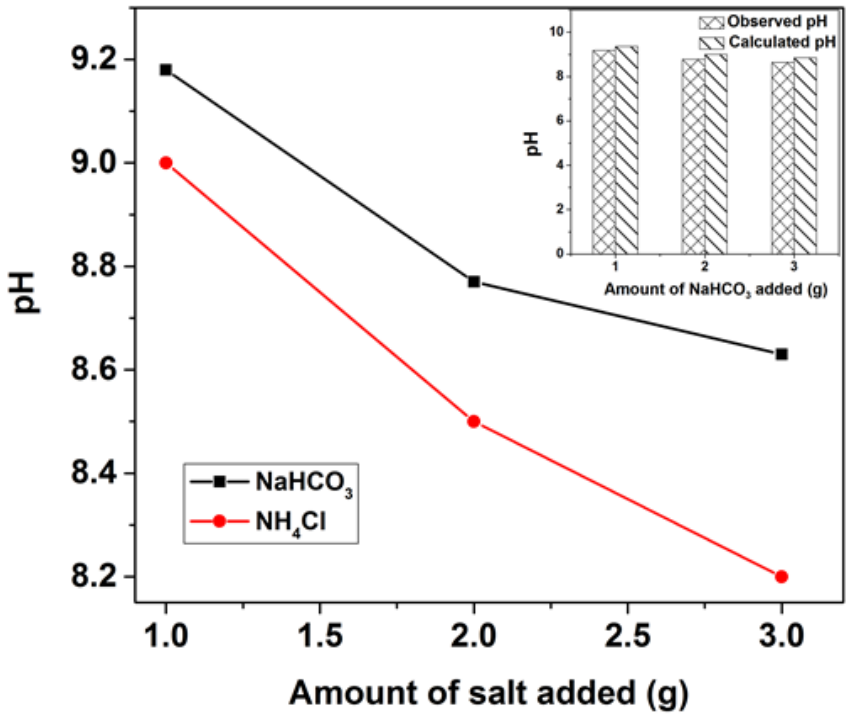

Environmental impact Ammoniacal nitrogen generation during conventional deliming process is one of the major environmental concerns. Fabrication of deliming recipe with sodium bicarbonate will pave a way towards an ecofriendly leather processing.

Economic Perspectives Utilization of a cheap, easily available chemical in the industry satisfies technical feasibility and cost-effectiveness. Employment of sodium bicarbonate in the newly developed recipe fulfills the economical feasibility. The total cost consumption for conventional and experimental deliming process is very much similar.

4. Conclusions

This study explores the utilization of $NaHCO_3$ for deliming, an important pretanning operation in leather manufacturing process. Sodium bicarbonate mediated alkali-mild alkali neutralization process could offer advantages in terms of waste minimization. Use of $NaHCO_3$ seems an innovative addendum in the ecofriendly process. Generation of huge amount of TSS in the experimental process might be a stumbling block of the developed recipe for tanners due to the stringent environmental concerns.

5. References

1. Covington A D, Tanning Chemistry: The science of leather, RSC Publishing, ISBN: 978-1-84973-434-9.

2. Saravanabhavan S, Thanikaivelan P, Rao J R, Nair BU, Ramasami T, Reversing the Conventional Leather Processing Sequence for Cleaner Leather Production.*Environ. Sci. Technol.*, 2006, **40,** 1069-1075.
3. Saravanabhavan S, Thanikaivelan P, Rao J R, Nair B U, Ramasami T, Sodium Metasilicate Based Fiber Opening for Greener Leather Processing,*Environ. Sci. Technol.* 2008, **42**, 1731–1739.
4. Vogel A I, Tatchell A R, Furnis B S, Hannaford A J, Smith P W G, *Vogel's Textbook of Practical Organic Chemistry (5th Edition),*John Wiley & Sons, Inc.,New York, 1978.

ECT P-66

ENZYMATIC EVALUATION OF Cr(III)-TOLERANT *B.AMYLOLIQUEFACIENS* TCCC 11319 ON DISPOSAL SOLID WASTES

Shan Cao*, Bin Xue ,Qinglong Xin,Shiting Zhou, Baozhen Cheng, Yu Li

College of Biotechnology, College of Food Engineering and Biotechnology, College of Material Science and Chemical Engineering, Tianjin University of Science and Technology, Tianjin, 300457, P. R. China

In recent years, biotechnology has got more and more attention in leather industry due to its high efficiency and cleanness. Compared with chemicaldegradation, biodegradation usually has more milder reaction conditions. Bacteria, fungi, and their enzyme can be used to treat CTLS since they have proved to be effective in the process. However, most of enzymes are deactivated by heavy metals. The chromium used in leather tanning process results in loss of collagenase acitivity in the waste-treatment of CTLS disposal. In order to solve this problem, it's important to improve the chromium tolerance of microorganism or enzyme which are used in leather wastes disposal.

In this paper, a strain isolated from tannery's soil has been identified as *B.amyloliquefaciens* and named as TCCC11319, which produced Cr(III)-tolerant fermentation broth with collagenase as the major component. Besides, there are alkaline protease, neutral protease and keratinase in the fermentation broth. All the proteases are significant for the degradation of wastes produced in leather production. Thus the strain can be applied for chromium-tanned leather shavings(CTLS) treatment. Furthermore, characteristics of collagenase in fermentation broth were analyzed. Under optimized conditions of inoculum 5%, pH 8 and temperature 37 ^{o}C, the collagenase activity of the crude broth reached 900 U/mL and exhibited relatively high tolerance to Cr(III)(≤900 mg/L). This strain has the potential application value for solid waste disposal of leather industry or other chromium contaminated industries.

Keywords:chromium-tanned leather shavings, biodegradation, *B.amyloliquefaciens*, Cr(III)-tolerance, collagenase.

1.Introduction

With the growth of leather industry, the effort of disposing wastes has unable to keep pace with the increasing amount of waste materials. This has often resulted in environment pollution. As known, 200kg of final chrome-containing leather product,and 250kg of chrome-containing tanned waste were generated when processing on metric ton of raw hide(Hüffer et al., 2004), namely, 25% of raw hides are converted into chromium-tanned leather shavings (CTLS).By previous studies, most of tanned wastes are treated through landfill or incineration processes but also with economic and environmental losses (Mu et al., 2003;. Pati et al., 2014)

Biotechnology include gene function, gene function, gene expression, protein interactions has developed rapidly and be widely used in medicine, food, breeding, aquaculture industries in these years(Mclaren et al., 2005). So far, biotechnology has got more and more attention in leather industry due to its high efficiency and cleanness(Bajza et al., 1998;. Bachate et al., 2013). However, chemical agents play the main roles in traditional leather process. Even though there are many researches of biotechnology, it's just at the starting stage in leather industry.

Biodegradation usually has more milder reaction conditions than chemical treatment. Bacteria, fungi, and their enzyme can be used to treat CTLS since they have proved to be effective in the process.In this paper, a new chromium-tolerant bacterial strain was isolated with gelatin plates from tannery, as well as the enzyme in fermentative broth produced by the strain were analyzed. Furthermore, the effects of CTLS hydrolysis by are evaluated to understand the application values of *B.amyloliquefaciens* TCCC 11319.

2.Materials and methods

2.1 Preliminary Screening and classification of Cr(III) tolerant Bacteria strain

CTLS (chromium-tanned leather shavings) and soil samples were collected from tannery. The new chromium-tolerant bacteria were isolated from soil samples by dilution plate technique method. After incubation, the colony morphologies were observed on plates through Gram straining method as described by Bailey and Scott(1996), and the species identification of the isolated chromium-tolerant bacteria strain was analyzed by 16S rRNA gene sequencing. Purified the genomic DNA of strain by the Wizard Genomic DNA Purification Kit (Promega, Madison, Wi, USA), and then that was used as a template for PCR amplification (30cycles, 95^{o}C for 45 s denaturation, 56^{o}C for 30 s primer annealing, and 72^{o}C for 1.5min extension). Respectively, evaluated the PCR products on 0.8% agarose gel via amplification on Primus 25 Advanced PCR machine (Peqlab Biotechnologie, GmbH, Germany). Compared with the homologous sequences, the gene sequences of strain were identified by BLAST technique(Altschul et al., 1997).

2.2 Enzymatic evaluation

Enzyme production was optimized using the following parameters: Inoculum radios of 1%, 2%, 5%, 7%, 10%(v/v), culture temperatures at range of 30 - 45 ^{o}C and pH 4-10 with fermentation time 32h. The optimum conditions were determined according to the collagenase acitivity. All experiments were carried out in triplicates.

The enzyme component was analyzed include collagenase, keratinase, neutral protease, alkaline protease. Crude enzyme extract was concentrated using a centrifuge (Eppendorf, 5480R, American) at 8000r/min for 10 mins. The collagenase activity was determined by ninhydrin colorimetric analysis for amino acids (Moore et al., 1954), and one unit of collagenase was defined as the amount of enzyme that released peptides from collagen equivalent in color intensity determined spectrophotometrically using 1μg of glycine in 1 min at pH 7.5 and temperature of 37^{o}C (Zhang et al., 2013). The keratinase activity was determined by the method from Letourneau et al's paper(Letourneau et al., 1998). One unit of keratinase activity is the amount of enzyme producing an absorbance change of 0.01 units(OD_{280}). Furthermore, the neutral protease and alkaline protease activity assay were based on the method described by Huang et al(Hwang et al., 2002). One unit of protease activity was defined as the amount of enzyme which releases 1μg of tyrsine per minute at 40^{o}C, pH 10.5 for alkaline protease and 30^{o}C pH 7.5 for neutral protease respectively.

3.Results and discussions

3.1 Classification of Cr(III) tolerant bacteria isolated from tannery

From the tannery's soil samples, an isolate strain was selected for further study by degradation of CTLS and numbered TCCC 11319 due to its Cr(III) tolerance property. It found that the characteristics of aerobic, Gram-positive and rod-shape of this strain as shown in Fig.1, and the strain is identified to

be a member of the genus Bacillus according to its morpho-physiological and biochemical characterizations. From 16S rRNA gene sequencing and phylogenetic analysis, the strain TCCC 11319 showed 99% sequence identity with *Bacillus amyloliquefaciens* strain when searched in Genbank nucleotide database (Fig.2).

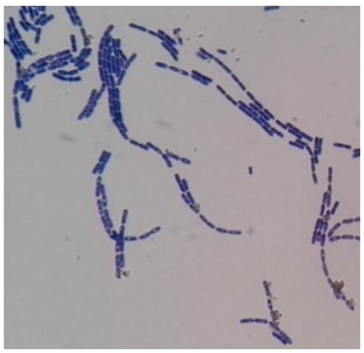

Fig.1 Individual morphology of bacterial strain TCCC 11319（100*10）

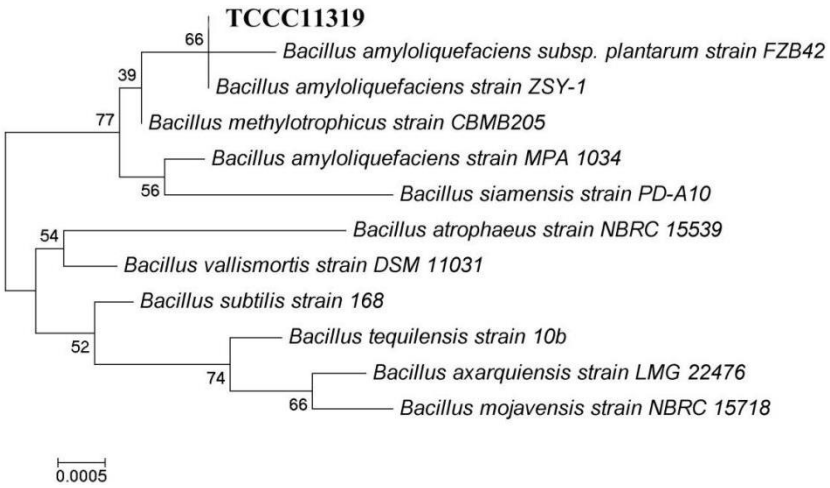

Fig.2 Phylogenetic analysis based on the 16SrDNA sequence of the strain TCCC11319

3.2 Enzyme properties

A summary of the crude enzyme from the culture medium of *B.amyloliquefaciens* TCCC 11319 is presented in Table 1. In the crude broth,the type of protease can be listed at least four main components - collagenase, alkaline protease, neutral protease, keratinase. As known, the main component of CTLS is collagen account for more than 70%. The collagenase of the enzyme plays a major role on degradation process. After the triple helix structures of collagenous domain of CTLS are digested by collagenase, the alkaline protease and neutral protease will be helpful to further hydrolysis to gelatin. Moreover, the keratinase can act on the hair in the solid waste simultaneously. In summary, all the componets of the enzyme are useful in leather wastes treatment. TCCC 11319 strain has potential value for the possible utilization in leather industry.

Table 1 The components of *B.amyloliquefaciens* TCCC11319 crude enzyme

Enzyme species	Enzyme acitivity（U/mL）
Collagenase	919.72
Alkaline protease	142.19
Neutral protease	90.33
Keratinase	53.47

The growth response curve of *B.amyloliquefaciens TCCC11319* strain at various concentrations of Cr(III)(100 mg/L, 200 mg/L, 300 mg/L, 400 mg/L, 500 mg/L) showed that the optical density attained by the strains depended on the concentration of Cr(III) in the solution (Fig.4a) . At the 300 mg/L Cr(III) concentration and above, the maximal bacteria density reduced about 40% compared with initial amount of bacteria. At the 400 mg/L and 500 mg/L concentration of Cr(III), the *B.amyloliquefaciens TCCC11319* strain could not grow on media obviously. Besides, there was a continuous research for Collagenase activity over a wide range of Cr(III). Thus, chromium sulfate was used as the substrate to determine the inhibitory effect of Cr(III) on collagenase activity. Cr(III) at a concentration of 1000 mg/L exhibited 80% inhibition to collagenase. The inhibition increase with increase of Cr(III) concentration and at 600 mg/L inhibition was obviously. The collagenase was inactivated when the Cr(III) concentration was over 1200 mg/L. Therefore, the strain of *B.amyloliquefaciens TCCC11319* has higher Cr(III) tolerance than other chromium tolerance bacteria presented so far.

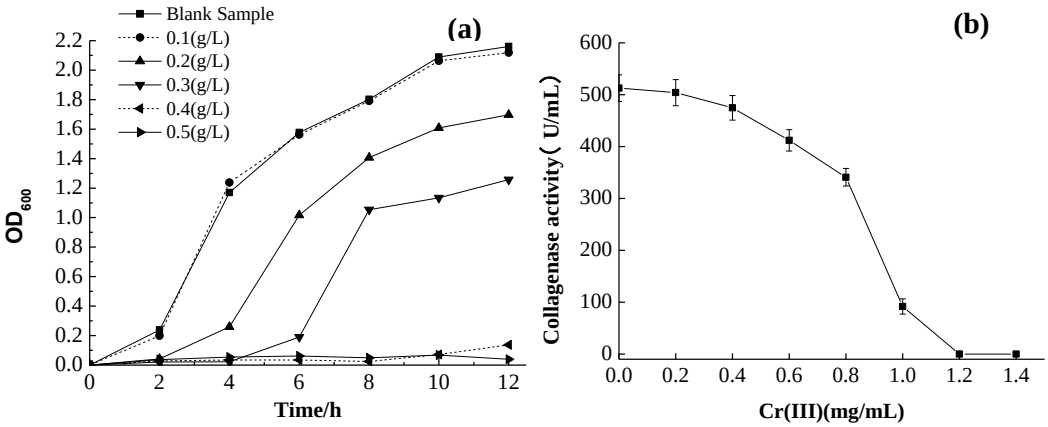

Fig.3 (a) Tolerance curve of *B.amyloliquefaciens* TCCC11319 for Cr (III) concentration (b) Tolerance curve of collagenase for Cr (III) concentration

4.Conclusion

The strain of *B.amyloliquefaciens* TCCC11319 exhibited high Cr(III) tolerance, and produced proteases include collagenase, alkaline protease, neutral protease and keratinase. The fermentation broth had the ability to tolerate 900mg/L Cr(III) concentration. The collagenase was significant for the degradation of leather shavings. Therefore, the present finding has the potential application value for solid waste disposal of leather industry or other chromium contaminated industries.

References

1.Hüffer, S., Taeger, T., 2004. Sustainable leather manufacturing: A topic with growing importance[J]. The Journ of the American Leather Chemists Association. 99(10), 424-428.

2.Mu, C., Lin, W., Zhang, M., 2003. Towards zero discharge of chromium-containing leather waste through improvet alkali hydrolysis[J]. Waste management. 23(9), 835-843.

3.Pati, A., Chaudhary, R., Subramani, S., 2014. A review on management of chrome-tanned leather shavings: a holistic paradigm to combat the environmental issues[J]. Environmental Science and Pollution Research. 21(19), 11266-11282.

4.McLaren, James S., 2005. Crop biotechnology provides an opportunity to develop a sustainable future. Trends in Biotechnology. 23(7), 339-342.

5.Bajza, Z. MarkoviI., 1998. Influence of enzime concentration on leather waste hydrolysis kinetics[J]. Journal of the Society of Leather Technologists and Chemists. 83(4), 172-176.

6.Bachate, S. P., Nandre, V. S., Ghatpande, N. S., et al., 2013. Simultaneous reduction of Cr (VI) and oxidation of As (III) by *Bacillus firmus* TE7 isolated from tannery effluent[J]. Chemosphere. 90(8), 2273-2278.

7.Bailey, R. W., Scott, E. G., 1996. Diagnostic Microbiology. Second ed. The C.V. Mosby Company. Saint Louis.

8.Altschul, S. F., Madden, T. L., Schäffer, A. A., et al. 1997. Gapped BLAST and PSI-BLAST: a new generation of protein database search programs[J]. Nucleic acids research. 25(17), 3389-3402.

9.Moore, S., Stein, W. H., 1954. A modified ninhydrin reagent for the photometric determination of amino acids and related compounds[J]. Journal of Biological Chemistry. 211, 907-913.

10.Zhang, Y., Fu, Y., Zhou, S., et al., 2013. A straightforward ninhydrin-based method for collagenase activity and inhibitor screening of collagenase using spectrophotometry[J]. Analytical biochemistry. 437(1): 46-48.

11.Letourneau, F., Soussotte, V., Bressollier, P., et al., 1998. Keratinolytic activity of *Streptomyces* sp. S. K1-02: a new isolated strain[J]. Letters in applied microbiology. 26(1), 77-80.

12.Hwang, I., Batchelor, B., Schlautman, M. A., et al., 2002. Effects of ferrous iron and molecular oxygen on chromium (VI) redox kinetics in the presence of aquifer solids[J]. Journal of hazardous materials. 92(2), 143-159.

FLS P-67

EVALUATION OF SPECIFICITY OF PROTEASE FOR DEHAIRING

Shanthi.C* and Shakilanishi S

Department of Biotechnology, School of Bio Sciences and Technology, Vellore Institute of Technology, Vellore 632014, Tamilnadu, India.

**E-mail:cshanthi@vit.ac.in*

Global concerns about environmental impact of leather industry have been forcing the tanneries to adopt cleaner leather processing technologies. Enzyme based leather processing methods have the potential to substantially reduce the pollution, toxicity and also improve leather quality. One such greener process option is the use of proteases in dehairing of skins and hides. But the important criterion in choosing enzymes for dehairing is the specificity towards the targeted biomolecules on skins. As the skin itself is a proteinous substance, use of non-specific proteases might degrade other skin proteins and cause damage to resultant leather. The present work deals with the comparative study on the specificity of a dehairing and non-dehairing protease isolated in our laboratory. Two proteases producing bacteria, *Bacillus cereus* VITSN04 and *Bacillus megaterium* VITSN02 were used in this study. Studies on the efficacy of enzymes to dehair goat skins revealed *B.cereus* protease exhibited potent dehairing efficacy whereas protease from *B.megaterium* did not. Dehairing and non-dehairing enzyme was identified as serine and metalloprotease respectively and optimal pH and temperature for activity were also determined. The activity of *B.cereus* enzyme to unhair was evaluated at its specificity level using protein substrates such as keratin, collagen and compared with *B.megaterium* protease. The results showed that the dehairing enzyme was non-keratinolytic and non collagenolytic. The SEM studies on the cross section of skin dehaired enzyme showed good fiber opening which could probably due to specific degradation of proteoglycanby the enzyme. This is yet to be confirmed using proteoglycan as substrate. The non dehairing protease had degraded keratin substrate but not collagen. This preliminarystudy signifies the importance of screening proteases for specificity before employing the enzyme for dehairing process.

Keywords: Protease, dehairing, non-dehairing, *Bacillus*

1. Introduction

At present, the concept “Eco-design” has been adopted by many industries for developing eco-friendly methods in order to reduce the environmental impacts of industrial pollutants. In this context, enzymes are considered as the major asset for cleaner technologies by acting as alternates to chemical processes and performing reactions with high specificity. One such enzyme is proteases which are been used in dehairing process of leather industry. It is accounted for 60-65% of total sales in world market and microbial source have become the choice for industrial use, rather than proteases obtained from the plant and animal sources (Genckal and Tari 2006). Proteases from *Bacillus* sp. are the best commercial sources available to date (Singh et al. 2004).Dehairing is one of the single largest constrained process involving the use of lime and sulphide, being the actual pollutants in tannery waste. During the process of unhairing, lime causes swelling up of skins, disassociation of proteoglycans bound to collagen fibril matrix and sulphide breaks the disulphide linkages of keratin together all leads the loosening of fibrilar matrix and removal of hairs. The enzyme action upon the skin and skin components for effective dehairing is not known till date. Though many proteases are been continuously produced from different micro-organisms and used for various applications, it’s not the same the protease that does all the work. Similarly, many proteases are screened for dehairing efficacy but not all kind of enzyme possesses the specificity to dehair animal skins. In the present study, an attempt has been made to evaluate dehairing efficacy of two proteases from micro-organisms isolated from same environment, and comparatively study the type of protease they belong to and its specificity towards skin proteins.

2. Material and methods

2.1. Micro-organisms

Protease producing bacteria, *Bacillus cereus* VITSN04 (Sundararajan et al., 2011)and strain 1isolated from soil samples collected near protein rich site, Vellore, India were used in the study.Morphology and Gram characteristics of strain 1 were studied. Molecular characterization was further studied by 16S rRNA gene sequencing method. DNA was isolated and amplified by PCR. The primer sequences 5C27 (5’-AGAGTTTGATCCTG-3) and RC1492 (5’-TACGGCTACCTTGTTACGACTT-3) were chosen from the conserved regions previously reported for the bacterial 16S rDNA (Marchesi et al. 1998). The 16S rRNA gene sequence similarities were studied using NCBI-BLAST search.

2.2. Crude enzyme and dehairing studies

One millimeter of seed culture (1 OD_{600nm}) was inoculated in nutrient broth and incubated at 37°C at 120rpm overnight. After 24h, the biomass was harvested by centrifugation at 8,000rpm for 10 min and enzyme purified from extracellular supernatant by ammonium sulphate precipitation method followed by dialysis and subjected for dehairing studies. Two halves of wet salted goat skins cut from butt portions (dimensions of 5×5cm) were used for enzyme application trials. Crude enzymes of both

strainswereapplied on flesh side of left and right halves of goat skins respectively. The skins were folded inside and left overnight. Next day the dehairing extent in the skins were assessed

2.3. Protease assay using azodye substrates

The substrate specificity of enzyme was determined by treating enzymes of both organisms with azodye conjugated substrates such as azocasein (Tomarelli et al. 1949), keratin azure (Wainright 1982) and azocoll (Chavira et al. 1894). One unit of protease activity is equivalent to change in the optical density of 0.01 per min under standard assay conditions. Standard deviation of each triplicate data was represented as error bars.

2.4. Characterization of enzymes

The enzymes from both organisms were characterized by studying the effect of pH, temperature and inhibitors on the proteolytic activity. For pH study, varying buffers such as citrate buffer (pH 3–5), Tris–HCl buffer (pH 6–8) and Glycine–NaOH buffer (pH 9–10) were used. Egg albumin (0.1%) and casein (2%) were used as substrates in acidic and alkaline pH respectively. The final concentration of each reaction mixture was adjusted to 0.2M with above mentioned buffers. To study the effect of temperature on proteolytic activity, reaction mixture was incubated at varying temperature ranging from 20 to 80°C at a constant pH of 8.0. To determine the class of proteases, the enzymes were treated with phenylmethylsulfonyl fluoride (PMSF), ethylenediaminetetraaceticacid (EDTA), 1,10-phenanthroline, iodoacetate and pepstatin A protease inhibitors (5 mM). The proteolytic activity was determined using casein as substrate (Kunitz 1947).

2.5. SEM studies

*B.cereus*VITSN04 protease treated leather was subjected for scanning electron microscope studies. The sample was sputter-coated with gold (Edwards E-306) and examined using FEI-Quanta 200 microscope at an accelerating voltage of 5kV.

3. Results and Discussion

3.1. Protease producing bacteria

Two highest protease producing bacteria isolated from soil sample collected milk vending shop were chosen for the study. One organism was identified earlier as *Bacillus cereus* VITSN04 (Sundararajan et al. 2011) and other organism (strain 1) was found to be rod-shaped, Gram positive and aerobic bacterium. Based on 16S rRNA gene sequencing analysis it was identified as *Bacillus megaterium*VITSN02.The16S rDNAsequence of *B.megaterium*VITSN02 has been deposited in Genbank database with accession number GQ406847. The phylogenetic tree (Fig. 1) was constructed by neighbor-joining method using Clustal W software.

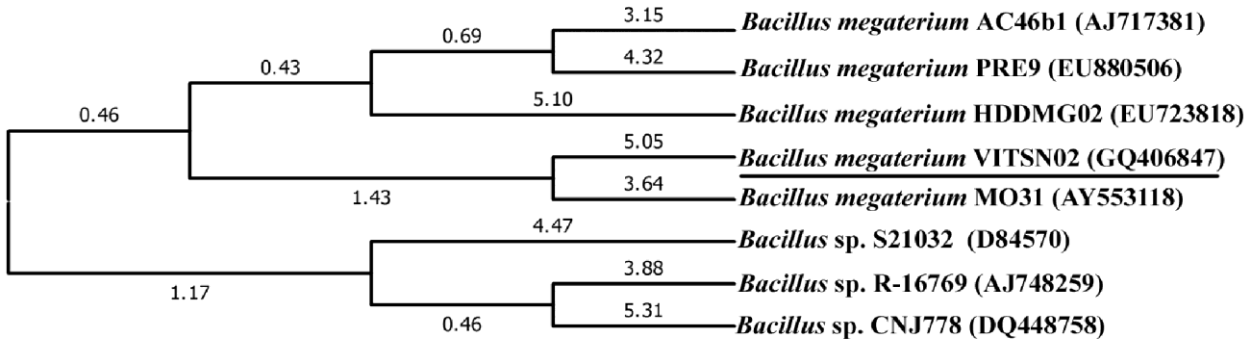

Fig. 1.Relationships between *Bacillus megaterium*VITSN02 (GQ406847) and members of the *Bacillus*spon rooted neighbor-joining tree based on 16S rDNA sequences.

3.2. Dehairing studies

The proteases from micro-organisms (*B.megaterium*VITSN02 *and* *B.cereus*VITSN04) isolated from the same environment were tested for dehairing efficacy. The study on treatment of enzymes on goat skins revealed (Fig.2) that *B.cereus*VITSN04 protease possesses good dehairing property (Fig. 2B) as reported earlier (Sundararajan et al., 2011) whereas the enzyme from *Bacillus megaterium*VITSN02 did not cause removal of hairs (Fig.2A) suggesting that the enzyme might lack specificity to initiate dehairing. Several proteases with dehairing function from *Bacillus* species (Briki et al. 2016; Anandharaj et al. 2016; Aravindhan et al. 2017) have been researched but details on the substrate specificity is still lacking.

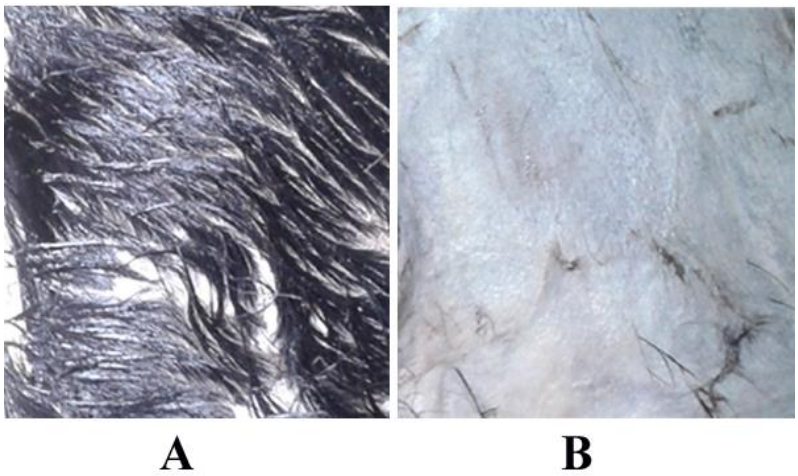

Fig.2. Dehairing of goat skins using enzyme (A) from *Bacillusmegaterium*VITSN02and (B) from *Bacilluscereus* VITSN04

3.3. Characterization of enzymes

The characteristics of enzymes from both organisms were studied in terms of pH and temperature optima for proteolytic activity and the class of the protease they belong to. The study on theinfluence of pH and temperature on enzyme activity revealed that the optimal pH for maximal proteolytic activity for *B.cereus* enzyme and *B.megaterium* enzyme was 8.0 and the optimum temperature was 30 and 40 °C, respectively. Inhibition studies revealed (Fig.3) that *B.cereus* enzyme was completely inhibited by PMSF and *B.megaterium* enzyme by 1,10phenanthroline and EDTA indicating the first one to be of the serine and the later a metalloprotease. Most of the dehairing enzymes are found to be serine alkaline proteases (Zhao et al. 2016; Wang et al. 2016).

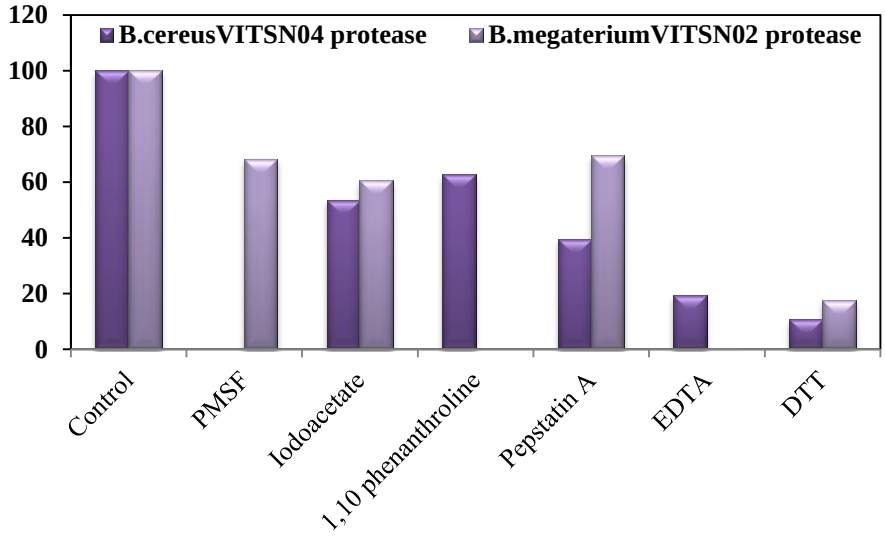

Fig.3. Effect of protease inhibitors on *B.cereus* enzyme and *B.megaterium* enzyme

3.4. Substrate specificity of enzymes

As skin itself is a proteinous substance, use of non-specific proteases might degrade skin and cause damage to leather. The suitability of proteases to act upon skin proteins viz., keratin and collagenwas evaluated using chromogenic protein substrates such as azocasein, keratin azure and azocoll. The treatment of both enzymes on azodye substrates showed that (Fig. 4) highest proteolytic activitywas observed with azocasein, since it is a non specific substrate and hence considered as common substrate for proteases (Barrett et al. 2012) *Bacillus megaterium* VITSN02 degraded keratin azure suggesting the enzyme to be keratinolytic probably by cleaving S-S bond of soluble keratin but not that of intact keratin of skin as evidenced (no dehairing) by intact hair Fig.1. The enzymes showed negligible activity for azocoll indicating both *strain* VITSN02 and VITSN04 proteases lack

collagenolytic activity. Overall, dehairing protease should be of a non-collagenolytic to produce good leather. Several researches are found the dehairing enzyme to be non-collagenolytic in nature (Rao et al. 2016; Wang et al. 2016)

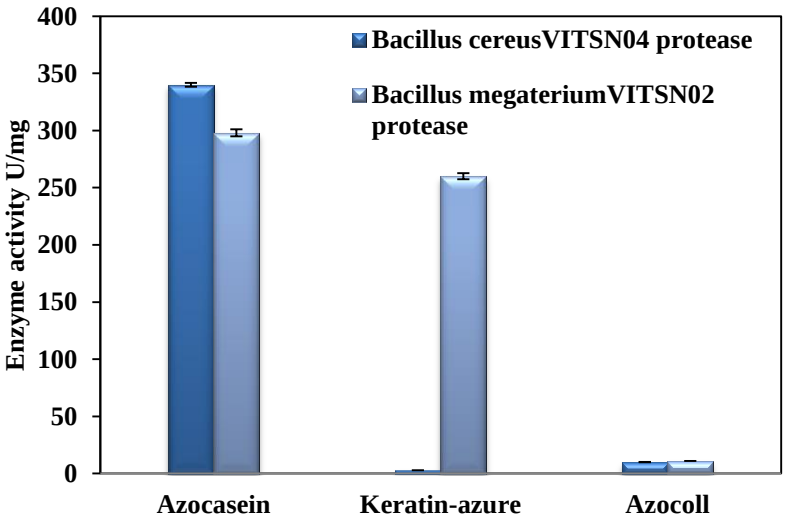

Fig.4. Hydrolysis of azodye conjugated protein substrates by *B.cereus*enzyme and *B.megaterium* enzyme

3.5.SEM analysis

The SEM analysis was carried out to check the effect of the enzyme on the firmness and integrity of the skin. Fig.5. depicts the cross section of leather treated with dehairing enzyme. The fibre bundles are well separated suggesting enzyme caused opening up of collagen fibre bundle at macro level may be due to disruption of proteoglycans which are bound to collagen fibril surface ultimately leading to loosening of ECM and removal of hairs.

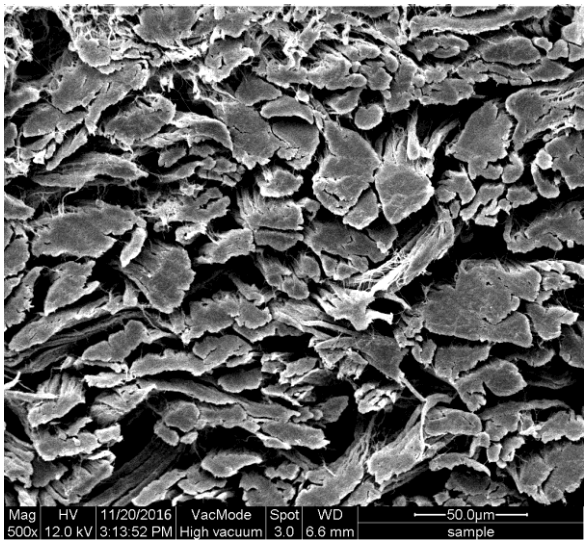

Fig.5. Scanning electron microscope-cross section of dehairing enzyme (*B.cereus*VITSN04) treated leather

3. Conclusion

Among two proteases, one from *Bacillus cereus* VITSN04 was found to be effective in dehairing and other enzyme from *Bacillus megaterium*VITSN02 does not possess such property. On further characterization of these enzymes, the optimal pH for both the enzymes was to be pH 8.0 and at temperature 30 and 40 °C the strain VITSN04 and VITSN02 protease showed maximum proteolytic activity respectively. The dehairing protease was a serine type of protease with non-collagenolytic and non-keratinolytic property whereas non-dehairing enzyme is a metalloprotease with non-collgenolytic property and keratinolytic on soluble keratins. Further studies with other constituent proteins in the skin such as proteoglycans as substrates would possibly indicate the screening procedure to be followed in isolating an efficient organism that can be employed commercially. This study gives a preliminary understanding of the specificity characteristics of dehairing proteases.

References

1. Anandharaj M, Sivasankari B, Siddharthan N, Rani R P, Sivakumar S. Production, Purification, and Biochemical Characterization of ThermostableMetallo-Protease from Novel *Bacillus alkalitelluris* TWI3 Isolated from Tannery Waste. Appl. Biochem. Biotechnol. 2016, **178**, 1666-1686.
2. Aravindhan R, Monika V, Balamurugan K, Subramanian V, Rao J R, Thanikaivelan P. Highly clean and efficient enzymatic dehairing in green solvents. J. Clean. Prod. 2017, **140**, 1578-1586.
3. Barrett A J, Woessner J F, Rawlings N D (Eds). *Handbook of proteolytic enzymes*; Elsevier academic press, Vol. 1. 2012.
4. Briki S, Hamdi O, Landoulsi A. Enzymatic dehairing of goat skins using alkaline protease from *Bacillus* sp. SB12. Protein Expr. Purif. 2016, **121**, 9-16.

5. Chavira Jr R, Burnett T J, Hageman J H. Assaying proteinases with azocoll. Anal. Biochem. 1984, **136**, 446–450.
6. Genckal H, Tari C. Alkaline protease production from alkalophilic*Bacillus* sp. isolated from natural habitats. Enzyme Microb. Technol. 2006, **39**, 703-710.
7. Kunitz M. Crystalline soybean trypsin inhibitor: II. General properties, Gen. Physiol. 1947, **30**, 291–310.
8. Marchesi J R, Sato T, Weightman A J, Martin T A, Fry J C, Hiom S J, Dymock D, Wade W G. Design and evaluation of useful bacterium-specific PCR primers that amplify genes coding for bacterial 16S rRNA. Appl. Environ. Microb. 1998, **64**, 795–799.
9. Rao R R, Vimudha M, Kamini N R, Gowthaman M K, Chandrasekran B, Saravanan P. Alkaline Protease Production from *Brevibacteriumluteolum* (MTCC 5982) Under Solid-State Fermentation and Its Application for Sulfide-Free Unhairing of Cowhides. Appl. Biochem. Biotechnol. 2016, **2**, 1-8.
10. Singh J, Vohra R M, Sahoo D K. Enhanced production of alkaline proteases by *Bacillus sphaericus* using fed-batch culture. Process Biochem. 2004, **39**, 1093-1101.
11. Tomarelli R, Charney J, Harding M L. The use of azoalbumin as a substrate in the colorimetric determination or peptic and tryptic activity. J. Lab.Clin. Med. 1949, **34**, 428.
12. Wainwright M A. A new method for determining the microbial degradation of keratin in soil. Experientia 1982, **38**, 243–244.
13. Wang C, Yu S, Song T, He T, Shao H, Wang H. Extracellular Proteome Profiling of *Bacillus pumilus* SCU11 Producing Alkaline Protease for Dehairing. J. Microbiol. Biotechnol. 2016, **28**, 1993.
14. Zhao H Y, Wu L Y, Liu G, Feng H. Single-site substitutions improve cold activity and increase thermostability of the dehairing alkaline protease (DHAP). Biosci. Biotechnol. Biochem. 2016, **80**, 2480- 2485.

FLS P-19

ROLE OF BOVINE COLLAGEN PEPTIDE ON CELL ADHESION AND PROLIFERATION

Shanthi C *, Sivaraman Kuppuswamy

Dept. of Biotechnology, School of Bio Science and Technology, VIT University, Vellore

632014, Tamil Nadu, India,

**E-mail address: cshanthi@vit.ac.in*

Collagen type I, which is the main component of the skin is found to have several biological roles in addition to structural role. Collagen is now well known to function by interaction with specific cell receptors like integrins and promote cell adhesion and proliferation. Hence use of collagen peptides and hydrolysates in therapeutics has increased tremendously. The aim of the present study was to determine the cell adhesion and proliferative property of short amino acid sequences in type I collagen. In earlier study, a larger peptide was isolated from bovine Achilles tendon collagen which showed cell adhesion in HeLa (epithelial) cell. Probable integrin binding sequences were identified from the larger peptide using bioinformatics tool. The activity of the identified small sequence was confirmed in HeLa cell line. The peptides were coated onto sterile cell culture microtiter plates at different concentrations and incubated for 6h for adhesion and 48h for proliferation assay. Bovine tendon collagen coated dishes were used as positive control. The cell count increased with increasing concentration of peptide when compared with uncoated surface. MTT assay also showed similar results. Proliferation assay was recorded as images, which showed effective proliferation of the cells in peptide coated surface when compared to uncoated surface. Fluorescent staining of the cell nucleus with Hoechst 53328 exhibited no visible DNA fragmentation and active dividing cells were also observed. The cell adhesion and proliferation assay was performed with fibroblast (3T3-L1 cells), keratinocytes (HaCaT) and compared with epithelial (HeLa) cell line. The concentration of peptides with highest cell adhesive and proliferative activity was determined. This basic study on bioactive collagen peptides would provide information for development of biocompatible biomaterials and scaffolds.

Keywords: Bovine tendon collagen, Peptide, cell adhesion, Cancer cell lines

Introduction

Collagen is a main component of the ECM, constituting about 25-35% of the whole of the body proteins in mammals, Collagen is a family of proteins containing about 28 types of collagen molecules classified into fibrillar and non-fibrillar type. Type I collagen is the most prevalent fibrillary form. The other types are present in lower proportions in various tissues and organs having

characteristic function in the particular organ or tissue [1, 2] Recently the focus on peptides within the parent protein is gaining popularity in finding novel peptides with diverse physiological and functional role, and such peptides are termed as cryptic peptides. Novel peptides from extracellular matrix proteins are being studied for the diverse functional role on cell signaling and interaction [3, 4, 5]. The highest number of novel peptides so far discovered are from ECM proteins [6]. Hence the information on cryptic peptides from ECM proteins paves way to explore unidentified peptides from type I collagen.

The fibril forming type I collagen, major form found in vertebrates, provides mechanical support for tissues and functional microenvironment for cells [7]. Cell adhesion is an important process that plays major role in the development of multicellular organisms. The cell adhesion process can be categorized into two major steps: the ECM binding sites interact with the cell adhesion receptors and the binding triggers the downstream proteins leading to cell attachment followed by remodeling of the cytoskeletal filaments supporting the cell shape and spreading of the cell on the substratum [8]. Among the cell adhesion receptors integrins are the largest family yet discovered [9]. Integrins facilitates the interaction between collagen type I and cells, they are involved in anchorage and bidirectional signal transfer. The whole of the signal cascade is operated through a series of protein signals which initiates the formation of protein aggregates, termed focal adhesion sites, these signals link integrins to the cytoskeletal proteins and other cascade of other cellular events involved in cell growth, development and apoptosis [10, 11]. Cryptic peptide with a molecular weight of (2.8kDa) was identified from type I collagen α chain from bovine Achilles tendon collagen which displayed cell adhesion, and proliferation. [12, 13].

The present study hypothesizes that the peptide regulated cell adhesion and proliferation of the cells may occur through the integrin receptors which was predicted through bioinformatics tools from our previous studies. The study focuses on identification of a smaller sequence that could have a probable role in cell adhesion and proliferative activity of the previously isolated larger peptide from Bovine Achilles tendon collagen. The cell adhesion activity of the peptide was carried out with the HeLa, 3T3-L1 (murine fibroblast) and HaCaT (Keratinocyte) cell lines.

Materials and methods

Custom synthesized peptide (GKNGDDGEA) was procured from Neo Scientific, USA. Cell culture work was carried out on HeLa, 3T3-L1 (murine fibroblast) and HaCaT (Keratinocyte) cell lines were procured from National Centre for Cell Science, Pune, India. All the cell culture work, peptide and collagen coating was done under sterile condition in a class II bio-safety cabinet (Clean Air Systems, Chennai, India). The T-flasks (Nunclon surface) were obtained from Nunc, Roskilde, Denmark and the microtiter plates were obtained from Tarsons Products Pvt. Ltd, New Delhi, India. The culture media DMEM was from GIBCO, antibiotic solution were obtained from HiMedia, India. Fetal bovine serum and 10x trypsin–EDTA solution were procured from Sigma–Aldrich, St. Louis, MO, USA.

Cell maintenance

HeLa, HaCaT and 3T3 (Keratinocyte) cell lines were maintained according to standard protocols [14]. Cells were cultured in DMEM supplemented with 10% fetal bovine serum and incubated at 37^{o} C in a 5% CO_2 humidified incubator. For experiments, cells reaching 80% confluence were detached from T-flasks with trypsin–EDTA, centrifuged and cell number was enumerated in a Neuber's chamber by trypan blue exclusion assay.

Peptide Coating on Microtiter Plate

The commercial peptide was coated onto sterile disposable microtiter plates for the cell adhesion and proliferation assay according to the standard procedures [15]. The peptide was coated with 3.2 × 10^{-3} to 1 × 10^{3} µg in each well of microtiter plates. Initially the peptide was diluted in PBS to desired concentration and added to the wells and incubated for 4h inside the biosafety cabinet at sterile condition. After the incubation process, the left over solution is removed off from the wells and the plate is stored under sterile condition at 4^{o}C until the experiment.

Cell Adhesion and Proliferation

Peptide were coated to the sterile cell culture microtiter plates at different concentration ranging from 3.2 × 10^{-3} to 1 × 10^{3} µg. For cell adhesion and proliferation study cells were seeded at a concentration of 3 × $10^{6}$and 5 × 10^{5} per well respectively and the dishes were incubated in a 5% CO_2 chamber for 6h and 48h respectively. The cells number and viability was enumerated as mentioned previously in cell maintenance section. The proliferation of the cells was observed using an inverted light microscope and photomicrograph at 400X magnification.

Hoechst 33258 staining

The cell lines were maintained under standard condition before the experiment. The cells were seeded on to peptide coated and uncoated coverslip in a 24 well cell culture plate with different concentration previously mentioned. For the proliferation study cells were seeded at a concentration of 5x10^{5} per well and incubated for 48h. the coverslips were rinsed with 1x PBS and the cells were fixed with 4% formaldehyde at room temperature for 10 min, again the coverslip was washed with 1x PBS and stained with 1x dye solution (Hoechst 33258) diluted in PBS for 15 min at room temperature. The coverslip was rinsed with 1x PBS and mounted onto a glass slide and imaged. The excitation light source was a mercury lamp with blue filter. Weswox Fluorescence Research Microscopes, FM-3000 was used at a magnification of 100 and 400X.

Statistical analysis

The cell adhesion assay was performed in triplicates, and the cell count was stated as mean ± SD. The results were checked for statistical significance by ANOVA and p values less than 0.05 were considered significant.

Results and Discussion

Table 1: HeLa , HaCat and 3T3 cell adhesion on surface coated with peptide				
Amount coated (µg)				
2.5x10^{2}	**1x10^{2}**	**0.8x10^{-1}**	**3.2x10^{-3}**	**Control**
Cell count (x10^{5}) ± SD				

HeLa					
Peptide	12.07 ± 0.6	8.7 ± 0.4	7.38 ± 0.44	6.36 ± 0.48	0.8 ± 0.04
HaCaT					
Peptide	3.30 ± 0.20	2.20 ± 0.26	1.50 ± 0.30	0.94 ± 0.05	0.19 ± 0.27
3T3					
Peptide	0.44 ± 0.12	0.30 ± 0.15	0.47 ± 0.10	0.37 ± 0.69	0.55 ± 0.07

Note: The peptide coating on the surface ranged from3.2 x 10^{-3} to 2.5 x 10^{2} µg. For adhesion assay cells were seeded at 3 x 10^{6} cells per well and the adherent cells were counted after 6h of incubation. All the assay was done in triplicates and the cell count (x10^{5}) mean and ± SD are given. Uncoated wells were used as a negative control and the cells failed to adhere to the surface within the observed period. The use of three different cell line sources was used to check the effectiveness of the peptide on cell adhesion and proliferation on different cell type and its microenvironment. Collagen positive control values (1x10^{2} µg – cell count was 15.7 ± 1.0 x 10^{5} cells). The cell count from the cell adhesion assay with peptide coated and uncoated the plates showed (Table-1) a significant cell adherence of HeLa cells in a concentration depended manner whereas the HaCaT cells showed less adherences. 3T3 cell line showed clumping of cells.

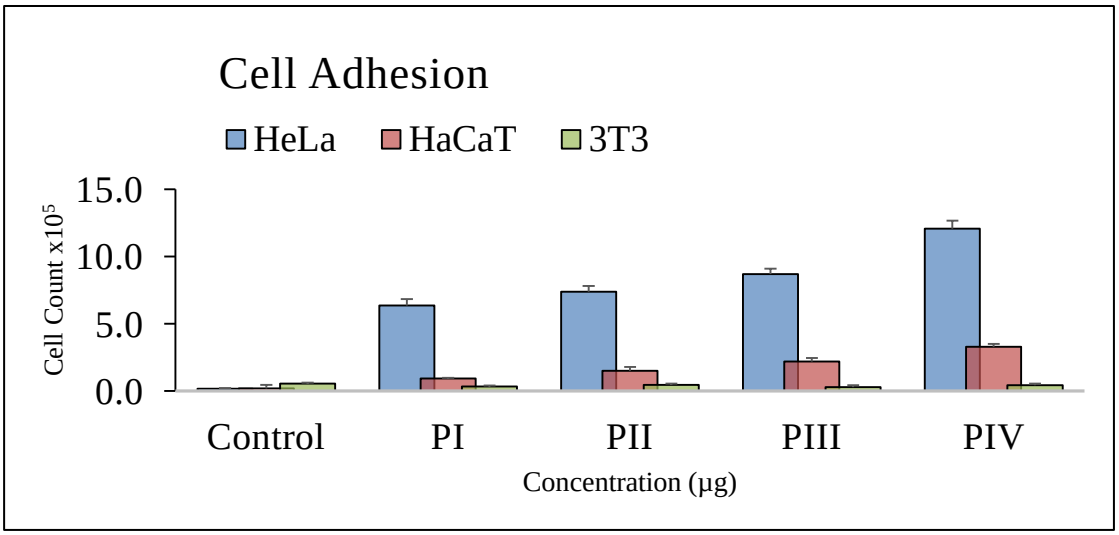

Fig 1: Cell count from the peptide coated dishes HeLa, HaCaT and 3T3 cell lines. The concentration of the peptide coated is represented as PI, PII, PIII and PIV (3.2 x 10^{-3}, 0.8 x 10^{-2}, 1 x 10^{2} and 2.5 x 10^{2} µg/ml respectively).

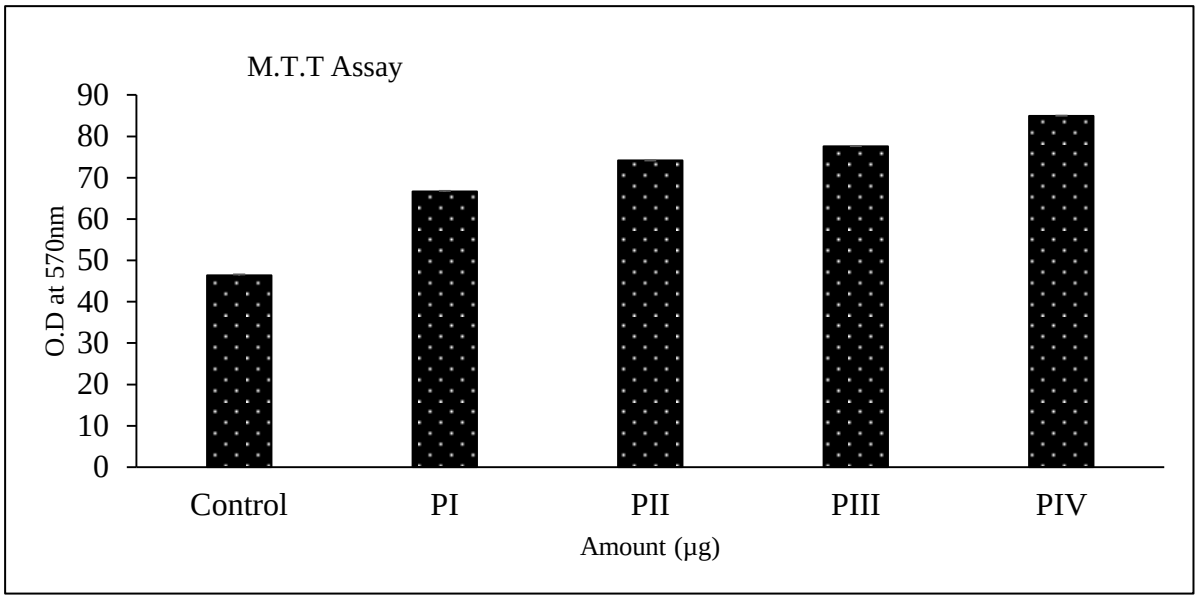

Fig 2: The MTT assay on HeLa. HeLa cells showed an increase in absorbance with increase in peptide coating concentration which indicates the increased adhered and live cells present, where as HaCaT and 3T3 cells showed insignificant observations hence data not shown.

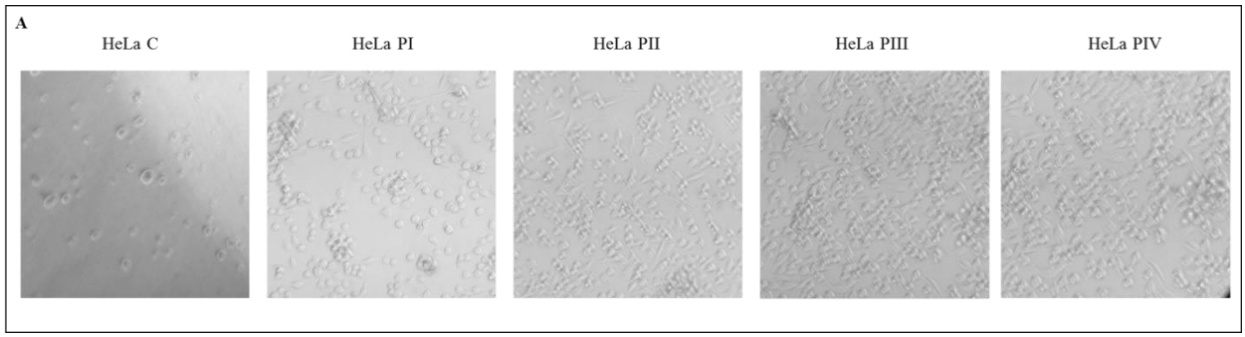

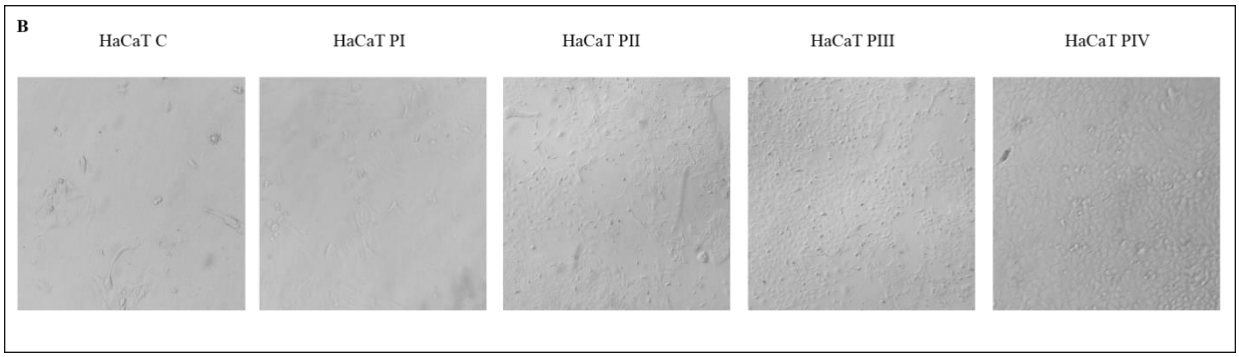

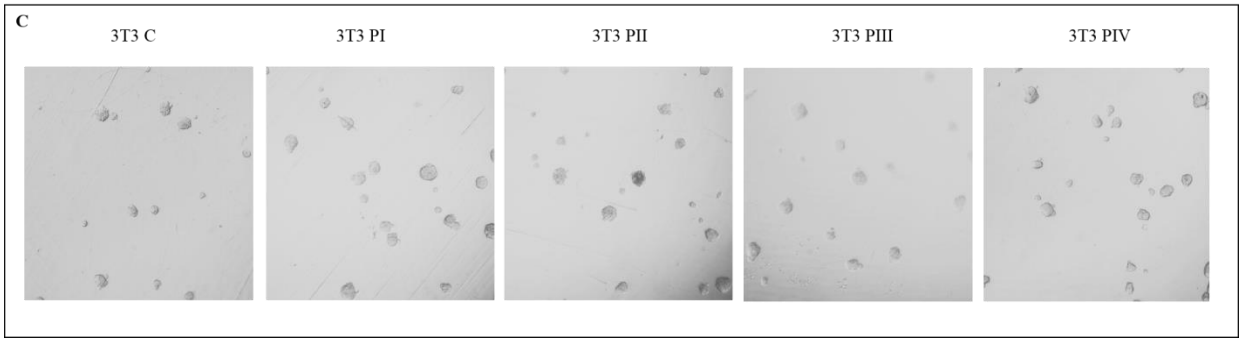

Fig 3: Bioactivity assessment of the peptide, photomicrograph of the cell adhesion. A – HeLa, B – HaCaT (Keratinocyte) and C – 3T3 (Murine Fibroblast) adhered to the peptide coated cell culture microtiter plates incubated for 6h and cell count was performed. The peptide concentration represented as PI, PII, PIII and PIV are as (3.2×10^{-3}, 0.8×10^{-2}, 1×10^{2} and 2.5×10^{2} µg per well respectively) and C represents uncoated control surface. The images photographed at 10x magnification. HeLa showed a significant cell adhesion on to the peptide coated surface and HaCaT cells showed very little adherence when compared to uncoated surface, whereas 3T3 cells clumped onto the surface.

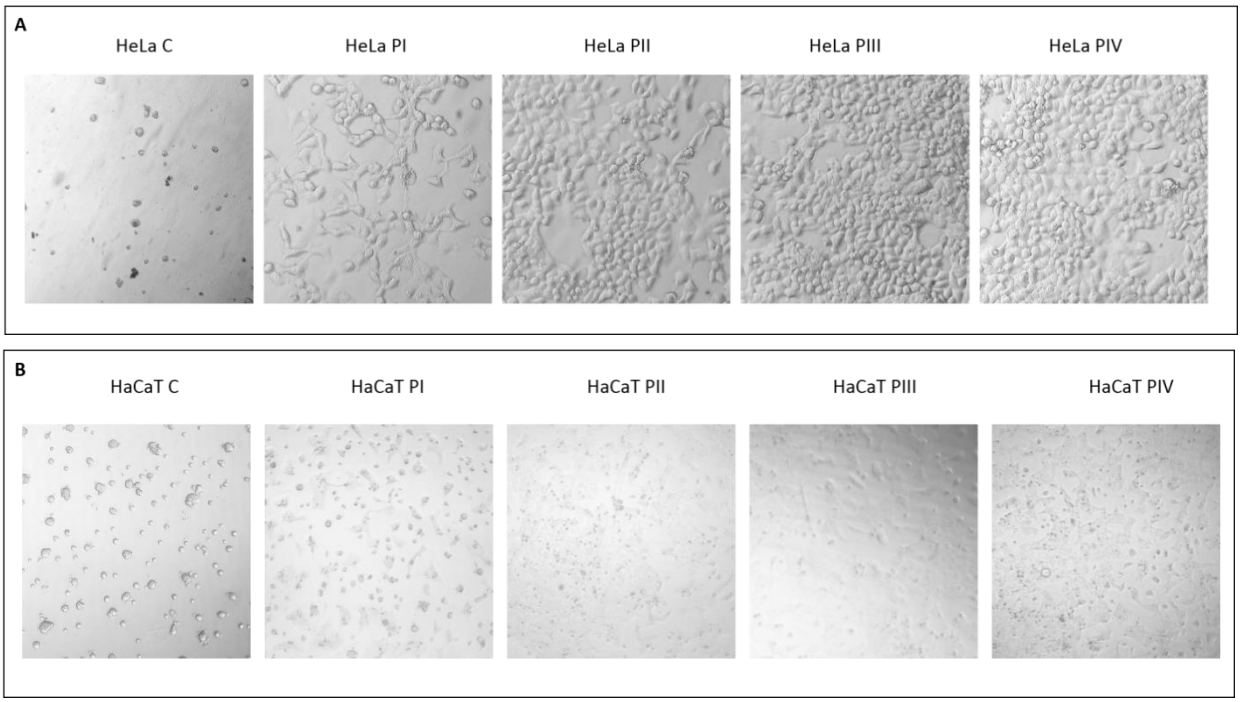

Fig 4: Photomicrograph of cell proliferation. A – HeLa and B – HaCaT (Keratinocyte) adhered to the peptide coated surface, incubated for 48h and proliferation was assessed. The peptide concentration represented as PI, PII, PIII and PIV are as (3.2×10^{-3}, 0.8×10^{-2}, 1×10^{2} and 2.5×10^{2} µg respectively) C represents uncoated control surface. The cell proliferation of HeLa increased significantly with increasing concentration of peptide, HaCaT cells showed some adherences of cells and 3T3 cell line did not show any adherence to the coated and uncoated surface. The insignificant cell adhesion on to the peptide coated surface may be due to insufficient cell seeding concentration which will be further confirmed by future experimentations. The images were photographed at 10x magnification.

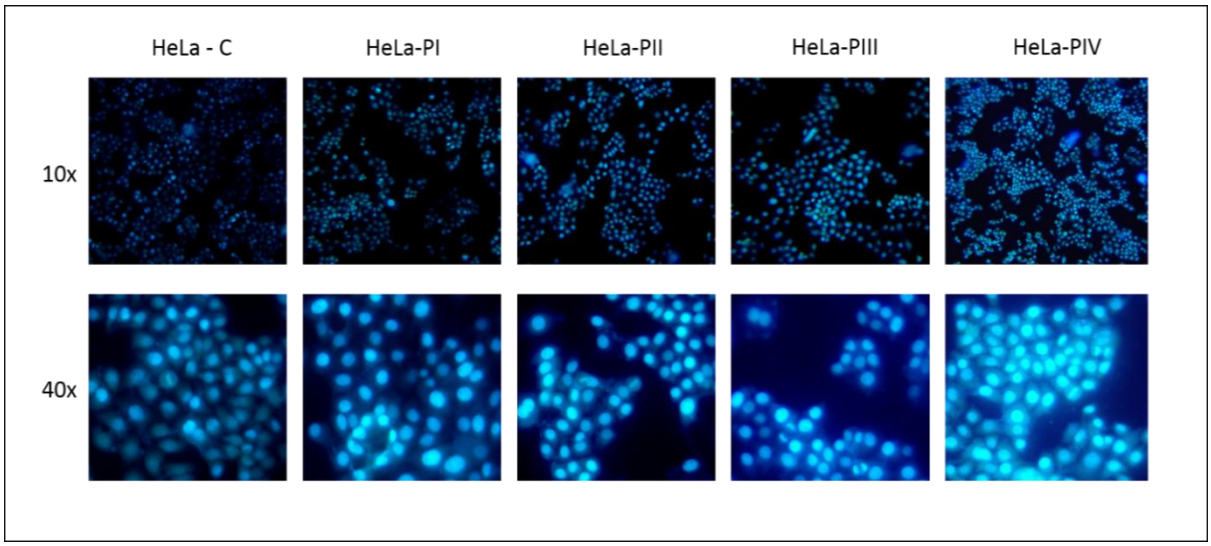

Fig 3: Fluorescent staining (Hoechst 33258) of HeLa cell. The peptide coating concentration is represented as PI, PII, PIII and PIV (3.2×10^{-3}, 0.8×10^{-2}, 1×10^{2} and 2.5×10^{2} µg respectively) C represents uncoated control surface. The images were photomicrographed at 10x and 40x magnification. The fluorescent staining with Hoechst 33258 is done to identify the DNA fragmentation and apoptosis. Clear nuclear staining and increase in number of cell with increase in concentration of the peptides confirms the role of the peptides in proliferation in HeLa cells.

Conclusion

The peptide showed a good adhesive and proliferative property with HeLa cells but similar results were not observed with HaCaT and 3T3 cells. In the case of HaCaT cells a delayed adhesion and proliferation occurred after an extended period of time. 3T3 cells were found clumped to the coated and uncoated surface of microtiter plates. Further studies have to be carried out to explain the above mentioned results.

Acknowledgements

This study was supported by research grant from DST, Government of India (SERB) and VIT University, Vellore.

References

1. Shoulders M D, Raines R T, Collagen structure and stability. *Annu Rev Biochem,* 2009, **78**, 929.

2. Kadler K E, Baldock C, Bella J, Boot-Handford R P, Collagens at a glance. *J. Cell Sci,* 2007, **120**, 1955-8.

3. Colorado, P C, Torre A, Kamphaus, G, Maeshima Y, Hopfer H, Takahashi K, Ericksen M B, Anti-angiogenic cues from vascular basement membrane collagen. *Cancer research*, 2000, **60**, 2520-2526.

4. Chow L W, Armgarth, A, St-Pierre J P, Bertazzo S, Gentilini C, Aurisicchio C, Stevens M M, Peptide-Directed Spatial Organization of Biomolecules in Dynamic Gradient Scaffolds. *Adv Healthc Mater*, 2014, **3**, 1381-1386.

5. Rubert Pérez C M, Panitch A, Chmielewski J, A Collagen Peptide-Based Physical Hydrogel for Cell Encapsulation. *Macromol Biosci*, 2011, **11**, 1426-1431.

6. Autelitano D J, Rajic A, Smith A I, Berndt M C, Ilag L L, Vadas M, The cryptome: a subset of the proteome, comprising cryptic peptides with distinct bioactivities. *Drug Discov Today*, 2006, **11**, 306-14.

7. Prockop, D J, Kivirikko K I, *Annu. Rev. Biochem*, 1995, **64**, 403–434.

8. Abedin M, King N, Diverse evolutionary paths to cell adhesion. *Trends Cell Biol*, 2010, **20**, 734-42.

9. Hynes R O, Integrins: bidirectional, allosteric signaling machines. *Cell*, 2002, **110**, 673-87.

10. Heino J, The collagen family members as cell adhesion proteins. *BioEssays*, 2007, **29**, 1001-10.

11. Takada Y, Ye X, Simon S, The integrins. Genome Biol, 2007, **8**, 1.

12. Banerjee P, Mehta A, Shanthi C, Screening for novel cell adhesive regions in bovine Achilles tendon collagen peptides. *Biochem. Cell Biol*, 2013, **92**, 9-22.

13. Banerjee P, Suseela G, Shanthi C, Isolation and identification of cryptic bioactive regions in bovine Achilles tendon collagen. *Protein J*, 2012, **374**, 86.

14. Ammerman N C, Beier Sexton M, Azad A F, Growth and maintenance of Vero cell lines. *Curr Protoc Microbiol*, 2008, A-4E.

15. Garcia A J, Vega M D, & Boettiger D, Modulation of cell proliferation and differentiation through substrate-dependent changes in fibronectin conformation, *Mol. Biol. Cell*, 1999, **10**, 785–798.

SFS P-39

NANOLAYEREDGRAPHENE OXIDE/MoS_2 COMPOSITES A NOVEL VISIBLE ACTIVE PHOTOCATALYST FOR SUSTAINABLE DYE HOUSE EFFLUENT TREATMENT

M. Suresh, A. Sivasamy*

Chemical Engineering Division, CSIR-Central Leather Research Institute, Adyar, Chennai-600 020
email: arumugamsivasamy@yahoo.co.in

Mineralization of dyes from various industrial effluents become an important issue pertaining to the environment. Advance oxidation process based semiconductor photocatalysis is considered as an emerging technique to overcome this problem.Graphene and its related materials possesses as an excellent electron acceptor/transport material, large surface area and can be applied as photocatalytic materials for environmental remediation. Hence, present investigation deals with nanolayers reduced graphene oxide/MoS_2 nanocomposite prepared by modified Hummer's method and sol-gel process. The prepared nanocomposite was characterized by XRD, FT-IR, FE-SEM and Raman analysis, thephotocatalytic activity was tested for the degradation of methylene blue dye under visible light irradiation. XRD results shows the pure crystalline nature of MoS_2 matrix in graphene oxide layers. The morphology of graphene oxide shows a sheet like form, where MoS_2 material were attached in between the sheets graphene oxide as layered structure. Raman analysis shows the purity of the graphitic nature. The preliminary photocatalytic studies such as effects of initial aqueous pH, different dye concentration and catalyst dosage were conducted. Neutral pH showed maximum percentage of degradation and same was considered for the further experiments. RGO-MoS_2 composite achieves maximum degradation of 96% at 240 min under visible light irradiation for MB dye molecules. The COD analysis of the sample was done at different time intervals.The kinetic rate constant results proves the photo reaction follows pseudo first order rate equation. The results demonstrate that RGO-MoS_2 could be a potential photocatalyst material for the photodegradation of organic dye molecule under visible light irradiation.

Keywords: photocatalyst, organic dye, visible light irradiation, nanocomposite.

1.Introduction

Effluents from industries such as textile, leather, paint etc., are the main sources for water pollution, which are highly colored, undergo chemical and biological changes and may affect human health as well as aquatic life (Liu P etal. 2016). There are number of conventional methods available for the treatment of colored effluents and are not feasible due to their inherent limitations. In the recent, many investigations have been carried out to degrade pollutants from aqueous phase, where

Advanced Oxidation Process (AOP) based semiconductor photocatalyis becomes an emerging technique for complete mineralization of effluent without byproduct formation (Dai S et al. 1996 ; Perez M.H et al. 2006). Semiconductor photocatalystsbased on metal oxide, graphene and Ag have a great attention on wastewater treatment due to their physical and chemical properties (Kowalska E et al. 2015;Ao Y et al. 2015). The traditional photocatalyst such as TiO_2, ZnO, ZnS have very low photocatalytic activity under visible light irradiation compared to UV light irradiation, this may due to their narrow band gap energy, low surface area etc (Yu X et al. 2016). Research has been made on the development of advanced photocatalytic material to overcome the limitations of above mentioned semiconductor photocatalysts (Xiang J et al., 2012). Graphene, a zero band gap energy material cannot be itself used for photocatalytic activity. Graphene as a support with other metal oxides as composite is totally different from graphene and can be considered as newer photocatalyst material (Min S. X et al. 2012). Graphene Oxide (GO), produced by the oxidation of graphite, while it is again followed by deoxygenation to yield Reduced Graphene Oxide (RGO). In recent years, sulfide based materials such as CdS, ZnS, MoS2, etc, have a great attention, where it acts asphotocatalystsas well as cocatalysts(Han SC et al. 2014;Li Y et al. 2009). Molybdenum disulfide MoS_2, a 2D transition metal dichalcogenide similar to graphite like structure have a great potential on wastewater treatment, where molybdenum is located in between the layers of sulfides. Due to its appreciable band gap energy and semiconducting properties, showed enhanced photo activity under visible light irradiations (Parzinger E et al. 2015;Chhowalla, M et al. 2013). Since, MoS_2 has some of the unique properties such as high surface area, reactivity, good electrical carrier and higher stability in water which can be act as photocatalyst(Laursen A. B et al. 2012). MoS_2 with a small band gap of 1.8 eV shows better response on visible region and exploited for photocatalytic activities due to its band gap of 1.22 eV as bulk material and 1.97 eV as single layer material (Splendiani, A et al. 2010;Mak K. F et al. 2010). MoS_2 can be prepared by various methods such as sol gel, CVD, ultrasonication, solvothermal, hydrothermal methods etc (Bessekhouad Y et al., 2003, ChoB, et al., 2015). One of the major demerits of $MoS_2$is that the recombination of electron hole pair, hence it should be resolved by improving the surface of the material. The combination of RGO/MoS_2 becomes an emerging photocatalyst due to their stability, flexibility, chemical and physical properties, etc. Graphene, an electron acceptor or donor and plays an important role in the field of photocatalysis, where it highly reduce the electron hole pair recombination and has been incorporated with photocatlysts to increase their efficiency(Chen Y et al. 2013;Zhang N et al. 2011;Pan L. K et al. 2013). Thus MoS_2can be incorporated with graphene for enhance photo activity under visible light irradiation, where MoS_2 act as a cocatalyst with graphene (Li J et al. 2014). Thus the graphene/MoS_2 composite not only applied in semiconductor photocatalysis but also used in various applications such as water splitting, energy storage and organic transformation reactions etc. RGO/MoS_2 composite can be prepared by various methods like hydrothermal, microwave and Hummer's method etc., (ChangK et al. 2011). Hence, the presentstudydeals with nanolayersRGO/MoS_2nanocompositematerial by modified Hummer's method and sol-gel process. The prepared nanocomposite was characterized by XRD, FTIR, FESEM and Raman analysis, and its photocatalytic activity was tested for the degradation of a model pollutantfor example, methylene blue dye under visible light irradiations in a slurry photoreactor.

2. Materials and methods

Natural graphite flakes,Molybdenum Oxide and L-Cysteinewas obtained from Sigma Aldrich, Potassium permanganate (KMnO4, 99%), Hydrochloric acid(HCl), Ethanol (C2H6O), sodium chloride (NaCl, 99.5%) were acquired from SD fine-chemicals Ltd, Mumbai, India. Hydrogen peroxide (H2O2, 30%), Potassium chloride (KCl, 99%), Nitric acid (HNO3 68%), Sodium nitrate (NaNO3 99%) sodium carbonate anhydrous GR ((NH4)2CO3), 99.9%) were procured from Merck, India Ltd. Magnesium sulphate (MgSO4.7H2O, 99.5%), potassium dichromate (K2Cr2O7, 99.9%) and ferrous ammonium sulphate ((NH4)2SO4.FeSO4.6H2O, 99%) were obtained from Qualigens fine chemicals, India. Concentrated sulphuric acid AR (H2SO4, 98%) and Sodium hydroxide pellets (NaOH, 98%) was received from Himedia laboratories private Ltd.

2.1Synthesis of RGO-MoS2 composite

Reduced Graphene oxide was prepared by modified Hummer's method using chemical oxidation technique. Natural graphite flakes were oxidized into graphite oxide followed by the exfoliation of graphite oxide to form graphene oxide employing sonication and centrifugation. The RGO-MoS2 nanocomposite were prepared by a solvothermal method. Typically, required quantity of graphite oxide is dissipated in 100 ml of ethanol in 250 ml beaker. In a separate beaker mixture of 0.3g of Na2MoO4 and 0.48g of L-Cysteine were dissolved in 50 ml of distilled water, after that transferred this solution into 250 ml beaker containing the graphite oxide solution.Then whole content was ultrasounicatedfor 30 min. After that the solution is poured in a Teflon- lined Stainless steel Auto clave kept it in muffle furnace at 180 °C for 6 hrs. Finally the product is washed with alcohol and distilled water for several times. The product was dried 80 °Cat vacuum oven for 24 hrs. The Black powder was sintered in a tubular furnace at 700°C for 2 hrs in N2 atmosphere and the RGO /MoS2 was obtained.

2.2 Characterization techniques

The crystalline phases of the synthesized RGO-MoS2 were identified by X-ray powder diffraction technique (PAN analytical X ray Diffractometer, Germany) with Cu kα radiation (λ = 1.5418 Å). The 2θ scan range was between 100 and 700 with an accelerating voltage of 40 kV and an emission current of 25 mA. Infrared transmission spectrum of the sample was obtained using a Fourier transform infrared spectrometer (Perkin Elmer). The purity of the prepared material were confirmed by Raman (Raman 11 System Nanophoton Corporation, Japan) instruments. The morphologies of the RGO-MoS2nanostructures were characterized by field emission scanning electron microscopy (FESEM,). Photocatalytic activity of the synthesized catalyst was studied for the photo degradation of MB using an annular slurry type visible photo reactor (Heber Scientific, Chennai, India) with a 500W tungsten filament lamp. The absorbance of the degraded solution was measured using a UV-Visible spectrophotometer and its chemical oxygen demand (COD) was determined using a COD digester (Thermo reactor HACH DRB 200).

2.3 Photocatalytic study

The photocatalytivity of the prepared RGO /MoS2wasevaluated for the degradation of methylene blue (MB) under Visible light irradiationThe preliminary experiments were conducted in 10 ml volume of the test solution with required concentrations of MB and irradiated under visible light for

6 hr. Similarly the kinetic studies were performed at a volume 100 ml MB solution with different initial dye concentrations and thephotocatalytic degradation was monitored at regular time intervals. 5 ml of the photodegraded sample was withdrawn, centrifuged and analyzed for residual dye concentration by recording at λmax 663nm (MB) using UV–visible spectrophotometer (Shimadzu-2450). The progress of photocatalytic degradation was also monitored by COD analysis using dichromate closed reflux method Hitachi U-3900 UV–vis spectrophotometer.

$$\%\ \text{degradation} = \frac{\text{Co} - \text{Ce}}{\text{Co}} \text{X}\ 100$$

Where, Co is the initial and Ceis residualdye concentration respectively.

3. Results and Discussion

3.1X-Ray diffraction (XRD) studies

The prepared RGO-MoS2was analyzed by XRD and results were shown inFig.1. It was observed that (Fig.1(a)) the diffraction peaks at 14.6°, 32.6°, 39.5°, 49.8°, and 58.0° were attributed to the (002), (100), (103), (105), and (110) crystal planes by indexing to the typical hexagonal structure of crystalline MoS2 and results are in accordance with that reported elsewhere (JCPDS card no. 37-1492)(Wang, X et al. 2014;Ji, H et al. 2015). All the diffraction peaks of the composite can be indexed to the MoS2 hexagonal phase with no impurities from incomplete sulfurization. The RGO-MoS2 composites shows the characteristic (002) reflection at 2ɵ 14.2° suggesting a well-stacked, layered structure.From the XRD patterns of RGO-MoS2nanocomposites, it can be said that the layered crystallinity is retained in the composites, envisaged by the presence of diffraction peaks due to MoS2.

3.2Fourier Transform-Infra Red (FT-IR) analysis

In order to determine the various functional groups of the prepared RGO-MoS2 nanocomposite material, FT-IR spectroscopic measurements were performed and the results are displayed in in Fig. 1(b). It can be clearly seen that GO shows the following characteristic absorption peaks: strong absorption in the range 3000–3500 cm−1 (O–H stretching vibrations), peaks at 1383 cm−1 (O–H deformation vibrations), 1724 cm−1 (carbonyl stretching vibrations), 1565 cm−1 (C–OH bending vibrations), 1228 cm−1 (C–O–C bond) and 1104 cm−1 (C–O stretching vibrations)(Weber T et al. 1996). After oxidation of GO during the solvothermal reaction, peak intensities of all oxygen-containing groups in the MoS2–RGO nanocomposite decrease remarkably as compared to those of GO. The Mo–S stretching vibrations can be assigned to the peak around 460 cm−1. Thus the peak around ~400-700 cm−1 appear, indicating that successfully deoxygenates the composite material.

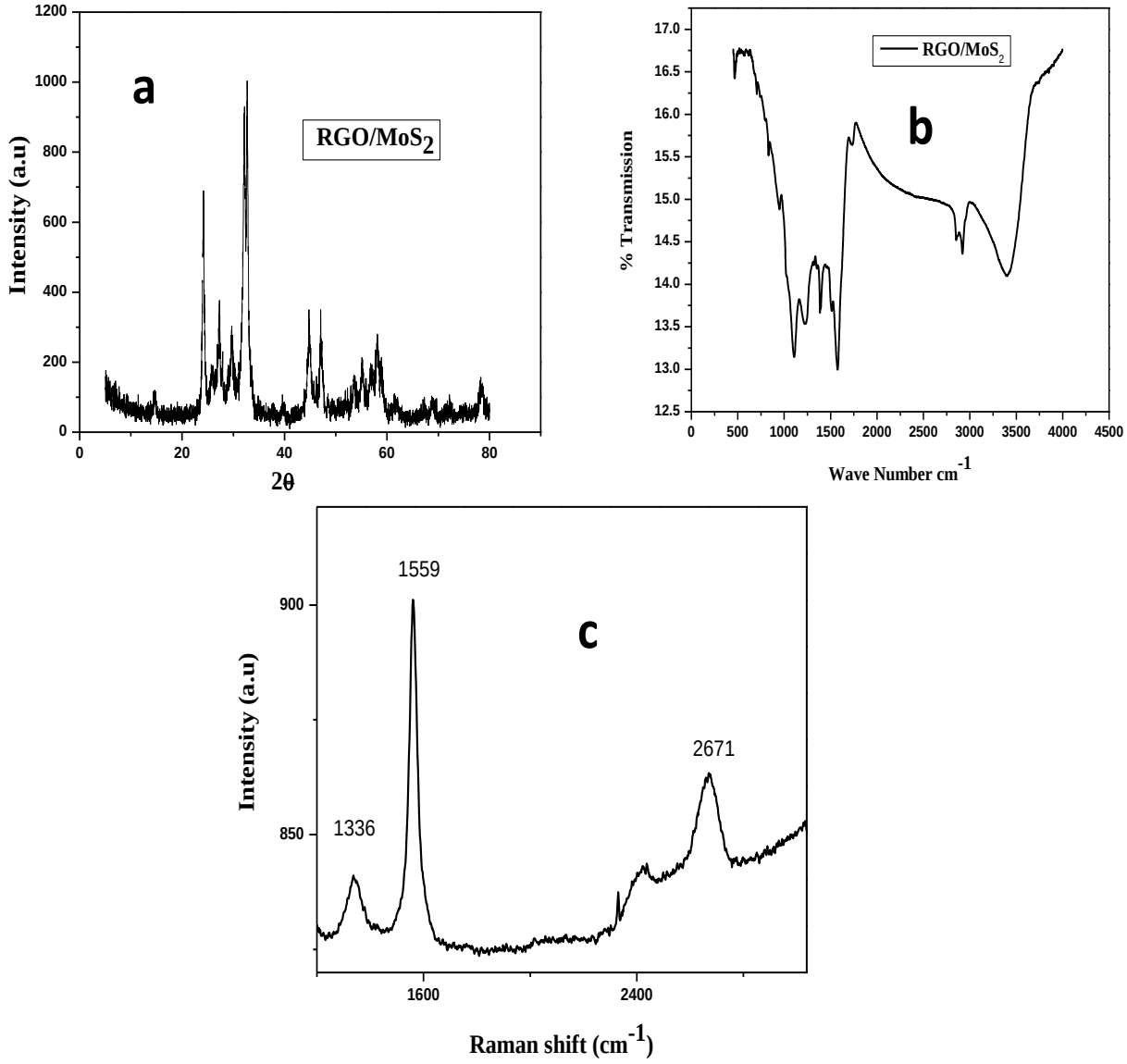

Figure1 (a): XRD analysis; (b): FT-IR spectrum; (c): Raman spectral analysis for reduced graphene oxide

3.3 Raman analysis

The Raman spectrum of the prepared RGO are shown in Fig 1(c). In the Raman spectrum D band indicated the extent of defects whereas G band shows the graphitic nature of GO, the D and G band of the Raman spectrum of RGO appeared at 1336 cm-1 and 1559 cm-1 and a slight 2D band occurs at 2671 cm-1, respectively. The D band response originating from the edges could be attributed to either the defects or to the breakdown of translational symmetry, while G band is corresponds to the first-order scattering of the E2g mode of sp2 hybridized carbon–carbon domain of graphite. Moreover, the relative strength of D band compared to G band depends strongly on the amount of disorder in the graphitic materials. Presence of D band and G band confirms the formation of graphene with lesser defects and higher crystalline nature.

3.4 Field emission scanning electron microscopic (FE-SEM) analysis

The surface morphology of the prepared RGO-MoS2 material were analyzed byfield emission scanning electron microscope (FE-SEM). FE-SEM image of the Reduced Graphene Oxide (RGO) and RGO-MoS2 is shown in Fig. 2 (a&b) respectively. RGO nanosheets are curled, corrugated, well defined and interlinked three-dimensional Graphene sheets, forming a porous network that resembles a thin layered sheet like structure. It is evident that the thin and aggregated flakes are stacked to each other with lateral sizes ranging from several hundred nanometers to several microns. The FE-SEM image of the synthesized RGO-MoS2composite displays the corrugated sheet like layers of MoS2 it shows the clear evidence for the formation of RGO-MoS2.

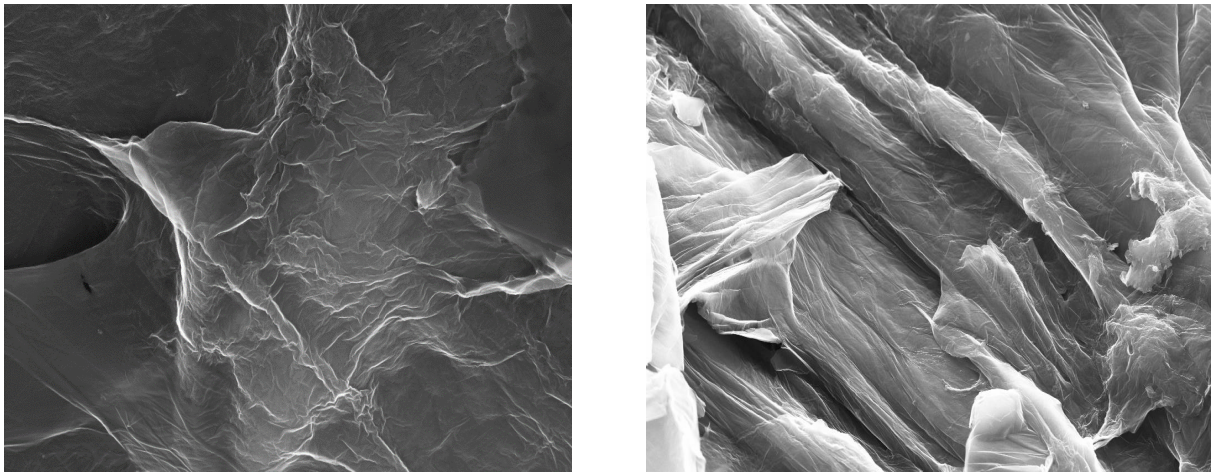

Figure2(a) FE-SEM image of RGO, (b) FE-SEM image of RGO-MoS2

3.5 Preliminary photocatalyticstudies

The photocatalytic activity of the prepared and characterized RGO-MoS2 composite was assessed by the degradation of MB dye under visible light irradiation in a slurry type photoreactor. Preliminary studies on the effect of aqueous phase pH, catalyst dosage and initial dye concentration were carried out.

3.5.1 Effect of aqueous phase pH

The pH plays an important role in the degradation of the MB dye molecules. The degradation of the dye molecules was investigated in the pH range of 2 to 12 at a fixed catalyst dosage and dye concentration (Fig. 3(a)). The initial pH of the solution was controlled by the addition of HCl for acidic and NaOH (0.1 N) for basic pH range. A catalyst dosage of 10mg/10ml was employed at each pH to treat 10ppm solution of MB dye molecule. It was observed that maximum degradation efficiency observed at neutral pH.The catalyst showed high activity at all thepH's with a maximum of 96% degradation at neutral pH. Thus all further reactions were carried out at neutral pH.

3.5.2. Effect of catalyst dosage

The loading of catalyst is significant parameter which controls the rate of photodegradation. The catalyst dosage of the RGO-MoS2 nanocomposite photocatalyst on the degradation of MB dye molecule was studied at a fixed concentration of the MB dye molecule inneutral pH under visible light irradiation. As shown in Fig.3 (b) the RGO-MoS2 nanocomposite was carried out by varying the photocatalyst load from 3 to 20 mg/10ml of 10 ppm dyeconcentration. In general, degradation efficiency was increased with increasing the amount of catalyst which maybe due to the availability of active sites and the number of electron-hole pairs generated.It was found that at minimum of 10 mg of catalyst the degradation efficiency was optimum. Thus, all further photodegradation studies were carried out with a catalyst dosage of 10mg/10 ml.

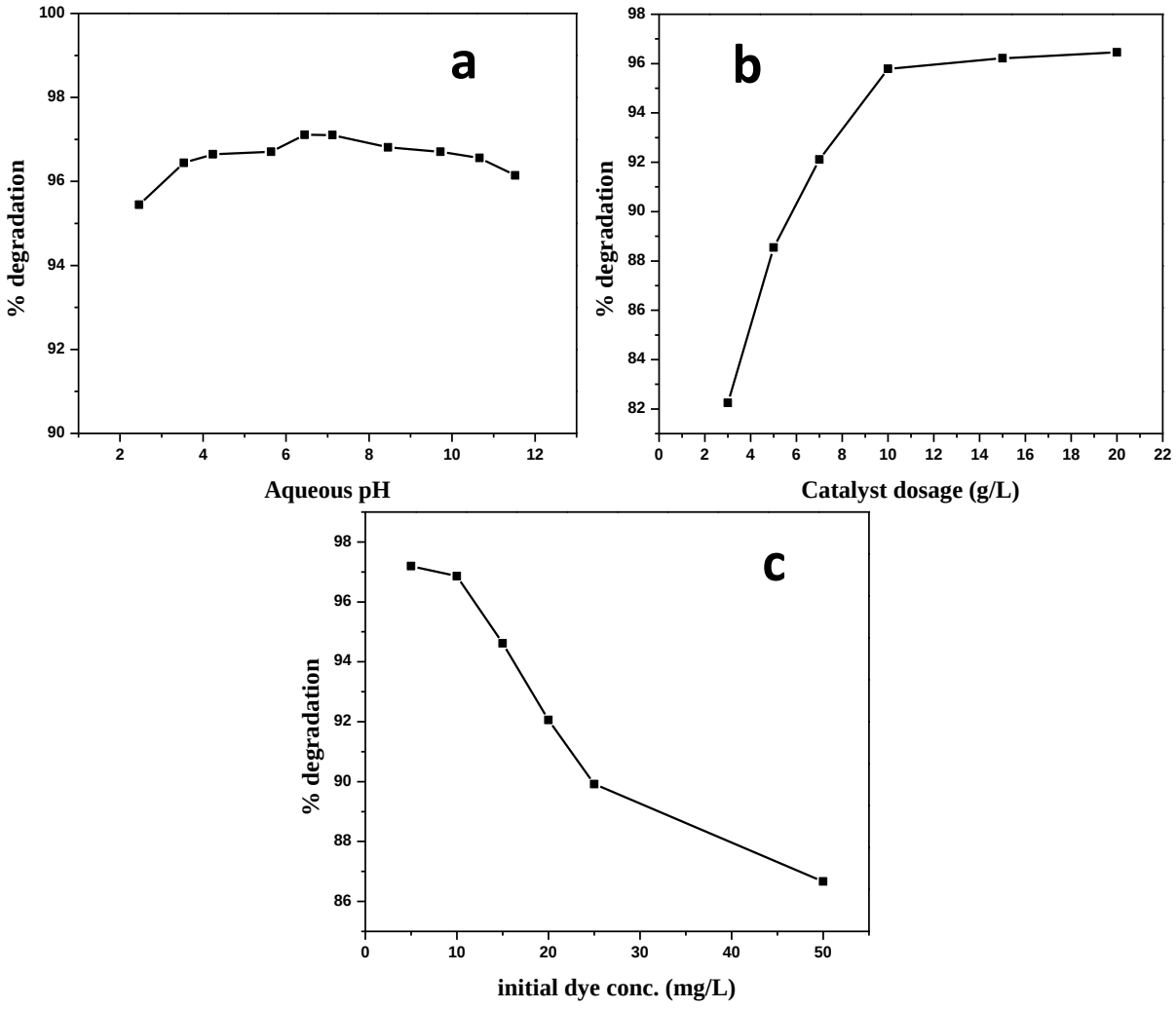

Figure 3 (a): Effect of pH, (b): Effect of catalyst dosage, and (c): Effect of initial dye concentration

3.5.3. Effect of initial dye concentration

The effect of initial dye concentration on the degradation efficiency was investigated by varying 5 to 50 ppm,the initial dye concentration plot as shown in Fig. 3 (c) optimized catalyst dosage of 10 mg/10ml with neutral aqueous phase pH. It was observed that, the degradation efficiency decreased with increasing dye concentration due to unavailability of active sites on the prepared photocatalyst.

3.6 Kinetic studies

Kinetic studies ofphotodegradation for the prepared RGO-MoS2 photocatalyst was achieved with various initial concentrations of MB dye molecule under visible light irradiation, the plot wasshowed in Fig 4 (a). The initial concentration of MB dye solution varied from 5 to 25 ppm at neutral aqueous pH and a desired amount of catalyst dosage was kept constant for the experiments. The sample was irradiated under visible light with constant stirring condition. The reactions were monitored by the withdrawal of 5 ml aliquots of sample at regular time intervals and the absorbance was measured by using UV-Visible spectrophotometer.Kinetics of the photodegradation of MB was analyzed by the pseudo first order reactions.

ln(Co/Ce)=kobst

where, C0 and Ceare the initial and final concentrations of MB dye with respect to time “t”, and kobs is the observed pseudo-first order rate constant.

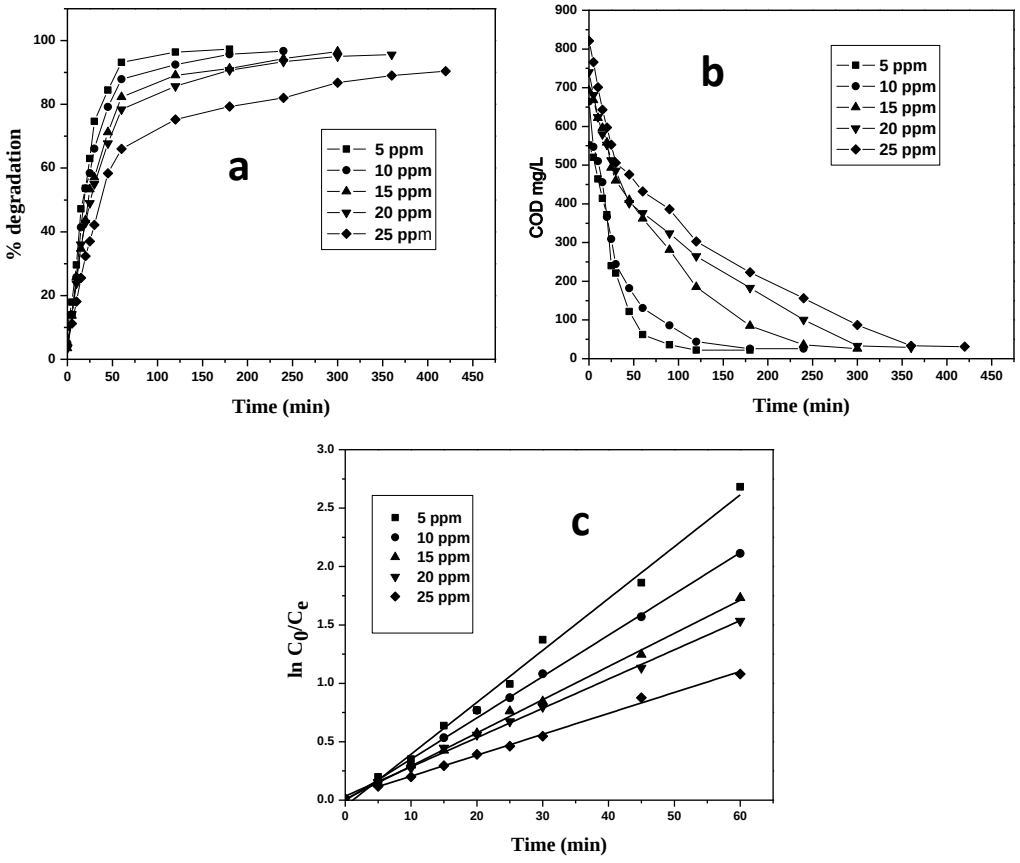

Figure 4 (a) Kinetics; (b) Reduction in COD; (c) Pseudo-first order kinetic plots

The photodegradation of MB solution by visible light irradiation employing the prepared RGO-MoS2as the photocatalyst followed a pseudo-first order kinetics (Fig.4 (c)) and therate constants were decreased from 3.55x 10-3 min-1 1.79 x 10-3 min-1 as the initial concentration of MB dye increased from 5 ppm to 25 ppm.The reduction of COD was also determined and the results are shown in Fig. 4 (b). It was observed that for 10 ppm, there is a reduction from 664 mg/L to below 30 mg/L, these results suggest that the prepared catalyst is highly active under visible light irradiations.

3.7 Effect of electrolytes

The effect of electrolytes on the photodegradation of MB dye molecules were also studied in the presence MgSO4, KCl, Na2CO3 and NaCl to evaluate catalyst efficiency along with inorganic anions such as chloride (Cl-), nitrate (NO3-), carbonate (CO32-), and sulfate (SO42-) may also present in the real wastewater, especially in practical effluents from the textile and dyestuff industries. The previously optimized pH and catalyst dosage were maintained for these reactions. 10mg/ 10 ml solutions of MB were photocatalytically degraded in the presence of varying the concentration of electrolytes from 1 to 7 wt %. The results were shown in Fig. 5 (a). It is observed that the presence of the electrolytes the photo degradation of the dye molecules does not affect the efficiency of the catalyst. Hence, the prepared RGO-MoS2 photocatalyst could be used to treat dye house effluents.

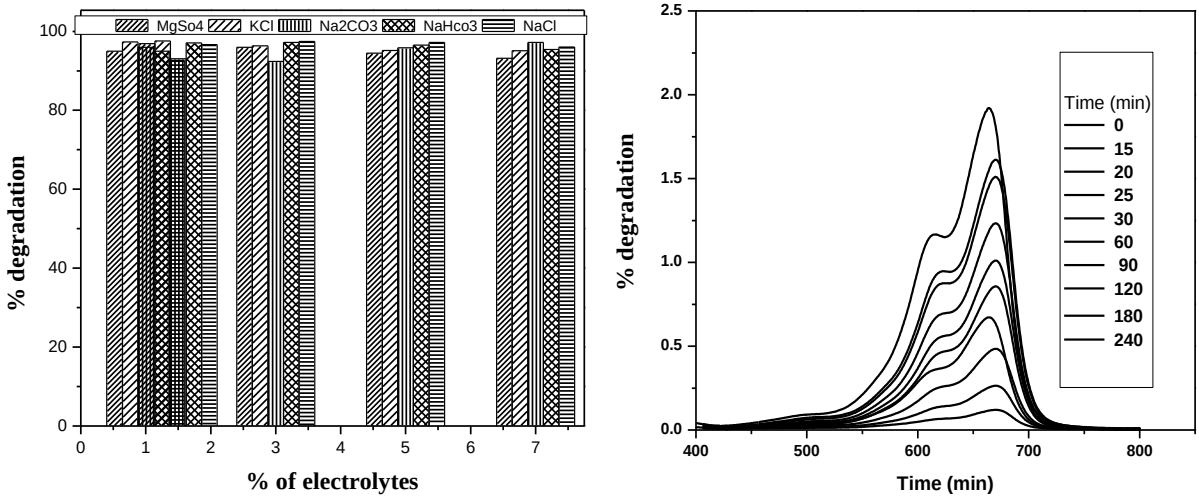

Figure 5 (a): Effect of electrolytes on dye degradation and (b) UV-Visible spectrum of MB dye

3.9 Analysis of photocatalytic degradation of MB dye molecules by UV-Visible spectroscopy

The photodegradedMBdye samples were analysed by UV-Visible spectrophotometer for the reduction of chromophore group present in the molecule. Fig.5 (b) shows the full scan UV-Visible absorption spectrum of neat and photodegraded MB dye samples. The samples withdrawn at regular time intervals were scanned from 200 – 800nm range. The absorption maximum at 663 nm which is responsible for the colour of the dye diminishes as the photodegradation reaction proceeds. The results clearly indicate the absence of any extra peaks and the absorbance maxima corresponding there is a gradual decrease in the absorption peak. It is observed that the 96% degradation of MB dye occurs at 240 min of visible light irradiation.

4. CONCLUSION

RGO-MoS_2 nanocomposite was synthesized by solvothermal method using modified Hummer's for graphene oxide. The prepared composite was characterized by various techniques such as XRD, FT-IR, FE-SEM, and Raman techniques. The crystallinity of the material was explained from the XRD analysis.The surface morphology were analyzed by the field emission scanning electron microscope (FE-SEM). Raman spectra confirms the presence of the G, 2D peak of RGO and its purity of graphene confirmed by the peak intensity ratio. The photocatalytic efficiency of the prepared RGO-MoS_2 composite was evaluated by the degradation of MB dye under visible light irradiation. Preliminary experiments showed maximum degradation at neutral pH with a catalyst dosage of 10mg/ 10ml. Reduction in COD was obtained according with percentage degradation. Kinetic study shows the photodegradation reaction to follow pseudo-first order kinetic model. The presence of electrolytes in the reaction solution did not affect the activity of the photocatalyst.

5. Acknowledgement

The authors would like to thank DST, New Delhi for providing fellowship under the INSPIRE-JRF and INDUS MAGIC 12 FYP progammefor the researchfacility.

6. Reference

1. Ao Y, Wang K, Wang P, Wang C, and HouJ Fabrication of p-type BiOCl/n-type $La_2Ti_2O_7$ facet-coupling heterostructure with enhanced photocatalytic performance ***RSC Adv.***, 2016,**6**, 48599-48609.

2. Bessekhouad Y, Robert D, Weber J.V.'Preparation of TiO2 nanoparticles by sol–gel route ,*Int. J. Photoener.,* 2003, **5**, 153 –158.

3.ChangK and ChenW.L-Cysteine-Assisted Synthesis of Layered MoS_2/Graphene Composites with Excellent Electrochemical Performances for Lithium Ion Batteries*ACS Nano*, 2011, 5, 4720–4728.

4. Chen Y, Ge H, Wei L, Li Z, Yuan R, Liu P and FuX. Reduction degree of reduced graphene oxide (RGO) dependence of photocatalytic hydrogen evolution performance over RGO/$ZnIn_2S_4$nanocomposites. *Catal. Sci. Technol.*, **2013,** 3**, 1712-1717.**

5. Chhowalla, M, Shin, H. S, Eda, G, Li. L, Loh, K. P, Zhang, H. The Chemistry of Two Dimensional Layered Transition Metal DichalcogenideNanosheets. *Nat. Chem*.2013, 5, 263–275.

6. Cho B, KimA R, ParkY, YoonJ, LeeY-J, LeeS, YooT J, KangC G, LeeB H, KoH C, KimD-H, and HahmM G.Bifunctional Sensing Characteristics of Chemical Vapor Deposition Synthesized Atomic-Layered MoS_2*ACS Appl. Mater. Interfaces*, 2015, *7* , 2952–2959.

7.Dai S, Song W, Li T and Zhuang Y, Study on azo dyes structure–biodegradability relationships, *Adv. in Environ Sci*. 1996 **4**, 1–9.

8.Han SC, Hu LF, Gao N,. Al-Ghamdi A, Fang X. Efficient self-assembly synthesis of uniform CdS spherical nanoparticles-Au nanoparticles hybrids with enhanced photoactivity. *AdvFunct Mater.* 2014, 24, 3725–3733

9.Ji, H, Liu C, Wang T,Chen, J, Mao Z, Zhao J,Hou W, Yang G. Porous hybrid composites of few-layer MoS2 nanosheets embedded in a carbon matrix with an excellent supercapacitor electrode performance. *Small*2015, **11**, 6480–6490.

10. Kowalska E, Wei Z, Karabiyik B, Herissan A, Janczarek M , Endo M, Markowska-Szczupak A, Remita H and Ohtani B. Silver-modified titania with enhanced photocatalytic and antimicrobial properties under UV and visible light irradiation *Catal. Today*. 2015, 252, 136-142.

11.Laursen A. B,.KegnaesS,.Dahl S,.Chorkendorff I, Molybdenum sulfides—efficient and viable materials for electro - and photoelectrocatalytic hydrogen evolution. *Energ. Environ. Sci.* 2012 5 5577-5591.

12.Li J, Liu X, Pan L, Qin W, Chen T and Sun Z. MoS2–reduced graphene oxide composites synthesized via a microwave-assisted method for visible-light photocatalytic degradation of methylene blue, *RSC Adv.,* 2014, 4, 9647–9651.

13.Liu P, Liu Y, Ye W, Ma J and Gao D, Flower-like N-doped MoS2for photocatalytic degradation of RhB by visible light irradiation. *Nanotechnol.* 2016, **27,** 225403.

14.Mak K. F, Lee C, Hone J, Shan J, Heinz T. F. Atomically Thin MoS2: A New Direct-Gap Semiconductor *Phys. Rev. Lett*. 2010, **105**, 136805.

15.Min S. X., Lu G. X. Sites for high efficient photocatalytic hydrogen evolution on a limited-layered MoS2 cocatalyst confined on graphen. *J. of Phy. Chem C* 2012, **116**, 25415-25424.

16.Pan L. K, Liu X. J, Sun Z and. Sun C. Q. Nanophotocatalysts *via* microwave-assisted solution-phase synthesis for efficient photocatalysis*J. Mater. Chem. A*,2013,**1** , 8299–8326**.**

17.Parzinger E, Miller B, Blaschke B, Garrido J A, Ager J. W, Holleitner A, WurstbauerU.Photocatalytic Stability of Single- and Few-Layer MoS_2 *AcsNano*. 2015,9 , 11302-11309.

18.Perez M.H, nuela G. P, Maldonado M.I, Malato O, Ibanez P.F, Oller I, Gernjak W and Malato S. Degradation of pesticides in water using solar advanced oxidation processes, *Applied Catalysis B:Environmental*2006, **64**, 272–281.

19.Splendiani, A, Sun, L, Zhang, Y, Li, T, Kim, J, Chim, C. Y, Galli, G, Wang, F. Emerging Photoluminescence in Monolayer MoS_2.*Nano Lett*.2010, 10, 1271–1275.

20.Wang, X.; Ding, J.; Yao, S.;Wu, X.; Feng, Q.;Wang, Z.; Geng, B. High supercapacitor and adsorption behavior of flower-like MoS2 nanostructures. *J. Mater. Chem. A*2014, **2**, 15958–15963.

21.Weber T,Muijsers J, Van Wolput J, Verhagen C and Niemantsverdriet J, Basic Reaction Steps in the Sulfidation of Crystalline MoO_3 to MoS_2, As Studied by X-ray Photoelectron and Infrared Emission Spectroscopy *J. Phys. Chem.*, 1996, **100**, 14144–14150

22.Xiang , J. Yu , M. Jaroniec , Synergetic effect of MoS2 and graphene as cocatalysts for enhanced photocatalytic H2 production activity of TiO2 nanoparticles. *J. Am.Chem. Soc*. 2012, 134, 6575.

23.Yu X, Shi J, Wang L, Wang W, Bian J, Feng L, Li C. A novel Au NPs-loaded MoS2/RGO composite for efficient hydrogen evolution under visible light. *j.mat let.*2016, 182 ,125-128.

24.Zhang N, Zhang Y, Pan X, Fu X, Liu S and Xu Y. J. Assembly of CdS Nanoparticles on the Two-Dimensional Graphene Scaffold as Visible-Light-Driven Photocatalyst for Selective Organic Transformation under Ambient Conditions *J. Phys. Chem. C*, 2011, 115, 23501–23511.

SFS P-40

SOLAR PHOTOCATALYTIC DEGRADATION OF LEATHER DYE HOUSE EFFLUENTS USING HEARTIN LIKE LAYERED BIOBR NANOPHOTOCATALYST

G. Tamilarasan, R. Pravina, A. Sivasamy*

Chemical Engineering Division, CSIR-CLRI, Adyar, Chennai, India-20

email: arumugamsivasamy@yahoo.co.in

The effluents from dye house and process industries are hazardous to human health, aquatic life and mainly cause enormous damages to the environment. In this study, BiOBr photocatalyst was synthesized by hydrothermal method and characterized by FT-IR, XRD, HR-SEM, UV-Vis DRS spectroscopy. The XRD analysis shows the crystalline nature of the prepared material. The FTIR analysis shows the surface functionalities present in the photocatalyst. HR-SEM analysis shows that the BiOBr photocatalyst, heartin like layered structure. Band gap energy of the prepared material was calculated from UV-vis-DRS data and it was found to be 2.92eV. The prepared photocatalyst was tested with real leather wastewater under solar light irradiation The wastewater analysis was done before and after the treatment with various parameters like Color, pH, oxidation Reduction Potential, total nitrogen, ammonia, total hardness, total dissolved solids, total solids, total suspended solids, chloride, total organic carbon, chromium and chemical oxygen demand analysis. The chemical oxygen demands for the photodegraded samples and untreated samples were 7680 and 176, where there was above 90% percentage of reduction achieved at a required time. The physico chemical parameters of photodegraded samples showed above 90 % removal with the untreated wastewater.

Keywords: Photocatalyst, effluent, treatment, layered structure.

1. Introduction

In the modern world a number of environmental problems are caused due to the industrial growth and their activities. In recent years, most of the industries discharge large quantities of wastewater into the water system without any treatment, which seriously affects the environment, aquatic eco-system and drinking water [Lahmar et al. 2012; Cavalcante et al. 2015; Kaur et al. 2010]. In many industries such as textile, pharmaceutical, leather industries etc., water is used in larger quantities for most of the processes [Gutterres et al. 2008]. Leather processing is very potential economic activity in growing countries all over the world and unrestricted release of effluents from

tannery into the natural water streams causes damages to the environment and causes many diseases to human and aquatic life [Sabumon 2016; Kongjao et al. 2008]. More than 90% dyes used in leather industry are azo dyes with chromophore units [Page et al. 2001]. In India, the present annual leather processing capacity which generates nearly 30-40 billion m^3 volume of leather wastewater contains significant concentration of organic compounds and hazardous pollutants [Mandal et al. 2010]. In general the quality of the water in effluents can be characterized by some physico-chemical characteristics namely, chemical oxygen demand (COD), total organic carbon (TOC), suspended solids (SS), biological oxygen demand (BOD). The complex characteristic of the wastewater collected from leather industry contains variety of mixed chemicals like organic, inorganic, syntans, natural tanning agents, soaking agents [Raghava Rao et al. 2003]. The tannery effluent contains high concentration of organic waste (COD/BOD) and inorganics likeNH_4-N, SO_4^{2-} /S^{2-}, Cr (III) and Chlorides [Kaul et al. 2001; Boshoff et al. 2004]. Numbers of conventional methods are available to treat the effluent generated from various industries, but they are all not facile to treat the presence of dyes and pigments. In the recent years researchers are developing the simple and eco-friendly process to overcome the drawbacks in treating the colored water. Tannery wastewater treatment includes primary treatment, chemical treatment, hydrogen sulphide removal, biological treatment and tertiary treatment [Rodrigues et al. 2008]. But the economic feasibility the above said treatment methods are require high cost for implementation and operation process [Fabbricino et al. 2013; Gutterres et al. 2008] in the field level. Advance oxidation process among other tertiary processes such as ozonation, fenton systems and electrochemical oxidation gained more importance for its high removal efficiency. In general, advance oxidation process is able to oxidize most of the organic molecules and reduce the inorganic species. Photocatalysis in AOP is sustained due to the high efficiency, low cost, sustainability, environment friendly, etc.

TiO_2 is proved as an important catalyst for the remediation of the environment. However, some of the intrinsic limitations of TiO_2 materials include its wide band gap energy, which can make its utilization as a visible driven photocatalyst is difficult [Li et al. 2015]. Among the available photocatalysts such as TiO_2, ZnO, CdS, SnO_2 andWO_3, etc [Devilliers 2006; Khan et al. 2014; Ansari et al. 2014; Anandan et al. 2012], bismuth oxybromide (BiOBr) are considered as potential materials for catalytic activities under UV and Visible light irradiations. From the literature BiOBr has become an efficient catalyst for the control of environmental pollution [Hem et al. 2003; Zhang et al. 2008; Ai et al 2009]. The unique features of the BiOBr material as superior photocatalyst are its excellent electrical, optical, luminescent and magnetic properties. Moreover BiOBr is a p-type semiconductor, which is in layered structure and is endowed with a unique polarization effect. This can be helpful for the separation of photogenerated electron-hole pair by Bi_2O_2 and bromine layer in the presence of internal static electric field [Gondal et al. 2011]. In addition to that the semiconductor material has indirect medium bandgap energy, which allows it to absorb the radiation from the visible region and also forces the excited electrons to travel a particular k-space distances and reduces the possibility

for recombination process of the valance band holes and excited electrons [Gondal et al. 2011]. In this study we successfully prepared BiOBr photocatalyst by hydrothermal technique. The prepared photocatalyst was characterized by FT-IR, UV-Vis-DRS, XRD, HR-SEM analyses. The prepared photocatalyst was tested for its photocatalytic activity on the degradation of a dye molecule in aqueous phase.

2. Materials and Methods

2.1. Preparation of the photocatalyst

The chemicals and reagents were purchased from sigma Aldrich (Bangalore, India) with analytical grade and used without further purification for the experiments. The BiOBr was prepared by hydrothermal technique which was already reported [Zheng et al. 2011]. In a typical synthesis, required quantity of bismuth nitrate was dissolved in 3 ml acetic acid (HAc), the resultant solution was added to 30ml de-ionized water containing 0.24 g of KBr under vigorous stirring. During the addition to KBr solution a yellow precipitate was formed and continuously stirred for another 20 min at room temperature. After 20 min, the suspension was transferred to a Teflon lined stainless steel autoclave and heated for 6 hrs at 120 ºC. The resulting precipitate was centrifuged and washed with water for several times to remove the ionic species present in the product and dried at 60 ºC for overnight and stored in an air tight containers for further use.

2.2. Analytical methods for characterization of the photocatalyst

The prepared material was characterized by X-ray powder diffraction (XRD) analysis employing (X' per PRO) instrument, FT-IR (Perkin Elmer 6X FT-IR) was used for the analysis of surface functional groups present in the sample. The morphology of catalyst was examined using a FEI Quanta FEG 200-High Resolution Scanning Electron Microscope (HR-SEM). UV–Vis-Diffuse reflectance spectra were recorded using shimadzu (UV-2450), Japan.

2.3. Characterization of dye house effluents

Total Organic Carbon analyzer (Model: SHIMADZU CORP 00291), was used to find out the organic content present in the wastewater and other physico chemical parameters were analyzed according to standard standard method (APHA, 1999).

2.4. Photocatalytic activity

The photocatalytic performance of the prepared catalyst was performed at the month of June 2016 under direct solar light irradiation. Dye house effluent (Lusgreen dark dye was used to dyeing of leather) collected from Tannery at CLRI after dyeing operation was completed. The % of photocatalytic degradation was calculated from the following equation.

$$\text{Degradation } (\%) = \frac{C_0 - C}{C_0} X100$$

where C_0 is the initial concentration of dye molecule and C is the concentration dye after solar light irradiation.

3. Results and Discussion

3.1. Band gap Energy

The band gap energy of the photocatalyst was analyzed by using UV-Vis-DRS analysis. The absorption spectrum of the prepared photocatalyst was plotted against wavelength and absorbance and the results shown in fig. 1 (i) indicate the prepared material has the absorption level under UV and visible light region. The band gap energy of the prepared photocatalyst was analyzed by using Kubelka–Munk function.

$$K = \frac{(100 - R)^2}{2R}$$

where R is the reflectance. A graph of $(Khv)^{1/2}$ vs photon energy (hv) was plotted, shown in fig 1(ii). The band gap energy of the photocatalyst was calculated from the above equation and it's found to be 2.92 eV. The results were well correlated with those of BiOBr photo catalysts as reported elsewhere [Kong et al. 2011].

3.2. FT-IR analysis

FT-IR techniques were used to analyze the functional groups present in the photocatalyst and results is shown in fig 1 (iii). The peak at 516 cm^{-1} is assigned to Bi-O bond symmetric stretching vibration [Li et al. 2012].

3.3. XRD analysis

The XRD pattern of the prepared photocatalyst with 001 facet (fig.1 (iv)) indicates the pure intense diffraction peaks and the good crystalline nature. The tetragonal phase of the prepared material was compared with JCPDS pattern and that were well matched. The diffraction peaks observed at 2ϑ = 10.76°, 21.80°, 25.06°, 31.61°, 32.15°, 39.24°, 46.15°, 50.62°, and 57.08° can be assigned to

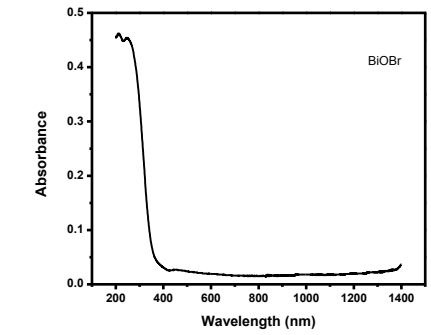

(i)

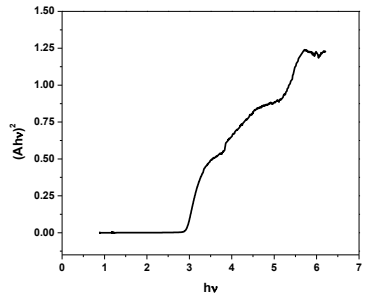

(ii)

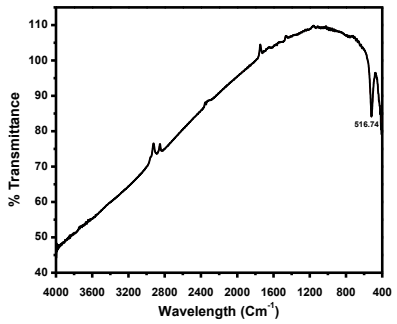

(iii)

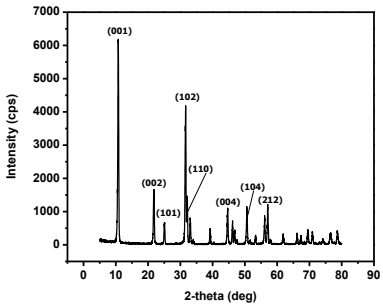

(iv)

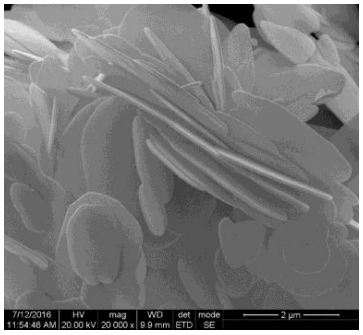

(v)

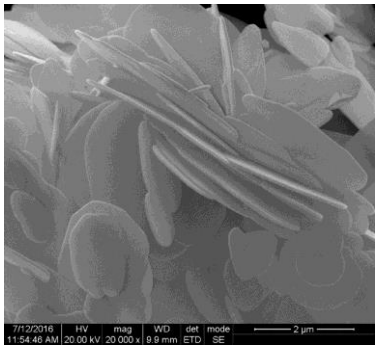

(vi)

Fig.1 (i) UV-Vis-DRS absorbance spectra, (ii) Band gap energy diagram, (iii) FTIR, (iv) XRD, (v) HR-SEM, (vi) HR-SEM

(001), (002), (101), (102), (110), (004), (104), and (212) planes of pure tetragonal BiOBr. The average crystallite size of the prepared photocatalyst (46.13 nm) was calculated using scherrer's equation 3:

$$d = 0.94\lambda/\beta\cos\theta$$

Where λ denotes the wavelength of the radiation equal to 0.154nm, $\beta$is the full width at half maximum and θ is the half diffraction angle.

3.4. Morphological analysis

The HR-SEM images of the prepared BiOBr material shown in fig.1 (v & vi). HR-SEM image shows the prepared photocatalyst in heartin like shape with smooth unique layered plates. Hence, HR-SEM results proved that the prepared catalyst are nanosized and may possess photocatalytic activity.

The photocatalytic efficiciency of the prepared BiOBr was evaluated for the degradation of commercial dye molecules under solar light irraiation in aqueous pahse. Preliminary photocatalytic studies were carried out for the optimization of initial aqeuous phase pH, catalyst dosage and initial dye concentrations.

3.5. Effect of aqueous phase pH

The effect of initial aqueous pH on the degradation of the dye molecule was studied in the range of 2 to 12. The pH solutions were adjusted by using 0.1 N HCl and NaOH. The test was made with 10 ml volume of each pH with dye concentration of 10 ppm using 10 mg of catalyst and the result shows the maximum degradation compared to adsorption study. Moreover above 90% of degradation was achieved at all the pH ranges under solar light irradiation shown in fig 2(i), while the extent of adsorption was 70%. The adsorption studies of the catalyst gives some more marginal adsorption ranges in acidic pH ranges. At neutral pH, above 95% of degradation was achieved whereas the percentage of adsorption was very low i.e., 20%. So we have fixed the neutral pH for further experiments.

3.6. Effect of catalyst dosage

The photocatalytic degradation and adsorption studies of the dye molecule were analyzed with different catalyst dosage. The result shows that by increasing the catalyst dosage, in the extent of adsorption increases through dark reaction, while the maximum degradation efficiency was obtained for very low catalyst dosage in photocatalytic process. From fig. 2 (ii) it was observed that the maximum photo-degradation of 99% achieved at 10 mg of catalyst with 10 ppm dye solution, with increasing catalyst dosage minimum variation in the degradation was found. So we fixed the optimum catalyst amount of 10 mg for further experiments at desired dye concentration.

3.7. Effect of initial dye concentration

The reaction was carried out with different initial dye concentration ranges from 5 to 50 ppm with desired amount of catalyst under solar light irradiation. The dark reaction studies were also conducted to differentiate the photodegradation process. From the fig. 2 (iii), it was found that photodegradation decreased with increasing the concentration of the dye molecule. This may be due to the lower penetration of light into the solution at increasing the concentration of the dye molecule covered by the active sites of the photocatalyst thereby making formation of the OH radicals more difficult at higher concentration and decreasing the photocatalytic activity. The dark

reaction studies show a decrease in adsorption by increasing the concentration of the dye molecule.

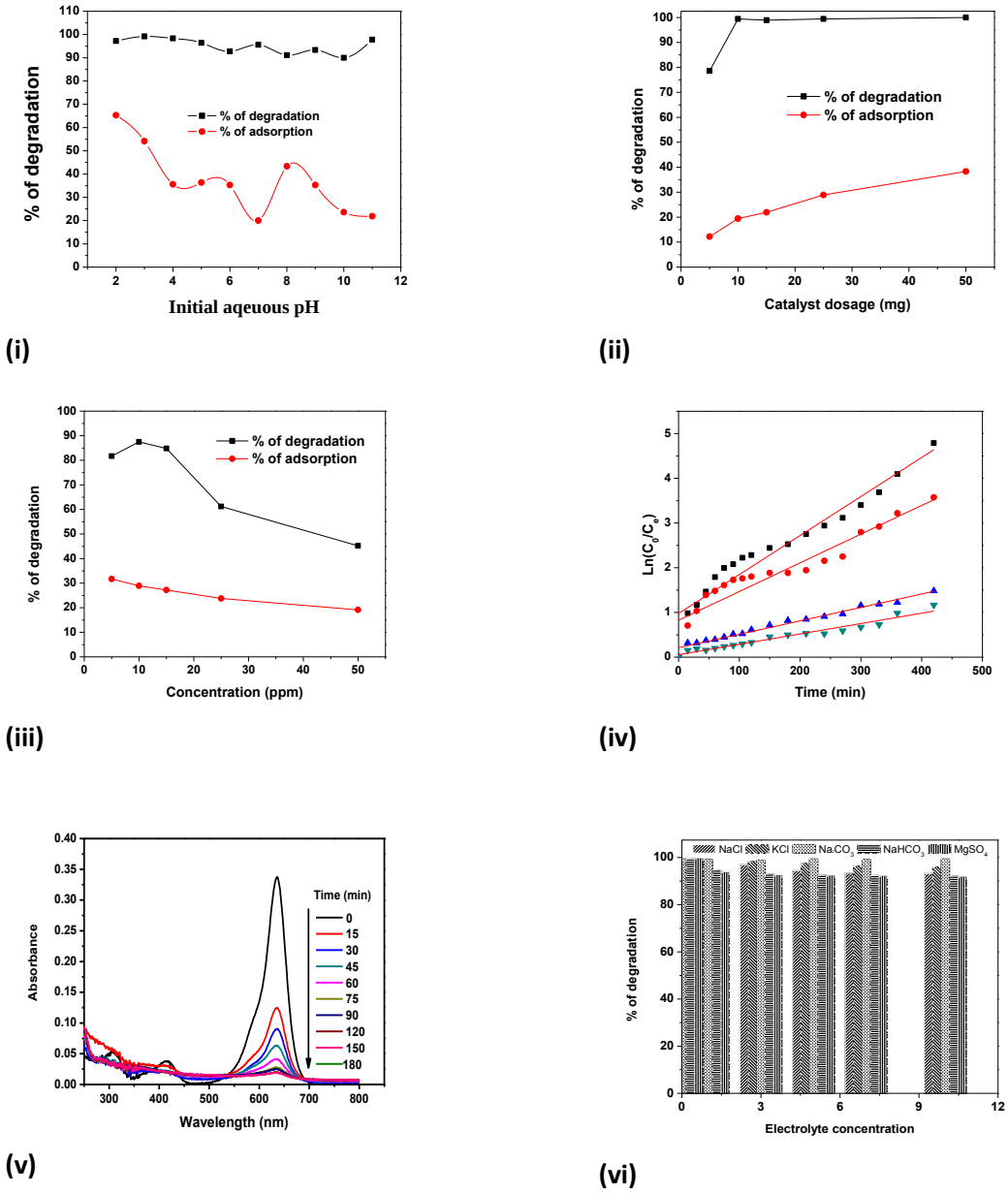

Fig.2 (i) Effect of aqueous pH, (ii) Effect of catalyst dosage, (iii) Effect of initial dye concentration, (iv) Pseudo-first-order plot, (v) Uv-Visible spectroscopy, (vi) Effect of electrolyte concentration

3.8. Kinetics of photodegradation

The kinetics of photodegradation of the dye house effluents carried out with different initial dye concentrations under solar light irradiation was shown in fig 2 (iv). The kinetic rate parameters of the degradation of the dye molecule was analyzed by using the following equation

$$\ln\left(\frac{C_t}{C_0}\right) = -k_{\text{obs}}t$$

where, k_{obs} is the pseudo-first-order rate constant; C_t is the concentration of dye molecule at time t and C_0 is the initial concentration at time t . The plot of time vs ln (C_0/Ce) gives the value of K_{obs}. From the results it is observed that the photodegradation follows pseudo-first-order rate and the rate of photodegradation was decreased with increasing the concentration of the dye molecules. The rate constants are found to be 8.73, 6.4, 3.0 and 2.3×10^{-3} for 5, 10, 25 and 50 ppm concentrations respectively.

3.9. Effect of electrolytes concentration

The effect of electrolyte concentration on the degradation of dye molecules is an important parameter, because the real dye house effluent consists different types of inorganic salts. In this study we have used the commonly used electrolytes namely NaCl, KCl, Na_2CO_3, $NaHCO_3$ and $MgSO_4$. There was a marginal decrease in the addition of electrolytes on the photodegradation of dye molecule. In case of all the electrolytes, above 90% of degradation was achieved and shown in fig 2 (vi). This proves that the catalyst will be active even in the presence of electrolytes.

3.10. Removal of COD level and UV-Vis Spectra analyses

The reduction in the chemical oxygen demand confirms the oxidation of organic dye molecule. The closed digestion method is used to find out the COD value. The percentage of photodegradation and the chemical oxygen demand was shown in fig. The complete mineralization of the sample was monitored with UV-Visible spectroscopy and COD analysis. During complete degradation, the chromophore unit will destroyed and the result shows in fig. 2 (v).

3.11. Reusability of the photocatalyst

The chemical stability of the photocatalyst was tested with different cycles for the economic perspective purposes. The recycling experiments were carried out for 10 ppm dye solution with used photocatalyst. It was observed that the above 90% of degradation achieved even the 3rd cycle of the operation without affecting the photocatalytic activity of the photocatalyst.

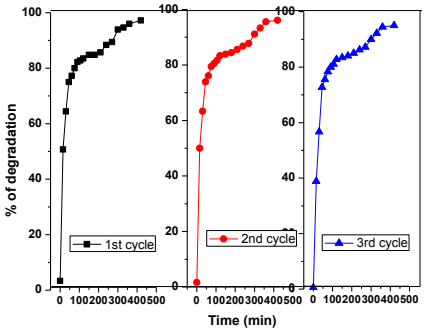

(i)

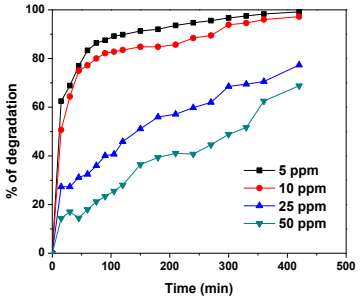

(ii)

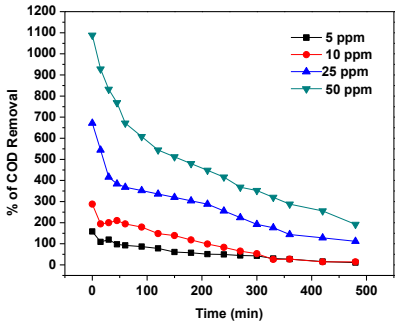

(iii)

Fig. 3 (i) Reusability of the photocatalyst, (ii) Kinetics of photodegradation, (iii) Reduction in COD level

3.12. Photodegradation of Real leather dye house effluent

The activity of the catalyst was checked with real dye house effluent. The real dye house effluent collected from tannery house in CLRI. The collected effluent was characterized by physico-chemical analysis. The wastewater analysis was carried out before and after the treatment with various parameters like Color, pH, Oxidation Reduction Potential, Total Nitrogen, Ammonia, Calcium, Total Hardness, Magnesium, Total Dissolved Solids, Total Solids, Total Suspended Solids, Chloride, Total Organic Carbon and Chemical Oxygen Demand analysis. The comparison of the real waste water and treated water varies with the parameters. The physico-chemical parameters of the dye house effluent and treated samples were listed in table 1.

Table 1. Physicochemical characteristics of the dye house effluent before and after photodegradation

S. No	Parameter	Untreated wastewater	Treated wastewater	Percentage of removal (%)
1	pH	3.47	7.85	-
2	COD	7680	176	97.70
3	TOC	2200	34.71	98.42
4	Sulphate	2151	274.89	87.22
5	Chloride	768	24.99	96.74
6	Total dissolved solids	66.186	1.204	98.18
7	Total Hardness	1320	410	68.93
8	Ammonia	65.1	0.84	98.70
9	TKN	3554	17.07	99.51
10	Chromium	-	73.51	-
11	ORP	+14	-20.0	-
12	Color	Green	Colorless	-

*All values except pH, color and percentage reduction are expressed in mg/L

The results clearly show the removal of organic and inorganic contaminants from the dye house effluent after treatment with the BiOBr photocatalyst. This indicates the high efficiency of the prepared photocatalyst in the treatment of real leather dye house effluent.

4. Conclusion

The present study revealed that the tetragonal phase of the layered BiOBr plates has been prepared by hydrothermal technique. The prepared photocatalyst was characterized through FT-IR, XRD, UV-Vis-DRS and HR-SEM analyses. The obtained layered plates have band gap energy of 2.92 eV. The BiOBr plates are highly active for photo-degradation of dye molecule under solar light irradiation under neutral pH. The photocatalyst also exhibits excellent stability of photodegradation organic molecules under visible light irradiation upto 3rd cycles without affecting the catalytic performance. The solar light active photocatalyst follows pseudo-first-order rate kinetic model for the photodegradation of organic dye molecule. The prepared BiOBr material serves as a promising photocatalyst for the treatment of real and simulated wastewater.

5. Acknowledgement

The authors would like to acknowledge the CSIR-CLRI for providing facilities under the scheme of INDUS-MAGIC CSC0123 in 12th FYP for the funding.

6. References

Ai Z H, Ho WK, Lee SC, Zhang LZ, Efficient photocatalytic removal of NO in indoor air with hierarchical bismuth oxybromide nanoplate microspheres under visible light. *Environ. Sci. Technol*. 2009, **43**, 4143–4150.

American Public Health Association, standard method for analysis of water and wasterwater, 1999.

Anandan S, Miyauchi M, Improved photocatalytic efficiency of a WO_3 system by an efficient visible-light induced hole transfer. *Chem. Commun*. 2012, **48**, 4323– 4325.

Ansari S A, Khan M M, Ansari M O, Lee J, Cho M H, Highly photoactive SnO_2 nanostructures engineered by electrochemically active biofilm, *New J. Chem*. 2014, **38**, 2462–2469.

Boshoff G, Duncan J, Rose PD, Tannery effluent as a carbon source for biological sulphate reduction. *Water Research*. 2004, **38**, 2651-2658.

Cavalcante RP, Dantas RF, Wender H, Bayarri B, González O, Giménez J, Esplugasd S, Amilcar MJ, Photocatalytic treatment of metoprolol with B-doped TiO2: effect of water matrix, toxicological evaluation and identification of intermediates. *Appl. Catal. B: Environ*. 2015, **176**, 173–182.

Devilliers D, Semiconductor photocatalysis: still an active research area despite barriers to commercialization. *Energeia,* 2006, **17**, 1–6.

Fabbricino M, Naviglio B, Tortora G, d'Antonio L, An environmental friendly cycle for Cr(III) removal and recovery from tannery wastewater. *J. Environ. Manag*. 2013, **117**, 1-6.

Gondal M A, Chang X, Ali MA, Yamani ZH, Zhou Q, Ji G, Adsorption and degradation performance of Rhodamine B over BiOBr under monochromatic 532 nm pulsed laser exposure. *Appl. Catal. A: Gen*. 2011, **397**, 192–200.

Gutterres M, Passos J, Aquim P, Severo L, Trierweiler J, Reduction of water demand and treatment cost in tanneries through reuse technique. *J. Am. Leather Chem. Assoc*. 2008, **103**, 138-143.

Gutterres, M, Passos J, Aquim P, Severo L, Trierweiler J, Reduction of water demand and treatment cost in tanneries through reuse technique. *J. Am. Leather Chem. Assoc*. 2008, **103**, 138–143.

Hem L J, Hartnik T, Roseth R, Breedveld G D, Photochemical degradation of benzotriazole, *J. Environ. Sci. Health. Part A.* 2003, **38**, 471–481.

Kaul S N, Tapas N, Vyas R D, Szpyrkowicz L, The Scope for Decreasing Pollution Load in Leather Processing, UNIDO (2000) Pollutants in tannery effluents, Regional Programme forPollution Control in the Tanning Industryin South-East Asia 2001.

Kaul S N, Tapas N, Vyas R D, Szpyrkowicz L, Wastemanagement in tanneries: Experience and outlook. *J. Indian Assoc. Environ. Manag*. 2001, **28**, 56-76.

Kaur A, Vats S, Rekhi S, Bhardwaj A, Goel J, Goel J, Tanwar RS, Gaur K, Physico-chemical analysis of the industrial effluents and their impact on the soil microflora. *Procedia Environ. Sci*. 2010, **2**, 595–599.

Khan M M, Ansari S A, Pradhan D, Ansari M O, Han DH, Lee J, Cho M H, Band gap engineered TiO_2 nanoparticles for visible light induced photoelectrochemical and photocatalytic studies. *J. Mater. Chem. A*. 2014, **2**, 637–644.

Kong L, Jiang Z, Xiao T, Lu L, Jones M O, Edwards P P, Exceptional visible-light-driven photocatalytic activity over BiOBr–ZnFe2O4heterojunctions. *Chem. Commun*. 2011, **47**, 5512–5514.

Kongjao S, Damronglerd S, Hunsom M, Simultaneous removal of organic and inorganic pollutants in tannery wastewater using electro coagulation technique. *Korean J. Chem. Engg*. 2008, **25**, 703-709.

Lahmar, H, Kebir, M, Nasrallah N, Trari M, Photocatalytic reduction of Cr(VI) on the new hetero-system $CuCr_2O_4$/ZnO. *J. Mol. Catal. A Chem.* 2012, **353**, 74–79.

Li D K, Pei L Z, Yang Y, Pei Y Q, Xie Y K, Zhang Q F, Synthesis and characterizations of BiOCl sheets. *e-J. Surf. Sci. Nanotechnol*. 2012, **10**, 161-164.

Li H, liu B, Yin S, Sato T, Wang Y, Visible light-driven photocatalytic activity of oleic acid-coated Tio_2 nanoparticles synthesized from absolute ethanol Solution. *Nanoscale Res. Lett*. 2015, **10**, 415

Mandal T, Dasgupta D, Mandal S, Datta S, Treatment of leather industry wastewater by aerobic biological and Fenton oxidation process. *J. Hazard. Mater*. 2010, **180**, 204–11.

Page C, What are leather dyes today? The relationship between the dye structure and its performance properties. In: XXVI IULTCS Congress Proceedings, Cape Town, 2001.

Rao J R, Chandrababu N K, Muralidharan C, Balachandran Unni Nair, Rao P G, Ramasami T, Recouping the wastewater: a way forward for cleaner leather processing. *J. Clean. Prod.* 2003, **11**, 591-599.

Rodrigues MAS, Amado FDR, Xavier JLN, Streit KF, Bernardes AM, Ferreira JZ, Application of photoelectrochemical–electrodialysis treatment for the recovery and reuse of water from tannery effluents. *J. Clean. Prod*. 2008, **16**, 605-611.

Sabumon P C, Perspectives on biological treatment of tannery effluent. *Adv Recycling Waste Manag.* 2016, **1:104**, 1-10.

Vyrides I, Stuckey D C, A modified method for the determination of chemical oxygen demand (COD) for samples with high salinity and low organics. *Bioresour Technol*.2009, **100**, 979-982.

Zhang X, Ai Z H, Jia F L, Generalized one-pot synthesis, characterization, and photocatalytic activity of hierarchical BiOX (X = Cl, Br, I) nanoplate microspheres. *J. Phys. Chem. C*. 2008, **112**, 747–753.

Zheng J, Yang F, Yang G D, Kong LA, Jones M O, Xiao T C, Edward P P, The hydrothermal synthesis of BiOBr flakes for visible-light-responsive photocatalytic degradation of methyl orange, *J. Photochem. Photobiol. A: Chem*. 2010, **212**, 8-13.

FLS P-20

USE OF TERNARY SOLVENT (WATER - ETHANOL – ETHYL ACETATE) MEDIUM FOR LEATHER PROCESSING: A POSSIBLE PARADIGM CHANGE

Solomon Fessehaye*, Bhargavi Narayana Reddy Gari, , Rathinam Aravindhan, Kalarical Janardhanan Sreeram, Jonnalagadda Raghava Rao1 and Balachandran Unni Nair

Chemical laboratory, CSIR-Central Leather Research Institute, Adyar, Chennai, India

Leather Technology Directorate, Leather Industry Development Institute 24692 code 1000, Addis Ababa Ethiopia, sfessehaye@gmail.com

An attempt to replace water (7-10 m3/ton) in leather processing with a ternary mixture of solvents that would have a lower boiling point than water (for easy recovery through evaporation) and also bring about maximum solubility of conventional dyes, syntans and fatliquors is reported. The ternary mixture (Water– ethanol – ethyl acetate) reported in this study provided for good solubility/dispersion of leather chemicals. Average particle size of the syntan/dye in solvent / water remaining the same, particle size distribution of dyes and syntans was advantageous in the solvent medium, leading to better diffusion. Amongst various trials, neutralization of the leathers after tanning in solvent medium followed by use of neutralization syntans was found to be more advantageous to obtain leather properties comparable to conventional controls. The adsorption studies of dye used in the present study followed Freundlich model in both solvent and water medium indicates multilayer adsorption. Physical properties of the leathers were similar to that of control, indicating clearly that the solvent had no adversary effect on collagen and also provided for good diffusion and fixation of chemicals. The method thus reported in this study could provide for a minimum change approach to leather processing with ample contribution to water saving.

Keyword: Ternary solvent, Freundlich model, diffusion

Introduction

During the last two decades, the leather industry is emerging out of its traditional practices to one adopting best clean practices. A review of the literature would suggest that there is a basket of technologies for each processing step, adoption of which could be more environmentally benign and economically sustainable than the dependence on end-of-pipe treatment system alone. A look into the historical setting of leather clusters would reveal that their locations were predominantly in water rich zones. Many of these zones had no inherent raw material but had to be transported in. Today, some of these zones have gone barren or are highly polluted, leading to either close down or

shifting of the industry from such locations.[1,2]

The growth of material science has enabled human kind to understand the benefits of using leather in some of our routines. Typical example is the case of footwear. It is slowly emerging that this industry may not be in a position to meet all the requirements of its customers, unless some out-of -box thinking and methodologies are developed to ensure independence from water in processing. Values such as 30-35 L/kg of hide/skin processed, effluent discharge of 50,000 m^3 /day from Indian leather sector alone etc.[3,4] need to be those of the past to ensure sustainable leather production.[5]

During the last two years, an approach towards use of solvents for diffusion of leather chemicals into the skin matrix has been reported. This includes use of eutectic solvents, extraction of vegetable tanning materials and subsequent leather tanning in solvent media, ionic liquids as the fibre opening agents etc.[6-8] While most of these research works have pertained to the emission intensive processes in pre-tanning and tanning stage, adoption of such methodologies in post-tanning is considered challenging. This is predominantly because of a large number of specialized auxiliaries – trademark products of industrial houses, which are in use to obtain customer desired properties. The common feature of these products is that they have been subjected to reactions such as sulfonation that would make them water soluble. In spite of this challenge, water consumption in post-tanning cannot be ignored as the contributes to about 23% of the water consumed in leather processing.[9]

Based on this background, in the initial survey leading to this publication, a set of solvents selected from the GSK Solvent Selection Guide were evaluated for their ability to dissolve or disperse a significant number of commercial auxiliaries drawn from various classes of compounds.[10] Such of those selected solvents were then tested for any adverse effect on collagen. Based on these initial studies, two solvents, viz., ethanol (EtOH) and ethyl acetate (EtOAc) were shortlisted based on the following considerations: a) good biodegradability and recyclability of these solvents and current use to replace water in processes such as dry cleaning, textiles and paints[11] and b) have no adverse effect on collagen.[12] Solvents chosen in this study are not marked in the red category with respect to VOC.[13] One of the major considerations, during our initial studies was the manner in which the identified solvents would interact with free water present in hides/skins or leather.

A further relook into these considerations led us to investigate various binary and ternary solvent mixtures involving water for dispersing/solubilizing commercial auxiliaries. This work reports in detail the results observed with one of the successful combinations, involving a set of auxiliaries employed for the manufacture of leather.

Experimental

Materials and Methods

A ternary mixture of water, ethyl acetate and ethanol (1:1:2) was employed in this study. The study reported here was carried out using analytical grade solvents to avoid interference from impurities. Auxiliaries selected for investigation were of commercial grade and those which were easily dispersed or had good solubility in the solvent mixture investigated were chosen for the leather trials. Wet blue goat skins were employed for the trials.

Dynamic Light Scattering Measurements

The changes in the particle size distribution of the syntans and dyes on dispersion into the solvent mixture was evaluated by dynamic light scattering technique using a Zetasizer Nano ZS (M/s. Malvern UK). The measurements were carried out at 25^{o}C using a 4 mW He-Ne laser operating at 633 nm. Data was collected at a scattering angle of 173^{o}.

Post Tanning Experiments

The experiments were carried out in tight fitting stainless steel drums without any acrylic transparent windows for observation. The speed of the drum was maintained at 15 RPM throughout the studies. Two wet blue goat shins were used for the study. The experiments were carried out employing the butt portion of the wet blue goat skins. Left sides were used for experiments trial, where ternary mixture was used for post tanning and the right sides were used for control trial, where water was used as medium. The post tanning process recipe is presented in Table I.

In order to have an understanding of the effect of neutralization on the processed leathers, neutralization was carried out in water as well as solvent and employing mild alkali/neutralization syntans. Scheme of work carried out is presented in Figure. 1 for better understanding. In all 3 trials (marked as **1** – **3**) was carried out with corresponding water based control (marked as **1a** – **3a**). Conventional mechanical operations were carried out on the crust leathers.

Characterization of the Leathers

Employing IUP methods for sampling and analysis, the strength parameters were determined for both control and experimental leathers.[14-16] Color fastness properties to and fro rubbing of the dyed crust leathers was tested according to ISO 11640:1993(E) test method. Dry rub fastness was measured using Giuliani Rub Fastness tester. Quantification of color was carried out by reflectance measurements using Techkon SpectroDrive (TKSDEB) in order to know intensity of dye on grain side of the leather surface. The CIELAB 1976 color coordinates were determined using in built software.

Scanning Electron Microscopic (SEM) Analysis

A sample from experimental (**1**) and control crust leathers (**1a**) were cut from official sampling position. All specimens were then coated with Gold using Edwards E306m sputter coater. A Leica Cambridge Stereoscan 440 Scanning electron microscope was used for the analysis. The micrographs for the grain surface and cross section were obtained by operating the SEM at an accelerating voltage of 20kVat different magnification levels.

Visual Assessment

The experimental and control leathers were visually evaluated for various properties by experts drawn from the industry. The ratings have been provided in a scale of 1-10, with 10 being the best.

Adsorption Equilibrium and Diffusion Coefficient Studies of the Dye in the Ternary Solvent Medium

Adsorption studies of the dye on the leather in the ternary solvent medium were carried out by contacting the leather with various initial concentrations of the dye solution. The samples for the experiments were obtained from the official sampling position (IUP 2) from a wet blue goat skin. In a shaker bottle, 6 g (dry weight) of the wet blue leather was weighed and 30 mL of dye solution containing various initial dye concentrations ranging from 167 to 1000 mg/L was added. The bottles were placed on a mechanical shaker for 2h at room temperature. The aliquots were drawn at every 15 min interval for 2h. The amount of the dye present in the samples was quantified using UV-Visible spectrophotometer (M/s. Shimadzu UV-1800) at 540nm. The absorbance was then converted into dye concentration value using a calibration graph. The amount of dye uptake was calculated by using the following formula

Where C_0 and C_e are the initial and equilibrium concentration of dye solution (mg/L) respectively, q_e is the equilibrium dye concentration on the leather (mg/g), V *is* the volume of the dye solution (L) and W is the weight of the leather (g).

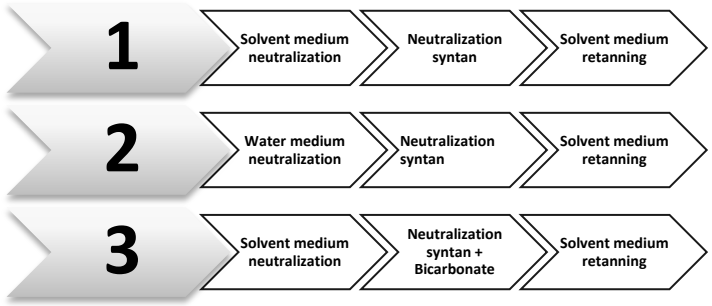

Figure 1. Scheme of trials employed to test the efficiency of ternary solvent mixture (Water-Ethanol-

Ethyl acetate) to replace water in post-tanning processes.

Results and Discussion

The selected solvents, water, ethyl acetate and ethanol were employed in the ratio of 1:1:2 and found to be able to provide maximum solubility of leather auxiliaries selected for this study. The properties of this ternary system is well documented in the literature.17-18 Interaction of these solvents with commercial leather auxiliaries, their performance on the leather was investigated.

Compatibility of Leather Auxiliaries with Ternary Solvent Mixture

The conventional leather auxiliaries are synthesized in such way to be completely soluble in water, so as to achieve better penetration. Accordingly, as expected, these auxiliaries were found to be insoluble in neat solvents (EtOAc and EtOH). When the solvents were in combination with water, i.e. ternary system, good solubility of the auxiliaries was observed. This has been attributed to the appropriate matching of dielectric constant of solvent mixture to the leather auxiliaries and/or reorientation of hydrogen bonding

Table I

Post tanning recipe (Product – Shoe Upper) employed to evaluate the efficacy of ternary solvent medium in leather processing.

Raw material: Wet blue goat skins. Ternary solvent: Water:EtOAc:EtOH (1:1:2). All percentages calculated on shaved weight of wet blue goat skins.

Process	Chemicals	%	Time (minutes)	Remarks
Washing	Water	100	10	Drained
Neutralization	Ternary Solvent (Trial 1, 3) or Water (Trial 2) or water (all controls)	100		pH adjusted to 5.2 – 5.4 and bath drained and washed with solvent
	Neutralization syntan (Trial 1 and 2) or Neutralization syntan: sodium bicarbonate 1:1 for Trial 3	0.7	20	
	Ternary solvent (for all trials) or water (for	150		

	control)			
	Acrylic syntan	2	20	
	Dye (anionic metal complex red)	2	20	
	Lecithin based fatliquor	3	30	Dispersed the products in ternary solvents (1:10 ratio) for addition
	Phenol-formaldehyde condensate based syntan	5	40	
Post-tanning	Melamine-formaldehyde condensate based syntan	5		
	Vegetable oil based fatliquor	3	60	
	Semi-synthetic fatliquor	3		
	Synthetic fatliquor	3		
	Formic acid	3	30x10+ 60	Addition in equal feeds of three, 10 min interval followed by 60 min
	Piled over night, toggle dry, staked			

between the auxiliary and the solvents in the ternary mixture. Water acts as co-solvent to make auxiliaries soluble in ternary mixture. Recently the possibility of solubilisation of oils in binary mixtures of solvents has been attributed to matching of dielectric constants of binary mixtures with that of water.[7]

Particle Size Distribution

Penetration of the dyes and syntans into the skin matrix depends on the particle size of the dispersion in solution. Lesser the particle size of syntans and dyes in solution, better will be the penetration down to the hierarchy.[19] It can be seen from Figure. 2 that a mono dispersed system is observed for the dye dispersed in solvent mixture, indicating a homogeneous dispersion and thus a uniform hue can be expected. In tune with the size distribution observed, visual assessment by experts indicated good penetration, color uniformity, depth of shade and dry rub fastness for leathers post-tanned using solvent as the dispersion medium.

The average particle size of the syntan in water as well as in solvent mixture was found to be around 260nm (Figure 3). The pores between fibre bundles in collagen is known to be 50-500 nm so the syntan can gently penetrate into the leather in solvent medium same as in conventional water processing.

Characteristic Features of the Leather

The Strength properties of the leather are presented in Table II. The physical strength values are a measure of efficiency of tanning and fatliquoring. The leathers processed both in solvent and in water medium are satisfying standard values. This indicates that the process developed using the ternary solvent medium does not deteriorating the quality of the leathers. A characteristic observation made in this study is that the neutralization in the solvent medium followed by retanning and fatliquoring in the solvent medium resulted (Trial **1**) in leathers whose strength properties matched well with control rather than those where neutralization was carried out in water (Trial **2**). This is possibly because in Trial **1**, the free water in leather was completely replaced with the solvent medium during neutralization process. Our earlier studies (data not shown) indicated that the solubility of alkalis such as sodium bicarbonate was minimal in the binary system of EtOH- EtOAc and hence the ability of the same to raise the pH during neutralization was poor. However, in Trial 3, the presence of water in the ternary system enabled the dissolution of the alkali and thus a combination of this system could uniformly raise the pH to desired values. A complete and thorough neutralization resulted in leathers with properties similar to that of control (Trial **3**).

Proper distribution of the dye through matrix, followed by its fixation is critical to achieve the desired levels of rub fastness. From Table II, it could be seen that the experimental leathers had excellent dry rub fastness, indicating that the fixation of the retanning and fatliquoring agents were good even in the presence of the ternary solvent medium.

Color Coordinates

$$\Delta E = \sqrt{(L_1 - L_2)^2 + (a_1 - a_2)^2 + (b_1 - b_2)^2}$$

Color difference calculated as

Where L_1, a_1 and b_1 are the color coordinates of trial and L_2, a_2 and b_2 are the color coordinates of control respectively, is presented in Table II. It can be seen that other than in the case of Trial **1**, the ΔE values are below 5, indicating that the color difference between control and trial leathers will not be perceptible to an untrained eye. A closer look at the color coordinates for **1** and **1a** (54.02, 20.29, 20.73 and 45.09, 21.01, 19.13, respectively for L, a* and b* of 1 and 1a) indicates that the perceptible change was only in the L (lightness value). The leathers from Trial **1** were lighter than the control leathers, where water has been used as dispersing medium. The color coordinates have been obtained from the grain side of the leather. It is likely that for a given concentration of dye, the predominant part of dye penetrated well into the matrix for **1**. A likely offshoot to this observation could be that the solvent based dispersion medium could be advantageous for making suede leathers. As a whole, color measurement values depict that no major difference exists between solvent processed and water control leathers.

Table II

Physical properties and color difference of the leathers (trial vis-à-vis respective controls).

Product	**Tensile strength (N/mm^2)**	**Percentage elongation at Break (%)**	**Tear strength (N/mm)**	**Dry rub fastness (scale of 0 – 5)**	**ΔE**
1	22.4	84.0	47.6	4	9.1
1a	24.9	83.9	51.0	4	
2	23.1	66.7	49.7	4/5	3.8
2a	29.0	97.1	58.1	4/5	
3	18.0	47.7	33.1	4	2.9
3a	18.2	51.4	34.6	4	

Visual Assessment

Three tanners have evaluated the crust leather from both control and experimental processes. Their evaluation in a scale of 0-10, with 10 being the highest is presented in Table III. Comparison between 1 and 1a reveals that the fullness for control trial is lesser by 1 unit. Deeper look at the Figure 3 would indicate that the maximum observed particle size when syntan in dispersed in solvent is 400 nm, while the same is slightly more aggregated in water (600 nm). Further the number of particles in the range of 1 – 10 nm, is significant in the case of syntan dispersed in solvent, indicating a better filling of the smaller pores leading to an increased grain smoothness (I unit more than control). Shade for experimental Trial 1 was lesser by 1 unit and this commensurate with observation on color coordinates. A further look into Figure 2, indicates that the particle size distribution of the dye employed in this study (indicated by black line in the figure) in solvent being homogenous and mono dispersed, a deeper penetration is expected compared to the same in water (indicated by red line in figure).

When neutralization was carried out in water medium, penetration was probably hampered due to aggregation of syntans at the interface of leather and solvent. This leads to a 2 unit decrease in fullness for Trial **2**. Aggregated particles create inhomogeneity leading to decreased rating when compared to control.

Except for dye penetration, softness and shade all parameters were similar between **3** and **3a.** This can be attributed to presence of neutral salts in the leather, arising from a bicarbonate neutralization, which was not completely removed by solvent washing after neutralization. An inter comparison between the three trials clearly indicates that a solvent neutralization followed by neutralization using syntans was the best way forward.

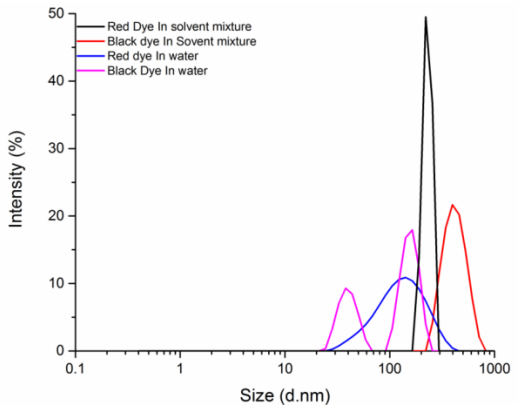

Figure 2. A comparison of the particle size distribution of dye dispersions in syntan water and ternary solvent mixture.

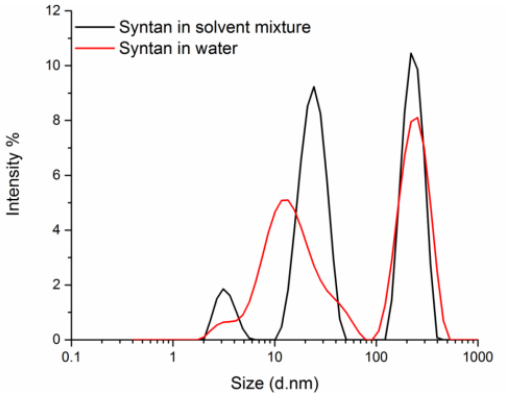

Figure 3. A comparison of the particle size distribution of a commercial aromatic syntan in water and ternary solvent mixture

Table III

Visual assessment rating (scale of 1 – 10) provided for leathers prepared using conventional

(water as diffusion medium) vis-à-vis experimental (solvent as diffusion medium).

Product	Full ness	Softness	Grain tightness	Grain smoothness	Dye penetration	Dye uniformity	Shade
1	7	8	8	8	8	8	7
1a	8	8	8	7	8	8	8
2	5	7	7	6	7	7	8
2a	7	8	8	9	9	9	8
3	7	6	7	7	5	7	6
3a	7	7	7	7	7	7	7

Morphological Evaluation of Leather

Morphological study of **1** and **1a** was carried out using scanning electron micrograph. The grain surface and cross-section of the control and experimental leathers at magnification of 30X and 500X respectively, are depicted in Fiure 4. It has been observed that the grain surface is clean without any foreign particles for both water and solvent processed leathers. This could be due to the optimal solubilization and dispersion of post tanning auxiliaries especially syntans and fatliquors. Pores are well opened and showed uniformity in grain pattern for both control and experimental leather. Cross section shows compact fibres, indicating solvents were not involved in damage of fibres of collagen.

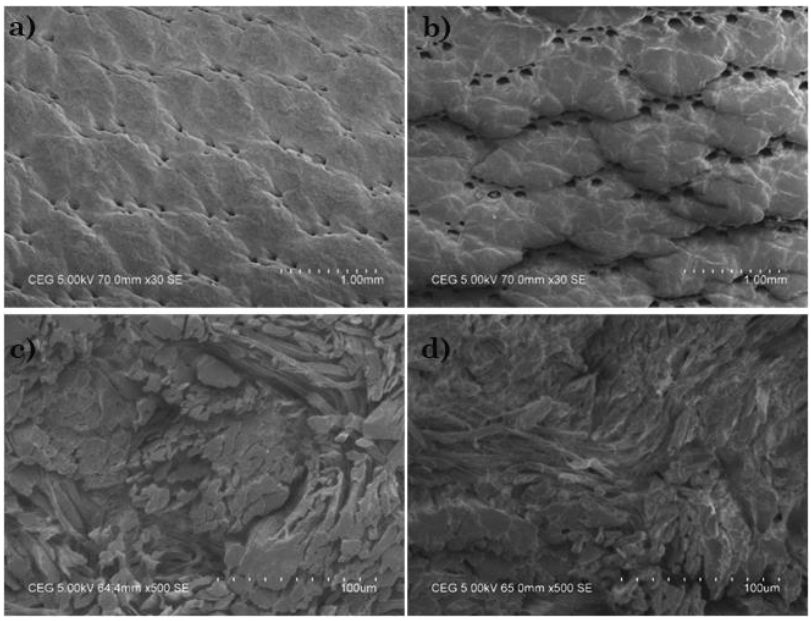

Figure 4. Scanning electron microscopic images a. grain **1**, b. grain **1a,** c. cross section of **1**, d. cross section of **1a**

Adsorption Isotherms

Adsorption studies have been carried out in order to find out the maximum uptake capacity of the wet blue leather for the dye used in the study. The studies have been carried out both in water and in solvent medium in order to establish the effect of solvent on the dye uptake behaviour of the wet blue leather. Adsorption of dye to the surface of the leather is limited by the number of active sites ($-NH_3^+$) available. The equilibrium dye uptake capacity of the wet blue leather in both water and solvent medium at various

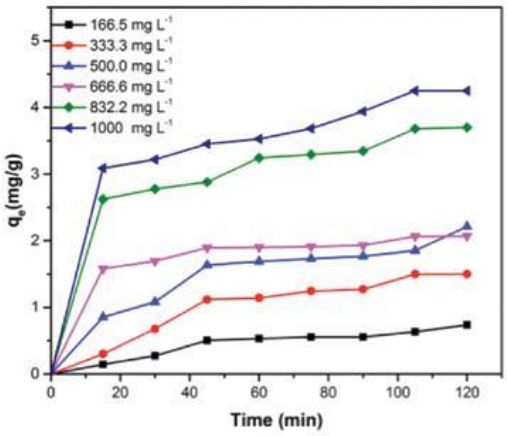

Figure 5. Trend in equilibrium dye uptake as against time in the solvent medium.

concentration of the dye are shown in Figure 5 and 6, respectively, It could be observed that the equilibrium dye uptake capacity of the wet blue (mg/g of leather) increased with increase in initial dye concentration, in both the medium. However, it is inferred from the data, trend in dye removal and

Table IV

Freundlich and Langmuir constants for water and solvent medium.

	Freundlich			Langmuir		
	K	n	R^2	q_0	b	R^2
Water	0.325	1.677	0.889	9.398	0.012	0.6141
Solvent	0.0121	1.1287	0.8939	6.25	0.0015	0.737

equilibrium dye uptake has been similar in both solvent and water. Hence, it could be inferred that the solvent does not affect the dye uptake behaviour of the wet blue leather.

The experimental data obtained has been analysed by two models namely Langmuir and Freundlich isotherm models in order to know the adsorption phenomena on the leather surface in the water and solvent medium. Langmuir isotherm assumes that the adsorbent surface is homogenous and the adsorbate forms a monolayer on the adsorbent surface. The Langmuir constants q_0 and b has been obtained from the

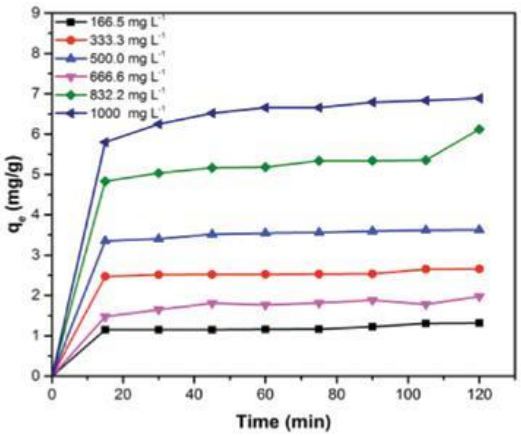

Figure 6. Trend in equilibrium dye uptake (experimental) as against time in the water medium.

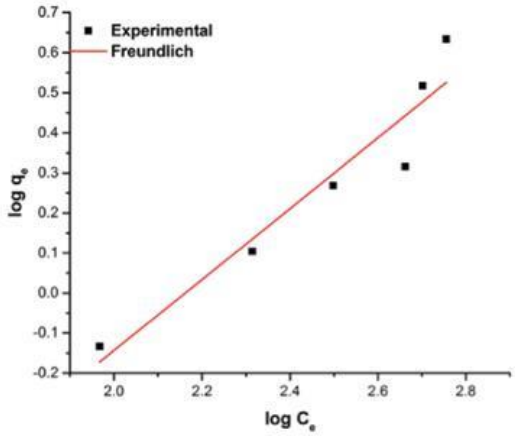

Figure 7. Comparison of solvent medium data by using Freundlich isotherms model fit

linear plot of C_e/ q_e versus C_e, which has a slope of $1/q_0$ and an intercept of $1/q_0b$. The linear form of Langmuir expression is given in the following equation.

$$\frac{C_e}{q_e} = \frac{1}{q_0 b} + \frac{C_e}{q_0}$$

The adsorption of dye by the wet blue leather has also been analysed by Freundlich isotherm model. This model express that the surface is heterogeneous and consists different adsorption sites. The Freundlich constants *n* and *k* were obtained from the following linear regression equation.

$$\log q_e = \log K + \frac{1}{n} \log C_e$$

Where n and K are Freundlich constants and can be obtained by liner plot of log *q*e versus log *C*e contains log K intercept and 1/n as the slope.

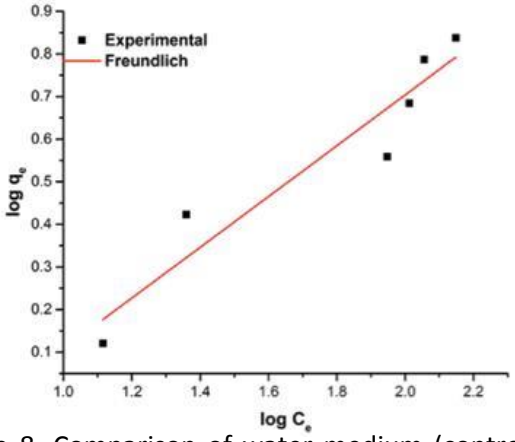

Figure 8. Comparison of water medium (control) data by using Freundlich isotherms model fit.

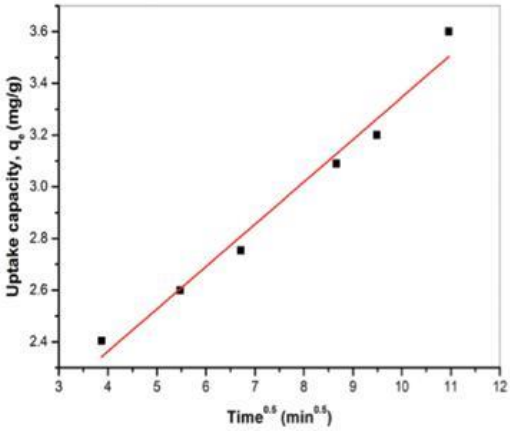

Figure 9. Plot to determine the diffusion coefficient of dye (red metal complex dye dispersed in ternary solvent medium) on leather.

Figure 7 and 8 shows Freundlich isotherm for the solvent and water medium, respectively. The obtained Freundlich and Langmuir constants for the solvent and water medium are presented in Table IV. From the table, correlation coefficient (R^2) value for water and solvent as per Freundlich model is higher compared to Langmuir model. This observation reveals that the adsorption of dye on

to the wet blue leathers in both water and solvent medium are heterogeneous in nature and follows Freundlich model.

Calculation of Diffusion Coefficient of the Dye in Solvent Medium

The process of transfer of solute from the solvent medium is studies by calculating diffusion coefficients for the initial concentration of 0.833×10^{-3} g.cm^{-3}. From the Figure 9, plot of dye uptake versus $t^{0.5}$, the slope of the linear plot was found to be 0.16386 mg/g.min. In order to predict the actual slow step involved, the kinetic data are further analyzed using Boyd kinetic expression, which is given by[20-21]

$$F = 1 - \frac{6}{\pi^2}\exp(-B_t)$$

and

$$F = \frac{q_t}{q_e}$$

Where q_e is the amount of dye adsorbed at infinite time (mg/g) and q_t represents the amount of dye adsorbed at any time t (min), F represents the fraction of solute adsorbed at any time t and B_t is a mathematical function of F, given by:

$$B_t = -0.4977 - \ln(1 - F)$$

The linearity of the plot of Bt vs time is used to distinguish whether external and intraparticle transport controls the adsorption rate. It is observed that the relation between B_t and t is linear (Average R^2=0.991) and does not pass through origin, confirming that surface diffusion is the rate-limiting step.[20, 22] The calculated B values are used to calculate the effective diffusion coefficient, D_i (cm^{2}s^{-1}) using the relation:

$$B = \pi^2 \frac{D_i}{r^2}$$

Where r represents the radius of the particle (assuming as spherical particles). The average D_i value was found to be 3.48 x10^{-4} cm^{2}s^{-1}.

Conclusions

The feasibility of use of green solvents in post tanning operations as alternative to water fol leather processing was explored in this researer. The judicial choice of the solvents from GSK solvent selection guide for the present study is of particular importanceA The green solvents chosen to be used as an alternative medium foe leathey processing shouln give the same or enhanced leathec propertieerand at the same tit should noh give rise to any pollution load. Tho physic-chemical

properties of the post tanning chemicals in the solvent medium present uniform size distribution, leading to good penetration into the matrix. Metal complex dyes in solvent mixture were found to have a homogenous and narrow particle size distribution compared to water medium which was also confirmed with respect to penetration, depth of dye and dry rub fastness on processed leather. When it comes to the neutralising medium solvent neutralised and solvent processed samples were having good appearance and properties. Adsorption isotherms of the dye in water and solvent medium follows same trend and fits to the Freundlich model, with multilayer adsorption being observed. The average diffusion coefficients of the dye in solvent medium was found to be 3.48×10^{-4} $cm^2.s^{-1}$ and found to be comparable with water mediated diffusion. Microscopic images of the leather treated with solvent mixture showed uniform grain pattern and compact cross section. The physical strength measurements of solvents processed leather portrays that solvents are not deteriorating the functional properties of collagen fibres.

This report thus opens up an opportunity to explore ternary solvent mixtures as a diffusion vehicle for current auxiliaries, leading to water reduction in leather processing with minimum change. Though not investigated as a part of the study, the boiling point of the ternary mixture being less than that of water, a complete recovery of the solvent through evaporative methods is feasible.

Acknowledgements

CLRI Communication Number 1165. The authors acknowledge the financial support of Supra Institutional project Research Initiatives in Waterless Tanning (RIWT) under the CSIR XII Plan programs. Authors thanks to Mr. G.C. Jayakumar for his support. Mr. Solomon Fessehaye thanks the Government of Ethiopia and the Twinning project between CLRI and LIDI for enabling him to carry out this research partly and CLRI and LIDI.

References

1. Tünay, O., Kabdaşli, I., Orhon, D., Cansever, G.; Use and minimization of water in leather tanning processes. *Water Science and Technology* ***40,***237-244, 1999.
2. Durai, G., Rajasimman, M.; Biological Treatment of Tannery Wastewater- A Review. *Journal of Environmental science and Technology* ***4,***1-17, 2011.
3. Ozgunay, H., Colak, S., Mutlu, M., Akyuz, F.; Characterization of leather industry wastes. *Polish J. Env. Stud.* ***16,***867, 2007.
4. MIDHA, V., DEY, A.; Biological treatment of tannery wastewater for sulfide removal. *Int. J. Chem. Sc****6,*** 472-486, 2008.
5. Jessop, P. G.; Searching for green solvents. *Green Chem.****13,*** 1391-1398, 2011.

6. Abbott, A. P., Alaysuy, O., Antunes, P., Douglas, A. C., Guthrie-Strachan, J., Wise, W. R.; Processing of Leather Using Deep Eutectic Solvents. *ACS Sustainable Chemistry& Engineering* 2015.

7. Bhargavi, N., Jayakumar, G. C., Sreeram, K. J., Raghava Rao, J., Nair, B. U.; Towards Sustainable Leather Production: Vegetable Tanning in Non-aqueous Medium. *JALCA**110,*** 97-102, 2015.

8. Jayakumar, G. C., Ami, M., Raghava Rao, J., Nishad Fathima, N.; Ionic liquids: new age materials for eco-friendly leather processing. *RSC Advances**5,*** 31998-32005, 2015.
9. Raghava Rao, J., Chandrababu, N., Muralidharan, C., Balachandran, U. N., Rao, P., Ramasami, T.; Recouping the wastewater: a way forward for cleaner leather processing. *J. Cleaner Prodn. **11,***591-599, 2003
10. Henderson, R. K., Jiménez-González, C., Constable, D. J., Alston, S. R., Inglis, G. G., Fisher, G., Sherwood, J., Binks, S. P., Curzons, A. D.; Expanding GSK's solvent selection guide– embedding sustainability into solvent selection starting at medicinal chemistry. *Green Chem.**13,*** 854-862, 2011.

11. Capello, C., Fischer, U., Hungerbühler, K.; What is a green solvent? A comprehensive framework for the environmental assessment of solvents. *Green Chem.**9,*** 927-934, 2007.

12. Ami, M., Raghava Rao, J., Nishad Fathima, N.; Can green solvents be alternatives for thermal stabilization of collagen? *Int. J. Biol. Macromol. **69,***361-368, 2014.

13. Henderson, R. K., Jiménez-González, C., Constable, D. J., Alston, S. R., Inglis, G. G., Fisher, G., Sherwood, J., Binks, S. P., Curzons, A. D.; Expanding GSK's solvent selection guide– embedding sustainability into solvent selection starting at medicinal chemistry. *Green Chemistry**13,*** 854-862, 2011.
14. IUP2. Sampling. *J. Soc. Leather Technol. Chem**84,*** 303-309, 2000.

15. IUP6. Measurement of tensile strength and percentage elongation. *J. Soc. Leather Technol. Chem**84,*** 317-321, 2000.

16. IUP8. Measurement of tear load - Double edge tear. *J. Soc.Leather Technol. Chem* 327-329, 2000.
17. Resa, J. M., Goenaga, J. M., Iglesias, M., Gonzalez-Olmos, R., Pozuelo, D.; Liquid-liquid equilibrium diagrams of ethanol+ water+(ethyl acetate or 1-pentanol) at several temperatures. *Journal of Chemical and Engineering Data**51,***

1300-1305, 2006.

18. Trofimova, M., Toikka, M., Toikka, A.; Solubility, liquid– liquid equilibrium and critical states for the quaternary system acetic acid–ethanol–ethyl acetate–water at 293.15 K. *Fluid Phase Equilibria* ***313,***46-51, 2012.

19. Burgess, D.; General aspects of fatliquoring: an introduction to the application and chemistry of fat liquoring. *Journal of the Society of Leather Technologists and chemists* ***78,***39-43, 1993.

20. Boyd, G., Adamson, A., Myers Jr, L.; The exchange adsorption of ions from aqueous solutions by organic zeolites. II. Kinetics1. *Journal of the American Chemical Society* ***69,***2836-2848, 1947.

21. Aravindhan, R., Rao, J. R., Nair, B. U.; Removal of basic yellow dye from aqueous solution by sorption on green alga Caulerpa scalpelliformis. *Journal of Hazardous Materials****142,*** 68-76, 2007.

22. Gupta, V. K., Ali, I.; Removal of DDD and DDE from wastewater using bagasse fly ash, a sugar industry waste. *Water Research* ***35,***33-40, 2001

NANO ZnO INCORPORATED HIGH PERFORMANCE ACRYLIC BINDER FOR LEATHER COATING

SudhaharSivaraj[1], Sneha.R[2], Sugunalakshmi[3]and Sanjeev Gupta[4]

1 :Department of Leather Technology, Alagappa College of Technology ,Anna University, Chennai, Pincode 600025, India, sudhahar02@gmail.com

2 :Department of Mechanical Engineering, Anna University, Chennai, Pincode 600025, India, sneh.pkr@gmail.com

3: Polymer Science and Technology, Central Leather Research Institute, Adyar, Chennai, Pincode 600020, India, suguna_clri@yahoo.co.in

4: Centre for Human & Organizational Resources Development, Central Leather Research Institute, Adyar,Chennai, Pincode 600020, India,sanjeevgupta@clri.res.in

Abstract

Poly acrylate /nanoZnO composite leather finishing agent was prepared by emulsion polymerization with Methyl Metha Acrylate, 2 Ethyl Hexcyl Acrylate, Lauryl Acrylate and Acrylic Acid monomers. The synthesized ZnO was functionalized in-situ during the polymerization process. The leather finished with ZnO incorporatedpolymer shows better color fastness to light, mechanical properties against control.

Keywords: Leather, ZnO, light fastness, emulsion polymerization, polymer nanocomposite

1. Introduction

The incorporation of inorganic building blocks into organic polymers is one of the most prominent routes in the synthesis of inorganic-organic composite materials. These materials are promising candidates for a wide variety of applications owing to their remarkable change in mechanical, thermal, electrical and magnetic properties (Kickelbick 2003).Aqueous acrylic dispersions have been preferred for coating applications owing to the advantages they offer such as low cost and good tolerance to additives and pigments (Briggs and Jialanella 2010).Acrylate polymers and copolymers are widely used in the leather finishing process.These polymers can take advantage of such inorganic

nanoparticles for enhanced properties such as UV stability, fire retardancy, scratch resistance, self cleaningetc (Fernando 2009).The properties of the produced nanocomposites depend greatly on the functionalized nano particle and the polymerization method. The addition of 0D nano particles such as SiO_2, TiO_2, ZnO, CdSe, ZnS, Al_2O_3 results in the improvement of thermal, physical properties and bioactivities of the latex. 1D nano materials such as carbon nanotubes alters the electrical properties such as conductivity and dielectricity whereas the addition of 2D nanofillers such as nanoclay, graphite and mica can strengthen the barrier property(Thomas Sabu, and Gennady Zaikov 2009).

Nano ZnO being a multifunctional inorganic nanoparticle has been the subject matter of interest as a potential filler material for polymer nanocomposites for enhancement in various properties (Xiong et al 2005, Li et al 2006 and Zhao et al 2006). In this article, copolymer latex of methyl methacrylate, ethyl hexyl acrylate, lauryl acrylate and acrylic acid incorporated with nano ZnO is synthesized to be used as a leather finishing agent which imparts light fastness to the full grain cow shoe upper finished leather.

The preformed nano particles of ZnO are made introduced into the polymerization vessel along with the surfactant to allow for in-situ formation of polymer nanocomposite. This process has is advantageous due to the fact that a poor dispersion is often encountered while attempting to incorporate nano fillers in a polymer melt (Demir et al 2006).The produced polymer nanocomposites films were characterized by Fourier transform infrared spectroscopy (FTIR), Differential scanning calorimetry (DSC) and Thermo gravimetric analysis(TGA). Leather samples were finished with the base coat of synthesized nanocomposites which showed enhanced UV stability than the ones finished without nanoZnO.

2. Materials and methods

2.1 Materials

Monomers Methyl Methacrylate (MMA), 2-Ethyl HexlyAcrylate(2-EHA),Lauryl Acrylate(LA), Acrylic Acid(AA) were purchased from Sigma Aldrich and were used without further purification. Initiator Potassium Per Sulfate (KPS) and surfactant Sodium dodecyl sulfate (SDS) were also obtained from Sigma Aldrich.

2.2 Synthesis of ZnOnanoparticles

To synthesis a ZnO nan0crystals, the analytical grade reagents were used as received without further purification. Briefly, 10 mM of $Zn(NO_3)_3.6H_2O$ and 1.5 g of urea were dissolved in 40 ml deionized (DI) water under stirring. After stirring of about 10 min, the clear solution was transferred to Teflon-lined stainless steel autoclave and kept in oven at 160 ºC for 12 h. The solution was cooled down to room temperature naturally and the precipitate was separated and washed with deionized (DI) water,

ethanol and acetone consecutively. Finally, the end product was dried at room temperature followed by the calcination at 300 ºC under air for 3 h.

2.3Synthesis of copolymer latex incorporated with ZnO nanoparticles

35% dispersion of MMA in combination with 2EHA, LA and AA was prepared. The monomer weight ratio MMA: 2EHA: LA: AArespectively was17.76:7.35:9.84:0.25.

To start with 0.5 gm of surfactant SDS was dissolved in 50 gm of deionized water and stirred well by vertex stirrer for 5 minutes. The monomers, MMA 17.76 gm, 2EHA 7.35 gm, LA 9.84 gm and AA 0.25 gm were added to three-fourth portion of the surfactant mixture and stirred well for 30 minutes. The ZnO nanoparticles were taken in concentrations of 0.01, 0.02, 0.03, 0.04 and 0.05 wt%for each trial and dissolved in the remaining one-fourth of surfactant by sonicating for 30 minutes. 0.75 gm of initiator, potassium per sulfate was dissolved in 20 gm ofdeionised water.

The ZnOnano particle and surfactant mixture was taken in a 250 ml 3-neck round bottom flask fitted with magnetic stirrer at 600RPM and heated in silicone oil bath to 80 ^{0}C, equipped with reflex condenser and thermometer. The initiator and monomer mixtures were added drop by drop under nitrogen atmosphere simultaneously into the reaction vessel. At the end of the reaction,a viscous latex was formed which was cooled andfiltered by using wattman filter paper. The nanocomposite films shown in Figure 2.1 were fabricated under atmospheric drying condition to study the property of the synthesized binder.

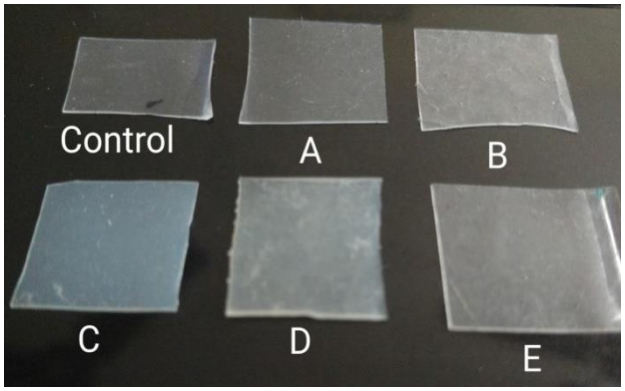

Figure 2.1 Films samples with A-0.01 wt % ZnO, B-0.02 wt % ZnO, C-0.03 wt % ZnO, D-0.04 wt % ZnO and E-0.05 wt % ZnO and Control

2.4 Application in leather finishing

The synthesized nanoZnO incorporated latex was used as a base coating for the finishing of upper leather. The coating mixture formulation consisted of water, ZnO functionalized acrylic binder,

polyurethane, casein, wax and pigment (Bacardit et al 2010 and Olle et al 2010). Further, the season mixturewas sprayed on the cow shoe upper leather by HVLP gun at 30 psi. The base coat deposition was 8 g/sft^2 applied by two cross coat spray, with intermediate drying. The dried leather was pressed at 80 °C/80 kg/cm^2 and further subjected to spraying of two cross coatings. After drying the leather was sprayed two cross coat of lacquer emulsion top.

2.5 ATR-IR, and DSC of cast films

The cast films of the ZnO functionalized acrylate polymer were characterized by attenuated total reflection-infrared spectroscopy (ATR-IR), Differential scanning calorimetry (DSC) and Thermo gravimetric analysis (TGA).

2.5 Testing of finished leather

Leather samples finished by both ZnO free polymer and ZnO functionalized composite were tested for color fastness to light by prolonged exposure to Xenon lamp for 20hours. The color fastness to rubbing and adhesion of finish were determined by standards SATRA TM8 and SATRA TM408.

3. Results and discussion

3.1 IR Spectra

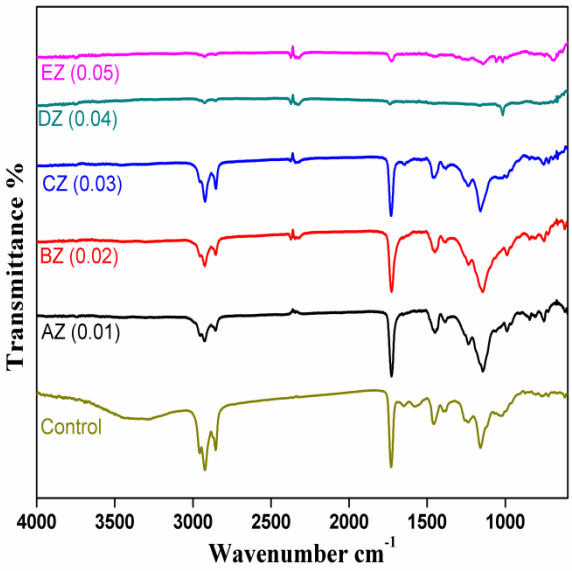

Figure 3.1 ATR-IR SPECTRA

The ATR-IR spectra reveal that all the films have similar IR vibrational modes as like control. The addition of ZnO nanoparticles does not alter the IR vibration even at high concentration of 0.05%.

However, it can be seen that there are diminishing intensity of vibrations due to the incorporation of ZnO.The peak at 1736cm^{-1} corresponds to C=O stretching, The C-OH stretch fundamental (1134 cm $^{-1}$), being a strong absorbance. An asymmetric stretching (CH) vibration at 2928 cm^{-1}, and the symmetric bending δs(CH_2) vibration at 1465 cm^{-1}.(Sachin et al 2016)

3.2 Differential scanning calorimetry (DSC)

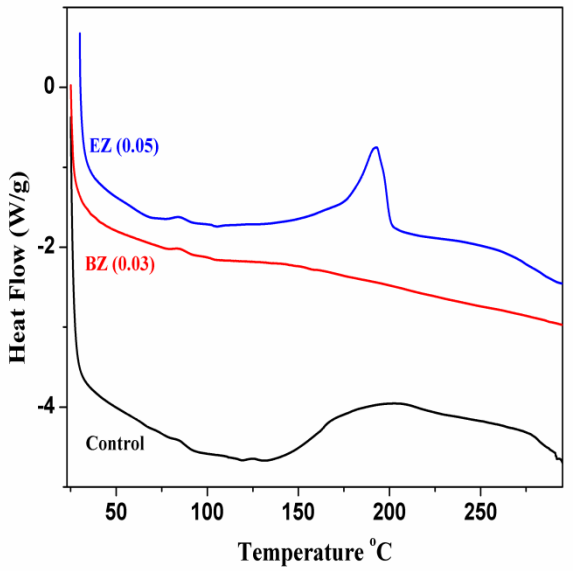

Figure 3.2 DSC

The control films have a glass transition temperature at about 150^{0}C with broad mass flow upto 300^{0}C. For the ZnO functionalized acrylate films show high stability upto300^{0}C.In particular, the lower concentrations of ZnO exhibit better stability due to the complete incorporation of nanoparticles within the acrylate matrix. While increasing the concentration of ZnO to greater than 0.04 wt %, the crystallinity of the films has been changed due to the segregation of the nanoparticles. In this case, the narrow glass transition peaks observed at 175^{0}C as shown in figure. This result indicates that the functionalization of ZnO nanoparticles with acrylate polymer significantly enhances the crystallinity and functional properties.

3.3 Color fastness to light

Table 3.1 shows the color fastness rating of the crust leather, leather finished with acrylic copolymer and the ones finished with acrylic copolymer incorporated with nanoZnO. All the leathers were

subjected to 20 hours exposure in Xenon arc light at 50^0C.It is evident that the finishing of leather with acrylate binder as well as addition of ZnO nanoparticles imparts a positive change in terms of light fastness of the samples when compare to crust leather.

Sample	Crust leather	Leather finished with acrylate	Leather finished with nano-ZnO functionalized acrylate
Rating	3.0	4.0	4.0

Table 3.1 Color fastness to light of samples

3.4 Color fastness to rubbing

The color fastness to circular rubbing of the samples shows increase due to the addition of ZnO nanoparticles against the control sample as shown in Table 3.2.

RUB FASTNESS	DRY		WET	
	MATERIAL	FELT	MATERIAL	FELT
CONTROL	3/4	3	3	2
A	4/5	4	4/5	4
B	4/5	4/5	4/5	3
C	4/5	4/5	4/5	4
D	4/5	4/5	4/5	4/5
E	4/5	4/5	4/5	4/5

Table 3.2 Color fastness to rubbing of samples with A-0.01 wt % ZnO, B-0.02 wt % ZnO, C-0.03 wt % ZnO, D-0.04 wt % ZnO and E-0.05 wt % ZnO and control

3.5 Finish film adhesion

The adhesion of finish increases with the addition of ZnO nanoparticles as seen from the Table 3.3 upto concentrations of 0.03 wt %. The decrease in adhesion for higher concentrations could be attributed to the agglomeration of nanoparticles.

SAMPLE	DRY	WET
CONTROL	2.87	2.21
A	3.17	2.5
B	3.42	2.78
C	3.48	2.44
D	2.60	1.96
E	2.49	2.34

Table 3.3 Finish film adhesion of samples with A-0.01 wt % ZnO, B-0.02 wt % ZnO, C-0.03 wt % ZnO, D-0.04 wt % ZnO and E-0.05 wt % ZnO and control

3.6 Organoleptic Properties subjective evaluation result for ZnOnano particles coated leather

All the finished leather were assessed for following organoleptic properties assessment parameters like gloss,covering,touch,filling.The ZnOnano composite acrylate binder coated leather showed better results than acrylate binder coated leather as seen from the Table 3.4

Properties	Control	AZ	BZ	CZ	DZ	EZ
Covering	2 or 3	3 or 4	4	4	4	4
Gloss	2 or 3	3	3 or 4	3 or 4	4	4
Touch	Dry	Dry,slippery	Dry,slippery, smooth	Dry,slippery, smooth	Dry,slippery, smooth	Dry,slippery, smooth
Filling	2 or 3	2 or 3	3	3 or 4	3 or 4	4
Levelness	4	4	4	4	4	4

Table 3.4Organoleptic Properties subjective evaluation
Rating description: 5-Excellent, 4-Good, 3-Medium, 2-Poor, 1-Very Poor

4. Conclusion

In this study, an acrylate copolymer incorporated with ZnO nanoparticles was synthesized and characterized. Further, the produced nanocomposite was used as a base coating formulation for the finishing of upper leather. The performance testing of the finished leather indicated that the addition of nanoZnO increases the color fastness to light as well as rubbing and the adhesion of finish of the leather than that of the samples finished with acrylic polymer without ZnO nanoparticles. The subjective evaluation properties of finished leather like covering, gloss, filling and levelness were better in ZnO nano composite acrylic polymer coated leather than the normal acrylic polymer coated leather.

5. References

1. Kickelbick Guido. "Concepts for the incorporation of inorganic building blocks into organic polymers on a nanoscale." *Progress in polymer science* 28.1 (2003): 83-114.

2. Briggs P.C, Jialanella G.L. (2010) *"Advances in structural adhesive bonding"*D.A.Dillard(ed.) chapter 6-pg 132

3.Fernando Raymond H. "Nanocomposite and nanostructured coatings: Recent advancements." *Nanotechnology Applications in Coatings* 1008 (2009)pg-9

4.Thomas Sabu, and Gennady Zaikov. "*Recent advances in polymer nanocomposites*" CRC Press, 2009. pg 155-156

5. Xiong, H-M., et al. "Bonding polyether onto ZnO nanoparticles: an effective method for preparing polymer nanocomposites with tunable luminescence and stable conductivity." *Advanced functional materials* 15.11 (2005): 1751-1756.

6. Li, Yuan-Qing, Shao-Yun Fu, and Yiu-Wing Mai."Preparation and characterization of transparent ZnO/epoxy nanocomposites with high-UV shielding efficiency." *Polymer* 47.6 (2006): 2127-2132.

7. Zhao, Hongxia, and Robert KY Li. "A study on the photo-degradation of zinc oxide (ZnO) filled polypropylene nanocomposites." *Polymer* 47.9 (2006): 3207-3217.

8. Demir, Mustafa M., et al. "PMMA/Zinc Oxide Nanocomposites Prepared by In-Situ Bulk Polymerization." *Macromolecular Rapid Communications* 27.10 (2006): 763-770.

9.Bacardit,A.,Olle,L.,Borras,M.D.,Cobos,M.,Jerico.A., and Sole,O. ''Aqueous Finishing with PolycarbodimideCoss-Linked Binders'',*Journal of SLTC*,Vol.94,117,2010.

10.Olle,L.,Shendryck,A.,Combalia,F.,Jorge.J. and Bacardit,A.,''Polysilane Crosslinked Binders for Aqueous Finishing''*Jounal of SLTC*,Vol.94,112,2010

11.Sachin U Chambhare,Gunwant,P.Lokhande and Jagtap,R.N., "Effects of incorporated imine functionality and dispersed nano zinc oxide particles on antimicrobial activity synthesized by RAFT polymerization", *Polym.Bull.,* DOI 1007/s00289-016-1800-6

FLS P-24

THE REDUCTION ABILITY OF THE ORGANIC ACID FOR HEXAVALENT CHROMIUM

Takeshi Onji*, Kyoji Sato

Technology Research Institute of Osaka Prefecture, 2-7-1 Ayumino, Izumi, Osaka 594-1157, Japan

E-mail:onji@tri-osaka.jp

Japanese Association of Leather Technology, Asahi-building, 129, Toyosawa, Himeji, Hyogo 670-0964, Japan

The chromium (Cr) included in the leather derived from a tanning agent often changes to harmful Cr (VI). It is evident that Cr (VI) is formed by the oxidation of the unsaturated fatty acid included in fat-liquoring agents or residual fat of chrome leather. Formed Cr (VI) is usually reduced to Cr (III) under the acid condition in the presence of adsorbed water and organic substance.

In this study, we focus on the ability of organic acid to reduction for Cr (VI). Formic acid, lactic acid, citric acid, and oxalic acid are used as organic acids which can apply to tanning processes. Propyl gallate and quercetin was adopted as reductants to compare with the reduction ability of those organic acids. In order to obtain reliable experimental findings, we have adopted the simple solution system. That is, Cr (VI) and gelatin solution system was prepared. The constant concentration of Cr (VI) and gelatin were adjusted to 50 □g/ml and 1g/100ml, respectively. By use of mineral acid, pH of the solution was adjusted to 3.5-3.8. In the presence of the organic acid, the concentration of Cr (VI) was determined at regular time intervals. The experimental results indicate that the reduction ability of organic acids is follows;

Propyl gallate = Quercetin ＞ Lactic acid ＞ Oxalic acid ≧Citric acid ≧ Formic acid

The lactic acid which is a mild acid practically applied to the tannage. We also studied a part of the reduction mechanism of Cr (VI).

Keywords: hexavalent chromium, reduction, organic acid, lactic acid

1. Introduction

There are great interests in prevention of auto-production of hexavalent chromium (Cr (VI)) in tanned leather for its harmfulness. [1)] It is evident that Cr (VI) is formed by the oxidation of the

unsaturated fatty acid included in fat-liquoring agents or residual fat of chrome leather.[2-4] On the other hand, in the absence of oil like unsaturated fatty acid, Cr (Ⅲ) weakly adsorbed under strong alkaline conditions easily became Cr (Ⅵ) by air oxidation. It was found that Cr (Ⅲ) strongly bonded with leather was hardly oxidized even under strong alkaline conditions. In addition, Cr (VI) is easily reduced to Cr (Ⅲ) under lower pH condition. Unsaturated fatty acids are present in the fat-liquoring agent, which is susceptible to air oxidation, so it is presumed that Cr (VI) is produced in fat-liquored chrome leather.[5-8] Normally, produced Cr (VI) is reduced to Cr (III) when water and organic substance exist under acidic conditions. In this report, we focused on the reduction effect of organic acids, and the reduction effect of various organic acids such as formic acid and citric acid used in the leather process was studied.

2. Material and methods

2.1 Measurement of Cr (VI) concentration change in gelatin solution.

Effect of different types of organic acids compounds on the reduction of Cr (VI) was investigated in 1% of gelatin water solution for a long incubation period. The solution was adjusted to pH 3.5-3.8 with hydrochloric acid or caustic soda solution. Organic acids (formic acid, citric acid, oxalic acid, lactic acid, propyl gallate, and quercetin) added to 0.1 M. Time-dependent change of Cr (VI) concentration was measured according to IUC18 method using diphenylcarbazide.

2.2 Oxidation of lactic acid in Cr(VI) solution.

A model experiment performed in order to confirm the oxidation of lactic acid by the Cr (IV). Equimolar potassium dichromate and lactic acid were dissolved in 50 ml of water. To measure the oxidative product of lactic acid, 5 ml of sample solution was collected in a test-tube. To the sampled solution, 5 ml of saturated solution of sodium chloride was added. Then, 10 ml of diethyl ether was added to the test-tube, and the content of the test tube was well shaken, and allowed to stand still. The upper ether layer was collected, and 1 g of anhydrous sodium sulfate was added. The ether solution was collected into a vial and ether was distilled off. The residue dissolved in 0.3 ml of diethyl ether, and deposit on the KRS-5 crystal surface. FT-IR was measured with a Perkin Elmer Spectrum One.

3. Results and Discussion

3.1 Measurement of Cr (VI) concentration change in gelatin solution.

Fig.1 shows the time depended concentration change of Cr (VI) in gelatin solution with organic acids. The test solution containing propyl gallate and quercetin decreased rapidly the quantity of Cr (VI). Lactic acid and oxalic acid decreased relatively quickly the quantity of Cr (VI). On the other hand, formic acid and citric acid decreased slowly the quantity of Cr (VI). These experimental results indicate that the reduction ability of organic acids is follows;

Propyl gallate = Quercetin ＞ Lactic acid ＞ Oxalic acid ≧Citric acid ≧ Formic acid

Fig.2 shows the time depended concentration change of Cr (VI) in gelatin solution with different concentration of lactic acid. The degree of decrease of Cr (VI) was proportional to the concentration of the added lactic acid. In the presence of lactic acid, it seems that lactic acid is oxidized, and the reduction to Cr (III) is occurred. Therefore, we decided to confirm that lactic acid is oxidized in the presence of Cr (IV).

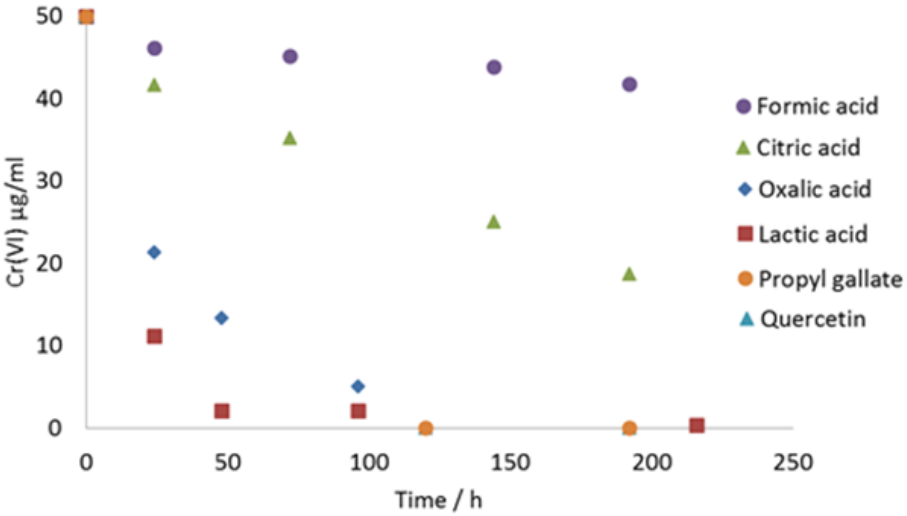

Fig.1 Time depended concentration change of Cr (VI) in gelatin solution with organic acids (formic acid, citric acid, oxalic acid, lactic acid, propyl gallate, and quercetin).

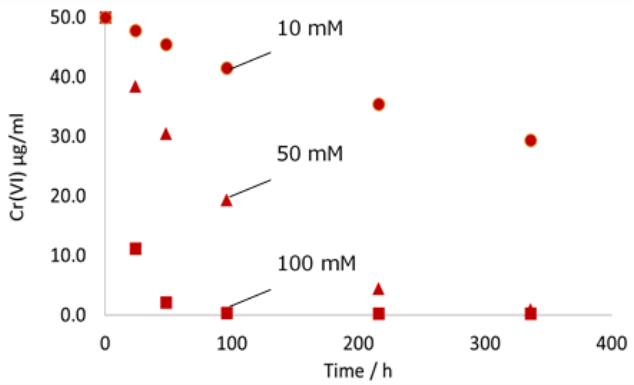

Fig.2 Time depended concentration change of Cr (VI) in gelatin solution with different concentration of lactic acid.

3.2 Oxidation of lactic acid in Cr(VI) solution.

Lactic acid was oxidized in the presence of Cr (IV). The oxidative product was extracted with ethyl ether. Fig.3 shows the spectra of the oxidative product. Comparing the spectra of lactic acid (upper) and oxidative product (center), absorption in 1050 cm^{-1} decreased and absorption in 1080, 1220 cm^{-1} increased. In the spectrum of the oxidation product, it is considered the peak of

1080, 1220 cm^{-1} is derived from pyruvic acid. It was suggested that lactic acid was oxidized by Cr (VI) and pyruvic acid was produced.

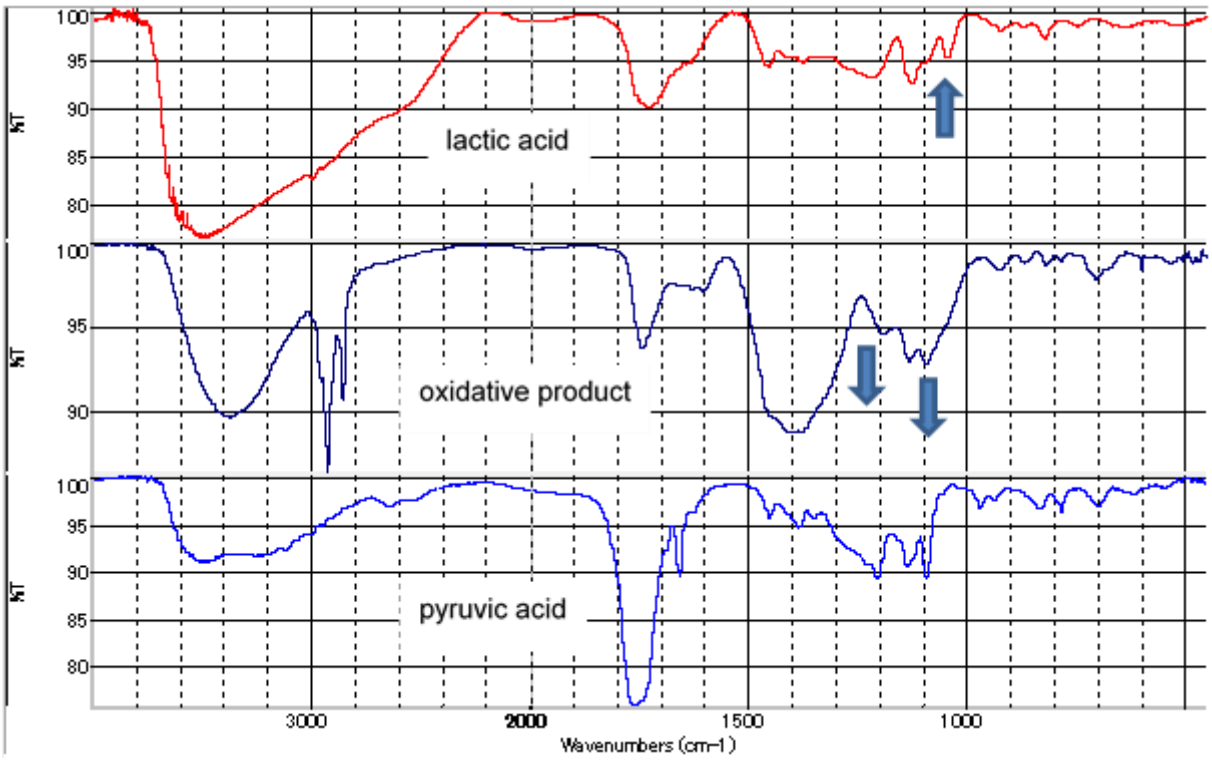

Fig.3 Spectra of lactic acid, the oxidative product and pyruvic acid.

4. Conclusion

Effect of acid type on Cr (VI) concentration changewas investigated in 1% of gelatin water solution. The lactic acid which is a mild acid practically applied to the tannage shows the reduction of

Cr (VI). Results by FT-IR analysis of the oxidation product of the reaction of Cr (VI) and lactic acid, it was found that lactic acid was oxidized by Cr (VI) and pyruvic acid was formed. Then it was suggested that lactic acid acts as a reducing agent, was found to reduce Cr (VI).

5. References

1) Nickolauss G. XXII congress of IULTCS p.47 (1995)

2) Dieter Graf, J. Am. Leather Chem. Assocn. 96, 169~179 (2001)

3) Renate M. and Heintz P., World Leather, June/July, 24, 14~17(2011)

4) L. Zang, C. Yu, H. Yung and Q. Hu, XXX congress of AIULTCS (2009)

5) Chandra Babu N. K., Asma K. Raghupathi A. Venba R. Ramesh R. and Sadulla S., Journal of Cleaner Production, 13, 1189~1195 (2005).

6) Palop R., Parareda J., Ballus O. and Marsal A. J. Soc. Leather Technol. Chem. 92, 200-204(2008)

7) Palop R., Parareda J., Ballus O. and Marsal A. J. Soc. Leather Technol. Chem. 92, 233-236 (2008)

8) Dieter G., J. Am. Leather Chem. Asoc. 96, 169-179(2001)

FLS P-25

BIOMIMETIC FABRICATION AND CHARACTERIZATION OF COLLAGEN/PS/NBAG SCAFFOLD FOR BONE TISSUE ENGINEERING

Tengfei Zhang, Xichan He, Yifei Chen, Fang Wang, Keyong Tang

College of Materials Science and Engineering, Zhengzhou University, Zhengzhou, Henan 450000, China, Corresponding author E-mail: kytang@zzu.edu.cn

The bone tissue engineering scaffold was developed by compounded the type I collagen with the porous scaffold of the sol-gel derived nano-bioactive glass in the system CaO-P_2O_5-SiO_2-Na_2O. In the present study, novel biomimetic composite scaffolds with similar properties to natural bone were prepared by blending and cross-linking with bioactive glass, type I collagen, and phosphatidylserine (PS). Several phospholipids, especially phosphatidylserine (PS) with high affinity for calcium ions have been shown to be an important component of them. Previous work had shown that PS is able to form complexes with both Ca^{2+} and $P_{i.}$, nucleate hydroxyapatite formation. Different collagen contents were chosen to confirm the maximum degree of collagen with the triple helix content. The molecular weight of collagen was characterized by electrophoresis, which affects the biocompatibility.

The collagen/PS/NBaG scaffold was croslinked with genipin (GNP) or 1-ethyl-3-(3-dimethylaminopropyl) arbodiimide (EDC) and N-hydroxysuccinimide (NHS). The collagen/PS/NBaG scaffold was prepared by using a freeze-drying technique and characterized by scanning electron microscopy (SEM) and Transmission electron microscope (TEM). The cross-section morphology shows that the collagen/PS/NBaG scaffold possessed a three-dimensional (3D) interconnected homogenous porous structure. The porosity of the collagen/PS/NBaG scaffold sample was tested according to the Archimedes principle. The mechanical properties of the scaffolds were analyzed using a texture analyzer. XRD analysis demonstrated the crystallographic properties of the scaffolds which immersing them in simulated body fluids (SBF). The functional groups of composite samples and nano-bioactive glass (NBaG) were examined by FTIR. All results demonstrated the Sol-Gel bioactive glass-type I collagen-PS scaffold with good biocompatibility and osteogenesis is a new ideal scaffold for bone tissue repair and regeneration.

Keywords: collagen, bioactive glass, phosphatidylserine , freeze-drying technique, scaffold

1. Introduction

For bone repairing, the surgeons preferred a bone substitute for bone graft, specifically the autograft, creating an increasing demand for these materials worldwide. Themain disadvantage associated with this approach is the requirement of surgeryto harvest the autologous bone, and the pain associated with theharvest site is often said to be more painful than the recipient site (Younger EM 1989).Biomaterials for bone tissue engineering have been extensivelystudied since there is a need for these materials to repair bones whichhave been lost or damaged due to trauma, injuries, disease or aging.Hence, the field of regenerative medicine aims to address this issue by developing new substitutes that can activate the body's own natural repair process omitting the need for donor tissue(Jones JR 2007). For advanced engineering of bone tissues, it has been a constant concern to take advantage of the unique properties of bioactive glasses (BG) to build scaffolding materials able to guide bone ingrowth (M. N. Rahaman 2011).

BG are known to efficiently stimulate bone regeneration(J. R. Jones 2013),and are even able to bond to soft tissues. Sol-gel processed bioactive glasses, with unique nanoporous structure was developed as a novel nanobiomaterial.45S5BGs (in wt%: 45% SiO_2, 24.5% Na_2O, 24.4% CaO and 6% P_2O_5) exposes critical concentrations of Ca, Si, Na and P ions, which have been shown to activate genes in osteoblast cells, stimulating new bone formation in vivo(V. Mourin 2012).BG scaffolds have been shown to have excellent biocompatibility, osteoconductivity and ability to form a bone-like mineral phase at the interface when in contact with living tissue. However, their brittleness is a serious drawback, and prevents them from sharing mechanical load with bone.

Composite materials consisting of BG particles dispersed in a bioresorbable polymer matrix show improved mechanical properties, but the absence of interfacial bonding between the organic and inorganic components, which usually have very different degradation rates, can cause instability and premature deterioration of the scaffold.(J. J. Blaker 2010)Biomimetic matrices may provide such a suitable microenvironment, which are envisioned through the application of biomimetic elucidated from bone assembly and structure. Bioactive materials such as calcium phosphates, bioactive glasses, and polymer/bioactive ceramic composites appear to be one of the promising classes of materials.The key is toprovide suitable scaffolds to insure cell differentiation andoptimal secretion activity. In addition a suitable scaffold for bone tissue engineering should have porosity more than 80% and pore size between 100 and 500 μm depending on the application of the scaffold.The nanoporous structure results in large surface area and has shown to enhances the surface adsorption ability and bio-mineralization ability(Chen XF 2007).

The bone matrix is approximately 35 wt% organic (mainly type I collagen) and 65 wt% inorganic material (mainly hydroxyapatite). Collagen have been widely used as scaffolds due to their similarity in composition to the extracellular matrix, their high biocompatibility, and their low

immunogenicity(Lee C H 2001).Thus, one of the aims of this study is to fabricate a collagen scaffold that is highly porous with interconnected pores and to maintain the existence of collagen nanofbers. Collagen is an organic component of bone and an extracellular matrix (ECM), and has a number of important functions, including tissue binding and support, as well as the maintenance of differentiation, growth, and plasma of cell matrix liquid. The extracellular matrices (ECMs) of hard tissue are composed of organic and inorganic phases. Presently collagen is mainly used in tissue engineering, such as a scaffold in 3-D cells cultures (Itoh 2001).

We had previously fabricated a composite containing collagen and bioactive inorganic material for bone tissue regeneration and demonstrated that a composite with a bioactive inorganic material exhibited better in vitro osteogenic properties than collagen alone.(Tsai S W 2008)Lately, a new porous bioactive nanocomposite that is composed of sol-gel bioactive glass (BG), collagen (COL), and phosphatidylserine (PS) was developed by a combination of sol-gel and freeze-drying methods.

2. Material and methods

2.1 Materials

Bioactive glasses were synthesized through sol-gel method. tetraethyl orthosilicate $Si(OC_2H_5)_4$(TEOS), triethyl phosphate $PO(C_2H_5)_3$ (TEP), calcium nitrate tetrahydrate $Ca(NO_3)_2.4H_2O$ and sodium nitrate $NaNO_3$,were used as the starting materials. They were mixed in deionized water and citric acid ($C_6H_8O_7$) to react. The solution was kept undisturbed at room temperature and 60℃.respectively, for an appropriate time period. Then, the dried material was sintered at 700℃ for 2 h. Type Ⅰ Collagen was extracted by acid - enzyme method (Shi Huiyang 2004)and we extracted collagen from pig skin.PS was supplied by Boao Medical Ltd. (Shanghai, China). EDC, NHS, morpholine ethanesulfonic acid (MES), and acetic acid were all chemical grade.

2.2 Sol–gel synthesis bioactive glass

The sol–gel synthesis of the bioactive glasses proceeded according to a conventional protocol for the synthesis of 45S5 bioactive glass(I. Cacciotti 2012;H. Pirayesh 2013).using the following chemical precursors tetraethyl orthosilicate $Si(OC_2H_5)_4$ (TEOS), triethyl phosphate $PO(C_2H_5)_3$ (TEP), calcium nitrate tetrahydrate $Ca(NO_3)_2{\cdot}4H_2O$ and sodium nitrate $NaNO_3$. Two different aqueous acid solutions prepared with nitric acid (HNO3) or with citric acid ($C_6H_8O_7$) were used to catalyze the hydrolysis reaction. The hydrolysis and condensation reactions were performed within a thermostated reactor to control the reaction temperature.

The molar ratio of TEOS, TEP, $NaNO_3$ and $Ca(NO_3)_2{\cdot}4H_2O$ were designed according to the molar ratio of SiO_2, P_2O_5, Na_2O and CaO in 45S5. To achieve a clear sol the molar ratio between the aqueous acid solution and the four chemical precursors was set to 10. Firstly, the acidic solution (26 mL) was magnetically stirred in the thermostated reactor at the desired temperature and TEOS (11.6 mL) and TEP (1 mL) were added dropwise to the solution and stirred until a clear solution was obtained. Next,

the $NaNO_3$ powder (4.66 g) was slowly added in the stirred solution until its complete dissolution. Finally the $Ca(NO_3)_2{\cdot}4H_2O$ powder (7.15 g) was added slowly to the solution stirred during 1 h to result in a transparent sol. Therefore the sol starts to transform into gel through polycondensation reactions. The gel was then kept at 60 °C for 12 h and finally dried at 200 °C and 700 °C for 5 h and 2 h respectively. After the drying step the gel was manually crushed to obtain a fine powder.

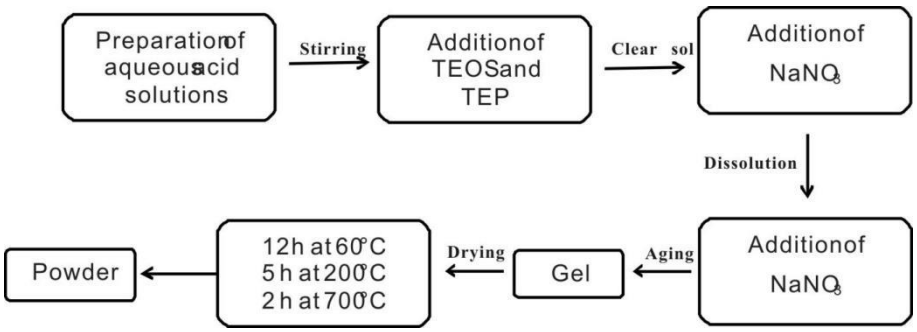

Fig. 1. Flowchart of the sol-gel process

2.3 Preparation of Composite Scaffolds

It was prepared by a combination of sol-gel and freeze-drying methods.Then the 45S5 BG was ground to particles and intensively mixed with the solution of COL-PS (wt ratio: 80-20) at a fraction of 65. 2.5 mg/mL crosslinking agents (1-ethyl-3-(3 dimethylaminopropyl) carbodiimide, EDC and N-hydroxysuccinimide, NHS (weight ratio of 4 to 1) were added to the mixture before it was frozen and finally freeze-dried at –50 °C for 24 h to develop porous composites.

2.4 Fourier transformed infrared spectroscopy (FTIR)

Structural characterizations of the powders were performed by FTIR spectroscopy. The FTIR spectra were obtained in reflexion mode with a FTIR imaging system (Spotlight, Perkin–Elmer, Courtaboeuf, France) coupled to a spectrometer (Spectrum 300, Perkin–Elmer) in the 400–4000 cm^{-1} range with a spectral resolution of 4 cm^{-1}.

2.5 Scanning electron microscopy (SEM) Observation

Scanning electron microscopy (SEM) (30XLFEG, Philips, The Netherlands) was used to observe the morphology of the composite scaffolds. The samples were sputter-coated with a layer of gold for observation at 20 KV and varying levels of magnification.

3. Results and Discussion

3.1 Fourier transformed infrared spectroscopy (FTIR)

Fig.2 and Fig.3 shows the FTIR spectra, in the 500-4000 cm^{-1} spectral range, for plain 45S5 bioactive glass and type Ⅰ collagen. The FTIR spectra of the two synthesized sol-gel glasses are presented in Fig.2 and compared with the spectrum of the sol-gel bioactive glass. The two broad bands at 925 cm^{-1} and 1035 cm^{-1} correspond to silicate adsorption bands which are respectively Si-O-Si stretching of

non-bridging oxygen atoms and Si-O-Si asymmetric stretching of bridging oxygen atoms within the silicate tetrahedron. Silicate bands for Si-O-Si bending mode are also observable at 510 cm^{-1} (H.A. Elbatal 2003). The peak at around 610 cm^{-1} and 870 cm^{-1} are attributed to P-O bending of PO_4^{3-} groups(A. Lucas-Girot 2011). The weak bands observed at around 1450 cm^{-1} are related to the presence of residual carbonate groups from the precursors [15].

FTIR spectra of plain collagen exhibited a number of characteristic spectral bands.such as: C = O stretch at 1662.1 cm^{-1} for amide I, N-H bend and C-H stretch at 1546 cm^{-1} for amide II, C-N stretch plus N-H in phase bending at 1244 cm^{-1} for amide III, N-H stretching vibration at 3298 cm^{-1} for the amide.

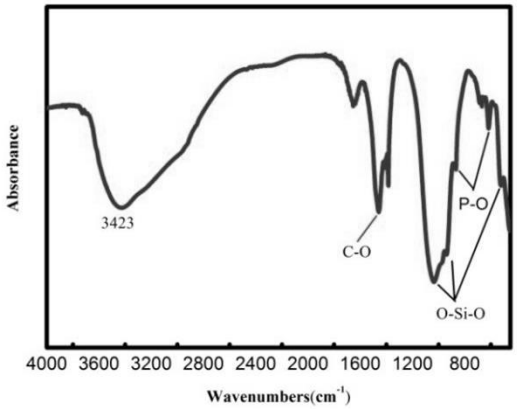

Fig. 2. FTIR spectra of the sol–gel 45S5 glasses.

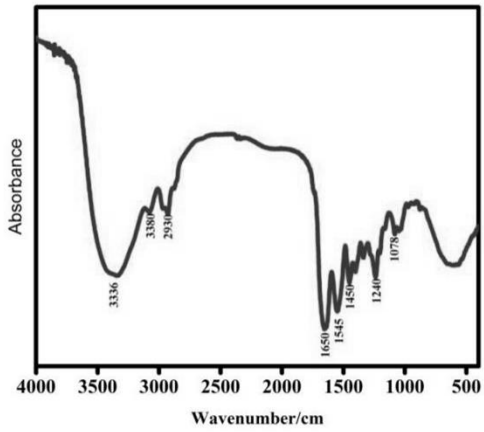

Fig. 3. FTIR spectra of the type Ⅰ collagen

3.2 Scanning electron microscopy (SEM) Observation

As shown in Fig. 4, the scanning electron micrographs show the highly porous architecture of the scaffolds, and an even distribution of bioactive glass was observed throughout the collagen matrix. Scanning electron micrographs showed that the structure of composite scaffolds were porous with pore diameters of approximately 50–150 μm.

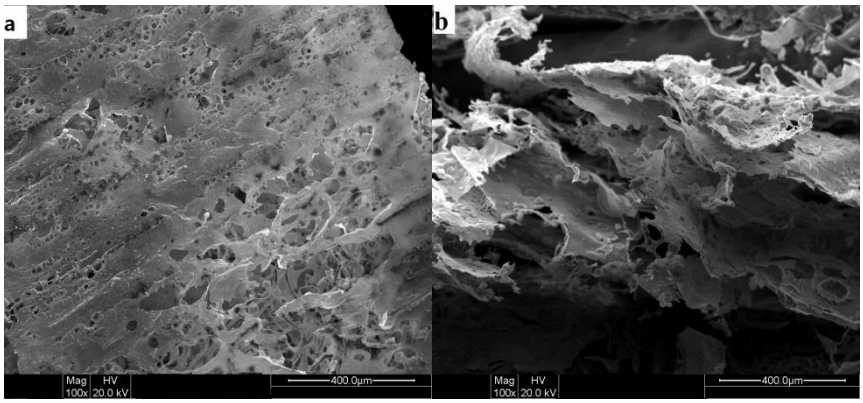

Fig. 4. SEM micrographs of the Collagen/PS/NBaG. (a) Longitudinal section, (b)cross section.

Conclusion

In this work we demonstrate that the 45S5bioactive glass powdercan be synthesized by the sol–gel process with a very low concentratedcitric acid solution instead the usual highly concentrated nitric acid solution to catalyze the hydrolysis reaction. Type Ⅰ collagen have high biocompatibility and low immunogenicity, which extract from pig skin.. Adopt freeze-drying methods can obtain 3-D macropous materials. PS is added to the scaffold as a growth factor can promote the formation of cell membrane . We will continue do some research about this aspect .

Acknowledgments

The financial supports from the National Natural Science Foundation Commission of China (No. 51373158) the Sci-Tech and Innovation Talent Foundation of Henan Province (No. 144200510018) are gratefully acknowledged.

References

1. Younger EM, Chapman MW. Morbidity at bone graft donor sites. J OrthopTrauma 1989;3:192e5
2. Jones JR, Gentleman E, Polak J. Bioactive glass scaffolds for bone regeneration.Elements 2007;3:393e9.
3. M. N. Rahaman, D. E. Day, B. Sonny Bal, Q. Fu, S. B. Jung, L. F. Bonewald and A. P. Tomsia, Acta Biomater., 2011, 7, 2355–2373
4. J. R. Jones, Acta Biomater., 2013, 9, 4457–4486.
5. V. Mourin, J.P. Cattalini, A.R. Boccaccini, Metallic ions as therapeutic agents in tissue engineering scaffolds : an overview of their biological applications and strategies for new developments, 2012 401–419.
6. J. J. Blaker, A. Bismarck, A. R. Boccaccini, A. M. Young and S. N. Nazhat, Acta Biomater., 2010, 6, 756–762
7. Chen XF, et al., “Nano-Structure Analysis of theSol-Gel Derived Bioactive Glasses”. Bulletin of theChinese Ceramic Society,Vol.26, pp.247-251,2007.
8. Lee C H, Singla A and Lee Y 2001 Biomedical applications of collagen Int. J. Pharm. 221 1–22
9. Itoh, H., Aso, Y., Furuse, M., Noishiki, Y., Miyata, T. (2001) Artif. Organs, 25, 213–217.

10. Tsai S W, Hsu F Y and Chen P L 2008 Beads of collagen nanohydroxyapatite composites prepared by a biomimetic process and the effects of their surface texture on cellular behavior in MG63 osteoblast-like cells Acta Biomater.4 1332–41
11. Shi Huiyang.Studies on Enzymatic Extraction of Collagen from Raw Pig Skin [D]. Beijing: Beijing University of Chemical Technology, 2004.
12. I. Cacciotti, M. Lombardi, A. Bianco, A. Ravaglioli, L. Montanaro, J. Mater. Sci. Mater. Med. 23 (2012) 1849–1866.
13. H. Pirayesh, J.A. Nychka, J. Am. Ceram. Soc. 96 (2013) 1643–1650.
14. H.A. Elbatal, M.A. Azooz, E.M.A. Khalil, A. Soltan Monem, Y.M. Hamdy, Mater. Chem. Phys. 80 (2003) 599–609.
15. A. Lucas-Girot, F.Z. Mezahi, M. Mami, H. Oudadesse, A. Harabi, M. le Floch, J. NonCryst. Solids 357 (2011) 3322–3327.

FLS P-26

MOLECULARLY ENGINEERED DUAL-CROSSLINKED HYDROGEL WITH GOOD ELASTICITY AND TOUGHNESS

Keyong Tang*,Xialian Fan, Xichan He, Keke Chen, Jingbao Huang, Pengyuan Yang,Tingting Yan, Jie Liu, Fang Wang, Yijin Li

College of Materials Science & Engineering, Zhengzhou University, Zhengzhou 450001, China

The Fifth Affiliated Hospital of Zhengzhou University, Zhengzhou 450001, China

Corresponding author E-mail address: keyongtangzzu@yahoo.com

Articular cartilage, covering the end of long bones in bodies with almost no friction, bears the great pressure from our gravity, and withstands high impulse or shear in a large range of movement. Therefore, it is essential to develop hydrogel with good elasticity and toughness in the field of artificial cartilage. Herein, a composite hydrogel with good elasticity and toughness was prepared, using gelatin (Gel), oxide cellulose, and acrylamide. Firstly, Gel and oxidized cellulose were used to form network structure though Schiff base reaction, and then, acrylamide was allowed to penetrate into the network structure of Gel/oxidized cellulose for radical polymerization. The interweaving of two networks provides the hydrogel with good elasticity and strength. And then the ionic coordination (CO_2LFe^{III}) was chosen as the third crossling to further strengthen the Gelatin/oxidized cellulose/pAAm hydrogel. The hydrogel has an advantage over each individual gels and could simulate partly the structure of native extracellular matrix of cartilage tissue. Besides, the influence of different forms of cellulose (microcrystalline cellulose, microfibrillated cellulose, cellulose nanowhisker, oxidized microcrystalline cellulose, oxidized microfibrillated cellulose, and oxidized cellulose nanowhisker) on the performance of hydrogel was investigated. The compression strength showed that the toughness of hydrogel gradually increased with increasing the content of cellulose. The loading-unloading test on the hydrogel showed the hydrogels are good in elasticity and able to recover quickly soon after removing the pressure. The results suggested that the hydrogel with good elasticity and toughness might serve as promising scaffolds for cartilage tissue engineering.

Keywords: cartilage; hydrogel; gelatin; cellulose; acrylamide

Introduction

Biopolymer-based hydrogels are widely used to emulate the extracellular matrix (ECM) for controlling stem cell differentiation and tissue regeneration because of the similarity between such hydrogels and native ECM in terms of their physical and biochemical properties(Wei K, 2016; Balakrishnan B, 2011; Van Vlierberghe S, 2011). However, they usually do not have enough mechanical strength due to its intrinsic structural inhomogeneity or lacking effective energy dissipation mechanism and largely limit their application in many fields(Lin P, 2011; Gong J P, 2010). Exploring ultrahigh strength hydrogels behaving like natural load-bearing soft tissue like tendon, cartilage, muscle, and blood vessels have many application potentials(Calvert P, 2009).

To this end, designing a hudrogel that combines mechanical strength with good elasticity and toughness is still a big challenge. In this study, we choose the biocompatible materials gelatin and environment friendly cellulose based on Schiff base to constitute an interpenetrating network, and then engineered acrylamide component into a chemically crosslinked network to form a woven structure on which a secondary crosslinking was imposed (**Figure 1**). The ionic coordination (CO_2LFe^{III}) was chosen as the third crossling to further strengthen the Gelatin/oxidized cellulose/pAAm hydrogel. Because the interpenetrating network of gelatin/oxidized cellulose was weak and the cellulose would shift under pressure, the woven structure was expected to be more efficient to obtain mechanical strength with good elasticity and toughness. Such hydrogels are robust enough to let nutrients or cells free in and out, support chondrogenesis of the human mesenchymal stem cells (hMSCs) and promote cartilage regeneration.

Experiment section

Materials. Gelatin with pharmaceutical grade and acrylamide were purchased from Aladdin. Ironchloride ($FeCl_3$), sodium hydroxide (NaOH) and concentrated sulfuric acid (H_2SO_4) were all supplied by Feng-chuan Chemicals Science and Technology Ltd., Tianjin, China. Microcrystalline cellulose (MCC) with pharmaceutical grade was provided by Qufu Tianli Medical Supplements Co. Ltd., China. Sodium periodate ($NaIO_4$) was from Tianjin Yongda Chemical regent Co. Ltd., China.

Preparation of MFC and CNC. The preparation of microfibrillated cellulose (MFC) was according to reference(Guo T, 2017). Briefly, 5 g MCC was dispersed in 100 mL sodium hydroxide solution with continuously stirring, the mixture was ultrasonic dispersed for 2 hours. Then the dispersion was treated with a homogenizer (APV1000/2000, SPX Flow technology Rosisita GmbH) at a pressure of 1250 bar for 30 cycles to obtain MFC dispersion.

Cellulose nanowhisker (CNC) was prepared using the methods previously described (Yang W, 2015). Generally, hydrolysis was carried out with 64% (wt/wt) sulphuric acid 45 ^{o}C for 120 min with vigorous stirring, followed by diluting the suspension into a 20-fold deionised water to quench the reaction. The suspension was then centrifuged at 5000rpm for 20 min to concentrate the cellulose and to

remove excess aqueous acid. The resultant precipitate was dialyzed against water for 3 days to further eliminate the acid until a pH of *ca.* 7.0 was obtained.

Sodium periodate oxidation of cellulose (MFC and CNC). An aqueous mixture of MFC (or CNC) and sodium periodate (Sodium periodate to MFC (or CNC) weight ratios was 0.7:1) was stirred for 2 days in absence of light at room temperature(Dash R, 2013). The product was dialyzed against deionized water for 2 days to remove the spent oxidant, and then freeze-dried for further use.

Gelatin/oxidized cellulose/pAAm hydrogel Fabrication. A three-step metod was used to synthesize dual-crosslinked hydrogels. 100 mL 10% (wt) gelatin solution was prepared in deionized water, and acrylamide was added to achieve 3 mol/L, then different weight ratios of oxidized cellulose (0, 3%, 6%, 9%, weight ratio of cellulose/total) was added in the solution, the mixture solution was stirred for 30 min. Then 1 wt% initiator KPS, 0.04mol/L chemical crosslinker N-N'-Methylene-bis-acrylamide (BIS) were added in the solution, the mixture was deaired for 10 min with argon gas. After that, 25 µL accelerator TEMED was added in the solution. The resulting solution was poured into a glass mold and placed at room temperature for 2 h to form chemically monocrosslinked hydrogel. Then the chemical monocrosslinked hydrogels were immersed in $FeCl_3$ (0.06 mol/L) solution for 16 h to form original physically crosslined network. At last, the Fe^{3+}-loaded hydrogels were immersed in deionized water for 48 h to remove superfluous Fe^{3+}.

Characterization. The cross-sectional morphologies of the hydrogels were investigated using the scanning electron microscopy (SEM, FEI Quanta 200, US). Compression test of the hydrogels were conducted using the texture analyser (TA.XT Plus, UK). Disk-shaped hydrogels samples (d=10mm, h=10mm) were made in custom-made molds and compressed at a fixed rate of 10mm/min to the target strain levels.

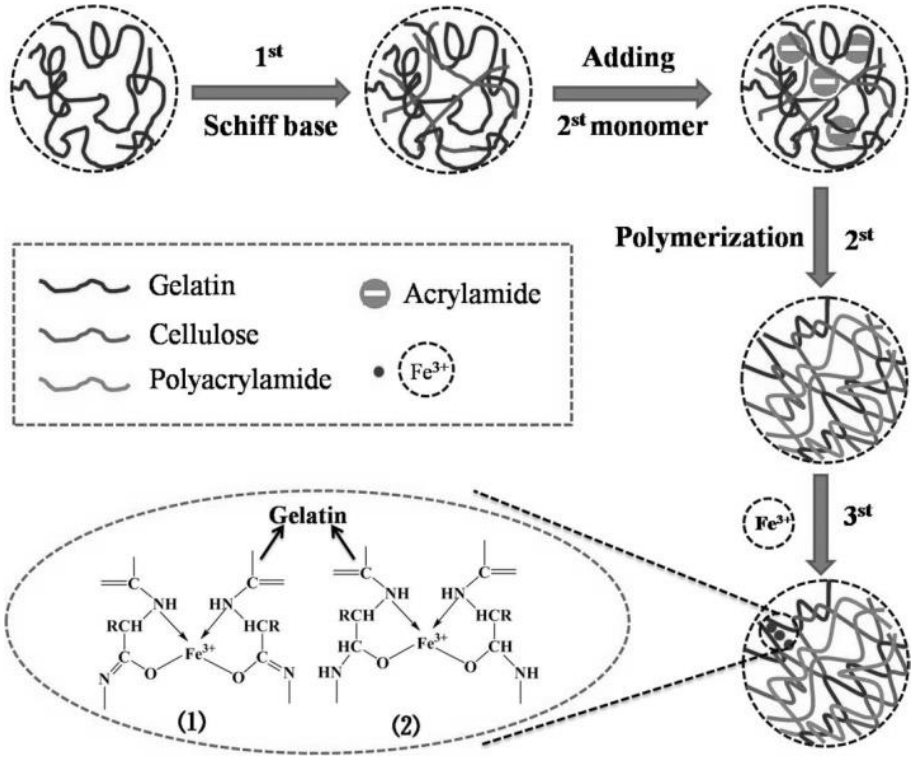

Figure 1. Schematic illustration of dual-crosslinked (chemically and physically) hydrogel: schiff base and in situ polymerization to form chemically crosslinked woven structure, Fe^{3+} coordination physically crosslinked network was formed after Fe^{3+} loading (The proposed structures of Fe^{3+}/gelatin: (1) enolization structure, (2) no enolization structure).

Result and Discussion

Articular cartilage as a complex and anisotropic material exhibits high mechanical and viscoelastic properties with a very low friction, which can withstand millions of cycles of joint loading-unloading over decades of wear(Liao I, 2013). Both polymer-filled voids and polymer entanglement with voids can effectively absorb and dissipate elastic energy around the cracks either by viscous dissipation or by large deformation of the polymer chains, preventing stress accumulation and crack propagation to a macroscopic level(Chen Q, 2015). However, once the fracture of polymer networks reaches irreversible damage caused by permanent bond breakage at high strain, the hydrogels will lose most of their mechanical properties after loadings, leading to the difficulty to recover from damage.

To overcome this problem, we present a new woven structure to improve the hydrogels with good elasticity and toughness. Figure 2a,b are the typical stress-strain curves of hydrogel-OMFC (1%, 3%, 6%, 9%), hydrogel-ONFC (1%, 3%, 6%, 9%). Figure 2c,d are the compression strength of hydrogel-OMFC (1%, 3%, 6%, 9%), hydrogel-ONFC (1%, 3%, 6%, 9%). It is seen that the compression strength of hydrogel-1% OMFC, hydrogel-1% ONFC are only ≈0.1MPa at the strain of 65%. In contrast, the compression strength of hydrogl-9% OMFC, hydrogel-9% ONFC can reach 0.4MPa, which are 4 times

higher than hydrogel-1% OMFC, hydrogel-1% ONFC. This indicates that the cellulose can significantly improve the mechanical strength of hydrogel. What's more, the compression strength of hydrogel-ONFC (1%, 3%, 6%, 9%) is higher than hydrogel-OMFC (1%, 3%, 6%, 9%), and the compression strength of hydrogel-6% ONFC is obviously 2 times larger than hydrogel-6% OMFC. This may be the structure of OMFC is interconnection network structure, the gelatin and OMFC could not well to constitute an interpenetrating network, results in uneven stress. Compared with OMFC, the structure of ONFC is short red-like, the gelatin and ONFC could to constitute a well interpenetrating network.

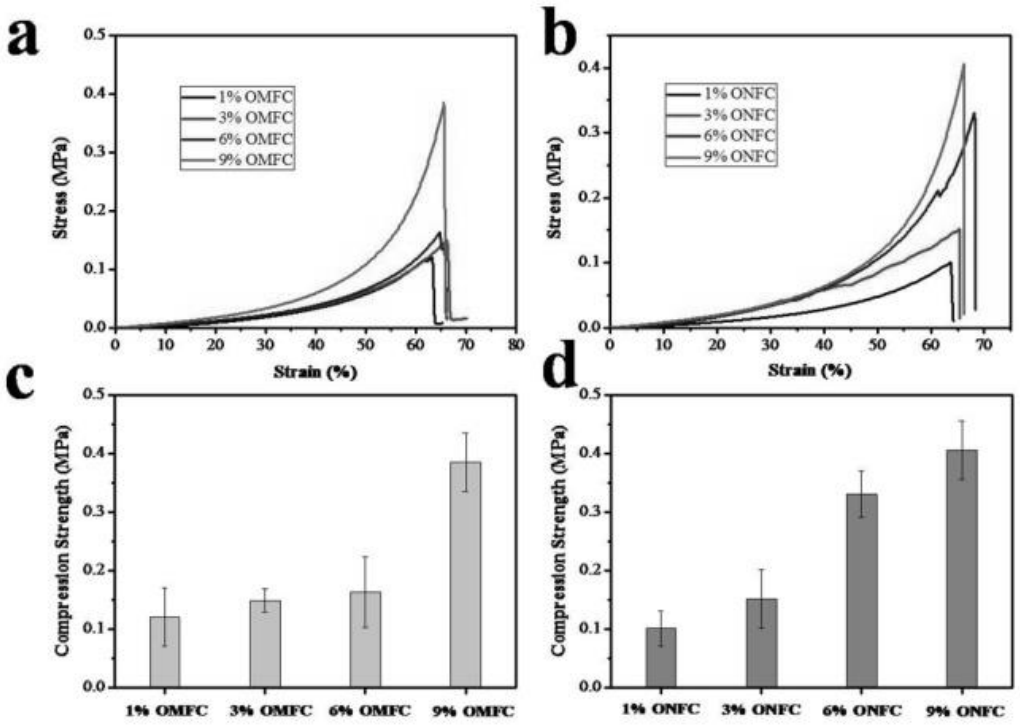

Figure 2. a,b are the typical stress-strain curves of hydrogel-OMFC (1%, 3%, 6%, 9%), hydrogel-ONFC (1%, 3%, 6%, 9%); **c,d** are the compression strength of hydrogel-OMFC (1%, 3%, 6%, 9%), hydrogel-ONFC (1%, 3%, 6%, 9%).

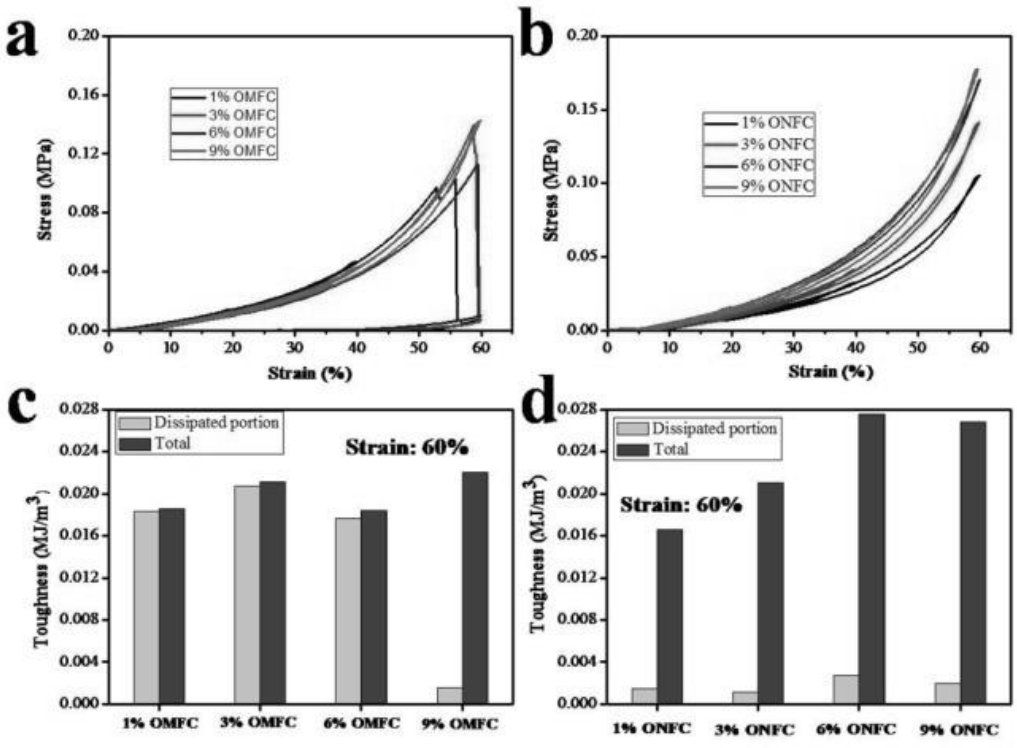

Figure 3. Loading-unloading test under various conditions: a) loading-unloading tests of hydrogel-OMFC (1%, 3%, 6%, 9%) under different strain (20%, 40%, 60%); b) loading-unloading tests of hydrogel-ONFC (1%, 3%, 6%, 9%) under different strain (20%, 40%, 60%); c) the toughness and the dissipated toughness of hydrogel-OMFC (1%, 3%, 6%, 9%) at strain of 60% calculated from the test (a); d) the toughness and the dissipated toughness of hydrogel-ONFC (1%, 3%, 6%, 9%) at strain of 60% calculated from the test (b).

Figure 3 shows the loading-unloading test of hydrogel under various conditions. As can be seen in Figure 3a, the hydrogel-OMFC (1%, 3%, 6%, 9%) under 20% or 40% strain all show good elasticity. However, the hydrogel-1% OMFC, hydrogel-3% OMFC and hydrogel-6% OMFC lost most of their elastic modulus under 60% strain, but the hydrogel-9% OMFC still keeps good elasticity. And the Figure 3c shows the toughness and the dissipated toughness of hydrogel-OMFC (1%, 3%, 6%, 9%) at strain of 60% calculated from the Figure 3a, it found that the hydrogel-1% OMFC, hydrogel-3% OMFC and hydrogel-6% OMFC lost most toughness to their original state under 60% strain, but the hydrogel-9% OMFC almost recovered to its original state, these might the woven structure becomes closely by increasing the content of OMFC. Compared to the hydrogel-OMFC (1%, 3%, 6%, 9%), the hydrogel-ONFC (1%, 3%, 6%, 9%) all show good elasticity, and they still keep good elasticity even under the condition of large deformation. The good elasticity in the hydrogel-ONFC (1%, 3%, 6%, 9%) was clearly illustrated in Figure 3b,d. With increasing the OMFC or ONFC content, all the toughness of hydrogel-OMFC (1%, 3%, 6%, 9%) and hydrogel-ONFC (1%, 3%, 6%, 9%) gradually increased. The hydrogel-OMFC and hydrogel-ONFC show different elasticity, these might be due to the structure of

cellulose. The structure of OMFC presents the network structure, and the ONFC presents short red-like. Because of interconnection network structure of OMFC, the gelatin molecule and OMFC could not well to constitute an interpenetrating network, results in low toughness and elasticity. The hydrogel-OMFC shows good elasticity under low deformation, this is mainly due to polyacrylamide molecule and the ionic coordination (CO_2LFe^{III}) between the gelatin molecules. The short red-like ONFC may be easier to enter the molecules of the gelatin, this is conductive to form an interpenetrating network and improve the elasticity of the hydrogels.

Figure 4a shows the hydrogels loaded with different concentration of Fe^{3+}, the hydrogels loaded with different concentration of Fe^{3+} have different toughness and elasticity. Based on this mechanism, we could prepare hydrogels with different properties to repair the damage of different parts of our body. Figure 4bshows the interaction mechanism of hydrogel under loading-unloading, it vivid shows the movement of molecular chain. Under the loading, the molecular chain of the gelatin and polyacrylamide stretches along the horizontal direction, and the cellulose chain under the traction of gelatin or polyacrylamide molecular chain to move along the vertical direction. Removal the loading on the hydrogel, the gelatin molecular chain recovered to its original state under the action of the ionic coordination (CO_2LFe^{III}), and the polyacrylamide molecular chain almost recovered to its original state under low deformation or most of the polyacrylamide molecular chain recovered its original state under large deformation. These might due to the sacrificing some C=C bonds to obtain high elasticity, and these bonds could not move back to its original state after removal the loading, and this results in the dissipated toughness of hydrogel.

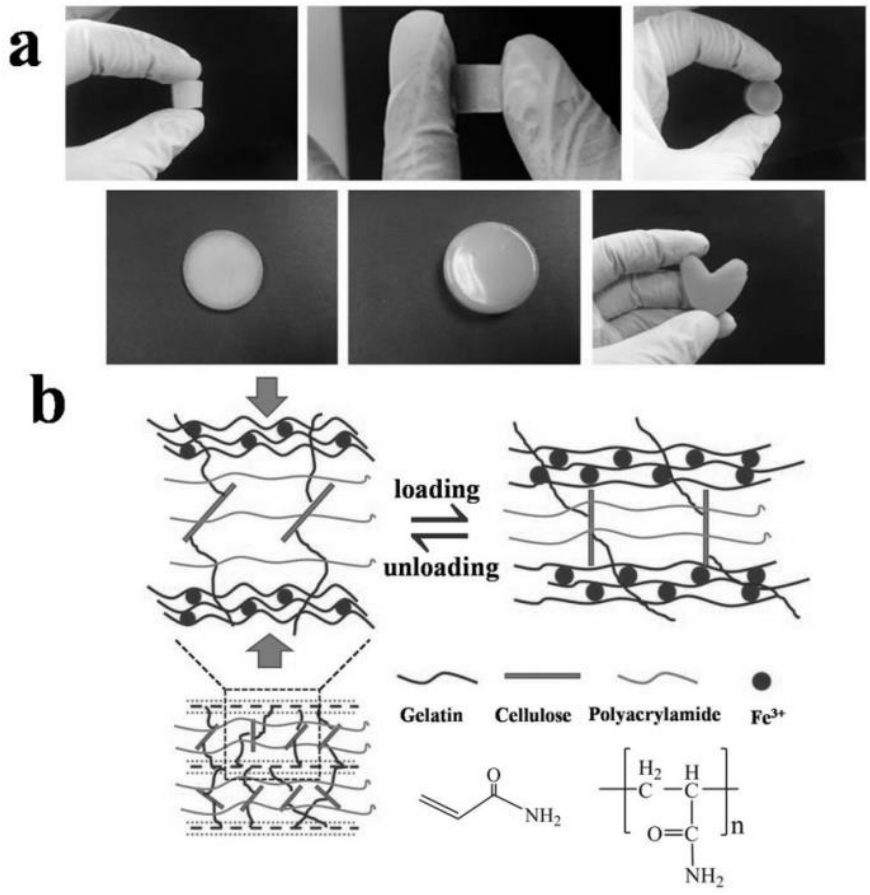

Figure 4. a)Hydrogelsloaded with different concentration of Fe^{3+}; b) Schematic of interaction mechanism of hydrogel under loading-unloading.

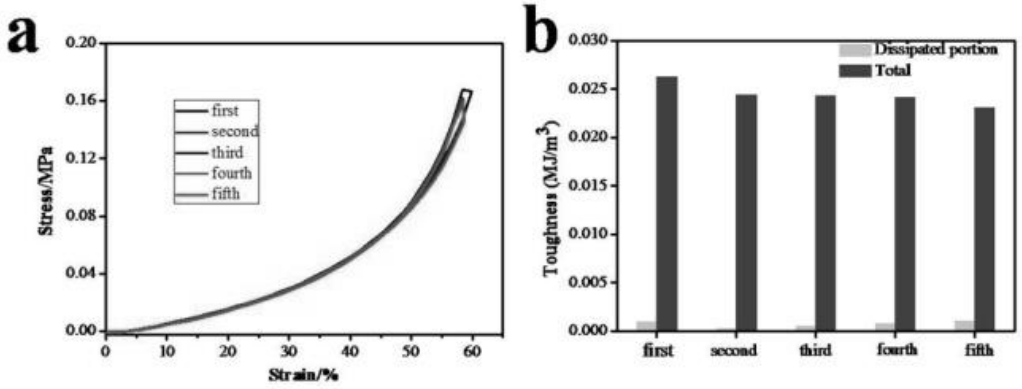

Figure 5. a) Five successive loading-unloading cycles of the hydrogel-9% ONFC; b) the toughness and the dissipated toughness of the hydrogel-9% ONFC calculated from the test (a).

A good elasticity was observed in the hydrogel. As depicted in **Figure 5a**, when finishing the five successive loading-unloading cycles test under 60% strain, the hydrogel-9% ONFC almost recovered to its original state. Figure 5bshows the toughness and the dissipated toughness of the hydrogel-9%

ONFC calculated from Figure 4a. It shows the dissipated toughness of the hydrogel-9% ONFC was little after five successive loading-unloading cycles. And the toughness recovered to 87.7% of its original value at the fifth loading-unloading. Five successive loading-unloading cycles were applied on the hydrogel-9% ONFC, such testing was aimed to make the hydrogel experience enough fatigue. As can be seen in Figure 5a, the compression curves almost superposed together under the five successive loading-unloading cycles test. Both gelatin/MFC hydrogel and DN hydrogel were prepared with two individual components that interact with each other through weak interaction. The present hydrogels have engineered acrylamide component into a chemically crosslinked network to form a woven structure on which a secondary crosslinking was imposed. And then the ionic coordination (CO_2LFe^{III}) was chosen as the third crossling to further strengthen the Gelatin/oxidized cellulose/pAAm hydrogel. The interaction mechanism in hydrogel may be clearly illustrated in Figure 4, the good elasticity of hydrogel might be due to the recorganizetion of the ionic coordination (CO_2LFe^{III}) and polyacrylamide molecular chain to form tridentates. These sacrificial bonds are homogeneously distributed in the main polymer chains at molecular level, which can provide strong, but reversible coordination interaction to dissipate energy efficiently.

Conclusion

In summary, a novel multiple-crosslinked hydrogel is prepared that combines both Schiff base, covalent crosslinking and multivalency ion pairing of Fe^{3+}-gelatin coordination. The ion paring interaction acts as the special dynamic junction, when the external loading was applied, the coordination bond serves as the reversible sacrificial bonds and rupture to dissipate energies. Based on the function mechanism, good elasticity and toughness property were achieved. Moreover, the mechanical property of the hydrogel can be easily tuned within a wide range for different applications by varying the concentration of gelatin, cellulose or Fe^{3+}-loading solution and so the number of ionic interaction. Because the interpenetrating network of gelatin/oxidized cellulose was weak and the cellulose would shift under pressure, and then engineered acrylamide component into a chemically crosslinked network to form a woven structure, the woven structure was expected to be more efficient to obtain mechanical strength with good elasticity and toughness. Such hydrogels are robust enough to let nutrients or cells free in and out, support chondrogenesis of the human mesenchymal stem cells (hMSCs) and promote cartilage regeneration.

Acknowledgments

The financial supports from the National Natural Science Foundation Commission of China (No. 51373158) the Sci-Tech and Innovation Talent Foundation of Henan Province (No. 144200510018) are gratefully acknowledged.

References

[1] Wei K, Zhu M, Sun Y, et al. Robust Biopolymeric Supramolecular “Host− Guest Macromer” Hydrogels Reinforced by in Situ Formed Multivalent Nanoclusters for Cartilage Regeneration[J]. Macromolecules, 2016, 49(3): 866-875.

[2] Balakrishnan B, Banerjee R. Biopolymer-based hydrogels for cartilage tissue engineering[J]. Chemical reviews, 2011, 111(8): 4453-4474.

[3] Van Vlierberghe S, Dubruel P, Schacht E. Biopolymer-based hydrogels as scaffolds for tissue engineering applications: a review[J]. Biomacromolecules, 2011, 12(5): 1387-1408.

[4] Lin P, Ma S, Wang X, et al. Molecularly Engineered Dual-Crosslinked Hydrogel with Ultrahigh Mechanical Strength, Toughness, and Good Self-Recovery[J]. Advanced Materials, 2015, 27(12): 2054-2059.

[5] Gong J P. Why are double network hydrogels so tough?[J]. Soft Matter, 2010, 6(12): 2583-2590.

[6] Calvert P. Hydrogels for soft machines[J]. Advanced materials, 2009, 21(7): 743-756.

[7] Guo T, Pei Y, Tang K, et al. Mechanical and drug release properties of alginate beads reinforced with cellulose[J]. Journal of Applied Polymer Science, 2017, 134(8).

[8] Yang W, Dominici F, Fortunati E, et al. Melt free radical grafting of glycidyl methacrylate (GMA) onto fully biodegradable poly (lactic) acid films: effect of cellulose nanocrystals and a masterbatch process[J]. RSC Advances, 2015, 5(41): 32350-32357.

[9] Dash R, Foston M, Ragauskas A J. Improving the mechanical and thermal properties of gelatin hydrogels cross-linked by cellulose nanowhiskers[J]. Carbohydrate polymers, 2013, 91(2): 638-645.

[10]Liao I, Moutos F T, Estes B T, et al. Composite three-dimensional woven scaffolds with interpenetrating network hydrogels to create functional synthetic articular cartilage[J]. Advanced functional materials, 2013, 23(47): 5833-5839.

[11] Chen Q, Chen H, Zhu L, et al. Fundamentals of double network hydrogels[J]. Journal of Materials Chemistry B, 2015, 3(18): 3654-3676.

FLS P-27

A TUNABLE BIOMATERIAL WITH GELATIN AND CARBOXYMETHYL CELLULOSE VIA TEMPLATE PRECIPITATION

Keyong Tang*, Ning Zhang, Xichan He, Tengfei Zhang, Yifei Chen, Xialian Fan, Fang Wang,

College of Materials Science and Engineering, Zhengzhou University, Zhengzhou, Henan 450000, *China,*

E-mail: kytang@zzu.edu.cn

A new gelatin/carboxymethyl cellulose(Gel/CMC) hybrid was prepared by an *in situ* precipitation method. Hydroxyapatie was precipitated in Gelatin and CMC bi-template and crosslinking sites were formed between the amino groups on GEL and the aldehyde groups on CMC through crosslinking using ethyl-3-(3-dimethylaminopropyl) carbodiimide iodide salt/N-hydroxysuccinimide (EDC/NHS). The gelatin/carboxymethyl cellulose/hydroxyapatite (Gel/CMC/HA) composite was successfully prepared with different template ratios in biomimetic environment. The structure and morphology of the composite were investigated by X-ray diffraction (XRD), Fourier transform infrared spectroscopy (FTIR), and scanning electron microscopy (SEM). Then this novel composite material was characterized, including mechanical properties. Moreover, biocompatibility was evaluated by 3-(4,5-dimethylthiazol-2-yl)-2,5-diphenyltetrazolium bromide (MTT) test.

The results revealed that hydroxyapatite (HA) was well assembled on the surface and inside both Gel and CMC molecular templates. Gel and CMC bi-template lead to more nucleation sites and active centers in comparison with a single Gel template system, and affect the orientation, size, and shape of the HA. SEM images showed that Gel/CMC/HA material had loose inner structure with irregular macro-pores, and HA crystals are almost completely cover the wall. The interconnected pores were in range from 100 to 300 μm in diameter. The high permeability of composite permitted the exchange of oxygen, nutrients, and soluble metabolites. It also possessed good mechanical properties and excellent biocompatibility. Based on the experimental results above, it was suitable for various clinical applications, such as cell scaffolds and tissue regeneration. This high-performance composite material was expected to be applied in fields of biomedicine as tissue guided regeneration material.

Keywords: gelatin, carboxymethyl cellulose, hydroxyapatite

1. Introduction

Tissue engineering material means that an ideal material is either used to induce tissue remodeling or as a carrier or template to implant cells and other growth factors for healing of tissue morbidity. Hence, it must be non-toxic, low-immunogenic, biocompatible, biodegradable, and have a corresponding matching mechanical property. Organic-inorganic composite systems have great potential in the development of biomaterials mimicking nature tissues.

Collagen is an important part of bone tissues in human and other mammals, with good biocompatibility. But its mechanical properties cannot satisfy for clinical requirements. Gelatin is an animal protein obtained by a controlled hydrolysis of fibrous insoluble collagen. It is easily obtained, with relatively cheap price. Reaction conditions to get gelatin are not so hard as collagen. Moreover, it has also been extensively explored as biomaterial for excellent properties, such as biocompatibility, biodegradation, non-toxicity, adsorption, and so on. So far, gelatin has been widely used for numerous biomedical applications as hard or soft capsules, hydrogels, microspheres and hydrogel fibers.(Dash, R 2013) However, the main disadvantages of gelatin are connected with its poor mechanical properties, which limit its applications as biomaterials. Cellulose is the most abundant natural resource in the world and possesses excellent biocompatibility. It has been used in both hard and soft tissue engineering.(Muller, F. A 2006) Carboxymethyl cellulose (CMC) is a linear polymer of b-D-glucose, which is fabricated by substitution of some of the hydroxyl groups of cellulose with carboxymethyl groups.(Muller, F. A 2006) Biomaterials based on cellulose or its derivatives have been widely used as hemodialysis membranes, enzymes or drug carriers and tissue repair matrices or scaffolds.(Ma, Z 2008; Laurence, S 2005; Fundueanu, G 2005) To date, many attempts have been made to modify the poor properties of gelatin including blending, compounding with natural fibers. Therefore, many researches introducing cellulose into gelatin are the effective work at the realm of reinforcement of gelatin in order to improve the mechanical properties of composite materials.(Martucci, J. F 2010) It is known that in nature human tissue, composites mainly comprised of hydroxyapatite (HA) nanocrystal and collagen (COL), under the micron size with excellent mechanical properties such as bone, teeth, are synthesized through self-assembling approaches.(Cui FZ 2007) In these structures, synergistic features are created by self-assembly of each component, usually comprising ordered distribution of hard segments in soft polymer matrix. A few researchers have developed various bio-mimetic ways to prepare composites, in situ precipitation method for example.

In the present work, gelatin/carboxymethyl cellulose/hydroxyapatite (Gel/CMC/HA) composites were prepared by an *in situ* precipitation method driven by collagen and cellulose template at 37 ^{o}C. Then, such biological cross-linker as ethyl-3-(3-dimethylaminopropyl) carbodiimide iodide salt/N-

hydroxysuccinimide (EDC/NHS) were used to obtain Gel/CMC/HA composite. Bi-templates (Gel and CMC), different ratio of two templates and EDC/NHS cross-linker were employed to investigate different effects on preparation of the resultant composites.

2. Material and methods

The Gel/CMC/HA composite was prepared by in situ precipitation method and lyophilization technique. Firstly, Gel and CMC were mixed at different weight ratio(0:10, 1:9, 3:7, 5:5, 7:3, 9:1, 10:0). Then, with the quality ratio of 3:7 (Gel+CMC: HA), Ca(NO3)2 and NH4H2PO4 was sequentially added into Gel/CMC system as a certain amount to regulate the properties of Col/Gel/BG composites. Biological cross-linker ethyl-3-(3-dimethylaminopropyl) carbodiimide iodide salt/N-hydroxysuccinimide (EDC/NHS) were used to obtain Gel/CMC/HA composite. Material was obtained by vaccum freeze drying at −50 ^{o}C for 72h (GT2-Type-8, LYOTECH).

Composition and morphology were respectively analyzed by Fourier transformed infrared spectroscopy (FTIR) (Nicolet iS10, USA), X-ray diffraction (XRD) (XD-3X, CHN) and scanning electron microscope (SEM) (Quanta200, USA). The compression performance of the composite scaffold was tested by universal testing machine (CMT4104, CHN).

The biocompatibility of Gel/CMC/HA composites was determined by a 3-(4,5-dimethylthiazol-2-yl)-2,5-diphenyltetrazolium bromide (MTT) colorimetric method. MTT test was carried out by mouse fibroblasts (Fbs) and the cytotoxicity of materials was evaluted according to ISO/TC194 file.

3. Results and Discussion

Figure 1 showed that the FTIR and XRD spectra of different Gel/CMC/HA composites. The results of FTIR and XRD indicated that carboxyl group of both Gel and CMC may serve as the deposition cite of calcium and phosphorus ions that these ions can deposit on Gel and CMC. It confirm incorporation well between HA and Gel or CMC template. Besides, amine groups(-NH_2) of Gel may have chelate reaction with calcium ion (Ca^{2+}) of HA. The calcium/phosphate ratio of different Gel/CMC/HA composites were also detected, about 1.67±0.6034. Combining the calcium/phosphate ratio test, inorganic phase of composite is similar to apatite in human bone tissue.(Clarke B 2008) After crosslinking by EDC/NHS, there has crosslinking reaction among composite material. And the orientation of hydroxyapatite(HA) along the c-axis is better as well as the higher crystallinity.

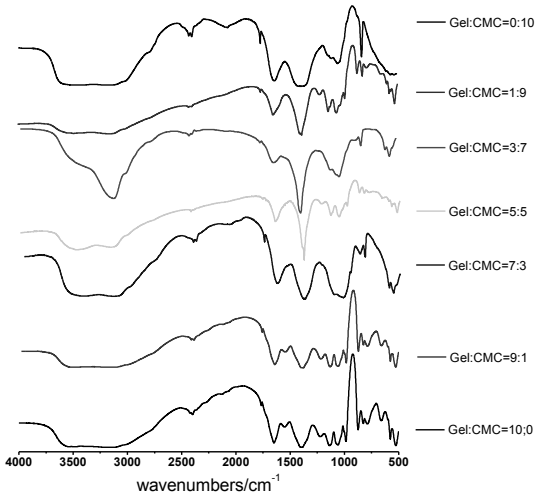
Gel:CMC=0:10
Gel:CMC=1:9
Gel:CMC=3:7
Gel:CMC=5:5
Gel:CMC=7:3
Gel:CMC=9:1
Gel:CMC=10;0
4000
3500
3000
2500
2000
1500
1000
500
wavenumbers/cm-1

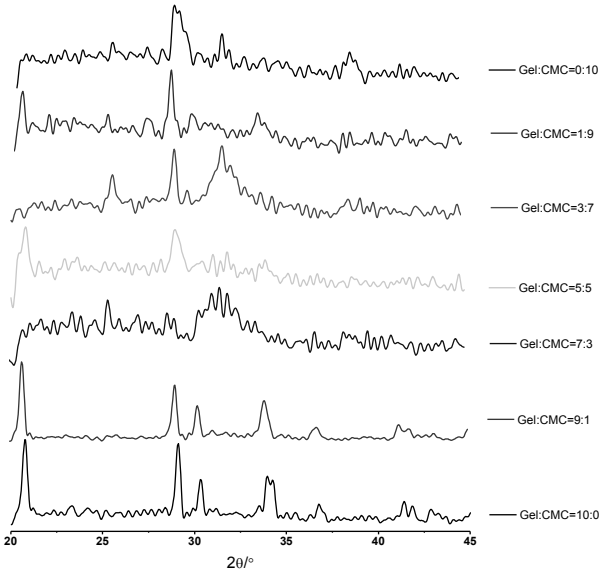
Gel:CMC=0:10
Gel:CMC=1:9
Gel:CMC=3:7
Gel:CMC=5:5
Gel:CMC=7:3
Gel:CMC=9:1
Gel:CMC=10:0
20
25
30
35
40
45
2θ/°

Figure 1 FTIR spectra and XRD spectra of different Cel/CMC/HA composites. The concentration for Cel/CMC and HA is 3:7 and the temperature is separately 37^{o}C.

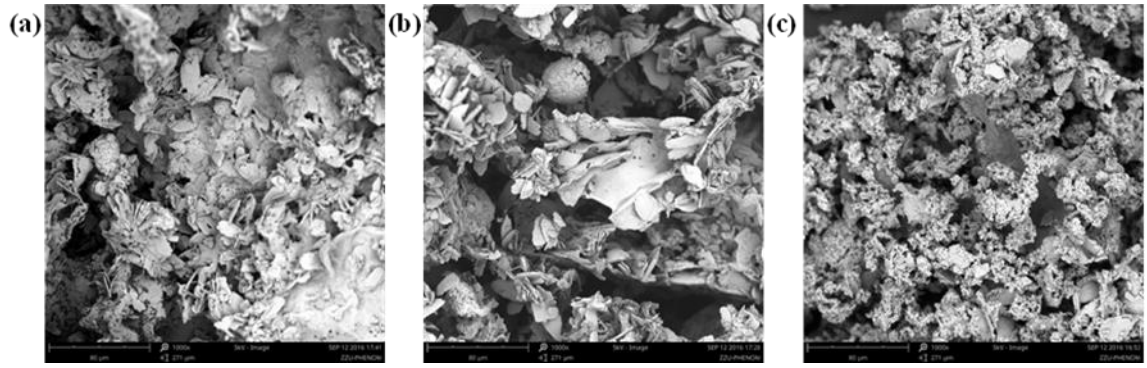

Figure 2 SEM images of different Cel/CMC/HA composites (cross section). The ratio of Cel/CMC: a is 3:7, b is 5:5 and c is 7:3. The concentration for Cel/CMC and HA is 3:7 and the temperature is 37^{o}C.

Figure 2 contained the section micromorphology of Cel/CMC/HA composites of different ratios. SEM images showed Figure 2 contains the section micromorphology of Cel/CMC/HA composites of different ratios all had irregular micropores and interior is compact. The resulting HA disperses homogeneously within Cel/CMC and combines with Cel/CMC durably. Composites formed an irregular and porous structure, with the diameters of a micrometer scale, dozens of micros. With the increasing CMC ratio in organic templates, more strip-like structure appeared and the deposition of HA was more compact. This micropore internal structure is desirable for bone cell growth. Moreover, the porosities observed in these composites suggest that they might be osteoinductive

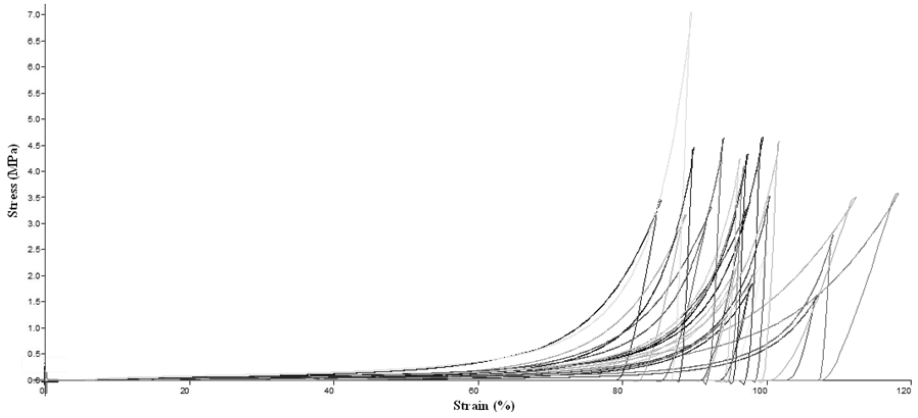

Sample	Weight ratio (Cel: CMC)	Weight ratio (Cel/CMC: HA)	Compressive strength (≈MPa)
Cel/CMC/HA	1:9	3:7	1.54
Cel/CMC/HA	3:7	3:7	1.86
Cel/CMC/HA	5:5	3:7	2.67
Cel/CMC/HA	7:3	3:7	4.53
Cel/CMC/HA	9:1	3:7	6.97
Cancellous bone	-		1-20

Figure 3 Mechanical properties of different Cel/CMC/HA composites.

Compressive strength of the prepared composite materials was shown in Figure 3. It gave the data obtained from mechanical compressive tests of composite samples and compares them with cancellous bone. Generally, compressive strength was increased with the induction of CMC into organic component. Besides, to a certain extent, Crosslinking reaction should increase the compressive strength. Phenomenon illustrated that the mechanical response was significantly affected by the proportion of CMC in the organic system. Mechanical property played an important role in the use of tissue engineering biomaterials. The compressive strength of all samples met the requirement of cancellous bone tissue.

In normal control group and the test materials group, cells were normal adherent growth, long spindle shaped, with lucent cytoplasm. The optical density (OD) values at 570 nm were as shown in Table 5. The cell relative growth rates of all Cel/CMC/HA composite are higher than 100%. According to cytotoxicity grading standards (0 to 5) and evaluation of results specified in ISO/TC194 file, it is known that the results for the diagnosis of grade 0, namely Non-cytotoxic. The MTT assay results indicated that Cel/CMC/HA materials exhibited non-cytotoxicity and good biocompatibility.

Table 1 OD values and RGR of MEF-WT cell being cultured for 2, 4 and 7 days.

Groups	2d		4d		7d	
score	OD value	RGR (%)	OD value	RGR (%)	OD value	RGR (%)
Normal control	0.545± 0.006		0.311± 0.001		0.132± 0.001	
50% Composite extraction solution	0.755± 0.075	153	0.521± 0.005	157	0.268± 0.019	122
100% Composite extraction solution	0.853± 0.024	224	0.636± 0.004	244	0.441± 0.016	278

Conclusion

According to the principle of in situ precipitation method, mineralization occured on the Gel and CMC organic templates. HA crystal are homogenously distributed inside and on the Gel/CMC as determined by SEM and XRD analysis. The chemical interactions between the inorganic component and Gel/CMC polymer probably take place via Ca2+ ions and carboxylate groups of the polymer. Mechanical properties of Cel/CMC/HA satisfy the requirement of biomaterial and could be changed with adding different ratios of CMC. The incorporation of HA improves the biological performance of the composites. Cel/CMC/HA materials exhibit non-cytotoxicity and good biocompatibility.

In summary, the obtained Cel/CMC/HA composites is a promising materials for bone tissue engineering. This biomaterial seems to show suitable properties to be considered as a good candidate for bone tissue engineering.

Acknowledgments

The financial supports from the National Natural Science Foundation Commission of China (No. 51373158) the Sci-Tech and Innovation Talent Foundation of Henan Province (No. 144200510018) are gratefully acknowledged.

References

1. Dash, R., Foston, M., Ragauskas, A. J. Improving the mechanical andthermal properties of gelatin hydrogels cross-linked by cellulosenanowhiskers. Carbohydrate Polymers, 2013, 91(2), 638–645.
2. Muller, F. A., Muller, L., Hofmann, I., Greil, P., Wenzel, M. M.; Staudenmaier, R. Biomaterials, 2006, 27, 3955–3963.
3. Hofmann, I., Muller, L., Greil, P., Muller, F. Surf. Coat. Technol. 2006, 201, 2392–2398.
4. Ma, Z., Ramakrishna, S. J. Membr. Sci., 2008, 319, 23–28.
5. Laurence, S., Bareille, R., Baquey, C., Fricain, J. C. J. Biomed. Mater. Res., Part A., 2005, 73A, 422–429.
6. Fundueanu, G., Constantin, M, Esposito, E, Cortesi, R., Nastruzzi, C., Menegatti, E. Biomaterials, 2005, 26, 4337–4347.
7. Martucci, J. F., Ruseckaite, R. A.. Biodegradable three-layer film derivedfrom bovine gelatin. Journal of Food Engineering, 2010, 99(3), 377–383.
8. Cui FZ, Li Y, Ge J. Self-assembly of mineralized collagen composites. Mater Sci Eng R, 2007, 57:1–27.
9. Clarke B. Clin J Am Soc Nephrol, 2008, 3, 131

ECT P-49

PRODUCTION OF SALINE TOLERANT ALKALINE LIPASE ENZYME BY USING HALOPHILIC ORGANISMS FOR THE TREATMENT OF HYPER-SALINE SOAK LIQUOR DISCHARGED FROM TANNERIES

Vasudha Priyadharsini, Maharaja.P, Shabarita, Mahesh.M, Swarnalatha.S, and Sekaran.G*

Environmental Science and Engineering Division, Council of Scientific & Industrial Research (CSIR), Central Leather Research Institute (CLRI), Adyar, Chennai 600 020, India

** Corresponding Author: Dr. G. Sekaran,*

Email: ganesansekaran@gmail.com

This present investigation was mainly focused on the enzymatic degradation of soluble bio molecules (lipids) present in hyper saline soak liquor discharge from tanneries. The halophilic organisms were isolated from different sources acclimatized with soak liquor and screened for their lipolytic activity at saline medium. The lipase was produced from two selected halophilic microbes were isolated from soak liquor (SL) and SL acclimatized deep soil and named as DS-1 and SOS-1. The biochemical characteristics and 16SrDNA analysis were done for the identification of organisms. The optimization studies on protease production was done and it was found to be time at 48 h; pH, 9-10; Temperature 40°C, substrate concentration 2% and the salinity of 4% show the maximum yield of lipase production. The produced lipase solution was purified by dialysis and the specific activity was evaluated. Additionally the stability of lipase was carried out by varying pH, temperature, TDS and metal ions. The degradation was carried out at different time interval and it was found that there was the complete degradation of lipid content of soak liquor was obtained at 120 min. The degradation efficiency was evaluated by the conversion of lipids into glycerol and fatty acids. The instrumental analysis such as UV-Visible and fluorescence spectroscopic studies were confirmed the enzymatic degradation of lipids into their smaller units in hyper saline soak liquor and it may favour for the effective treatment of soak liquor by further unit operations.

Key words: soak liquor, lipase, halophilic organisms, lipids, enzymatic degradation

1. Introduction

There has been constant research on bioremediation of lipid-rich wastewater, either aerobically or anaerobically. The treatment of lipid laden waste water is a serious problem as they reduce the BOD and COD of the water which poses a great threat to aquatic life if not treated efficiently (Kanmani et al., 2015). Enzymes have been demonstrated to be efficient biocatalysts in many biomass conversion processes and are becoming a cost effective alternative in many applications compared to the whole microorganism (Kobayashi et al., 2001). Applications of enzymes and whole cell biocatalysis for

producing diverse types of chemical and biological substances have become a proven technology in chemical and pharmaceutical industries because enzyme-based reactions usually lead to a reduction in the process time, number of reaction steps (Jung-Min et al., 2015) .In particular, enzymes provide a more powerful way of producing enantiomeric pure compounds mainly through high chemoselectivity, regioselectivity, and streoselectivity.

Lipases (triacylglycerol hydrolases, E.C. 3.1.1.3) have innumerable application significance importance due to their wide range of reactions. Lipases are ubiquitous enzymes of considerable physiological significance and industrial lipases catalyse the hydrolysis triglycerides to diglycerides, monoglycerides, glycerol and fatty acids In particular, lipases from thermophiles are expected to play a significant role in industrial processes as they are thermostable and resistant to chemical denaturation. (Liu et al., 2011; Cammarota & Freire, 2006; Hasan et al., 2006). Lipases that are produced from thermophilic bacterial strains increase the efficiency of the lipid hydrolysis process. Halophiles have expressed greater importance in hydrolysis of oil because of the increased miscibility of lipids and other hydrophobic substrates in water; increased reactant mobility, higher temperature associated faster reaction rates; and thus the efficiency of hydrolysis of lipid by halophiles was higher than the mesophiles (Reis & Miller, 2009). Recently, several lipases have been isolated identified and characterised from halophilic isolates, mainly Pseudomonas sp. Amongst the various bacterial lipases that are researched upon, the strains from the genera *Pseudomonas* and *Bacillus sp* have distinct properties of high enantio selectivity and halo tolerant stability activity in broader range of pH, enabling them as catalysts of choice by most pharmacists, microbiologist's environmentalists (Hills, 2003; Bastida et al., 1998).

Hyper saline effluents are generated by various industrial activities. This wastewater, rich in both organic matter and total dissolved solids (TDS), is difficult to treat using conventional biological wastewater treatment processes (Wilson et al., 2006). Use of halophilic bacteria is required the interest in treating that kind of wastewater is growing at a fast rate. Among the industries generating hypersaline effluents, tanneries are prominent in India. Due to the variety of chemicals added at different stages of processing of hides and skins, the wastewater has complex characteristics. In this study, tannery wastewater was collected after the soaking of hides and skins. Salt (sodium chloride (NaCl)) is used to preserve the fresh skins from decomposition immediately after they are stripped in the slaughterhouse, and the excess of salt has to be removed in the tannery before further processing. This is done by soaking, using a lot of water, which generates the first source of effluent (Sekaran et al., 2011;Gholamreza & Behnam, 2009). (Karthikeyan et al., 2011). The soak liquor is characterised by high organic load, high suspended solids (sand, lime, hair, flesh, dung, etc.) and high salinity. Because of that high salt content, this waste- water is generally segregated and sent to solar evaporation pans (SEP's). Lipolytic strains isolated from industrial effluents show potential ability in degradation and bioremediation (Hasan et al., 2006). The hypersaline water obtained from tannery industry act as suitable substrate upon which salt tolerant lipase having various salt concentration can be used e can effectively use to degrade the lipids present in the tannery waste water. The present investigation is focused on the isolation and identification of halo tolerant organism for the production of lipase enzyme for the degradation of lipids present in the soak liquor.

2. Materials and methods

2.1. Materials

All the chemicals such as Lipase enzyme (produced from *Pseudomonas japonica* strain), Poly vinyl alcohol, triton-X-100, sodium chloride, calcium chloride, sodium orthophosphate, disodium hydrogen phosphate ethanol, acetate, phenolphthalein indicator, phospho vanillin, diethyl ether brought from Hi-media chemicals.

2.2. Isolation and Screening of lipase producers at saline medium

Bacterial strains were isolated from the soak liquor effluent, which was serially diluted and the higher dilutions were plated on minimal media supplemented with 1% (v/v) and 1% sewage water incubated overnight at 37°C. Discrete colonies were sub-cultured in the same medium and pure cultures were obtained. They were streaked on tributyrin agar (TBA) plates to screen for lipase activity. Lipase producers show a zone of clearance around the area of growth that is attributable to the butyric acid released upon tributyrin hydrolysis. Based on the size of the zones in the agar plates, the lipolytic microorganisms were selected and maintained in nutrient agar slants and stored at 4 °C. The isolated colonies were continuously sub cultured to maintain the viability of the cultures. These cultures were grown on special media- Tributyrin Agar with different concentrations of salt viz. 1%, 2%, etc. till 4%. The plates were incubated for the observation of clear zone of an individual organism in all 4 different concentrations. Those organisms which were grown in all 4 concentrations were selected for the production of the enzyme and also chosen for further assays.

2.3. Molecular identification

The two best isolates were identified using 16S rRNA gene sequence based molecular technique. Single colonies from freshly streaked agar plates were inoculated into nutrient broth. Sequence data obtained were analysed and consensus sequences were generated from forward and reverse sequences using 'Aligner' software. These sequences were subjected to BLAST (Basic Local Alignment Search Tool) with NCBI (National Center for Biotechnology Information) Gen Bank database and the cultures were identified. Phylogenetic trees were constructed using the neighbour joining method. Further studies were restricted to the single best lipase producer (Gururaj et al., 2016).

2.4. Production extraction and purification of bacterial culture

Minimal media was prepared by the following composition with 1% dextrose as sole carbon source. The trace elements were added in the concentration of 2mL/1000L. The media was enriched with the given substrate- animal fat at a concentration of 1% for 100mL. After the centrifugation of sample from the production medium, acetone precipitation was carried out and it was incubated at 18°c for overnight. The precipitate was then collected by centrifugation at 4°c and suspended in corresponding pH solution.

2.5. Optimization studies

The effect of time was estimated at different intervals viz., 12, 24, 36, 48, 72 h at 37˚C and the estimation of lipids, lipase activity, estimation of fatty acids and glycerol was performed after every time of the study. The study was performed for different pH analysis viz 2-10 pH and the lipase activity, lipid,

fatty acid and glycerol were estimated under the standard conditions. The culture broth was added and incubated at different temperature 20-60°C and the lipase activity, lipid, fatty acid and glycerol were estimated under the standard conditions. The pH of the medium was adjusted to the optimized value and incubated at optimized time and temperature and different concentration of salt (NaCl) viz., 1-6% was added to the media and the culture broth was added and further studies were carried out.

2.6. Analytical Methods

2.6.1. Determination of lipase activity

Lipase activity was determined by using 5ml of olive oil substrate is mixed with 2ml of 0.03% Triton X-100 , 2ml of 3M NaCl , 1ml of $CaCl_2$soln , 4ml of phosphate buffer(at pH 7) followed by 5 min shaking. Then 1ml of enzyme solution was added and kept in shaking incubator for 15 min.10ml of 1:1 Ethanol: acetone solution and phenolphthalein indicator was added followed by 0.02N of sodium hydroxide titration (NaOH). The appearance of pale pink color is the end point. This was done with reference to (Naci & Ali, 2002) with minimal modifications. The lipids present in the soak liquor sample was estimated by using phospho vanilin reagent (Joseph et al., 1972). For fatty acid determination diethyl ether and ethanol mixture was added to the sample and blank and titrated against NaOH.For glycerol determination sodium peroxidase & acetyl acetone reagents were used and the absorbance was taken at 410nm. The extracted lipase enzyme was characterized by the instrumental analysis such as FT-IR, TGA and DSC analysis.

2.7. Preparation and degradation Studies for fat content of soak liquor

1 kg of animal hide soaked in 3 L of water for overnight and left it for settling for about 2 h, and then it was taken after the primary clarification using $AlCl_3$. The degradation studies were carried out by introducing the lipase enzyme derived from the microorganism *Pseudomonas japonica* by altering the various parameters such as time, temperature and pH.

2.8. Instrumental Analysis

The lipase enzyme sample was mixed with KBr of spectroscopic grade and made in the form of pellets at a pressure of about 1 MPa. The pellets were about 10 mm in diameter and 1 mm in thickness. The samples were scanned in the spectral range of 4000–400 cm−1. Thermo gravimetric analysis (TGA) Differential Scanning Calorimetric analysis (DSC) were carried out under nitrogen atmosphere from 30 to 800 with a temperature gradient of 10°C min^{-1} and scans were recorded using a TGA Q50. The degradation of soak liquor was studied by UV visible absorption spectra using CARY 5E UV–VIS-NIR Spectrophotometer, USA. The fluorescence spectrophotometer study was carried out to determine the excitation and emission characteristics of both soak liquor and the degraded products, in range of λ 200-800nm (Cary Eclipse, USA).

3. RESULTS AND DISCUSSION

3.1. Bacterial isolation and identification for lipase activity at saline medium

The bacterial strains that were isolated from soak liquor were screened for lipase secretion by selection on tributyrin agar plates.

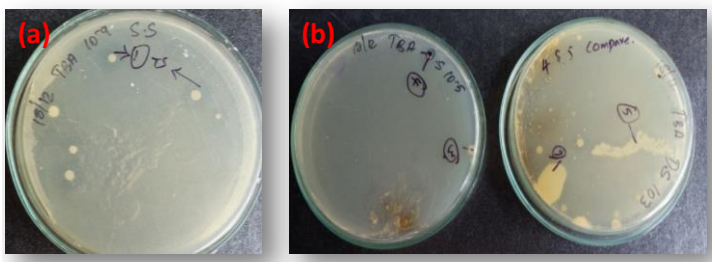

Fig.1. (a) Screening of organisms from acclimatized soak liquor sample (b) Deep soil sample

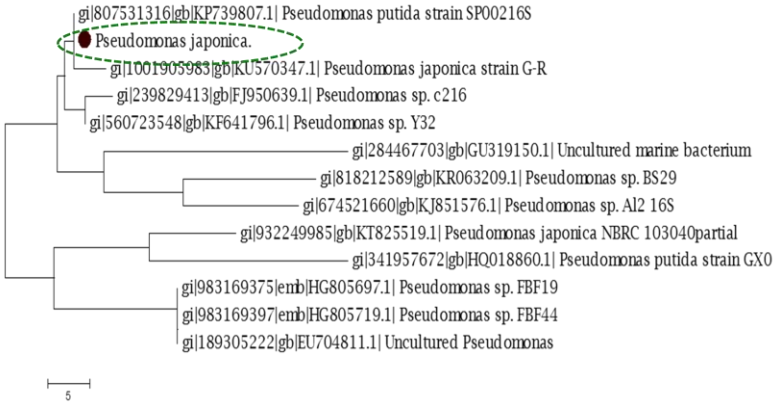

Fig.2. Phylogenetic tree analysis lipase producing organism- *Pseudomonas japonica*

The SOS-1 strain that showed a larger zone of clearance around the colony was selected for further studies (Fig:1). Biochemical characterization revealed that the strain is aerobic, gram negative and non-motile. The strain was confirmed as *Pseudomonas sp*. (Fig:2) SOS-*1* by 16S rDNA sequencing which is in accordance with Bergey's Manual of Determinative Biology. The zone of hydrolysis at various concentration such as 1%, 2%, 3% and 4% was observed and the salt tolerant ability of the microorganism was found to be effective at 4% of (4g/100ml) concentration.(Fig.3h). Thus we conclude the microorganism was able to grow in effectively at saline conditions.

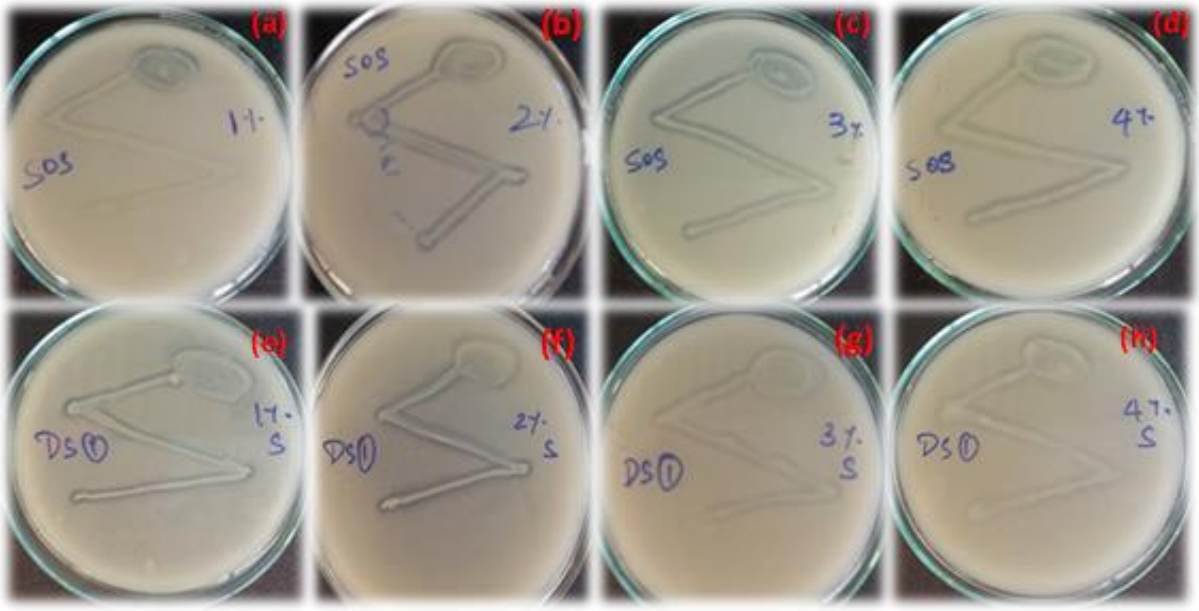

Fig.3. Salt tolerant assay at various NaCl concentrations for the samples SOS-1, (a-d) and DS-1(e-h)

3.2. OPTIMIZATION STUDIES

The optimum time of the lipase activity was found to be 36hrs (12.6 U/mL). Lipase activity increased with increasing pH and peaked at pH 9 (28.5 U/mL), after which it gradually dropped. Based on this observation, it could be inferred that the enzyme is alkaliphilic in nature. These results reveal that the enzyme is moderately thermophilic in nature (Kim et al., 2009) .The optimum temperature for lipase activity was 40 ˚C (Snellman , et al., 2004) .The enzyme activity increased with increasing temperature and peaked at 40°C .After which it dropped down at 30˚C. The stability of SOS-1 lipase was maintained upon pre-incubation at temperatures up to 50°C (Fig.6) Exposure to 60°C or higher, caused thermal denaturation of the lipase.

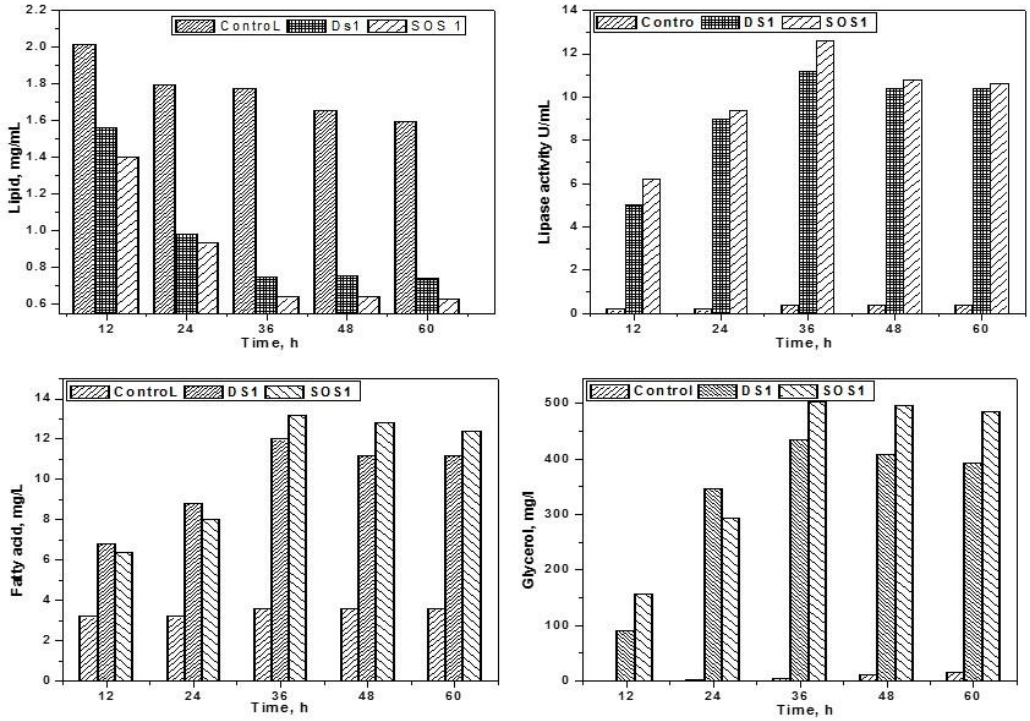

Fig.4. Optimization studies on the effect of time for the production of lipase using *Pseudomonas japonica* with respect to (a) lipid degradation, (b) lipase activity (c) Glycerol and (d) fatty acid formation

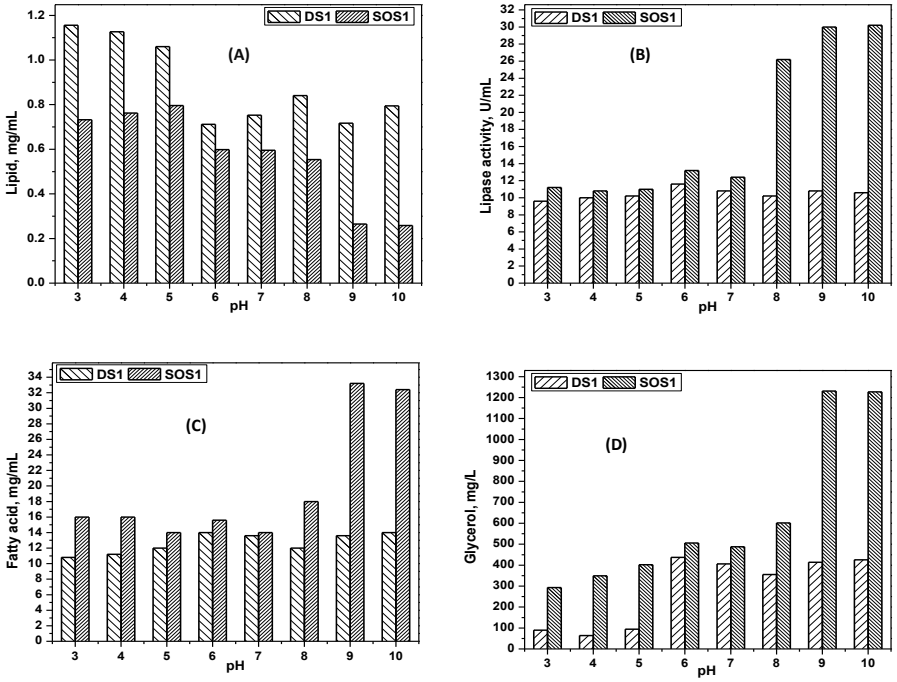

Fig.5. Optimization studies on the effect of pH for the production of lipase using *Pseudomonas japonica* with respect to (a) lipid degradation, (b) lipase activity (c) Glycerol and (d) formation

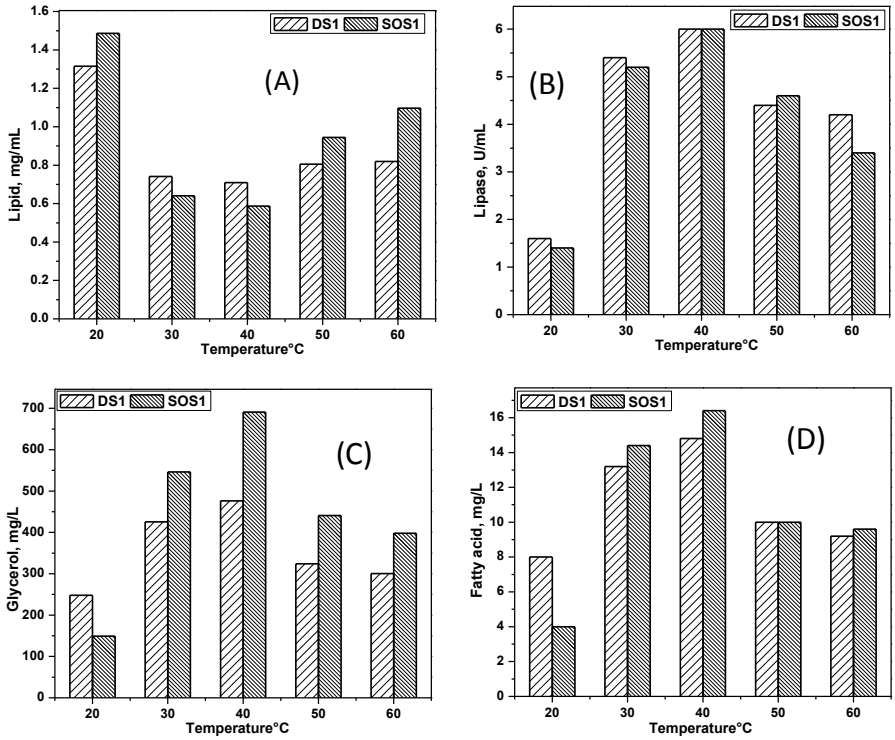

Fig.6.Optimization studies on the effect of temperature for the production of lipase using *Pseudomonas japonica* with respect to (a) lipid degradation, (b) lipase activity (c) Glycerol and (d) formation

3.3. Characterization of Lipase extracted from *Pseudomonas japonica*

The FTIR spectra of lipase enzyme were shown in Figure. FT-IR spectra showed (Fig.) a broad envelope ranging from 3600 cm−1 to 3100 cm−1 (centred on 3461 cm−1) which corresponds to the N–H stretching vibrations of peptide whereas N-H bending was around 1640 cm−1 for primary amine. The peak at 1402 and 992 cm−1 corresponds to O-H bend in carboxylic acid and its C-N stretching around 1112 cm-1.

The presence of peptide bond in lipase was confirmed through the amide stretching at 1640 cm-1. TGA thermogram of extracellular lipase enzyme showed 3.01% weight loss at the temperature 245.25°C due to the removal of moisture. Thereafter, 11.06% of weight loss occurred at 411.77°C, where the actual stable compounds are degraded. After this decomposition, there was a decrease in weight loss of 21.58% was observed at 565.68°C o and the final residue of 75.89% reveals the thermal stability of the enzyme at the end of the scan (800°C). The TGA of Lipase enzyme from *SOS-1 species* showed better stability behaviour. The DSC spectrum of lipase showed three thermal transitions by showing the endothermic peaks appear at 76.23°C and 232.3

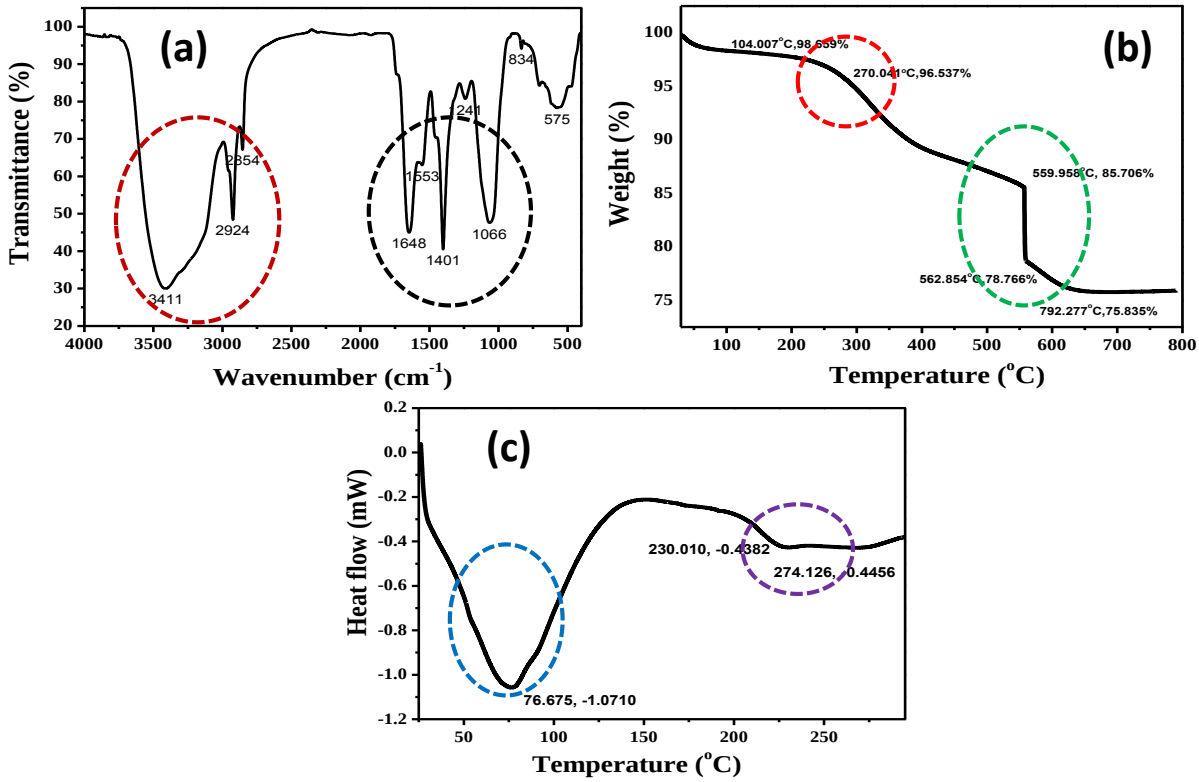

Fig.7. (a) FT-IR Spectra (b) TGA and (c) DSC analysis of the lipase enzyme isolated from *Pseudomonas Japonica*

3.4. DEGRADATION STUDIES

The optimum time for the degradation of soak liquor using the lipase enzyme was found to be at 60 min. This can be inferred from the hydrolysis of the lipids which was 58(mg/L) initially converted into to their smaller constituents such as fatty acids and glycerol which were 25(mg/L) and 20(mg/L) at the end of the reaction. The effect of pH (2–10) on the degradation of lipids using liapse (2 mg) was studied. The activity of lipase increased with increase in pH and it was observed that the maximum amount of formed glycerol and fatty acids were formed at time, 60 min and pH 7.

The degradation of lipids in soak liquor effluent using lipase was active in the weakly basic of pH 7 and 10 with the glycerol and fatty acids formation of about 25 (mg/L) and 20 (mg/L) respectively and thus attained stability (Fig 6.) At other pH hydrolysis did not occur which be attribute to the loss of its activity. It is known that change in pH always affects the activity of wide spectrum of intracellular enzymes, and they may be involved in opposing systems that are activated or inhibited .The ideal temperature for the degradation of the of the lipids was recorded to be 40˚C. The initial amount of lipid content was found to be 30 (mg/L) which hydrolysed effectively into 15(mg/L) of glycerol and fatty acids.

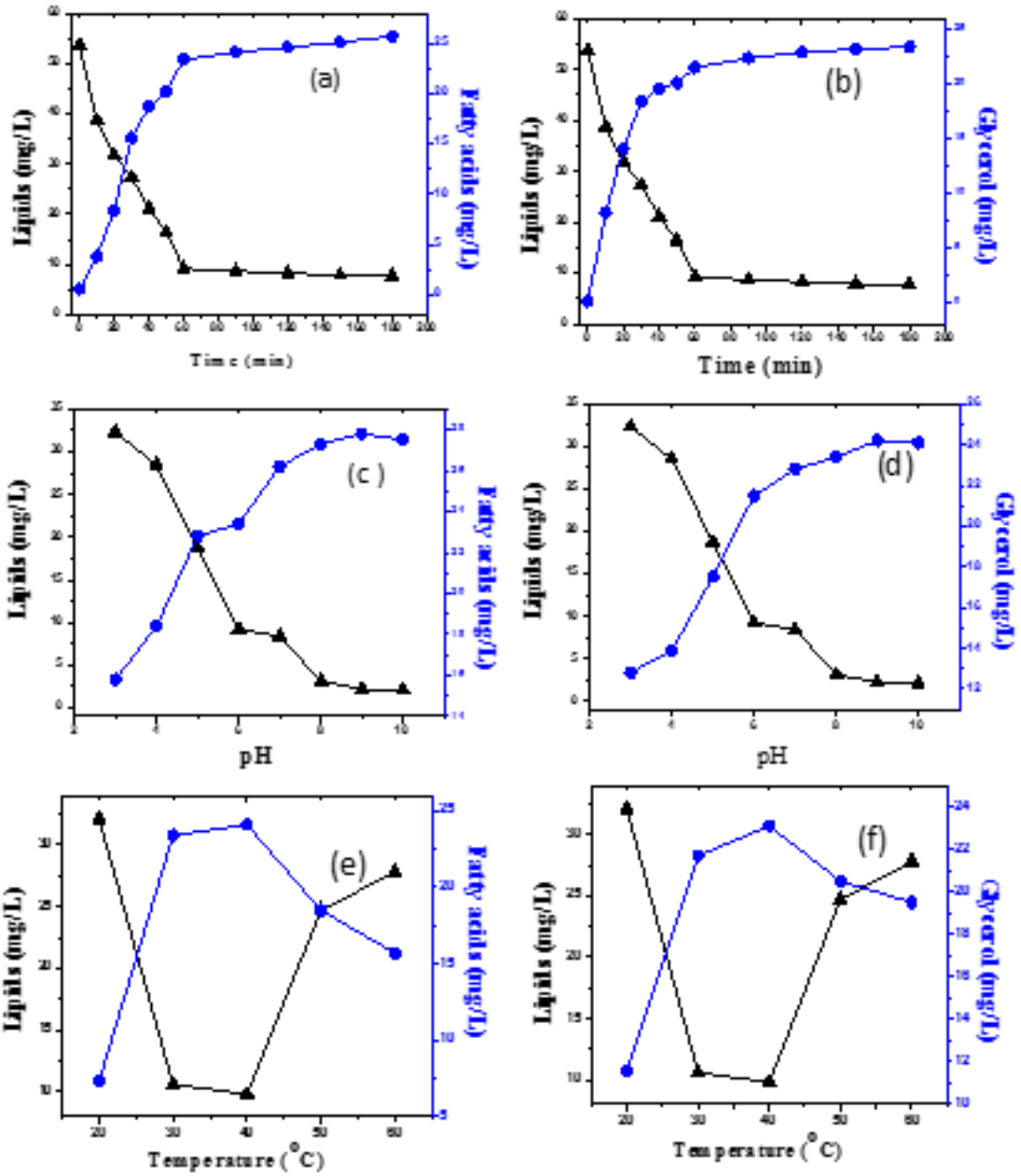

Fig.9. Optimization of (a, b) time (c, d) pH and (e, f) temperature for the degradation of lipid content of soak liquor with respect to fatty acid and glycerol formation

3.5. INSTRUMENTAL STUDIES FOR LIPID DEGRADATION

The degradation of fat content of soak liquor was confirmed by UV-Visible and Fluorescence spectroscopy studies were shown in Fig. 9(a) and Fig. 9 (b). The UV spectrum show the peaks at near

280nm and 220nm, reason for the presence of fatty components of soak liquor. After the treatment with different time interval from 20 min to 60 min, the intensity of the respective peaks were decreased and also shifts in the peaks were observed. This was confirmed the degradation of fat content of soak liquor.

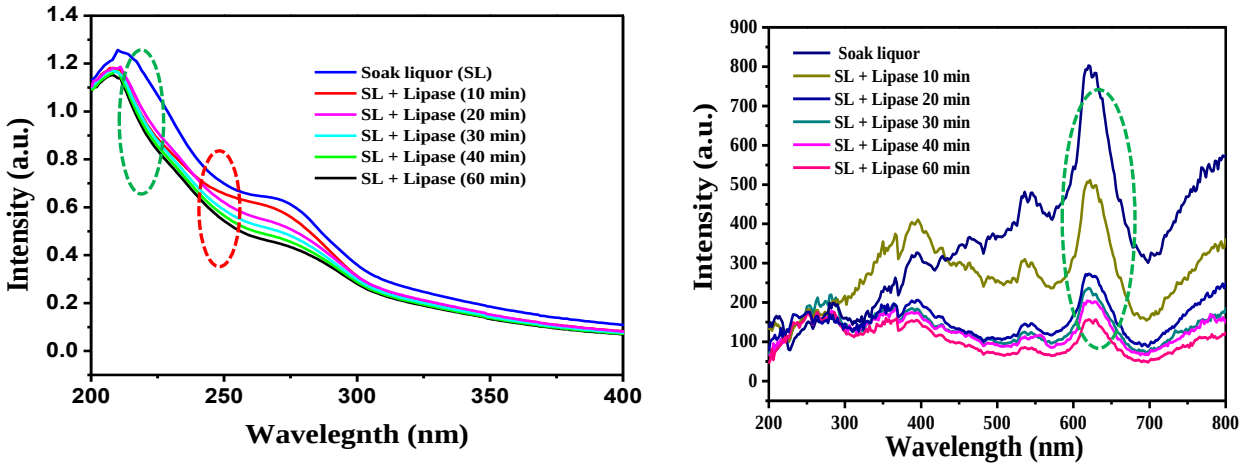

Fig.8. a) UV-Visible Spectroscopy study indicating the treatment of soak liquor with lipase enzyme b) UV-fluorescence Spectroscopy denoting the degradation of fat content in soak liquor

4. CONCLUSIONS

SOS-1 *was* isolated from different soil samples of CLRI, the isolates were screened for lipolytic hydrolysis by rapid screening methods. 2 isolates were taken and streaked over TBA plates with different salt concentration to determine their saline tolerance. Out of these 2, 1 best organism was isolated based on their lipolytic hydrolysis zones. This organism was taken for morphological, bio-chemical and physiological characterization. The isolates were identified as *Pseudomonas sp.* The production of lipase was carried out in minimal media with animal fat as substrate supplemented with carbon source-dextrose and trace elements. The results of optimization studies showed analysis of the enzyme activity which amounted uptp 1360 U/ml .Hence this strain was selected and 16s rRNA study was performed. The enzyme was extracted by acetone precipitation method. The lyophilized powder of the enzyme was subjected to FTIR analysis and TGA-DSC. The FT-IR analyses of the extracted enzyme were given positive results for the presence of lipase by analysing functional group. The FT-IR absorption peak values for lipase from the isolated culture results and the standard results were compared. The findings from the present investigation suggest that lipase produced from *Pseudomonas Japonica* .

SOS-1 and the lipase produced by it are quite promising and can be used for further studies. Pseudomonas is predominantly used in the degradation of oils and fat substances with ease compared to the other bacterial strains producing lipase enzyme and thus this isolate consists desirable features that could be favourably exploited for the treatment of wastewaters high in fat and oil contents. . Purification and characterization of lipase from SOS-1 has further revealed its industrially useful properties such as stability at high pH values, high temperatures, and in the presence of high salinity.

Such traits mean that the use of this enzyme could be extended to diversified industrial sectors such as detergents production, thereby giving it an edge over other.

5. ACKNOWLEDGEMENTS

The authors acknowledge CSIR-CLRI, India for granting financial support from STRAIT project (CSC 0201) and INDEPTH BSC 0103 to carry out this research work.

6. REFERENCES

1. P. Kanmani, K. Kumaresan and J. Aravind, "Utilization of coconut oil mill waste as a substrate for optimized lipase," Electronic journal of Biotechnology, pp. 20-28, 2015.
2. S. Kobayashi, H. Uyama and S. Kimura, "Enzymatic polymerization.," chem rev,**12**, pp. 3793-3818, 2001.
3. C. Jung-Min, H. Sang-Soo and K. Hak-Sung, "Industrial applications of enzyme biocatalysis: Current status and future aspects," 2015.
4. G. Liu, Z. Liang, S. Yang, P. Du, Y. Yang and Y. Chen, "Bio-treatment of grease wastewater: Research progress," Chin J Appl Ecol, pp. 2219-2226, 2011.
5. M. Cammarota and D. Freire, "A review on hydrolytic enzymes in the treatment of wastewater with high oil and grease content.," Bioresource Technology, pp. 2195-2210, 2006
6. F. Hasan, A. Shah and A. Hameed, "Industrial applications of microbial lipases," Enzyme Microbial Technology, **29**, pp. 235-251, 2006.
7. P. Reis, K. Holmberg, H. Watzke, M. Leser and R. Miller, "Lipases at interfaces: a review," , pp. 237-250, 2009.
8. G. Hills, "Industrial use of lipases to produce fatty acid esters," **105**, pp. 601-607, 2003.
9. Bastida, A, P. Sabuquillo, P. Armisen, R. Fernández Lafuente, J. Huguet and Guisan, "A single step purification, immobilization and hyperactivation of lipases," **58**, pp. 486-493, 1998.
10. L. Wilson, J. Palomo, G. Fernandez-Lorente, A. Illanes and J. Guisan, "Effect of lipase–lipase interactions in the activity, stability and specificity of a lipase from Alcaligenes sp," pp. 259-264, 2006.
11. G. Sekaran, S. Karthikeyan, K. Ramani, B. Ravindran, A. Gnanamani and A. Mandal, **9**, pp. 499-504, 2011.
12. M. Gholamreza, M. Maryam and B. Behnam, **43**, pp. 1295–1302., 2009.
13. S. Karthikeyan, S. Titus, A. Gnanamani, A. B. Mandal and G. Sekaran, **42**, pp. 438-455, 2011.
14. D. Naci and A. Ali, "Partial purification of intestinal triglyceride lipase from Cyprinion heckel and effect of pH on enzyme activity.," **26**, pp. 133–143., 2002.
15. Hassan F, Shah A, Hameed A. Industrial application of microbial lipases. Enzyme Microb Technol pp.35–51,2006
16. Gururaj P, Process optimization for production and purification of a thermostable, organic solvent tolerant lipase from *Acinetobacter sp.* AU07. *Braz J Microbiol.* (2016)

17. Joseph AK, Shauna A, James M. Chemical basis of the sulfo-phospho-vanillin reaction for estimating total serum lipids. Clin Chem pp.199–202,1972
18. In-Hye P, Kim SH, Lee YS, Purification, and characterization of a cold-adapted lipase produced by *Acinetobacter baumannii* BD5. *J Microbiol Biotechnol* :pp128–135 , 2009.
19. Snellman EA, Colwell RR. Acinetobacter lipases: molecular biology, biochemical properties and biotechnological potential. *J Ind Microbiol Biotechnol*. pp.391–400,2004.
20. Saisubramanian N, Sivasubramanian S, Nandakumar N,Indirakumar B, Chaudhary N, Puvanakrishnan R. Two step purification of *Acinetobacter* sp. lipase and its evaluation as a detergent additive at low temperatures. *Appl Biochem and Biotechnol*. 150 pp.139–156,2008.

IVL P-35

LEATHER JACKET FISH SKINS - EXPLORED POTENTIAL RAW MATERIAL FOR LEATHER INDUSTRY

R Venba, MalathyJawahar, Abhinandan kumar, R Aravindhan,V Karthik N.K.Chandra Babu

Central Leather Research Institute, Adyar, Chennai – 600 020, India

venba@clri.res.in, venbakasi@yahoo.co.in

ncreasing price of conventional raw material and absence of technology among tanners for the conversion of alternative raw materials into leather poses a niche area. There is a great potential to develop technologies for the conversion of skins from unexplored sources into leather for the tanning industry. Leather jacket fish skin has been explored as a potential raw material due to the availability and exotic grain pattern. Leather jacket fishes are non endangered species and consumed without the skin. Skins of these fishes are removed and discarded as waste before being exported from fish processing centres. Experiments were carried out to investigate the feasibility of turning these fish skins to leather.

Leather jacket fish skins were explored for their aptness in leather manufacturing process as a raw material by analyzing the physical, chemical and histological characteristics. Suitable modifications were done in the pretanning process and appropriate enzymes were utilized to achieve proper fibre opening and to remove melanin from the skin. Leather process technology was developed andstandardized for the conversion of fish skin into leathers. Histological characteristics were studied at different stages of processing using optical microscopic technique. Organoleptic properties and physical strength properties of the crust leathers were analyzed.

Development of leather process technology using this explored new raw material would enable to make wealth from waste.

Keywords : Leather jacket fish skin, potential raw material, exotic pattern, fibre opening, histological characteristics, organoleptic properties.

Introduction

Increasing demand of conventional raw material and absence of technology among tanners for the conversion of alternative raw material into leather poses a niche area. There is a great potential to develop technologies for the conversion of skins from unexplored sources into leather for the tanning industry. Only conventional raw materials from goat, sheep, cow and buffalo are processed for leather manufacture by tanners. The cost of these raw materials is higher and their availability is not consistent and varies depending on the season: (UNIDO 2010). Alternate source of raw materials could offset the cost of leather and leather product manufacture making the business more competitive and profitable.Skins of a wide variety of animals, birds and fishes can be used as raw materials for leather processing. But the texture, pattern and usage vary depending on the type of hides or skins used for makingleather. Hence, exploring new raw materials for leather making is continuously required to produce new type of leather distinguished from conventional leather.

Utilization of fish skins for leather production have gained interest as an additional source of raw material for leather production (Karthikeyan and NK Chandrababu 2009). It also provides an economical and environmental solution for the fish industry to utilize the skins.Fish skin is available in enormous quantity as a byproduct of fish processing centres**.**Skins from many variety of fishes like Salt-water eel, crap, salmon shark and ray fishes and other similar varieties have been earlier investigated by many researchers for leather production (Karthikeyan and NK Chandrababu 2011; Ramesh Duraisamy et al 2016; Püntener A.G et al 2013; Arife Candaş et al 2015).

Fig 1.Leather Jacket fish

Fig.1 shows the image of Leather jacket fish. Leatherjackets derived their name due to the skin, which has to be removed before serving. The skin is inedible and is usually discarded. The scientific name of leather jacket fish is Oligoplite Saurus and the common names are jack fish,butter fish and trigger fish. The fish weighs around 1.5 Kg.The thickness of the fish skin is around 0.7mm,length ranges from 30 to 70cmand width 20 to 40cm. The skin is rough without scales and has firm texture. The distinguished features of leather jacket fishes are prominent dorsal spine and leathery sand paper like skin.

Leather jacket fish skin is neither consumed by the people nor converted into high value products; most of them go as a waste**.**Treatment and conversion of waste into value added productswould help not only to strengthen the economy of acountry but also to protect the environment from pollution and to improve the socio-economic status of the people by creating employment. The leather jacket fish has beautiful grain structure with minute tube like projections which makes it to resemble sand paper and can be used for the production of decorative leather for ornamental goods. Leather jacket fish skin is thus explored as a potential raw material for leather industry due to its availability and exotic nature.

Hence to create awareness and to provide technology to the leather sector, an attempt has been made in this study to investigate the feasibility of turning leather jacket fish skins into leather. The aptness of leather jacket fish skin in leather manufacturing process as a raw material has been studied by analyzing the physical, chemical and histological characteristics.Enzyme assisted liming process has been designed according to skin characteristics and full chrome and semichromeprocesses have been adopted to make crust leathers from leather jacket fish skins.

Materials and Methods

Fresh leather jacket fish skins (200 Nos) were collected from Chennai based fish processing where the skins are removed and are discarded as wastes. The skin were easily removed after cutting the head portion by peeling the skin starting from the head portion and werewashed with water for 15 minutes. Controlled processing conditions and careful treatment is required in the beam house,to protect the grain texture of the leather jacket fish skins.

Chemical Characterization of Leather jacket fish Skin

Determination of Protein Content

The protein content of the raw fish skin sample was estimated utilizing the Kjeldahl method (Bradstreet R. B.,1954),The protein content in percentage = % nitrogen x 6.25.

Determination of Fat Content

The fat content of the raw fish skin sample was estimated as per the standard IUC method SLC 4.(Herts, 1996) The sample is continuously extracted with dichloromethane. Solvent is then evaporated from the extract which is then dried at 102^0C.

Fibre Opening & pigment removal : (Enzyme assisted Method)

In 200% water, commercial grade protease enzyme 0.2%, Amylase0.2%, and xylanase 0.5% were added to the drum and the drum was run for 60minutes under 3rpm.

Lime 3.5% was then added and the drum and was run for 10 minutes for every one hour upto 8 hours and left overnight.

Deliming and Bating:

Deliming was done with Ammonium sulphate 1.0% in 100% float and the drum was run under 3 rpm for 45 minutes and washed with water**.**

Tanning trials with full chrome and semi chrome process

The tanning trials were carried out as given in Table 1.

Table 1.Fish skin tanning trials

Full chrome process	Semi chrome process

Vegetable tanning (% based on pelt weight)

(Drum rpm was controlled at 5rpm)

Partial pickling

Water 50%

Salt 5% - run for 10min

Formic acid 0.5%

2x10min+30min pH 4.5-5.0

Vegetable tanning

Pretanning syntan 3% 30min

Wattle 10%

Sulphited Veg based fatliquor 1% 1h

Wattle 10%

Sulphited Veg based fgatliquor 1% 1h

Myrobalan 5% 45min

pH adjusted to 3.0-3.2.

Drained, rinsed, piled for 2 days.

Semi Chroming:

Wetting Agent 0.5% 30 min, Drain, Wash.

Water 200%

Borax 1% 60 min

Drain, Wash.

Oxalic acid 1% 30min, Drain, Wash

Water 50%

Chrome syntan 5%

Chrome tanning (% based on pelt weight)

(Drum rpm was controlled at 5rpm)

Pickling

Water 100%

Salt 10% - run for 10min

formic acid 1% -run for 15min

Sulphuric acid 0.5%

-run for 3x10min+60min pH 2.8-3.0.

Chrome tanning

Drain 50% pickle water. Add

BCS powder 8% 90min

Water 50%

Sodium formate 1% 30min

Sodium bicarbonate 0.75% 3x10min + 60min

pH 3.8. Drained, rinsed and piled.

Rechroming

Water 100%

Chrome syntan 5%60 min

Sodium formate 0.5%(in 10% water)

Sodium bicarbonate 0.5% 2x10min + 45min (in 10% water)

pH 4.0 Drained, rinsed and piled overnight.

Histological Studies with H & E (Hematoxylin & Eosine) Staining

The histological studies for the soaked, limed, chrome and vegetable tanned fish skin leathers were carried out. After the completion of the above mentioned full chrome and semi chrome processes, the samples were cut and preserved in 10% formalin for 48 h. The fixed samples were dehydrated in a series of solutions of alcohol of different concentrations (50 to 100%) and then cleared in xylene. They were finally embedded in paraffin wax into moulds. Thin sections (10µm thick) were cut on a microtome, mounted on glass slides , stained with Hematoxylin and counterstained with Eosine.

Post Tanning Process

All the tanned leathers were neutralized to pH 5.0-5.5 and washed. Table 2 illustrates the post tanning process.

Table 2 Post tanning process

Process	Chemicals	%	Drum running time	Remarks
Neutralization	Water	100		
	Neutralizing syntan	1.0	20 min	Check
	Sodium formate	0.75	3x10+30min	pH 5.0 -5.5
	Sodium bicarbanate	0.3		Wash/drain
Retanning	Water	100		
	Acrylic Resin syntan	4	30 min	
Dyeing and	Acid Dye 2%	2	30 min	Check
Fatliquoring	synthetic fatliquor	3	15 min	penetration
	Phenolic syntan	3		
	Resin Syntan	3	40 min	
	Sulphited fish oil basedfatliquor	3		
	Sulphited veg oil based fatliquor	3		
	synthetic fatliquor	5		
			60 min	
	wattle Powder	3	30 min	
Fixing	Formic acid	1.5	3x10+30min	

Drain, wash and pile over night. Next day, dry, stake by hand and trim

Physical Testing and Visual Assessment

The samples for physical testing were cut from the chrome tanned and semi-chrome tanned crust

leathers and conditioned at 80±4^{o}F and 65±4% R.H. for 48 h. The tensile strength and % elongation were measured as per the IULTCS methodIUP: 6 (2000). Experienced technologists assessed the organoleptic properties such as fullness, feel, grain tightness and general appearance and the leathers were rated on a scale of 0-10 points for each functional property.

Results and Discussion

Chemical Characterization of Leather jacket fish skin

Analytical values of moisture, total protein and fat content of fish skin is presented in Table 3.

Table 3Chemical characteristics of leather jacket fish skin

S No	Characteristics	Value in % w/w
1.	Nitrogen content	4.11
2.	Protein content	25.86
3.	Fat content	1.2

Fat content of leather jacket fish skin was found to be low ie 1.2% which indicates that degreasing process is not essential for this type of fish skins.

Histological Studies of Chicken Leg Skins with H & E Staining

The optical microphotographs taken for the soaked, limed, leather jacket skins as shown in the Figures 2 to 5.

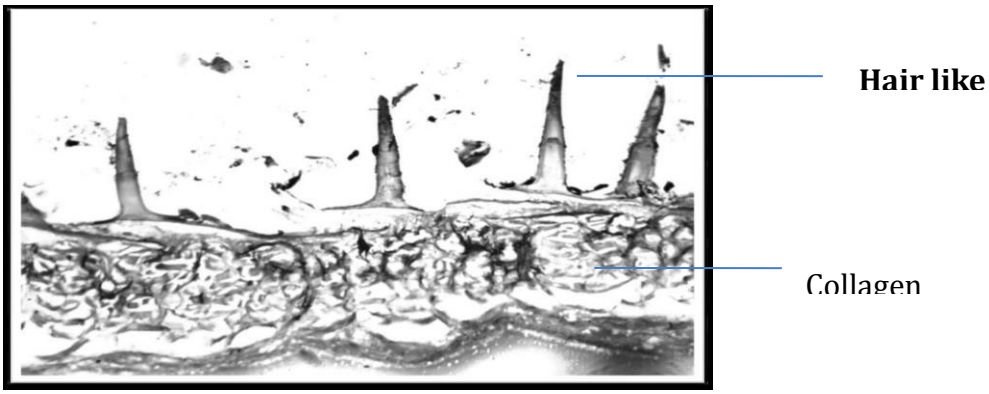

Fig 2. H & E stained optical micrographof Soaked Leather jacket fish skin

The soaked leather jacket fish skin (Fig 1) show absence of scales but has hair like projections which indicates the characteristic surface pattern of Leather jacket fish skin.This surface pattern is found to be unique to leather jacket fish skin. The unique surface pattern or "grain" is a major economic feature of the leather made from the skin, making it more valuable.

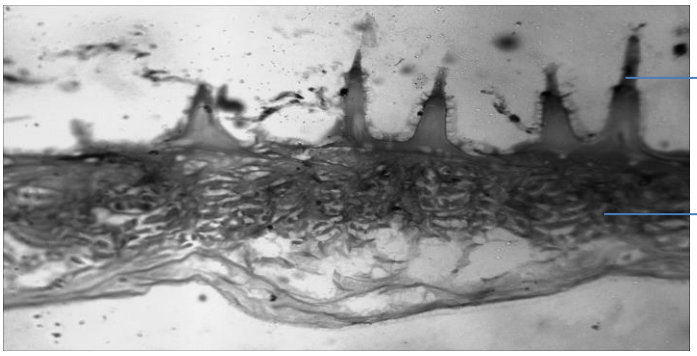

Fig 3. H & E stained optical micrograph of Limed Leather jacket fish skin

The enzyme assisted liming process show opened up fibre structure without destructing the characteristic surface pattern of the leather jacket fish skin.

Effect of Tanning System on the Fibre Structure of fish skin Leather

The following are the H &E stained optical microscopic pictures of full chrome and semichrome leather jacket fish skin leathers

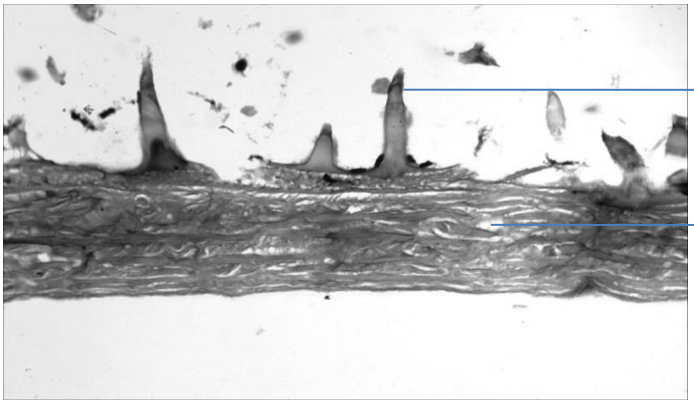

Fig 4. H & E stained optical micrograph of Full chrome Leather jacket fish leather

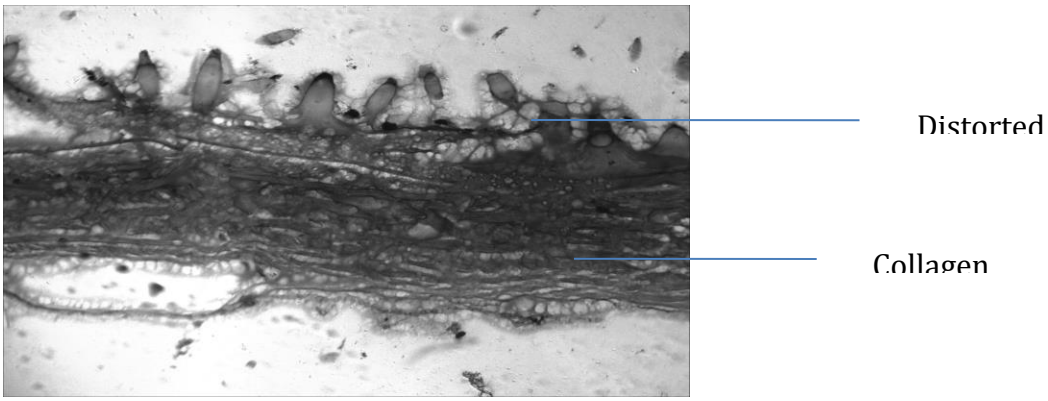

Fig 5. H & E stained optical micrograph of Semichrome Leather jacket fish leather

From the microscopical studies , it is clearly seen that the grain pattern remained same after chrome tanning process but the characteristic grain pattern is much affected in the case of semichrome leather. Fibre bundles are separated well in semi-chrome tanned leather, and has lead to fuller leather compared to fullchrome leather.

Strength characteristics and visual assessment

Table 4.Physical Strength Characteristics of full chrome and semi chrome tanned leathers

S No	Parameter	Chrome tanned	Semi chrome
1.	Tensile Strength N/mm^2	7.90	7.04
2.	Elongation at break %	28.01	24.16
3.	Tear Strength N/mm	47.11	43.94

Physical strength testing results presented in Table 4 reveal that thefull chrome crust leathers of leather jacket fish skin has comparatively higher strength characteristics and elongation at break when compared to semichrome leathers.

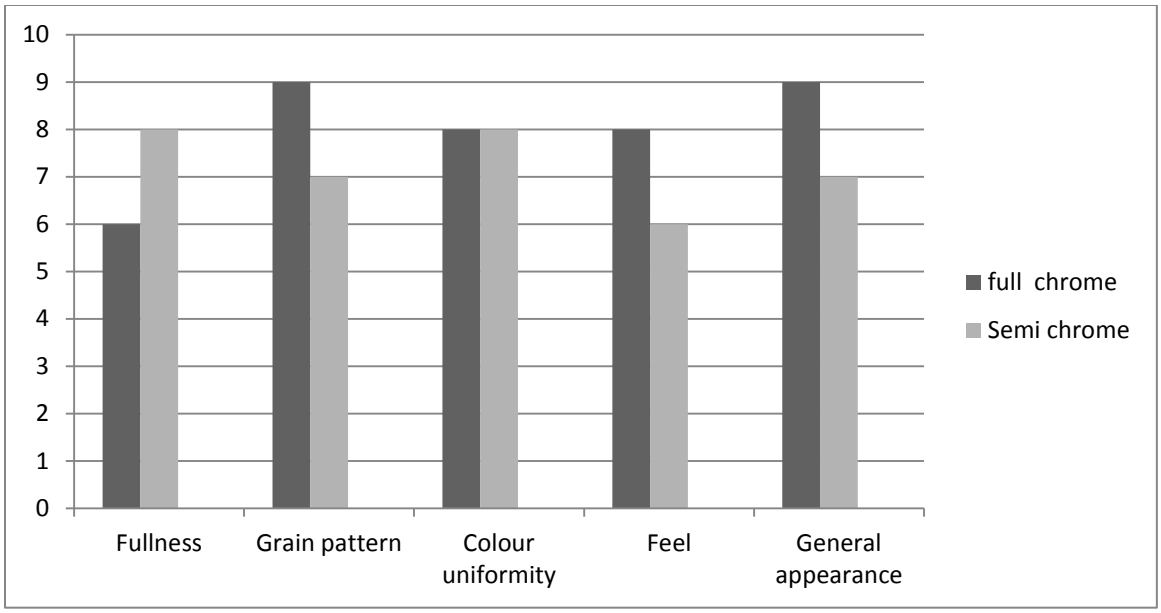

Fig 6. Visual assessment on organoleptic properties

Visual assessment data of crust leathers assessed by experienced technologists on a scale of 0-10 points for each functional property is presented in Fig 6. It is evident from the figure that the organoleptic properties such as grain pattern, uniformity of colour and feel are better for full-chrome leathers whereas semichrome crust leathers show better fullness propertycompared to chrome tanned leathers. These results show that full chrome process is more suited for leather processing using leather jacket fish skin raw material.

Conclusion

Leather jacket fish skin was explored as a new raw material for leather industry and the feasibility of turning this to leather was investigated. The technology developed for the conversion of leather jacket fish skins into finished leather would catch the attention of commercial tanners. Enzyme assisted fibre opening and full chrome tanning process has resulted in softleather with better strength characteristics. Microscopic analysis and visual assessment data indicates that the characteristic grain pattern of leather jacket fish skin is maintained in leathers processed by full chrome tanning process.

Acknowledgment

The authors acknowledge the financial support from CSIR, New Delhi under the Supra Institutional Project S&T Revolution in Leather with a Green Touch (STRAIT) (CSIR-CLRI Communication No. 1230).

References

1. Karthikeyan, R. Chandra Babu, N.K. Mandal, A.B. Sehgal, P.K., A new depigmentation and fibre opening method for the conversion of stingray skins into leathers, *Journal of the American Leather Chemists Association,* 2011**, 105**, 25-32.
2. N.K. ChandraBabu, A.B.Mandal and P .K. Sehgal (), "Studies on the Preparation of Soft Leathers from Himantura (Family Dasyatidae) Stingray Skins and their Applications in Foot and Hand Reflexology",*International Union of Leather Technologists & Chemists Societies,* 2009, *349*
3.Püntener A.G., Donkan A., Fish Leather a Traditional Crafts and Industrial Goods, *XXXII. Congress of IULTCS*, May 29th–31th, Istanbul, Turkey, 2013.
4.Arife Candaş Adıgüzel Zengin1, Fish Skins: Valuable Resources for Leather Industry
XXXIII IULTCS Congress November, 24th – 27th, 2015 Novo Hamburgo/Brazil

5.Herts ,SLC4: Dertermination of fat contect in: 'Official Methods of Analysis', *Society of Leather Technol Chem,* 1996.

6.Bradstreet R. B.,Kjeldahl Method for Organic Nitrogen,*Anal Chem,* 1954. **26,** 185–187.
7.IUP: 6, Measurement of tensile strength and percentage elongation, *Journal of the Society of Leather Technologists and Chemists,* 2000, **84**, pp.317-321.

8. Future Trends in the World Leather and Leather Products Industry and Trade,*United Nations Industrial Development Organization* Vienna, 2010.

9. Ramesh Duraisamy, Seguye Shamena, Abiyu Kerebo Berekete, A Review of Bio-tanning Materials for Processing of Fish Skin into Leather, *International Journal of Engineering Trends and Technology (IJETT)* September 2016, **39** Number 1.

IVL P-36

SUBSTANCE IMPROVEMENT AND VALUE ADDITION IN LEATHER THROUGH ECO-BENIGN APPROACH

Venkatasubramanian Sivakumar*,Resmi Mohan, Chellappa Muralidharan

[1]Chemical Engineering Department, [2]Tannery Division, CSIR-CLRI

CSIR-Central Leather Research Institute (CLRI), Adyar, Chennai -600 02, India,

A large proportion of hides/skins especially of Asian origin lack substance and possess inherent defects leading to difficulty in producing high quality leathers. In this regard eco benign, simple and cost effective methodology has been developed to improve the substance (bulk properties) as well as surface characteristics of leather using selected polymers and bio-degradable materials. The effect of this treatment has been studied during various stages of leather processing. The substance improvement has been quantified. Strength property and pore-size analysis have also been studied. The results indicate that there is up to 30% improvement in substance for different types of substrates and end products. This methodology could be a lucrative way of upgrading low value leathers.

Keywords: Leather, Substance improvement, Bio-degradable, Eco-benign, Value addition

Introduction

Hides and skins are most commonly a by-product of meat, milk or wool production. The properties of leather vary considerably depending upon the type and quality of both the skins and the tanning process. The advantages of using biopolymers in the leather are filling the loose portions such as belly, neck etc and impart fullness to the grain.

The objective of the present study is to improve the substance of low quality leather by using biodegradable polymers such as polyvinyl alcohol (PVA). Polyvinyl Alcohol (PVA, sometimes referred to as PVOH) is a water soluble polymer used widely in adhesives, paints, sealants, coatings, textiles, plastics etc. PVA has excellent film forming, emulsifying and adhesive properties. It is also resistant to oil, grease and solvents. It is odorless and nontoxic. It has high tensile strength and flexibility, as well as high oxygen and aroma barrier properties.

Materials and methods

Chemicals and raw materials

Polyvinyl alcohol (grade 173) was purchased from Suraj chemicals, Chennai. The cow hide for the experiments were taken from tannery division of CSIR-CLRI. The hide was soaked in water for the rehydration of the skin. Then after liming (hair removal) and de-fleshing process the skin was cut into two pieces through the backbone and marked as left and right. Then the weights of hide pieces were taken. Then the skin was processed till pickling process and stored in pickling solution.

Biopolymer preparation

The % of polyvinyl alcohol (PVA) used for the treatment is based on % *w/w* of hide weight. The PVA were dissolved in 100% water (with respect to hide weight) which is heated up to 70°C by continuous mixing process. This solution was used for the treatment process.

Influence of PVA on cow hide at tanning stage

The left side piece of the cow hide was taken as control and right side was taken for experiment process, for the treatment with selected biodegradable polymer. Both the control and experiment process were carried out separately in different drums. For the control process conventional tanning process were carried out. For the tanning process 8% (% *w/w* w.r.to hide wt.) chromium sulphate was used. First 4% (% *w/w* w.r.to hide wt.) was taken and added in the drum. After 1 hr of treatment again 4% chromium sulphate was added in the drum and treated for 1 hr.

For the experiment process, polymer based (sandwich model) tanning process were carried out. For the tanning process 4% chromium sulphate (% *w/w* w.r.to hide wt.) was used and treated for 1 hr. After treating with chrome, prepared 5% (% *w/v* w.r.to hide wt.) PVA solution was added in the drum and treated the hide for 2 hrs. Then again hide is treated with 4% chrome for 2 hrs.

In control process, instead of PVA 100% water was added after treating with 8% chrome. After tanning process both the control and experiment process are treated with sodium formate (1%) and sodium bicarbonate (1%) in order to adjust the pH at 4. Then the both hides are taken out from the drum and kept for aging 36 hrs.

Influence of PVA on cow hide at pickling stage

The left side (control) and right side (experiment) of the hide pieces were treated in separate drums. In the control process, hide was treated with 100% pickle liquor (% *w/v* w.r.to hide wt.) for 15 minutes. For the tanning of the hide 8% (% *w/w* w.r.to hide wt.) chromium sulphate was used. First 4% (% *w/w* w.r.to hide wt.) was taken and added in the drum. After 1 hr of treatment again 4% chromium sulphate was added in the drum and treated for 1 hr.

For experiment process, once the hide is treated for 2hrs with 5% (% *w/w* w.r.to hide wt.) with PVA solution the hides were tanned using 8% chrome for 2 hrs.

Basification process is carried out in order to adjust the pH of the hide at 4 for both control and experiment process by adding 100% water (% *w/v* w.r.to hide wt.) is added to both the drums. And then sodium formate (1%) and sodium bicarbonate (1%) was added and treated for 2 hrs. Then the both hides are taken out from the drum and kept for aging 36 hrs.

Crusting process of cow hide

During crusting process the tanned hide is re-tanned, dyed and lubricated. Crusting process is begins with neutralization process, in which tanned hide is treated with sodium formate (0.5%) and sodium bicarbonate (0.5%) in order make the pH of the hide at 5.5. This process is necessary for the leather in order to allow it to properly absorb the various chemicals that are used. Once the pH levels of hides are neutralized, retanning process is done by using syntans and hide is dyed at this stage. Once desired color is achieved, fat liquoring process is used to lubricate the leather fibres with wax and oils. Formic acid (3%) is used for fixation process, in which all the chemicals used previously are either bonded within the leather or removed from it.

During setting process, excess of water from the hide is removed and flatness of the hide is achieved. After setting process, leather is dried and then staking process has carried out in order to make leather softens and conditioned. The thickness of the hides of control and experiment are measured at this stage by using gauge machine and compared the results by calculating mean thickness and standard deviation.

Calculation

$$\sqrt{N}$$

Mean ($\overline{X}$) = $\frac{\Sigma X}{N}$ Standard deviation (σ) = $\frac{1}{N} \sum_{i=1} (X_i - \overline{X})$

N = total no. of values

X = each value in the population

Shrinkage temperature analysis

SATRA STD 114 shrinkage apparatus is used for the analysis. This apparatus enables shrinkage temperature to be measured up to 115°C. When leather is slowly heated in water, a sudden shrinkage occurs at a temperature which is characteristic of the tannage. If the shrinkage temperature is above 100°C it is necessary to use water pressure greater than atmospheric to determine its value. Tanning aims to bring about stability against thermal and enzymatic degradation of skin matrix properties. One of the characteristic features of skin is its dimensional change under the action of heat. Skin undergoes length reduction at a characteristic temperature to a level of one third of its original dimension.

Strength analysis

The hides were tested for various physical properties such as tensile strength and tear strength which are important for its application. Tensile strength was measured using Instron universal testing machine.

Pore size Analysis

Analysis of pore structure of skin is important to understand process of diffusion and adsorption involved during any application of the skin matrix. Pore structure renders skin many unique properties. Insight into the pore structure of the skin matrix is required to understand mass and heat transport properties as well as fracture mechanism of material under flexural stress [2,3]. The changes brought about in the pore structure have been studied using mercury intrusion porosimetry.

Results and discussions

Influence of PVA on cow hide at tanning stage

Table 1 shows the mean thickness and standard deviation of the cow hides of both control and experiment from different regions of the hides. The results shows that 0.38 mm of substance have been increased in the belly region of experiment when compared with control. In the backbone region of the experiment also have 0.28 mm improvement in the substance compared to control. In case of butt region there is no improvement. This is may be because of the butt region is already filled there is no empty places so the polymer can go and attach.

Table1 The mean thickness and its standard deviation in the different regions of cowhides.

	EXPERIMENT		**CONTROL**	
	MEAN	**S.D**	**MEAN**	**S.D**
Backbone	2.91	0.12	2.63	0.22
Butt	3.04	0.068	3.05	0.097
Belly	2.44	0.217	2.06	0.089

Table 2 Comparative studies of strength properties polymer treated hide and control at tanning stage.

	EXPERIMENT		**CONTROL**	
	Along	**Across**	**Along**	**Across**
Tensile strength (N/mm^2)	24.65	22.43	27.12	26.07
Tear strength (N/mm)	101.83	107.68	101.48	100.77

Shrinkage temperature analysis shows that experiment have shrinkage temperature of 101° C when compared to control which is 100°C. These results indicate that polymer treatment doesn't reduce any native properties of leather.

In the pore size analysis, the mean flow pore diameter of the experiment is 0.3006 microns and the control is 0.1793 microns. This study shows that the mean flow pore diameter of experiment increased when compared to control. This means that the polymer has absorbed (mass transport) inside collagen matrix of cowhide treated with PVA.

Influence of PVA on cow hide at pickling stage

The thickness in the different regions of cow hides of experiment and control are given in the table 3. The results shows that there is no substance improvement in the cow hide when compared to control.

Table 3 The mean thickness and its standard deviation of cowhides.

	EXPERIMENT		CONTROL	
	MEAN	S.D	MEAN	S.D
Backbone	1.20	0.010	1.22	0.0089
Butt	1.36	0.0134	1.34	0.012
Belly	1.26	0.020	1.27	0.034

Table 4 Strength analysis results of polymer treated cow hide and control at pickling stage.

	EXPERIMENT		CONTROL	
	Along	**Across**	**Along**	**Across**
Tensile strength (N/mm^2)	15.75	16.87	13.75	12.26
Tear strength (N/mm)	80.14	88.44	104.21	105.32

Shrinkage temperature analysis shows that polymer treated hide can withstand the temperature up to 103°C where as control 102°C. And it also shows that the polymer didn't reduce the native properties of tanned leather.

Conclusion

In this present study, the hides treated with PVA at tanning stage (sandwich model) have good substance improvement when compared to treatment at pickling stage. The PVA doesn't reduce any strength properties of leather. So this sandwich method can be used for upgrading the low value leathers. This method is simple, cost effective and eco-friendly and can be used to improve the substance of leathers for the production of high quality leather.

Acknowledgements

Authors thanks STRAIT Project (WP 1.2.11) under XIIth plan project of CSIR-CLRI and also CSIR, New Delhi for the financial support in the research work.

References

[1] R.R. Stromberg, M. Swerdlow, Pores in collagen and leather, *J. Am. Leather Chem. Assoc*.,1954, **47**, 336–351.

[2] T.J. Carter, J.R. Kanagy, A flex tension test for leather, *J. Am. Leather Chem. Assoc*., 1954, **49**, 23–42.

IVL P-37

AN ECO-FRIENDLY LEATHER COATING MATERIAL

U Venkateswarlu

Advanced Materials Lab, Central Leather Research Institute, Adyar, Chennai- 600020, India; e-mail: venkateswaralu@clri.res.in

Hen egg white (A) and gelatin (B) composition that was used as a bio-degradable binder was prepared and the product is cross-linked with Glutaraldehyde (C). The composition thus formed (ABC) was standardized with tensile strength and characterized with FTIR, TGA, CD spectra. The tensile strength test was conducted on ABC composite at a speed of 5 mm/min and it shows an optimum tensile strength of 40 Mpa with elongation (170%) for AB and C at the ratio of 50:1. The Circular Dichroism (CD) spectra was performed between 185 nm-250 nm and the AB composite shows an helical structure that confirms presence of peptide bond and for ABC composite an unordered random coil structure with negative peak at 197 nm i.e. helical structure was converted into random coil that confirms the concept of cross linking of AB composite with Glutaraldehyde. The FTIR spectra of AB composite shows protein peaks at 1654 cm-1 (Amide-I), 1561 cm-1 (Amide-II), 1244 cm-1 (Amide-III) whereas for ABC composite, the amide-III band was absent, this is due to glutaraldehyde link with amide group. Thermal gravimetric analysis of AB composite shows 60% weight loss between 235^{o}C to 400^{o}C and for ABC composite it was 8% between 235^{o}C – 375^{o}C. Water absorption studies were conducted on samples and it was concluded that the AB composite was disintegrated within an hour whereas ABC composite (in the ratio AB:C = 50:1) was intact even after 24 hours and has water absorption capacity of 173%/mm^3, 233%/mm^3, 245%/mm^3, 153%/mm^3 after 1 hr, 2 hr, 3 hr and 24 hrs respectively. The ABC composite is tested for peel strength by giving a coat on a standard leather surface and it was found to have 4.8 N/mm on dry condition and 3.2 N/mm on wet condition. Therefore the proposed hen egg white–gelatin–glutaraldehyde (ABC) composite possesses excellent characteristics and can be used as a coating agent for Leather.

Key words: hen egg white, gelatin, Glutaraldehyde, FTIR, TGA, CD, Tensile strength, water absorption

1. Introduction

Hen egg white is a viscous fluid that contains albumen, poggle, glair, proteins and water. Hen egg white in combination with gelatin was used as a binder [1]. The glutaraldehyde was cross linked with Bovine serum albumin and used as bio-glue [2] for tissue adhesive and as a sealing agent for kidney during partial nephrectomy. Glue was prepared using albumin and glutaraldehyde as a tissue adhesive for sealing pulmonary parenchyma and bronchial anastomoses [3]. The immobilization of Lysozyme in hen egg white was cross linked with glutaraldehyde that can be used for continuous lysis of bacterial cells. Enhancement of Lysozyme action by cross linking hen egg white in the presence of N-acetyl glucosamine was observed by Kamalroohk [4]. The unique property of hen egg white to form stable foam has been

reported by Marolia [5] in developing a novel method for immobilization of naturally present Lysozyme in egg with glutaraldehyde. Kulkarni [6] has developed a new inter penetrating polymer network of sodium alginate and gelatin with egg albumin cross linked with glutaraldehyde for in-vitro release of cefadroxil. Gelatin is common substance used extensively in pharmaceuticals, leather, food ingredient and packing. Bigi [7] has investigated gelatin- glutaraldehyde films for its mechanical, thermal and swelling properties and verified the influence of glutaraldehyde concentration on the stability of the films. Tabata [8] had prepared gelatin- glutaraldehyde hydrogels and implanted the same after incorporating bFGF in the hydrogel in the rats to find out the revascularization of bFGF release from the hydrogels. Chen [9] had prepared anticancer biodegradable and hydrophilic glutaraldehyde cross-linked microspheres and quantified the in-vivo release of anticancer drugs from microspheres. Sharma [10] studied the LASER light scattering of gelatin-glutaraldehyde solutions using static and dynamic Laser light scattering measurements. Similar method has been studied by Kennedy [11] for the surface mobilization and entrapping of enzymes on glutaraldehyde cross linked gelatin particles. Martucci [12] has studied creep behavior of glutaraldehyde-gelatin films by short time flexural tests at 30^{o}C. Chemical cross linking yields an increase in strength and decrease in viscous creep. In the present study, I have developed hen egg white-gelatin-glutaraldehyde composite and characterized it for FTIR, TGA, CD and Tensile strength.

2. Material and methods

2.1 Materials:

Fresh hen egg white was separated from chicken egg and used as such. Gelatin used was purchased from MBD, Mumbai, India. Glutaraldehyde was obtained from Merck, Germany. All other reagents used were of analytical grade.

2.2 Methods:

2.2.1 Preparation of Albumin solution (A): Egg white was separated from broken egg and kept in a conical flask.

2.2.2 Preparation of Gelatin solution (B): 20 grams of gelatin powder was dissolved in 200 ml of water at 55^{o}C in a water bath and stored in a flask.

2.2.3 Preparation of AB film: 5 ml of solution (A) was added to 20 ml of (B) at ration of 1:4 and stirred for about 10 minutes to get uniform solution. It was then poured in a polythene tray and dried at room temperature (20-25^{o}C) for about 24 hours. Then so formed film was named as (AB).

2.2.4 Preparation of ABC film: 30 ml of solution (A) was added to 120 ml of (B) and different composition films were prepared by adding solution (C) as per concentrations shown in below table-1.

Sample ID	AB (ml)	C (ml)
1	25	0.25
2	25	0.50

3	25	0.75
4	25	1.00
5	25	1.25
6	25	1.50

Table-1: Preparation of ABC composites

These six samples were dried and made into films as per procedure mentioned in section 2.2.3.

2.3 Characterization:

The AB and ABC films were characterized by using FTIR spectra, Thermo Gravimetric Analysis, Circular Dichroism, Tensile strength and water absorption.

2.3.1Water Absorption (%): The samples were tested for water absorption capacity according to the following method. Each sample was cut in to 6 pieces of 10 mm x 10 mm in size. These six samples were placed in a chamber which maintains at 20^{o}C and 65% RH for about 24 hours in order to get uniform condition for all samples. Then take weight for each sample individually and denote it as (W_i). Then place all samples in a beaker of 100 ml size and pour 50 ml of double distilled water in to the beaker. Then take weight of each sample (W_f) after 1 hr, 2 hr, 3 hr and 24 hrs and recorded. Before taking weight, the sample should be blotting with filter paper to remove unabsorbed water particles on the surface of the sample. The water absorption was calculated in terms of percentage per unit area as follows.

Water Absorption: $\mathbf{E_s = \{(W_f - W_i) / W_i\}}$ %/mm^2

2.3.2 Tensile Strength: Three samples of dumbbell shape of sized 4 mm wide and 10 mm length were used to find tensile property using Universal Testing Machine (INSTRON Model 1405) according to method described by Vogel [11]at elongation rate of 5 mm/min.

2.3.3 Infrared Spectroscopy: The concept of cross linking of AB composite with glutaraldehyde is tested with FTIR spectra using Nicolet Impact 400using 500 mg KBr pellet containing 2-6 mg of the sample.

2.3.4 CD Spectroscopy: The CD measurements were recorded using JASCO J-715 spectropolarimeter (Japan). The instrument was calibrated using ammonium-d10-camphor sulfonic acid. The path length used was 1 mm. The spectra were recorded with 1 nm bandwidth and 0.2 nm step resolution. This spectrum will record average value of 5 readings. The resulting spectra were baseline-corrected and smoothened. The samples AB and ABC were obtained by dissolving 0.5 ml of the sample in 10 ml of distilled water. All the spectra were collected from 190-250 nm which is the band in analyzing the secondary structure of protein and peptides.

2.3.5 Thermal Gravimetric Analysis: The thermal stability of the substance was determined using Perkin-Elmer over temperature range of 37^{o}C to 585^{o}C at heating rate of 20^{o}C / min under nitrogen atmosphere.

3. Results & Discussion

3.1 Tensile Strength: In this study AB is cross linked with varying amounts of glutaraldehyde and the tensile strength of these components were given in Table-2. Based on studies [1], AB sample was prepared at a ratio of 1:4 (A: B) which gave highest tensile strength (20.9 Mpa) and hence it was used as a standard composition in the present study. With increasing the amount of glutaraldehyde, the tensile strength increases first and then decreases. The composition ABC with 2% glutaraldehyde gives highest tensile strength when compared to other concentration. At this concentration GTA would have been reacted completely with NH_2 groups present in AB backbone as shown in fig-1. With increase in glutaraldehyde concentration, it homo polymerizes and hence decrease in tensile strength and elongation at break was observed.

Sl. No	AB (ml)	C (ml)	Tensile Strength (Mpa)	Elongation at break (%)
1	25	0.00	20.9	112
2	25	0.25	33.3	129
3	25	0.50	40.0	170
4	25	0.75	36.2	143
5	25	1.00	32.1	68
6	25	1.25	28.4	45
7	25	1.50	25.2	39

Table-2: Tensile Strength of hen egg white-gelatin-glutaraldehyde composite

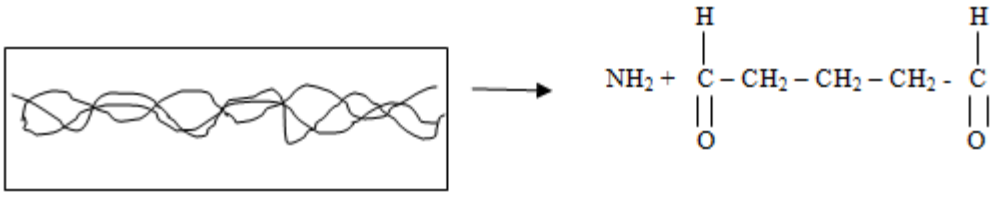

Fig-1: Partial Cross linking of hen egg white-gelatin composite with Glutaraldehyde

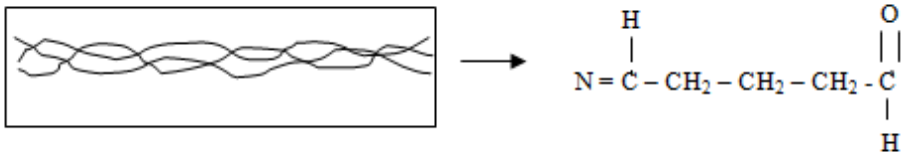

Fig-2: Fully cross linking of hen egg white-gelatin composite with Glutaraldehyde

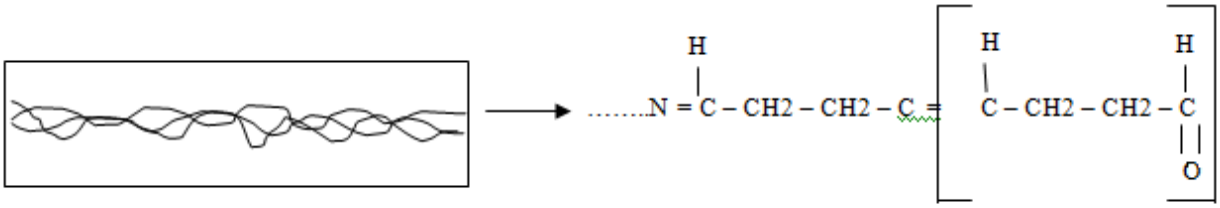

Fig-3: Homo polymerization of Glutaraldehyde

3.2 Water Absorption: Water absorption property of above samples is shown in below table-3.

Sl. No.	Time (hr)	Sample-1 AB alone	Sample-2 %	Sample-3 %	Sample-4 %	Sample-5 %	Sample-6 %	Sample-7 %
1	1	Disintegrated after 1 hour	187	173	170	167	157	125
2	2		256	233	224	219	198	148
3	3		368	245	234	228	205	156
4	24		300	153	125	129	119	103

Table-3: Water absorption of hen egg -gelatin and hen egg-gelatin-glutaraldehyde composites

The hen egg white-gelatin composite as such was disintegrated within a hour whereas samples cross linked with glutaraldehyde were intact even after 24 hours. With increase in glutaraldehyde concentration, the water absorption property increases first and then decreases, this is due to hydrophilic groups (NH_2, COOH, OH) on the AB backbone would have contributed to dissolving membrane in water. With the addition of glutaraldehyde, the NH_2 groups on the AB would have reacted with the –CHO group on glutaraldehyde and increased the hydrophobicity as shown in fig-2. With further increase in concentration of glutaraldehyde, lower values of percentage water absorption were observed due to the homo polymerization of glutaraldehyde as shown in fig-3.

3.3 FTIR Spectroscopy: The FTIR spectra of hen egg – gelatin composite shows protein peaks at 1654 cm^{-1} (Amide-I), 1561 cm^{-1} (Amide-II), 1244 cm^{-1} (Amide-III) as shown in fig-4.

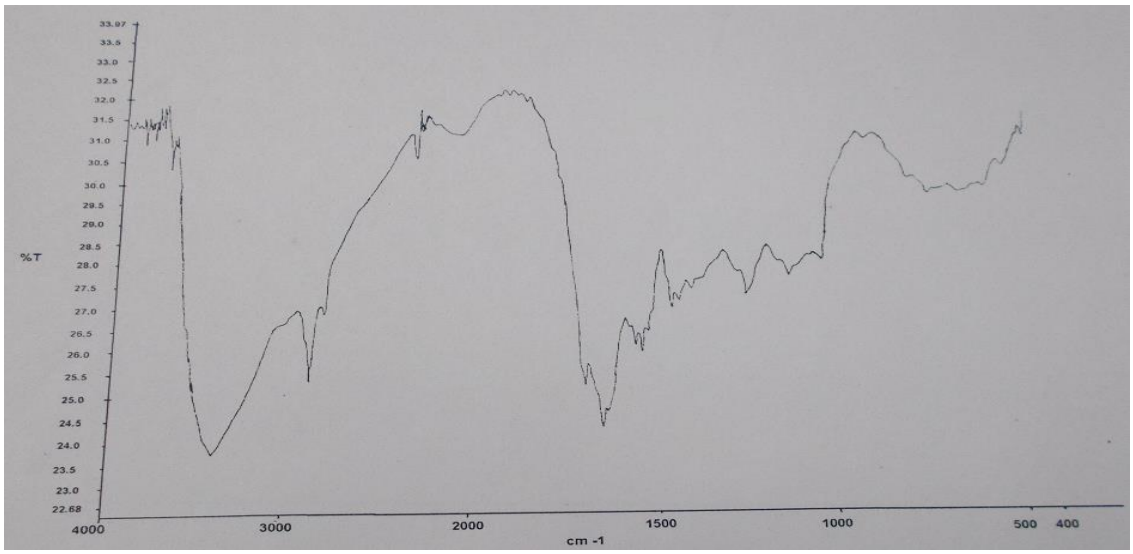

Fig-4: FTIR Spectra of Hen egg white-Gelatin composite

In the FTIR spectra of hen egg-gelatin cross linked glutaraldehyde, the amide-III band is absent; this is due to linking of glutaraldehyde with amide groups as shown in fig-5.

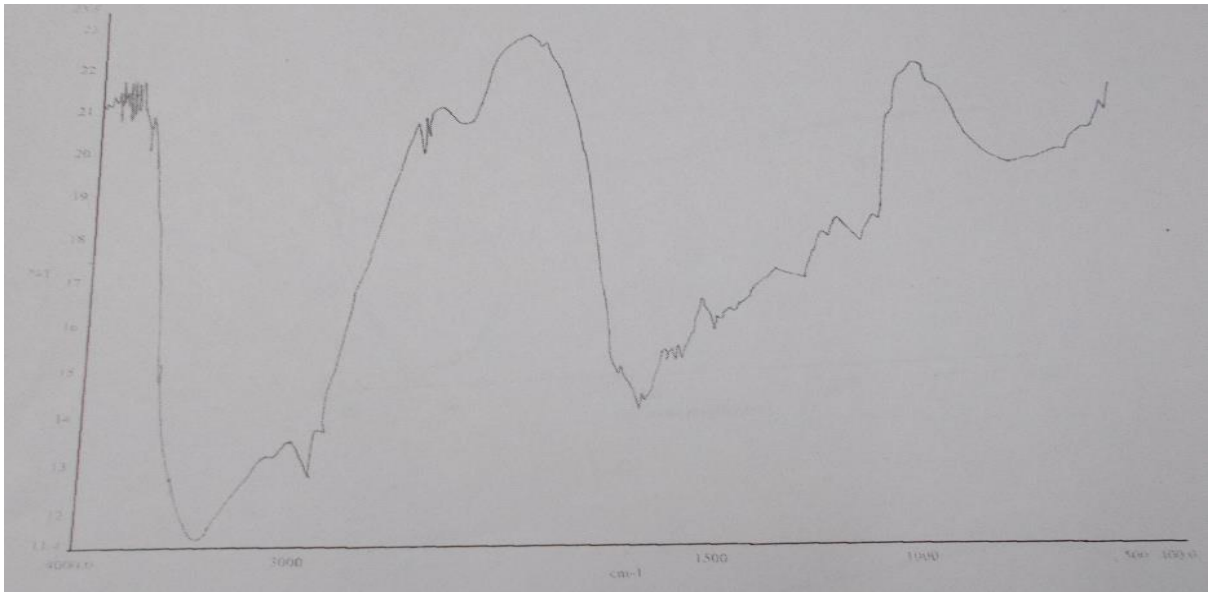

Fig-5: FTIR spectra of Hen egg white-Gelatin-Glutaraldehyde composite

This is an indication of cross linking of glutaraldehyde with hen egg-gelatin composite.

3.4 Thermal Gravimetric Analysis (TGA)

In thermo gravimetric analysis, the loss of weight due to evolution of H_2O and CO and evaporation of other pyrolysis products are collectively measured as percentage of original weight. In this investigation, AB and ABC were heated steadily from 37^{o}C to 585^{o}C. The initial weight loss of 25.38% and 13.08% were observed at 235^{o}C for AB composite and ABC composite respectively. About 60% of weight loss was observed between 235^{o}C to 400^{o}C for AB as shown in fig-6 whereas for ABC about 8% of weight loss was observed between 235^{o}C – 375^{o}C as shown in fig-7.

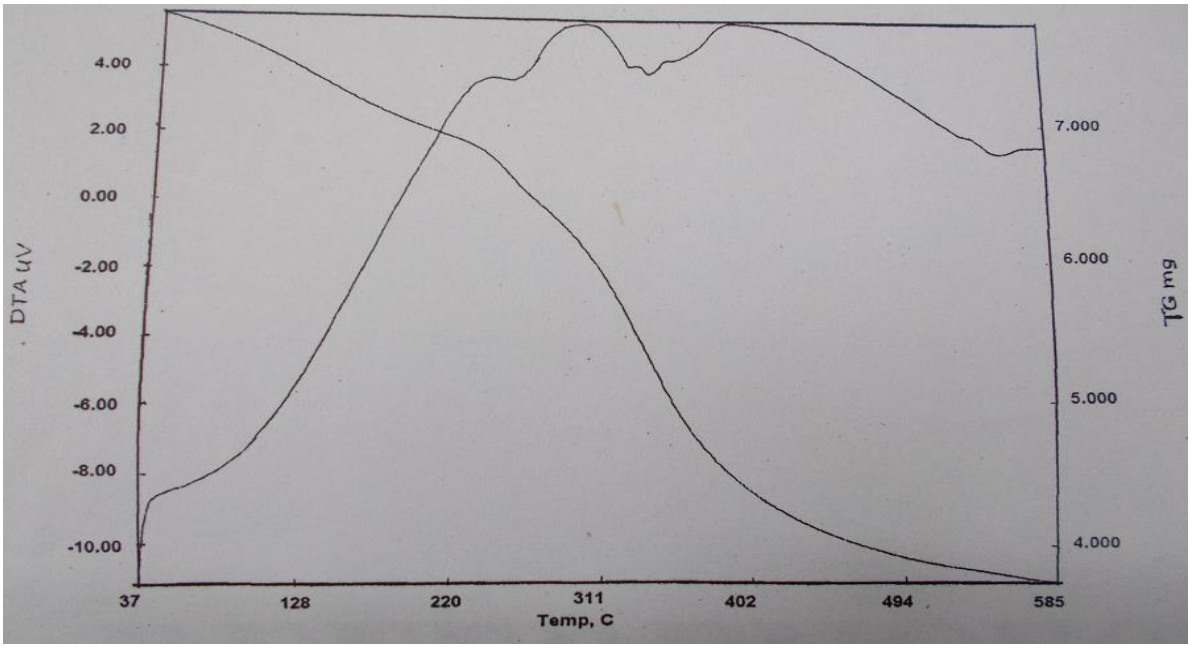

Fig-6: TGA analysis of Hen egg white-Gelatin composite

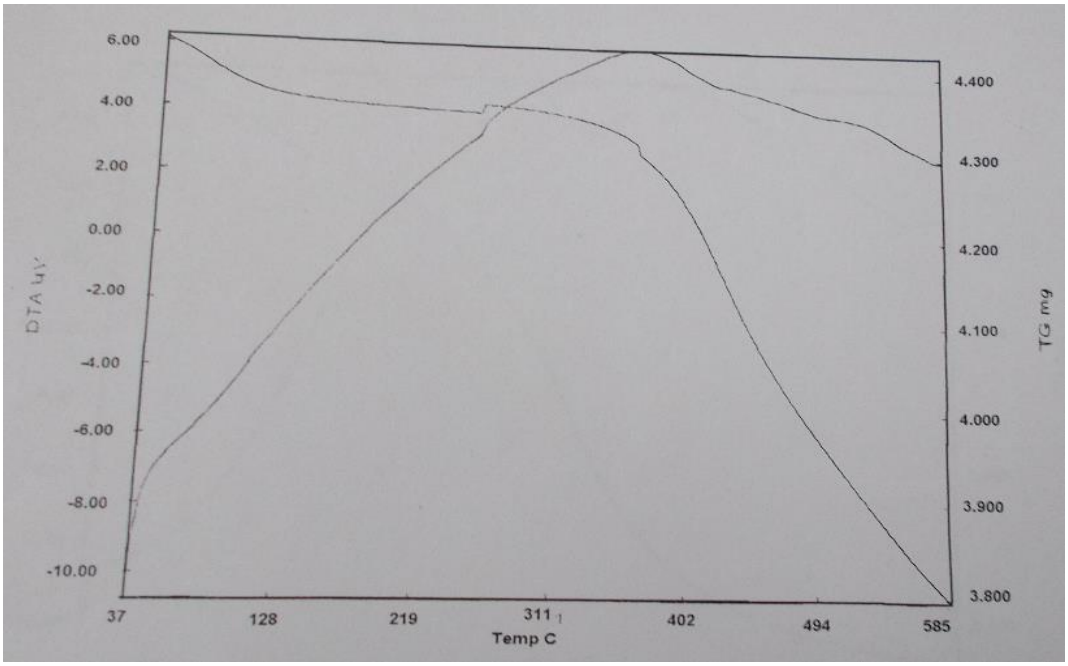

Fig-7: TGA analysis of Hen egg white-Gelatin-Glutaraldehyde composite

A sudden decomposition was observed between 375^{o}C – 585^{o}C for ABC. The ABC sample was thermally stable up to 375^{o}C whereas gradual thermal decomposition was observed between 235^{o}C – 585^{o}C in the case of AB. A 100% thermal decomposition was observed in both the cases at 585^{o}C. Higher value of thermal stability in ABC composite is due to cross linking of glutaraldehyde with the functional groups in the backbone of AB composite.

3.5 Circular Dichroism

It was known from the previous study [1] that the composite AB shows α-helical structure which confirms protein present in the composite. The far UV spectral studies (185 nm - 250 nm) were conducted on ABC composite and it was observed that an unordered random coil structure with negative peak at around 197 nm as shown in fig-8.

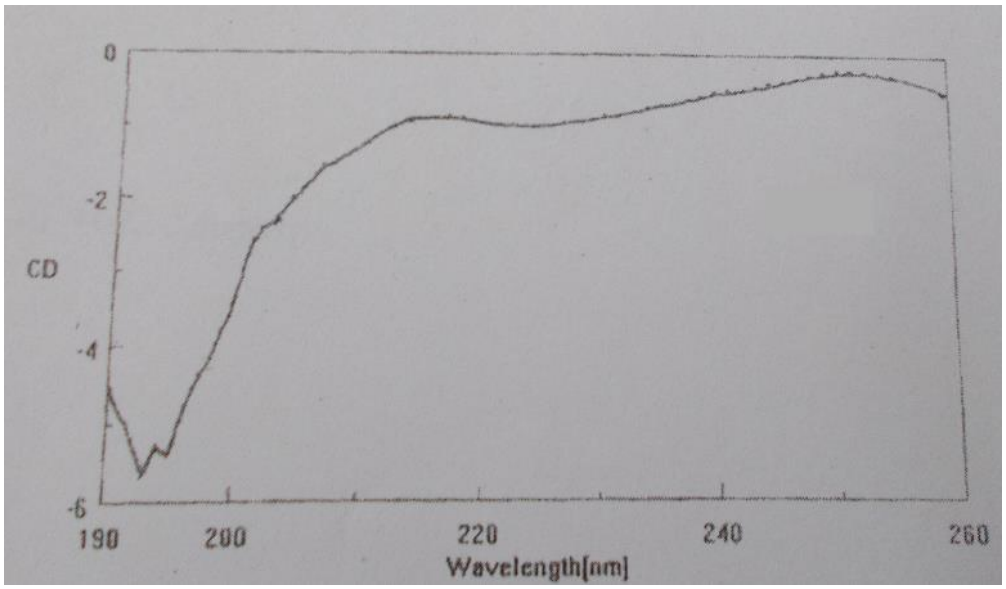

Fig-8: CD spectra of Hen egg white-Gelatin-Glutaraldehyde composite

The breakage of helical structure in AB and converted in to random coil is due to cross linking of glutaraldehyde with AB composite.

4. Conclusion

Hen egg white which is natural food nutrient is used in making a bio-polymer material by cross linking with gelatin and glutaraldehyde. This bio-polymeric film possesses excellent tensile strength and high temperature withstands and hence the product can be used as a coating agent on materials to prevent rust and thereby improving the life of the material.

5. References

1. U. Venkateswarlu, Kamala Bhoopalan, R. Mohan, B.N Das and T.P Sastry, Studies on chemically modified hen egg white and gelatin composites. *J. Applied Polymer Science.* 2006, **100**, 318-322.

2. G. Hidas, A. Kastin and M. Mullerad, Sutureless nephron-sparing surgery: Use of albumin glutaraldehyde tissue adhesive (BioGlue). *Urology*, 2006, **67**, 697-700.

3. Georg W. Hergeta, Mulugeta Kassaa, Ursus Nikolaus Riedeb, Yao Lua, Ludwig Brethnera and Joachim Hassea, Experimental use of an albumin–glutaraldehyde tissue adhesive for sealing pulmonary parenchyma and bronchial anastomoses. *Eur. J. Cardio-Thoracic Surgery*, 2001, **19**, 4-9.

4. Kamalrookh Z Marolia and Stanislaus F D'Souza, Enhancement in the Lysozyme activity of the hen egg white foam matrix by cross-linking in the presence of N-acetyl glucosamine. *J. Biochem. Biophys. Methods,* 1999, **39**, 115-117.

5. Kamalrookh Z Marolia and Stanislaus F D'Souza, A simple technique for the immobilization of Lysozyme by cross-linking of hen egg white foam. *J. Biochem. Biophys. Methods*, 1993, **26**, 143-147.

6. Anandrao R. Kulkarnia, Kumaresh S. Soppimatha, Tejraj M. Aminabhavia and Walter E. Rudzinskib, In-vitro release kinetics of cefadroxil-loaded sodium alginate interpenetrating network beads. *Eur. J. Pharmaceutics and Biopharmaceutics*, 2001, **51**, 127-133.

7. A Bigi, G Cojazzi, S Panzavolta, K Rubini and N Roveri, Mechanical and thermal properties of gelatin films at different degrees of glutaraldehyde cross linking. *Biomaterials*, 2001, **22**, 763-768.

8. Yasuhiko Tabata and Yoshito Ikada, Vascularization effect of basic fibroblast growth factor released from gelatin hydrogels with different biodegradabilities. *Biomaterials*, 1999, **20**, 2169-2175.

9. Yan Changhong, Li Xiongwei, Chen Xiaoli, Wang Danqing, Zhong Dachang, Tan Tianzhi and Hiromi Kitano, Anticancer gelatin microspheres with multiple functions. *Biomaterials*, 1991, **12**, 640-644.

10. Jitendra Sharma and H.B. Bohidar, Gelatin–glutaraldehyde supramolecular structures studied by laser light scattering. *Eur. Polymer Journal*, 2000, **36**, 1409-1418.

11. J.F. Kennedy, B. Kalogerakis and J.M.S. Cabral, Surface immobilization and entrapping of enzymes on glutaraldehyde cross linked gelatin particles. *Enzyme and Microbial Technology*, 1984, **6**, 127-131.

12. J.F. Martucci, R.A. Ruseckaite and A. Vázquez, Creep of glutaraldehyde-cross linked gelatin films. *Materials Science and Engineering*, 2006, **435**, 681-686.

13. T.P. Sastry and K. Panduranga Rao, Hydrogels Based on Amniotic Collagen Poly (Hydroxyethyl Methacrylate) Graft Copolymers. *J. Bioactive and Compatible Polymers*, 1990, **5**, 430-438.

IVL P-38

ULTRASONIC STUDIES ON VEGETABLE TANNIN MATERIALS

U Venkateswarlu

Advanced Materials Lab, Central Leather Research Institute, Adyar, Chennai- 600020, India

e-mail: venkateswaralu@clri.res.in

Ultrasonic studies were performed on Myrobalan, Mangustan and soap berry tannin compounds. These tannin materials were extracted using Proctor Method (PR) and Ultra Sound (US) methods. The properties of density, velocity, viscosity, adiabatic compressibility, acoustic impedance, absorption coefficient, viscous relaxation time and free length were calculated at different concentrations and temperatures using both PR & US extraction methods and their results were found to be having similar behavior at temperatures between 20^{o}C and 80^{o}C in step of 5^{o}C. Ultrasonic velocity of the tannins increases with increase in temperature. Viscosity of the tannins decreases with increase in concentration and temperature. Adiabatic compressibility (which is a measure of molecular interactions in binary and ternary mixtures) for tannins decreases with increase in temperature. Inter molecular free length (which is a measure of molecular association) of tannins increases with increase in temperature. Absorption coefficient (structure dependant) for tannins decreases with temperature. Acoustic impedance (which accesses molecular interaction between components) increases with temperature. All the above mentioned ultrasonic parameters show an increase in its values with increase in their concentrations. Finally, it was concluded from the study that the Ultrasonic method is a simple and non-destructive powerful technique in analyzing the tannin materials.

Keywords: Myrobalan, Mangustan, soapberry, ultrasonic, proctor, tannin.

1. Introduction

Myrobalan tannin [1] is a fruit of Terminalia chebula was obtained by well crystallizing substance which gave on hydrolysis either with dilute sulfuric acid or with emulsion, 1 mol. ellagic acid and 2 mol. Glucose. Myrobalan extracts provide a light greenish yellow color to tanning liquors and leathers and they are used especially in the first steps of tanning sole leathers. The extracts are available both in liquid and powder form and give leathers a uniform color and a soft touch. Due to myrobalan's high sugar content, the extracts ferment easily. Ultrasonic power was used in extraction of myrobalan [2] as a tanning agent. Mangustan is a tropical fruit of the tree Garcinia mangostana and has a deep reddish-purple colored exocarp (rind) when ripe. Tannin is obtained from the bark [Abbiw]. The fruit shell contains 7-13% tannin and the seeds contain 3% oil [Burkill]. The rind of the fruit contains tannin, a resin and a bitter principle called mangostin. The rind contains 5.5% of tannin, and a resin as well as a yellow crystalline bitter principle, mangostin ($C_2OH_{22}O_5$) or mangosim isolated from the rind. Mangostin is obtained by boiling the rind in water, and tannin is removed by exhausting by boiling in alcohol and evaporating; resulting product is mangostin and resin; resin is precipitated by redissolving it in alcohol and water, and evaporating the water. It occurs in small yellow scales, tasteless neutral, insoluble in water, but readily soluble in alcohol and ether [3]. Soapberry was extracted and used for the prevention of a skin infestation [4] by an organism that impairs leather quality. The berries are preferably first dried and ground, and then extraction is carried out in an alcoholic solvent and the extract material subjected to alkaline hydrolysis. The above tannin extracts were collected and used for our study to analyze ultrasonic parameters. The parameters such as Ultrasonic densities (ϱ), velocities (u), and viscosities (η), are measured for the above said tannin solutions and the acoustical parameters such as adiabatic compressibility (β), free length (Lf), absorption coefficient (α/f^2), viscous relaxation time (τ), characteristic (acoustic) impedance (Z), are calculated for these solutions to study solute-solvent interactions according to the method published by Venkateswarlu [6].

2. Material and methods:

2.1 Materials: Myrobalan, Mangustan, Soapberry were crushed and freed from seeds and the flesh portion was taken for tannin extraction by (i) Procter extraction method (PR Method) and (ii) high power ultrasound extraction method (US Method).

2.1.1 PR Method: Myrobalan nuts (4g) were taken and tannins were extracted in hot water for 2 hours using Procter extractor to obtain 1000 ml of 0.04% solution with respect to tannin concentration.

2.1.2 US Method: The crushed myrobalan nuts free from seeds (4g) were taken in a beaker and kept in a high power ultrasonic bath having a power output of about 150 w at a frequency of 40 kHz. Extraction was carried out using distilled water for 30 min. at room temperature to obtain 1000 ml of 0.4% solution with respect to tannin concentration.

2.1.3 PR Method: Mangustan nuts (8g) were taken and tannins were extracted in hot water for 2 hours using Procter extractor to obtain 1000 ml of 0.04% solution with respect to tannin concentration.

2.1.4 US Method: The crushed Mangustan nuts free from seeds (8g) were taken in a beaker and kept in a high power ultrasonic bath having a power output of about 150 w at a frequency of 40 kHz. Extraction was carried out using distilled water for 30 min. at room temperature to obtain 1000 ml of 0.4% solution with respect to tannin concentration.

2.1.5 PR Method: Soapberry (8g) was taken and tannins were extracted in hot water for 2 hours using Procter extractor to obtain 1000 ml of 0.04% solution with respect to tannin concentration.

2.1.6 US Method: The crushed Soapberry free from seeds (8g) were taken in a beaker and kept in a high power ultrasonic bath having a power output of about 150 w at a frequency of 40 kHz. Extraction was carried out using distilled water for 30 min. at room temperature to obtain 1000 ml of 0.4% solution with respect to tannin concentration.

2.2 Method: Tannin solutions obtained by PR and US methods were used to measure ultrasonic velocity at different temperatures ranging from 20°C-90°C with an increment of 5°C using an ultrasonic interferometer vibrating at a frequency of 2 MHz, Viscosity and density measurements were also carried out for all these solutions at different temperatures.

3. Results & Discussion

Ultrasonic densities, velocities and viscosities are measured for solutions prepared with tannin materials of (i) myrobalan (ii) Mangustan (iii) Soapberry nuts by using ultrasonic method(US) and Procter method (PR) at temperature range 20°C-80°C in the step of 5°C. The density (ϱ) values of above said tannin extracts at different temperatures and concentrations are shown in below fig.1.

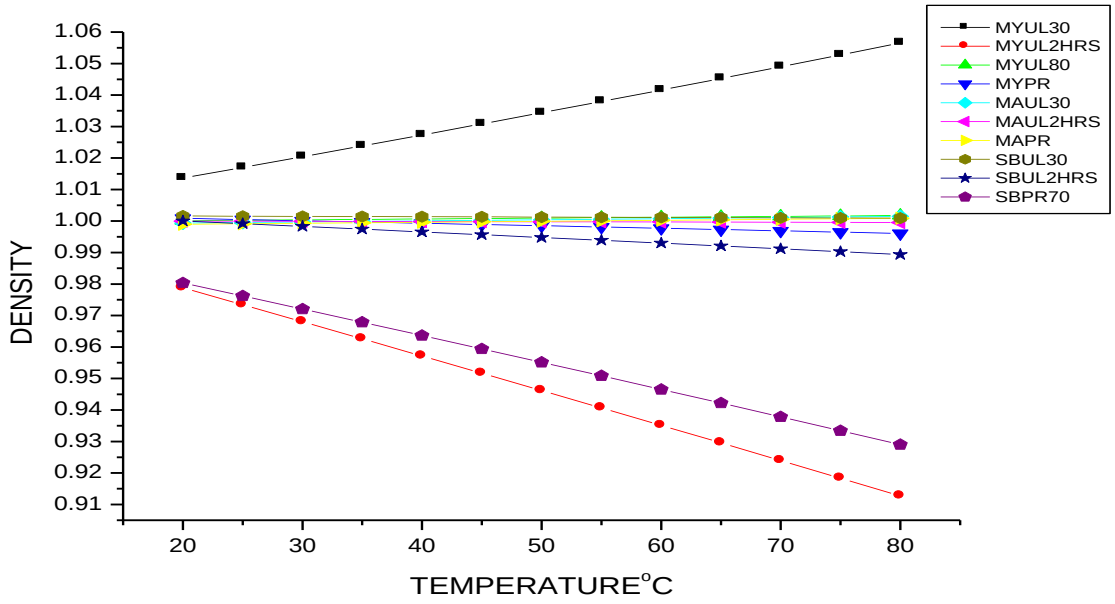

Fig.1 Density (ϱ) versus temperature at different concentrations

Ultrasonic velocity (u) against concentration for these solutions between 20°C and 80°C are shown in fig.2.

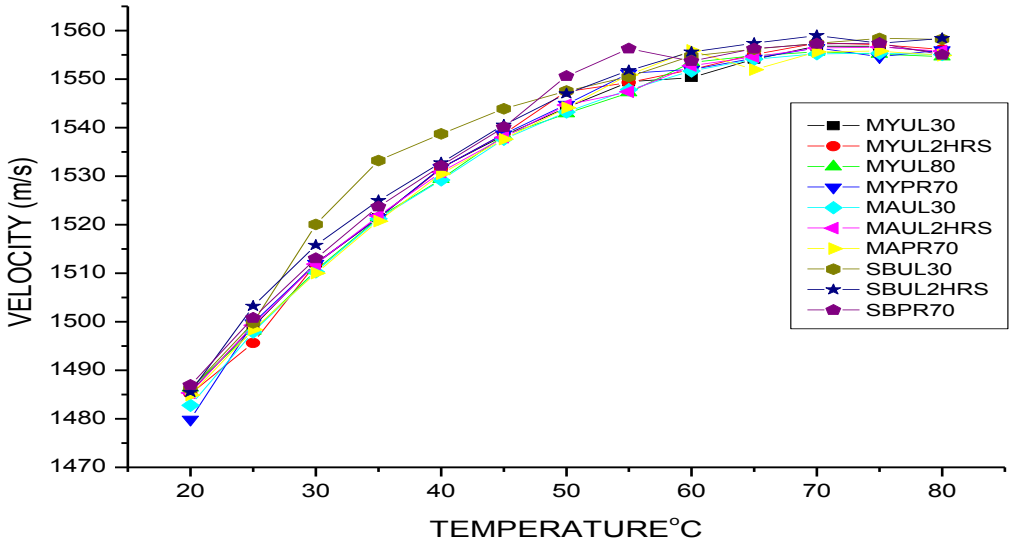

Fig.2 Ultrasonic velocities (u) versus temperature at different concentrations

It indicates that the ultrasound behavior in the solutions prepared by US and PR methods depends on structure of tannin materials and the influence of temperature. The impact of water behavior is observed invariably the samples extracted both (PR) and (US) methods. These observations indicate that the intermolecular attractions are similar to that of water. Viscosity (η) of tannins at various concentrations was measured from 20°C to 80°C and was shown in fig.3.

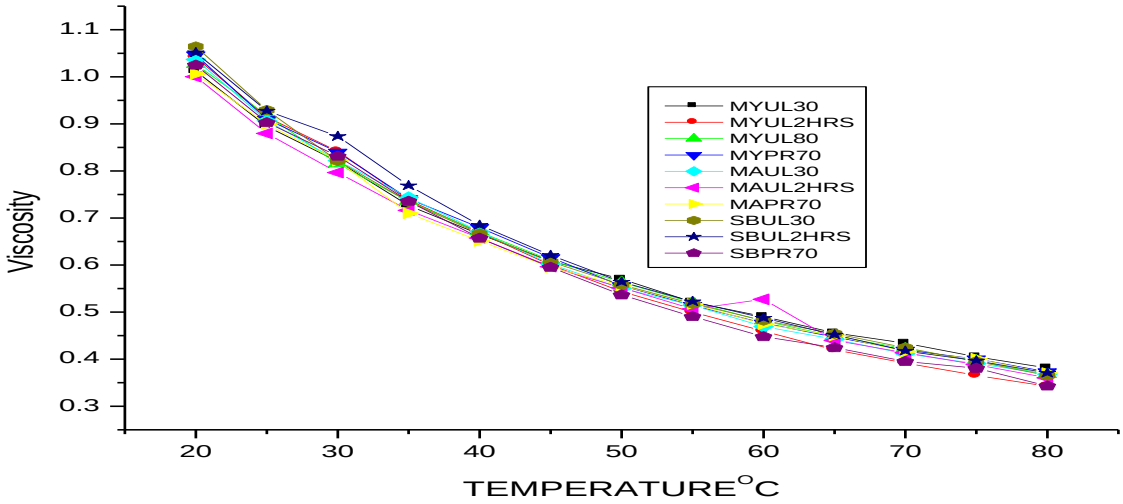

Fig.3 Viscosity (η) versus temperature at different concentrations

Adiabatic compressibility (β) is another parameter used in the study of molecular interactions in binary and ternary liquid mixtures. Salvation studies can be made from the β values. In the present investigation, β values are calculated from the ultrasonic velocities and densities at different temperatures in solution extracted from the tannin materials and are presented in fig.4.

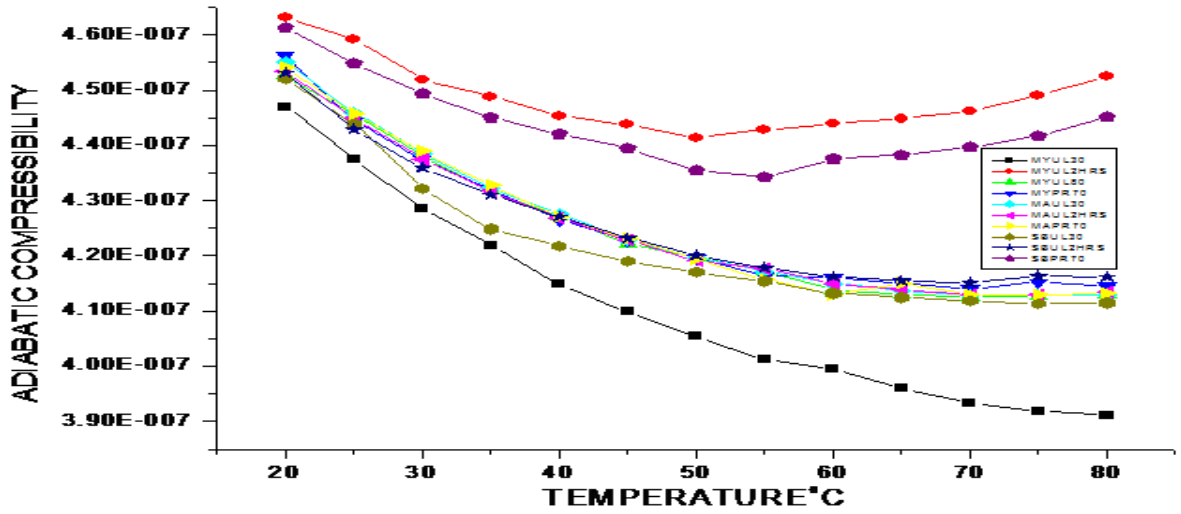

Fig.4 Adiabatic compressibility (β) versus temperature at different concentrations

It was clear from the plot that for all the solutions, the compressibility factor decreases with increase in temperature. Inter molecular free length (L_f) in a liquid system is a measure of molecular association. In the case of binary mixtures, L_f values depend on the interaction between the component molecules. In order to compare the intermolecular attraction in these solution, intermolecular free length values are computed from the solution extracted from the tannin materials of (i) myrobalan (ii) Mangustan (iii) Soapberry nuts and presented in fig.5.

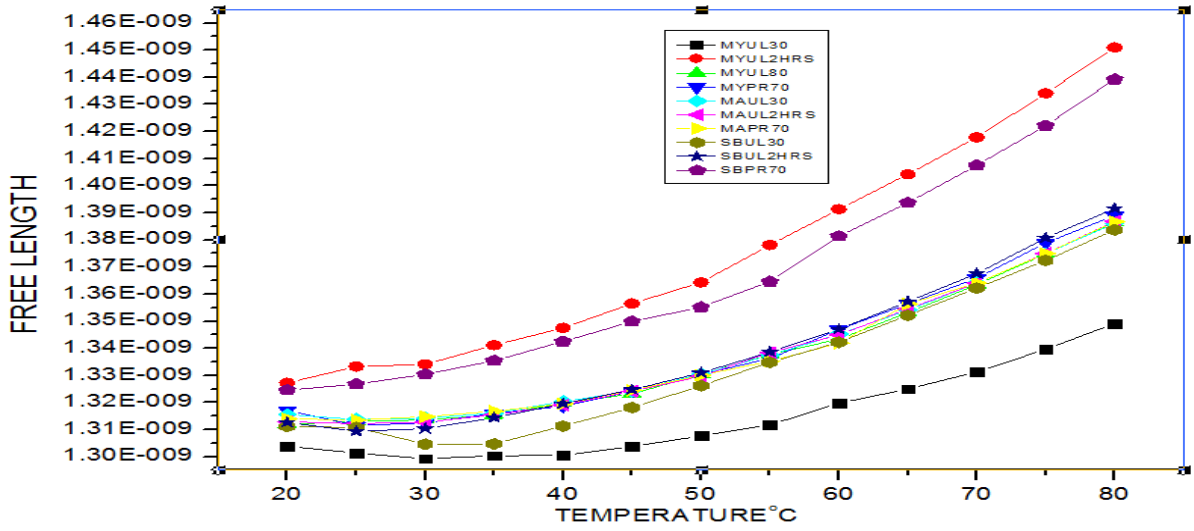

Fig.5 Intermolecular free length (L_f) versus temperature at different concentrations

It may be mentioned here that for all the solutions, the free length factor increases with increase in temperature. Absorption coefficient (α/f^2) is characteristic of a compound and depends on its structure. The tannin materials taken for this study are structurally different and hence study of the (α/f^2) solutions may throw light on the intermolecular attraction and are shown in fig.6.

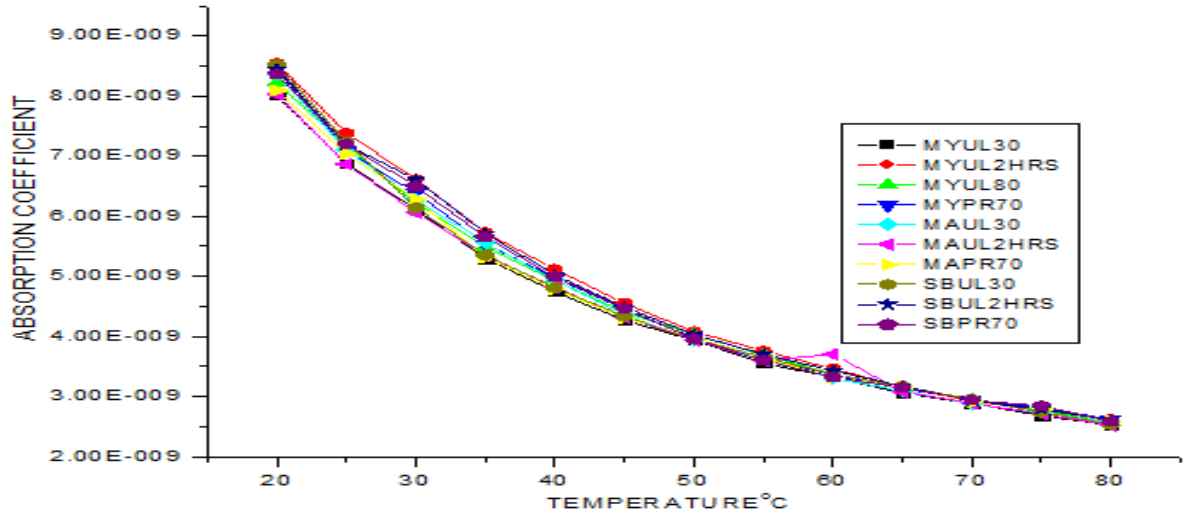

Fig.6 Absorption coefficient (α/f^2) versus temperature at different concentrations

It is found that (α/f^2) values do not change significantly with decrease with increase in temperature. This is because in aqueous solution solvent-solvent interactions are much stronger than solute-solvent interactions. In case of viscous relaxation time (τ) the same trend is observed and the data is presented in fig.7.

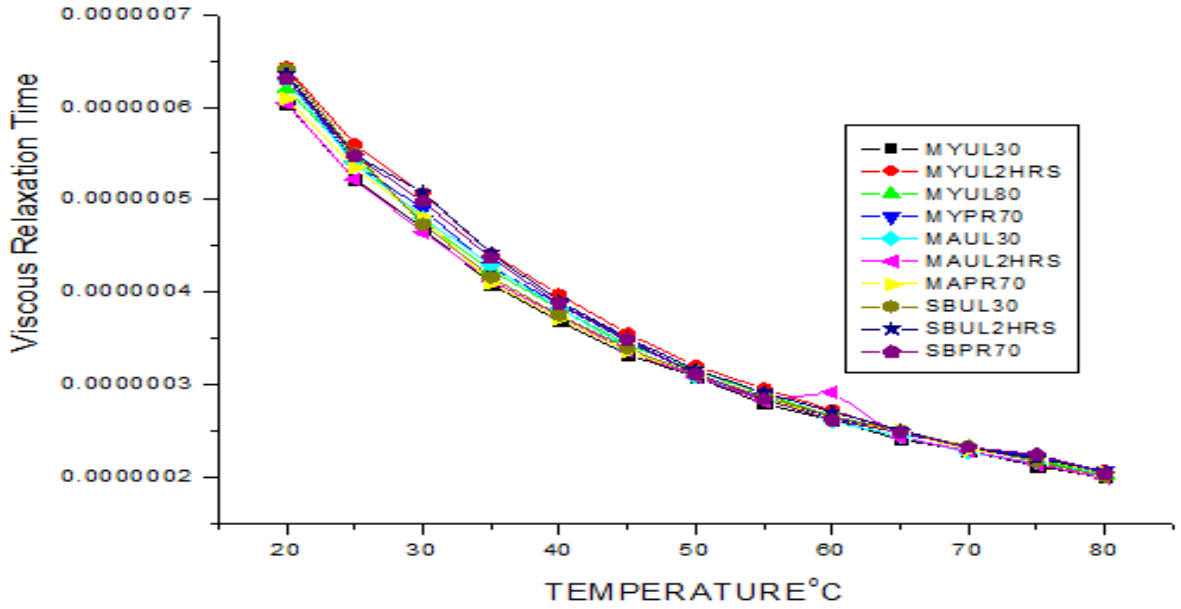

Fig.7 Viscous relaxation time (τ) versus temperature at different concentrations

Acoustic impedance (Z) in a liquid system can be used to assess the molecular interaction between the components plots of Z against solutions at all temperatures are given in fig.8.

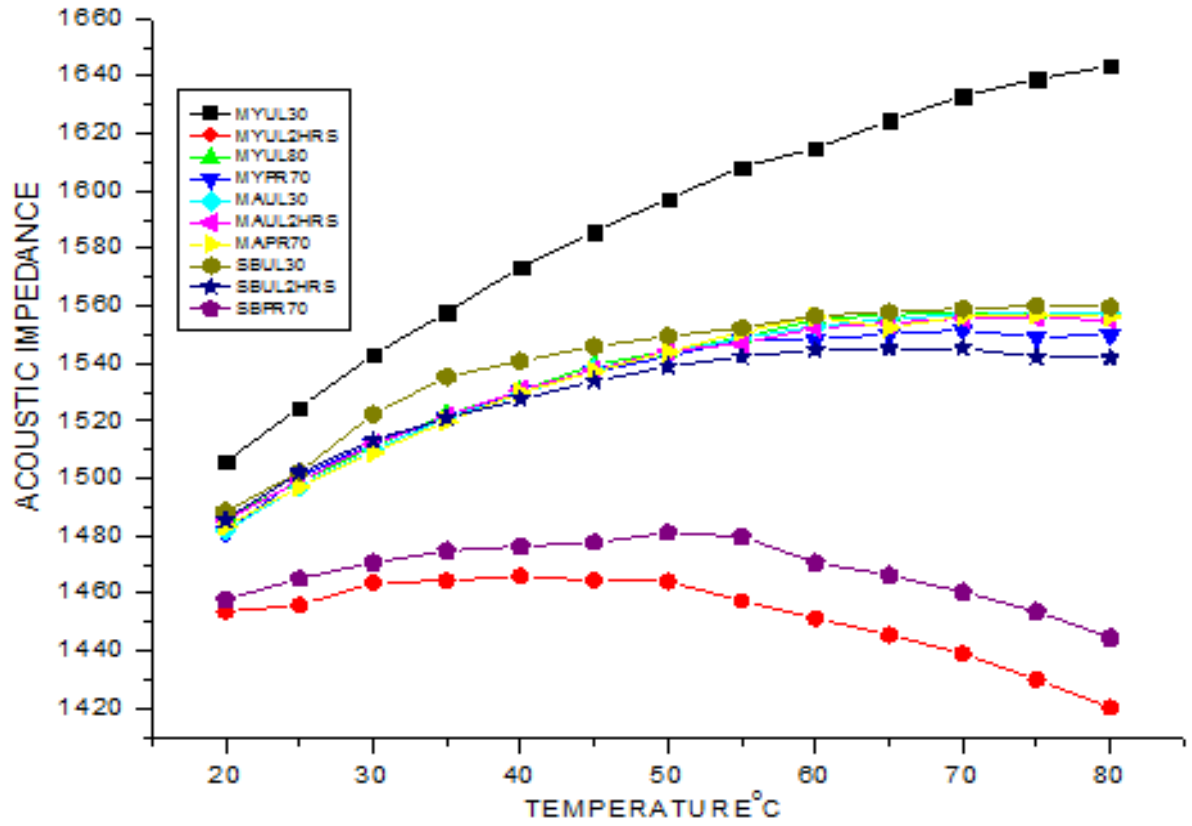

Fig.8 Acoustic impedance (Z) versus temperature at different concentrations

In general it is observed that Z values increase with increase of temperature for UL extraction than PR method.

Finally, analysis of tannin solutions of myrobalan is done using PR method and US method and the values are shown in below table-1. It was found that the amount on tannins present per 100 g total soluble is almost same by both the methods of extraction which gives 73.77% and 73.35% tannins per 100 g of total soluble respectively.

CHARACTERISTICS	PROCTER METHOD (PR)	ULTRASONIC METHOD (US)
Moisture (%)	9.5375	9.5375
Total soluble (%)	68.5333	62.0444
Tannins (%)	50.5600	45.5111
Non-tannins (%)	17.9733	16.5333
T/NT ratio	2.8130	2.7526
Tannins per 100 g Soluble	73.77	73.35

Table-1 Analysis of Myrobalan tannin using Proctor & Ultrasonic methods

4. Conclusions

Extraction obtained by PR and US methods are comparable with respect to thermo dynamical parameters. The extraction obtained by the US method at room temperature in shorter duration (30minutes) has intense color which is very much suitable for tanning leather. Hence it is concluded that the US method is more suitable than the existing PR method.

5. References

1. M. Nierenstein, and J. Potter, The distribution of myrobalan tannin. J. Biochem, 1945, **39**, 390-392.

2. V. Sivakumar, V. Ravi verma, P.G. Rao and G. Swaminathan, Studies on the use of power ultrasound in solid-liquid myrobalan extraction process. *J. Cleaner Production*, 2007, **15**, 1813-18.

3. K. M. Nadkarni, and A. K. Nadkarni, Indian Materia Medica - with Ayurvedic, Unani-Tibbi, Siddha, Allopathic, Homeopathic, Naturopathic and Home remedies. ***ISBN No. 81-7154-142-9***, 1999.

4. Bayoh, Tiruneh and Kassa, Treatment relating to leather. ***PCT/GB2003/004367***, 2004.

5. Zhang Junjie, Calculation of Ultrasonic Velocity in Binary Liquid Mixtures of Benzene. *Journal of University of Science and Technology of China*, 1984, **2**, 298-300.

6. U. Venkateswarlu, Ultrasonic studies on sargassum dye using water/ethanol extraction at different temperatures. *International Research Journal of Engineering and Technology*, 2015, **2**, 1130-1138.

SFS P-46

DEVELOPMENT OF DEGREASING ENZYME (LIPASE) USING SOLID WASTE FROM LEATHER INDUSTRY

Vimudha Muralidharan, Renganath Rao Ramesh, Michael Selvakumar Arokianathan and Saravanan Palanivel

Leather Process Division, Central Leather Research Institute, Adyar, Chennai - 600 020, India. Mail id: dermagroup@yahoo.co.in

Leather making process involves usage of hazardous chemical inputs for the conversion of skin to leather. Pre-tanning and tanning operations contribute to about 80-90% of the total pollution load. Among solid wastes, hide fleshing wastes accounts for 50-60% of wastes generated from the process. On the other hand, conventional degreasing process of animal skins is done using surfactants and solvents that are environmentally problematic. Fat from hide fleshing wastes was utilized for production of lipase enzyme using lipolytic bacteria sourced from putrefied animal skin. Such lipase was used for degreasing animal skin. Five lipolytic strains were screened and selected for the study. Among all, one strain showed maximum lipase activity when fleshing fat used as lipase inducer. About 20 - 30 g of fleshing lipid was obtained per kg of hide fleshing wastes. Lipase from optimized fermentation with carbon, nitrogen and fleshing lipid yielded maximum activity of 810 U/ml and used for degreasing of animal skins containing around 18 - 22% fat at the initial stage. The fat content in the skins was found to be reduced to around 4 - 6% after the degreasing enzyme treatment. The current study focused on researching the possibilities of using a skin putrefying bacteria based lipase for degreasing purpose, which was found to be more specific in its action with respect to natural grease present inside the skin matrix. Also, the fleshing wastes generated from the leather industry was optimally utilized for the cleaner and greener processing, which promised to be a sustainable solution for the industry.

Keywords: putrefaction; lipolytic bacteria; lipase; fleshing wastes; degreasing

1. Introduction

Leather and leather products are still in-vogue in the synthetics dominated world. Nevertheless, the leather industry is notorious for the pollution generation. The process steps, pre-tanning and tanning operations contributes to about 80-90% of the total pollution load (Saravanabhavan et al. 2005). Hide fleshings that accounts for 50-60% of total solid wastes, are disposed off with difficulty (Dayanandan et al. 2013). Utilizing such organic-rich component for fruitful innovations could lead to cleaner and sustainable solutions. Degreasing of animal skins is one of the most important processing steps since the consequences of inadequate degreasing can result in irreversible damage to the finished leather. The solvents and surfactants used for this purpose are problematic to environment. Lipase that has the ability to hydrolyze the lipid can be effectively utilized for degreasing purpose. Although, the strategy of using lipase for degreasing is already known and reported. Some of the works include degreasing of sheep skins using fungal lipases from *Rhizopus nodosus*, *Aspergillus flavus, Aspergillus niger* (Kamini et al. 1999) and bacterial lipases from *Bacillus spp.* (Saran et al. 2013), *Geobacillus spp.* (Deeya et al. 2016) and *Pseudomonas spp.* (Ramani et al. 2010). But there exists an inadequacy of these lipase in meeting the requirements, which solely calls for further developmental works in this area. The choice of micro-organisms for the production of enzymes is the key factor in obtaining efficacious lipase that could act as degreaser. The micro-organisms associated with the degradation of natural grease during putrefaction have been isolated and identified. Also, the medium which becomes the substrate for the organism, could decide the efficacy of the enzyme so produced. The present workwas aimed at developing an efficacious degreasing enzyme using a microbiological production medium that would employ the lipid extracted from tannery fleshing waste and an appropriate organism, thereby minimizing the pollution load altogether.

2. Materials and Methods

2.1 Materials

All chemicals were procured from Sigma Aldrich Pvt. Ltd. Microbiological media components were procured from HiMedia Pvt. Ltd. Pickled New Zealand sheep skins were used as raw materials for degreasing.

2.2 Methods

2.2.1 Isolation and characterization of lipolytic strains

Five lipolytic strains were screened and selected from the set of putrefactive bacteria isolated from putrefying goat skin. The isolates were tested on Tributyrin agar plate for lipid hydrolysis. The strains were inoculated in olive oil enriched nutrient media and incubated at 37^{o}C for 24 h. The fermented broths were centrifuged at 10,000 rpm at 4^{o}C for 10 min and the supernatant was spectrophotometrically assayed for lipase activity using p-nitrophenyl palmitate as substrate. (Winkler and Stuckmann 1979). Protein content of the supernatant was also determined using spectrophotometer. Bovine Serum Albumin standard was used. (Lowry et al. 1951)

2.2.2 Extraction of fleshing lipid from limed animal fleshing wastes

Limed fleshing wastes were pretreated using ammonium salts to remove the lime. Pretreated, washed and thermally hydrolyzed for 120 min at 121^{o}C and 15 psi. After hydrolysis, the lipid part and protein part gets separated. Hydrolyzed wastes were then cooled to room temperature and lipid was collected. The fleshing lipid was heated at 60^{o}C for 45 min to remove the moisture and then stored for further use.

2.2.3 Optimization of enzyme production parameters

Lipase enzyme was produced using Submerged fermentation. Parameters such as inoculum size, temperature, pH, incubation time along with carbon and nitrogen sources were optimized using OVAT (One-Variable-At-a Time) approach (Deeya et al. 2016). Fleshing lipid was used as lipase inducer and the concentration of lipid was also optimized. Carbon and nitrogen sources required for the production of enzyme were also optimized in the similar approach.

2.2.4 Characterization of crude lipase enzyme

Selected strain was inoculated in the optimized fermentation medium and the lipase was characterized for pH and temperature stability. The molecular weight of the crude lipase was determined using SDS-PAGE electrophoresis technique (Ramani et al. 2010). The gel was stained using Silver nitrate staining technique.

2.2.5 Application of degreasing enzyme for skin degreasing

Pickled New Zealand sheep skins with fat content ranging about 18 – 22 % were taken for evaluating the efficacy of the fleshing lipid based lipase enzyme, taking commercial degreasing enzyme as control. Table 1 explains the processing details of degreasing.

Table 1 Degreasing process of animal skin

Unit Process	**Input**	**Process Parameters**
Raw Material:		**Pickled New Zealand Sheep skins (Weight: 1.4 kg, pH – 3.8)**
Depickling (Drum)	Water 1.5 L (100%) Hypo 28 g (2%)	The skin piece were drummed for an hour and pH noted till 8.0.
Degreasing	Water 1.5 L (100%) Enzyme (X) (10%)	Drummed for 2 hours and then pelts were washed
Washing	Water 2 L (150%)	Drum run at 6 rpm for 20 minutes
Then the pelts were chrome tanned conventionally after adjusting the pH		

Crude lipase enzyme produced using animal fleshing lipid as lipase inducer of activity unit 810 U/mL was used for the degreasing application. The samples were collected after and before degreasing and the natural grease content was determined. The natural grease content in the pelt was determined by Soxhlet extraction method using Petroleum – ether solvent as a prescribed method of IULTCS (Sivakumar 2009). The wet pelt sample was cut into small pieces and taken in an evaporating basin and dried at 30^{o}C – 35^{o}C for 16 – 18 h. Then the actual weight of the pelt was recorded as W_1. The dried pelt was transferred to extraction thimble made out of Whatmann No.1 filter paper. The extraction flask was cleaned and dried in an oven at 102^{o}C and cooled in a desiccator and its weight along with the boiling porcelain bits was noted as W_2. The Soxhlet extraction was carried out with apparatus of 100 mL capacity using Petroleum – Ether as solvent for 5 h and the solvent from the flask was subsequently distilled. The extract was dried in the oven for 4 h at 102^{o}C, cooled in the desiccator and the weight of the flask was recorded. The drying – cooling – weighing cycle was repeated until the difference was less than 10 mg. Then the final dried weight of the flask was noted as W_3. The solvent extractable from the samples were measured using the equation

$$\%\text{Fat Content} = \left(\frac{(\text{W3} - \text{W2})}{\text{W1}}\right) \times 100$$

The fat content on skins were reported as percentage solvent extractable.

3. Results and Discussions

3.1 Identification of lipolytic strain

Among all five strains, two strains were found to be more potent in hydrolyzing the lipid. Two of the strains were identified by 16sRNA technique. Strain No. 4.2 and Strain 3.3 were identified as *Pseudomonas mendocina* and *Staphylococcus xylosus* respectively. Strain No. 4.2 was selected for the purpose of degreasing high fat content sheep skins.

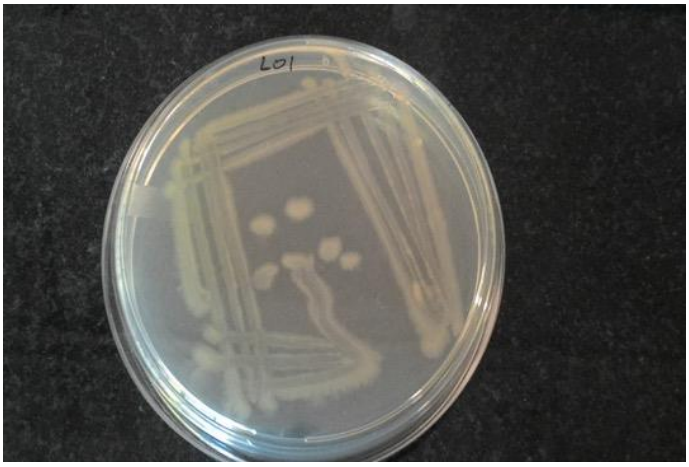

Figure 1 Strain No. 4.2

3.2 Extraction of fleshing lipid from limed animal fleshing wastes

Thermal hydrolysis of 1 kg of animal fleshing waste yielded 20-30 g of fleshing lipid. The fleshing lipid was collected and stored till further use. Fig shows the thermal hydrolysis of animal fleshing wastes.

a) b) c) d)

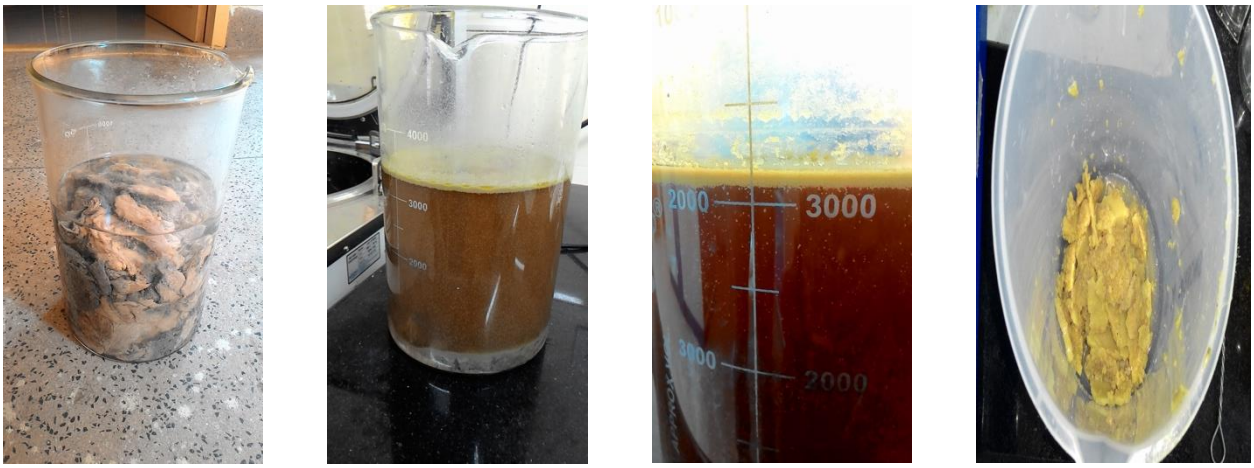

Figure 2 Thermal hydrolysis of limed fleshing wastes. a) pretreated washed fleshings; b) After thermal hydrolysis; c) Separation of layers; d) Animal fleshing lipid

3.3 Optimization of enzyme production parameters

The fermentation conditions such as inoculum size, pH, incubation temperature, concentration of fleshing lipid, effect of carbon and nitrogen sources were optimized for production of lipase with better lipase activity. Fleshing lipid was found to be the key carbon source and lipase inducer for lipase enzyme production. The carbon and nitrogen sources were screened by replacing 1% w/v of the respective source in the Fleshing Fat-Nutrient media.

The selected strain (Strain No. 4.2) showed better activity with even very low concentration of substrate (0.2%v/v) as compared to that of Olive oil based lipase. This reveals the strains' higher capability of hydrolyzing the animal fat rather than the vegetable oil. This could be taken as a lead factor for considering the strain to be a potent degreasing enzyme producer. The animal fat in the fermentation media also acts as the prime carbon source as it is revealed by the screening test where the other carbon sources have very little to no effect on the lipase production. The following figures are shown to represent the optimized conditions for lipase production with animal fleshing lipid as lipase inducer. The table below describes the optimized conditions for lipase production.

Table 2 Optimized parameters for production of lipase using animal fleshing lipid

PARAMETERS	**OPTIMUM CONDITIONS**
Inoculum (%v/v)	7
pH	9.0
Temperature (^{o}C)	37
Fleshing lipid (%v/v)	0.2
Incubation Time	48 h

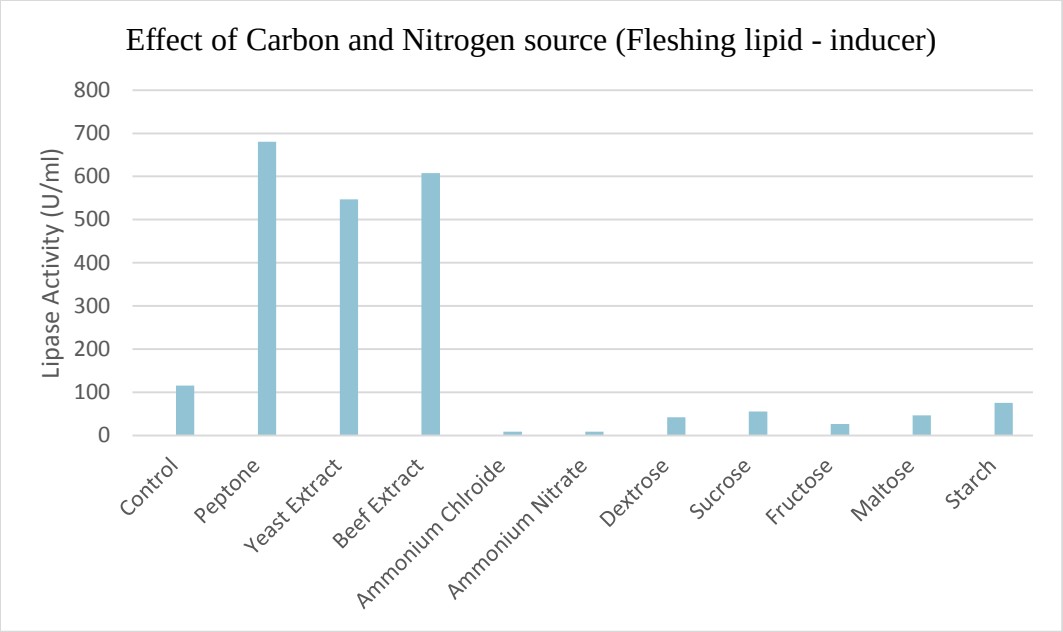

Figure 3 Effect of carbon and nitrogen sources on lipase production

3.4 Characterization of crude lipase enzyme

The crude lipase enzyme produced using Strain No.4.2 on fleshing lipid was characterized for its thermal (Fig) and pH stability (Fig). The crude enzyme was subjected to electrophoresis (Fig) against the standard protein marker of range 14.3 kDa – 97.4 kDa (GeNei from Merck Millipore Pvt. Ltd.).

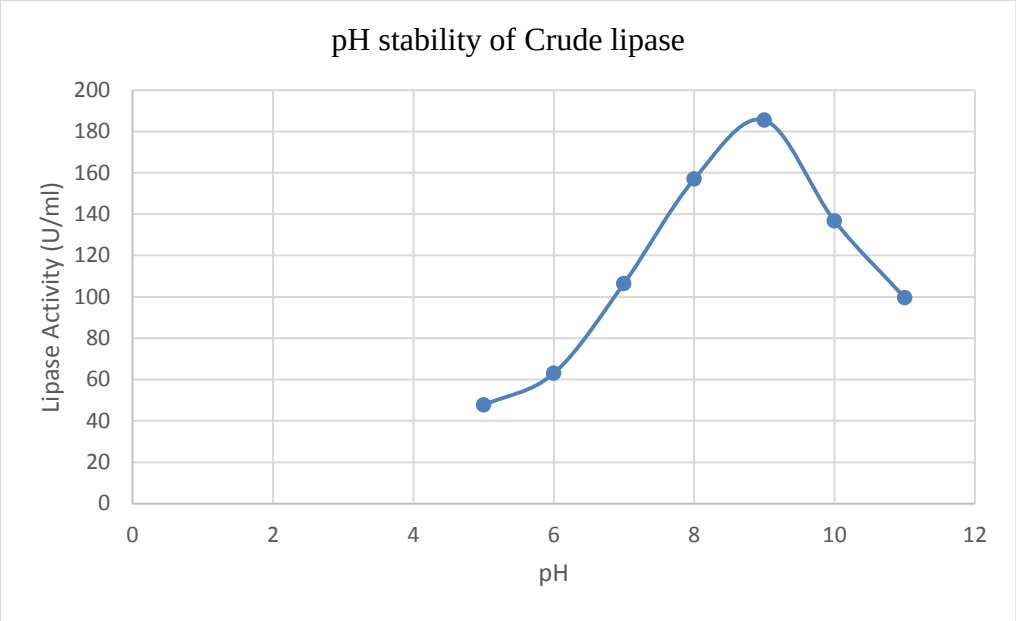

Figure 4 pH stability of lipase enzyme

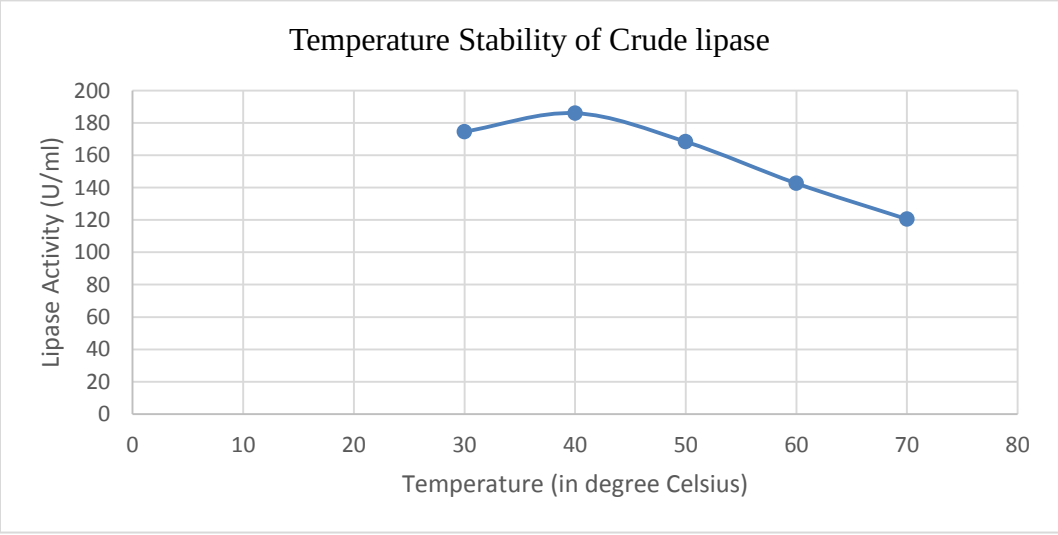

Figure 5 Temperature stability of lipase enzyme

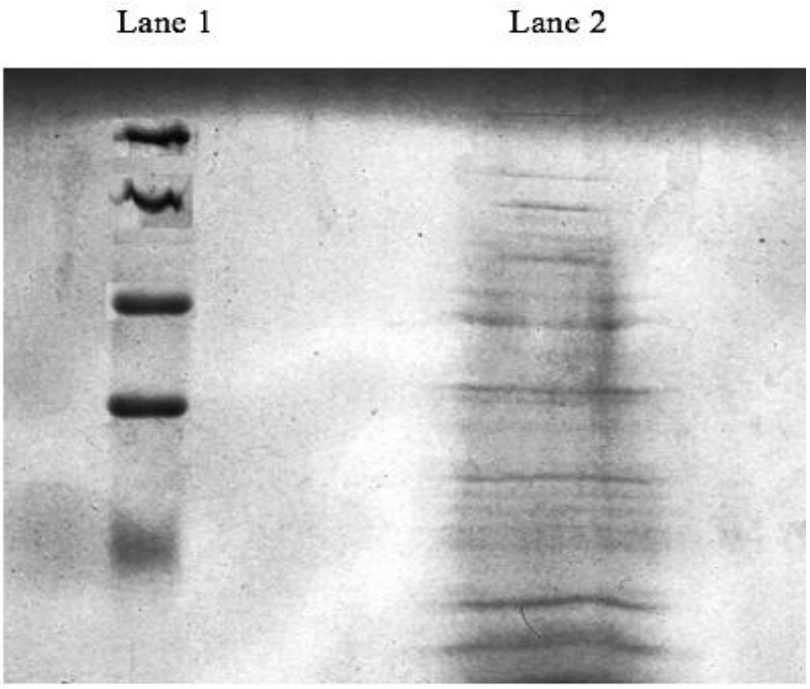

Figure 6 SDS-PAGE (12%) Silver stained gel

The Fig represents a 12% SDS-PAGE gel that revealed resolution of lipase enzyme to give majority of bands around 30 kDa to 97.4 kDa. Lane 1 represents the protein marker showing 5 bands from 20.1 kDa – 97.4 kDa (bottom to top). Lane 2 represents bands for crude lipase enzyme having major bands around 27 kDa,32 kDa, 43 kDa, 59 kDa, 67 kDa and 97 kDa. The crude lipase enzyme was found to be stable at pH 9.0 and at a temperature around 40^{o}C.

3.5Evaluation of enzyme's ability for skin degreasing application

The fat content before and after degreasing were determined using Soxhlet extraction and tabulated below.

The pelt after degreasing operation were found to have a clean smooth surface and the texture of the pelt was better than commercially degreased pelts. Fleshing lipid based lipase treatment rendered the skin with lowered fat content ranging to about 4 – 6%. Though the solvent treated skins had the least fat content but it was found to be harmful to environment and the quality of leather. The standalone effect of the enzyme was better and it could be further improvised by fermentation technologies.

Table 3 Efficacy of lipase enzyme for degreasing

Experiment	Initial Fat Content of Skin (%)	Final Fat Content of Degreased Skin (%)	Percentage reduction (%)
Commercial Degreasing Enzyme	18	5.1	71.6
Fleshing lipid based Lipase enzyme	21	4.2	80
Commercial Degreasing solvent	22	2.3	89.5

4. Conclusions

The current study focused on researching the possibilities of using a skin putrefying bacteria based lipase for degreasing purpose, which was found to be more specific in its action with respect to natural grease present inside the skin matrix. Further, the fleshing wastes generated from the leather industry was optimally utilized as raw material for the production of lipase leading to the development of cleaner and greener degreasing process in leather manufacturing. The wastes have been put to beneficial use to the same industry's cleaner processing leading to a sustainable option.

5. Acknowledgement

The authors of this work acknowledge the ZERIS CSC 0103 project work and CSIR-CLRI for providing funds and helping with the laboratory equipment.

6. References

1. Dayanandan A, Hilda V R S, Shanmugavel M, Gnanamani A, Suseela Rajakumar G, Enhanced production of *Aspergillus tamarii* lipase for recovery of fat from tannery fleshings. *Braz. Jou. of Microbio*. 2013, **44**, 1089-1095.
2. Deeya M A F, Reda A B and Hassan M A, Production of thermoalkaliphilic lipase from *Geobacillus thermoleovorans* DA2 and application in leather industry. *Enz. Res.* 2016, 1-9.
3. Kamini N R, Hemachander C, Mala J G S, Puvanakrishnan R, Microbial enzyme technology as an alternative to conventional chemicals in leather industry. *Curr. Sci*. 1999, **77**, 80-86.
4. Lowry O H, Rosebrough N J, Farr A L and Randall R J, Protein measurement with Folin Phenol reagent. *J. Biol. Chem.* 1951, **193**, 265-275.
5. Ramani K, Kennedy J L, Ramakrishnan M and Sekaran M, Purification characterization and application of acidic lipase from *Pseudomonas gessardii* using beef tallow as a substrate for fats and oil hydrolysis. *Proc. Biochem*. 2010, **45**, 1683-1691.
6. Saran S, Richi V, Rekha K, Jasmine I and Saxena R K. Enzyme mediated beam house operations of leather industry: a needed step towards greener technology. *Jou. Cle. Prod.*, 2013, **1**, 47-52.
7. Saravanabhavan S, Aravindhan R, Thanikaivelan P, Raghava Rao J, Nair B. U. and Ramasami T, A source reduction approach: Integrated bio-based tanning methods and the role of enzymes in dehairing and fibre opening. *Clean Tech. Envi. Pol.* 2005, **7**, 3-14.
8. Sivakumar V, Chandrasekaran F, Swaminathan G and Rao P G. Towards cleaner degreasing method in industries: ultrasound-assisted aqueous degreasing process in leather making. *Jou. Cle. Prod*. 2009, **17**, 101-104.
9. Winkler U K and Stuckmann M, Glycogen, hyaluronate and some other polysaccharides greatly enhance the formation of exolipase by *Serrate marcescens*. *Jou Bact.,* 1979, **138**, 663-670.

IVL P-39

LIME FREE LEATHER PROCESSING USING SODIUM ALUMINATE

Valeika Virgilijus, Kestutis Beleska , Justa Sirvaityte, Rasa Alaburdaite & Violeta Valeikiene

Kaunas University of Technology, Department of Physical and Inorganic Chemistry, Radvilenu pl. 19, 50254, Kaunas, Lithuania Email: virgilijus.valeika @ktu.lt; rasa.alaburdaite@ktu.lt
Kaunas University of Technology, Department of Polymer Chemistry and Technology, Radvilenu pl. 19, 50254, Kaunas, Lithuania Email: kestutis.beleska@ktu.lt; justa.sirvaityte@ktu.lt; violeta.valeikiene@ktu.lt

A major contributor to the pollution from the tanning industry is conventional unhairing using sodium sulphide and lime. After the process, a sludge containing lime polluted with sulphides and proteins degradation products forms.
In this study, an attempt has been made to change the lime by soluble sodium aluminate. This material has strongly alkaline properties, non-toxic and good solubility in water. Also, sodium aluminate is an important commercial inorganic chemical for various industrial technical applications.
Therefore, the investigation of the possibility to replace lime by sodium aluminate in unhairing systems was done. There were investigated hair degradation quality, behaviour of hide tissue during unhairing process and the influence of unhairing parameters on the process run and finished leather quality.
Keywords: hide, unhairing, collagen, sodium aluminate, enzyme.

1. INTRODUCTION

Leather technologists and chemists could say when chromium salts were begun to be used in tanneries; they also could indicate the period when such materials as aniline dyes, enzymes etc. had been applied for the leather manufacture. Herewith**, in all probability** nobody knows when that serious chemical material, having title „lime“, has been first time employed for leather processing. Thereby, the lime is very good known, simple, relatively cheap, not very hazardous material, which is also usable for many other industrial purposes, and this is the main reason why till now it seems not irreplaceable for leather makers.
Despite the facts mentioned above, attempts to eliminate the lime from leather processing technologies are carrying out again and again. The main reason is, probably, the bad solubility of lime. On the one hand, this property of lime is very useful for a regulation of alkalinity during the liming process. On the other hand, it is the reason why the major part of lime added for the liming is threw out afterward. As write Thanikaivelan et al. (2001) “huge amounts of lime sludge and total solids formation are the main drawbacks of lime”. Herewith, the wastes are toxic and characterized by a high concentration of sulphur, mineral compounds, a high alkalinity and a high organic load. Cleaning process of the wastes is expensive, complicate and lingering.

After liming follows a deliming process. The lime which got into derma during liming must be removed as much as it possible reaching to produce a qualitative leather. Ammonia compounds or carbon dioxide are usually used for the deliming. The application of ammonia compounds leads to the pollution of wastewater by ammonia; the use of carbon dioxide requires special equipment for the process. Accordingly, the next reason, which leads to the elimination of lime from leather technologies is an appearance of a possibility to simplify the unhaired hide neutralization process or obviate the need of such process overall.

Nowadays there are few methods, which investigators use reaching to develop lime free leather manufacture processes. 1st way is to use enzymes. Pure enzymatic unhairing (Dettmer et al. 2013) or unhairing using mixtures containing enzymes with soluble alkalis (Valeika et al. 2009, Thanikaivelan et al. 2001), with reducers (Xu et al. 2010) or with oxidizers (Morera et al. 2016) can be applied for the producing of the leather, which, according to investigators' opinion, meets the quality requirements.

The next widely presented lime free method is a use of oxidizers. An application of such oxidizers as hydrogen peroxide (Bronco et al. 2005); magnesium peroxide (Gehring et al. 2006), calcium peroxide (Gehring et al. 2003); chlorine dioxide or even chlorine (Krawiecky and Sabat, 1984) is proposed.

The simplest way, which allows avoiding the formation of solid lime sludge, is a replacement of lime by other strong alkalis soluble in water. First of such very known alkalis is, of course, sodium alkali. Thorstensen and Dubost (1985) investigated various unhairing systems containing NaOH: NaOH with $NaHSO_3$; NaOH with amines; NaOH with carbamide; NaOH with carbamide and $NaBH_4$ etc. They concluded that sodium alkali is more effective unhairing agent comparing with lime. The strong action of sodium hydroxide on collagen can be weakened by addition of salts: sodium chloride, sodium sulphate, sodium formate or disodium hydro phosphate (Valeika et al. 1997). The developed lime-free method of unhairing-dermal opening up allows diminishing of consumption of sulphides and reaching of properties of chromium tanned leather not worse than those of leather produced using conventional method (Valeika et al. 2000).

The next alkali investigated as possible substitute of lime is sodium metasilicate. Munz and Sonleitner (2005) state that lime in the unhairing process can be substituted by sodium silicate without problems. They developed methods of unhairing applying sodium silicate as lime substitute, which lead reduced effluent loading, and so also sludge volumes from effluent treatment decreases. Saravanabhavan et al. (2005) investigated a lime and sulphide-free unhairing process using a commercial enzyme with the activation using sodium metasilicate. The process led to significant reduction in chemical oxygen demand and total solids by 53 and 26%, respectively. Liu et al. (2009) developed novel method based on system containing sodium silicate, enzyme, surfactant and urea. This method allows achievement an equivalent effect on fibre opening, shrinkage temperature and mechanical properties of crust leather compared with a conventional liming process. The environmental factors were all superior to the conventional liming process.

Herewith, sodium silicate like lime can be used for hair save process. It was investigated (Valeika et al. 2015) that sodium silicate acts as an effective immunization agent whose efficiency increases with increased treatment duration and treatment solution concentration. The effect was applied for a development of new hair save unhairing method (Sirvaityte et al. 2015). The parameters of the unhairing process have also been optimized evaluating qualitative indexes of the hide during processes and the leather obtained as well. It was established that hair removal quality and chemical and strength

properties of the experimental leathers are comparable to those of control leathers. A significant reduction in chemical oxygen demand (COD), biochemical oxygen demand and total Kjeldahl nitrogen were obtained in comparison with the comparative data for the conventional unhairing with hair burning.

After the searching of other materials suitable for the replacement of lime in unhairing process, authors of this paper have focused on one more interesting material: sodium aluminate. The material has strong alkaline properties, good solubility in water, and, comparatively, is cheap. Furthermore, it is an important commercial inorganic chemical for various industrial technical applications.

Possibilities to use the sodium aluminate as an alkaline agent instead of lime for hide unhairing process were investigated. The paper briefly presents summarised results of the investigation.

2. MATERIAL AND METHODS

Materials

Wool of merino sheep was used for the establishment of immunization effect of alkalis. The wool treatment by alkalis solutions was carried out pouring 100 ml of alkali solution on 1 g of the wool and shaking with agitation 120 rpm at 20-22^{o}C. The immunization effect was evaluated basing on changes of wool mass loss and content of nitrogen in treatment solution.

Salted cowhide after soaking and washing according to conventional technology were cut into pieces 10x10 cm and experimental series were prepared from these pieces. Samples were soaked and washed. Parameters of unhairing of the experimental were varied according to conditions of experiments. The unhairing for the control samples was carried out as follows: H_2O 40%, temperature 20-22^{o}C, $Ca(OH)_2$ 2.3%, Na_2S(100%) 1.2%, 1 h run continuously, $Ca(OH)_2$ 2.3%, 1 h run continuously, H_2O 100%, 2 h run continuously, later 5 min. every 3 h (% are based on hide weight in descriptions of unhairing methods).

Analytical sodium aluminate ($NaAlO_2$) containing Na_2O 40-45% and Al_2O_3 50-56% was used in this study. The chemicals used for the technological processes and for the analysis were of analytical grade. Other chemical materials used for technological processes were of commercial grade.

Enzyme preparations (EP) *Erhavit LSU* (TFL, Germany) and *Vilzim PRO ALK* (Baltijos enzimai, Lithuania) were employed for an enzymatic process.

Evaluation of unhairing quality

The quality of unhairing was evaluated according to the following scoring system:

1 – the hair is affected weakly;

2 – the hair is affected strongly but residuals of hair and epidermis are remained on derma and cannot be removed mechanically;

3 – residuals of hair and epidermis are remained on hide but easily can be removed mechanically;

4 – hide surface is clean.

Determination of hide and leather properties

Shrinkage temperature of hide was measured according to standard (Standard ISO 3380, 2002).
The swelling was calculated as ratio of increase in weight of hide during unhairing and soaked hide weight, and expressed in percent.
The amount of collagen proteins removed was estimated from the amount of hydroxyproline in the treatment solution. The amount of hydroxyproline was determined using a photo colorimetric method (Zaides et al. 1964).
Measurement of samples pH was carried out according to standard (Standard ISO 4045, 2008). The amount of removed non-collagenous proteins was calculated as the difference between the total proteins and the collagen proteins in the treatment solutions. The total proteins were established by Kjeldahl's procedure (Golovteeva et al. 1982).
Porosity of hide was determined according to method described in the literature (Golovteeva et al. 1982). Before the evaluation of porosity, the hide samples were dehydrated with acetone (Patent USSR, 1980).
Strength properties, the amount of chrome compounds in leather, soluble matter in dichloromethane, and volatile matter were determined according to standards (Standard EN ISO 3376, 2003; Standard ISO 5398-2, 2009; Standard ISO 4048, 2008; Standard EN ISO 4684, 2006).
Shrinkage temperature of chromed leather samples was determined as described in the literature using special equipment and replacing the distilled water with glycerol (Golovteeva et al. 1982).
Scanning electron microscopy (SEM) of hair was carried out using scanning microscope *JSM–840A* (*Joel,* USA). SEM parameters: 150 and 1200 times, accelerating *voltage* 25 kV, detector SE, *high vacuum regime*. The samples were coated by gold-palladium using equipment *JFC–1110 FINE COAT ION SPUTTER* (*Joel,* USA).
The main indexes of pollution load were determined according to standard methods (Standard ISO 15705, 2002; Standard ISO 5815-1, 2003).

3. RESULTS AND DISCUSSION

Unhairing with hair immunization

The previous investigation of hide unhairing using sodium silicate (Valeika et al. 2015; Sirvaityte et al. 2015) was the basis trying to reach similar effect using sodium aluminate. Experiments using merino wool revealed that sodium aluminate immunization efficiency increases while prolonging treatment duration and increasing treatment solution concentration. It was established that for appropriate immunization of the wool should be used solutions 2-3% sodium aluminate (Valeika et al. 2014). The immunization effect lasts even when the pH is about 13. Accordingly, the sodium aluminate has been confirmed as effective immunization agent having high immunization ability almost the same as the one for calcium hydroxide. Photographs of the wool treated by solutions of calcium hydroxide or sodium aluminate (solutions' concentration 2%) are presented in Fig. 1.
For the investigation of the unhairing effect the hide samples were treated as follows: H_2O 100%, temperature 20-22 ^{o}C, $NaAlO_2$ 2% or 3%, 1 or 2 hours run continuously, Na_2S(100%) 0.9%, 2 hours run continuously. After that the treatment solution was percolated through textile for released hair

removal, and returned into the treatment vessel; further run continuously 5 minutes every 4 hours. Total duration of the process 24 hours.

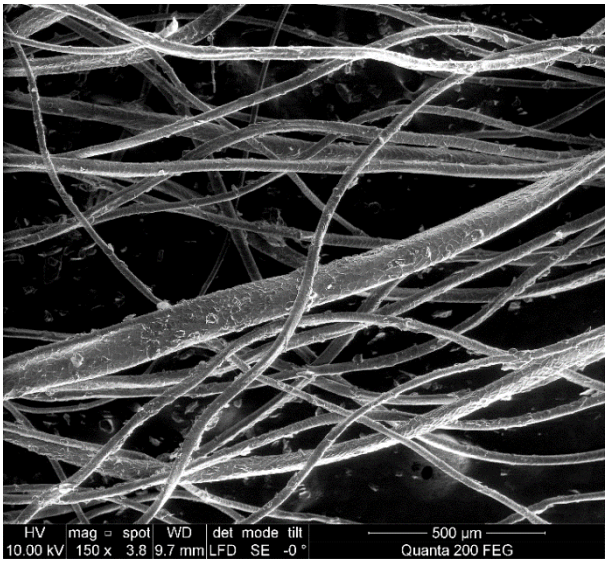

a

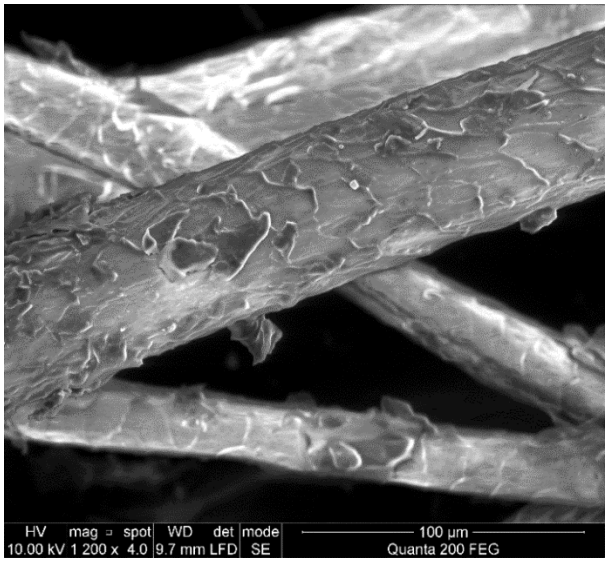

b

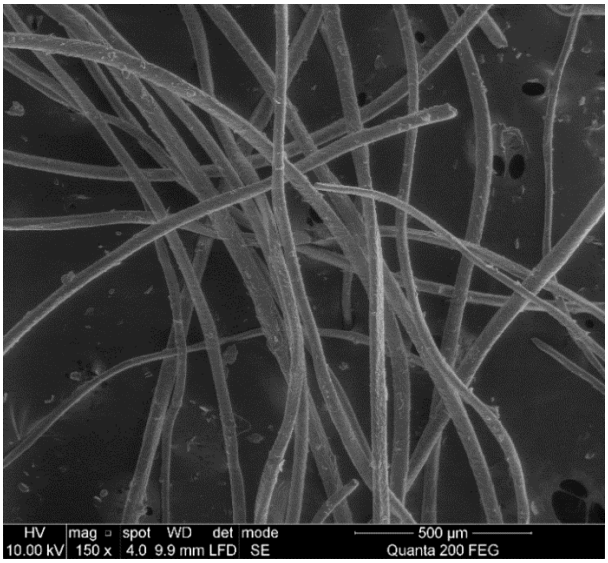

c

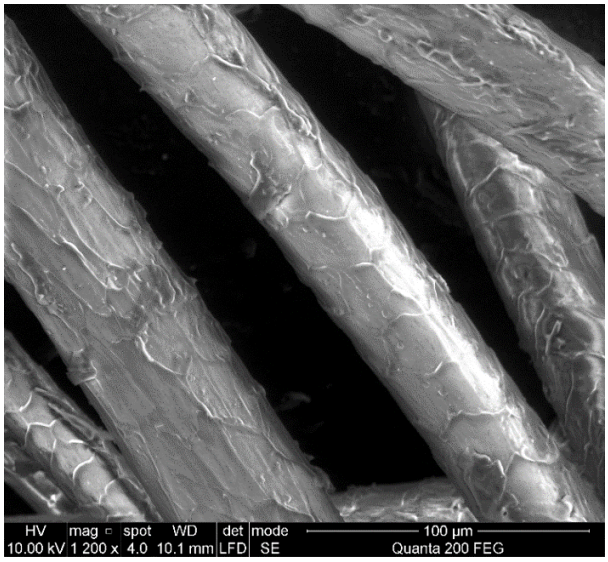

d

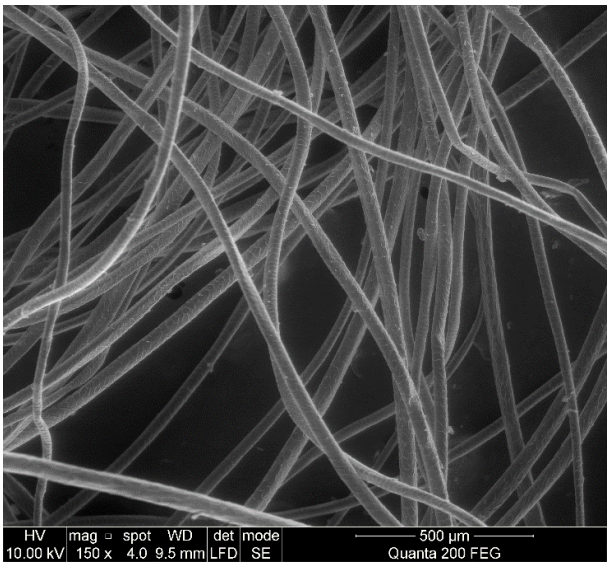

e

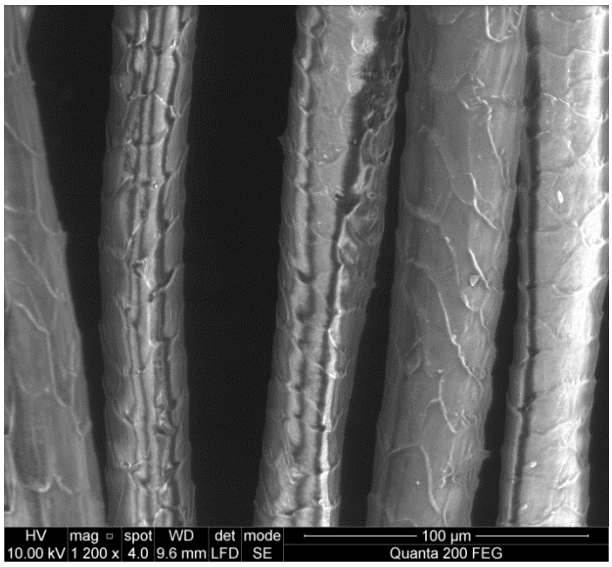

f

Figure 1. SEM photographs: **a, b** – native wool; **c, d** – wool treated 24 hours with $Ca(OH)_2$ **e, f –** wool treated 24 hours with $NaAlO_2$ (magnification: **a, c, e** – 150; **b, d, f** – 1200 times).

After the treatment a quality of the obtained pelt was assessed by analysis methods and organoleptically (Table 1).

Table 1. Data of assessement of pelt obtained by unhairing with hair immunization

Amount of used $NaAlO_2$, %	Total amount of removed protein materials, g/kg of hide		Amount of removed collagenous proteins, g/kg of hide		Shrinkage temperature, °C		Unhairing quality, points	
	Duration of treatment of hides by $NaAlO_2$, hours							
	1	2	1	2	1	2	1	2
2	1.84	2.18	0.08	0.08	57.0	58.0	3	3
3	2.09	1.47	0.09	0.09	58.0	58.0	3	3
Control unhairing	–		0.38		56.8		4	

The organoleptic estimation (Table 1) of the unhairing quality has shown that qualitative release of hair and epidermis is not reached using the unhairing with immunization. Despite the fact that residuals of hair could be removed from hide surface using blunt knife, the patches of epidermis left on the surface of hide even after wiping with the knife. We suppose that epidermis is immunized to strong, and does not surrender to action of sodium sulphide as a reducer.

Assessing other indexes of the pelt and the unhairing process, it can be proposed that hide tissue is affected markedly weaker than during control process. Collagen of pelt is affected in less level; shrinkage temperature of the pelt is higher than after the control unhairing-liming.

Now, the investigations of the unhairing using sodium aluminate based on the hair immunization are stopped.

Unhairing with hair degradation

The next step was the exploration of simultaneous action of sodium aluminate with sodium sulphide reaching to degrade hair. The qualitative degradation of hair and epidermis was achieved using solution containing 2-3% of sodium aluminate and 1.3-1.5% of sodium sulphide (Sirvaityte et al. 2016) The effect of such process on collagen is weaker than of conventional one. Increase of temperature up to 30^{o}C does not lead to better hair removal but significantly enhances effect on collagen.
Qualitative derma opening up level can be reached adding NaOH 0.5% into unhairing solution after 2 hours of the process beginning and the process continued for 22 hours. The NaOH addition leads to better removal of non-collagen proteins.
The pelt unhaired and opened up using sodium aluminate, sodium sulphide and sodium alkali due to the absence of calcium compounds in the derma can be neutralized using 2% of ammonia sulphate or 3% of boric acid (Beleska et al. 2016). The pelt after neutralization-bating had similar properties as conventionally neutralised one. Accordingly, after chroming these pelts were also very close in their properties. On the other hand, the experimental leather has less chromium content comparing with control one.

Table 2. Chemical and physical indexes of crust leather

Indexes	Crust leather	
	experimental	control
Moisture content, %	15.7	16.2
Cr_2O_3 content, %	5.09	5.13
Shrinkage temperature, ^{o}C	116.0	116.3
pH of leather	3.43	3.42
Amount of matter soluble in dichloromethane, %	4.49	4.31
Tensile strength, N/mm^2	19.7	19.9
Grain strength, N/mm^2	14.6	16.2
Relative elongation at the break, %	54.9	53.6

Industrial trials of the lime free unhairing using sodium aluminate and neutralization with reduced amount of ammonia sulphate has shown that produced leather by main qualitative indexes somewhat yields to conventionally produced one but it absolutely meets the quality requirements for shoe upper leathers (Table 2).
The lime free unhairing leads to less pollution of wastewater. The unhairing when sodium aluminate is used allows decrease of pollution load by TSS, Kjeldahl nitrogen, and especially by sulphides (Table 3). By the way, still it is not clear the reason of such low amount of sulphides in the end of the experimental unhairing.

Table 3. Indexes of pollution load (g/1 kg of hide) and pH of waste water after unhairing-dermal opening process (Sirvaityte et al. 2016)

Index	Unhairing-dermal opening up method	
	experimental	control
Total dissolved solids	81	97
Total suspended solids	4.2	6.4
Na_2S	1.3	13.4
BOD	32.8	25.9
COD	48.0	90.7
Total Kjeldahl nitrogen	14.8	19.9
pH	12.46	12.52

Enzyme assisted unhairing with hair degradation

Experiments to explore the simultaneous action of sodium aluminate, sodium sulphide and proteolytic enzymes were done as well.

The experiments have shown that addition of 0.1% EP *Vilzim PRO ALK* or 0.2% of *Erhavit LSU* allows decreasing the initial concentration of Na_2S down to 9 g/l simultaneously reaching qualitative degradation of hair during the process (other conditions: H_2O 100%; $NaAlO_2$ 2%, temperature 22-25^oC, duration 24 h).

The unhaired hide obtained using EP *Vilzim PRO ALK* was processed (subsequent processes were carried out according to conventional technology) getting chromed leather. The indexes of hide during the subsequent processes are presented in Table 4.

Table 4. Indexes of hide unhaired using system EP+$NaAlO_2$+Na_2S during processes

Index	Unhairing method	
	experimental	control
After unhairing:		
Shrinkage temperature, ^oC	57.5	52.0
Amount of removed collagenous proteins, g/kg of hide	0.60	0.39
After neutralization (deliming)-bating:		
Shrinkage temperature, ^oC	64.0	62.0
Amount of removed collagenous proteins, g/kg of hide	0.22	0.22
After chroming:		
Shrinkage temperature, ^oC	114.0	116.5
Cr_2O_3 content, %	4.43	5.46

The markedly higher amount of removed collagenous proteins during unhairing process allows proposition about overmuch strong effect of enzyme on collagen. Despite the fact that high shrinkage temperature was achieved during chroming process, the experimental leather has less amount of chromium. Furthermore, it has shrunk grain. Accordingly, these faults again indicate too strong effect on hide during processing.

The investigation of enzyme-aluminate unhairing now is in progress.

4. CONCLUSIONS

Sodium aluminate was confirmed as effective hair immunization agent. The treatment by solution containing 20 g/l of sodium silicate during 3 h allows reaching high immunization ability almost same as of calcium hydroxide in presented conditions. The immunization effect stays when the pH is about 13. The unhairing of hides when they at first are treated by sodium aluminate during 2 hours, and, afterward, are treated with sodium sulphide (total process duration 24 hours) does not release epidermis completely. Presumably, the epidermis is immunized to strong, and does not surrender to action of sodium sulphide as a reducer.

The qualitative removal of hair is achieved using solution containing 2-3% of sodium aluminate and 1.3-1.5% of sodium sulphide. The effect of such process on collagen is weaker than of conventional one.

Qualitative derma opening up level can be reached adding NaOH 0.5% into unhairing solution after 2 hours of the process beginning and the process continued for 22 hours. The NaOH addition leads to better removal of non-collagen proteins. The unhaired hide due to the absence of calcium compounds in the derma can be neutralized using 2 % of ammonia sulphate or 3% of boric acid. After chroming the experimental leather has very close properties comparing with conventional one.

The addition of enzymes into system containing sodium aluminate and sodium sulphide leads to decrease of sodium sulphide consumption reaching qualitative unhairing with hair degradation. Herewith, the use of EP *Vilzim PRO ALK* characterizes by stronger action on the hide. Due to this, the chromed leather with lower quality is processed from the hide obtained by enzyme assisted process.

5. ACKNOWLEDGEMENT

The research was carried out according to Research teams' project MIP021/2014 BEKALCE ODA funded by Research Council of Lithuania.

6. REFERENCES

1. Beleska K, Valeika V, Sirvaityte J, Alaburdaite R, Valeikiene V, Peculiarities of neutralization of lime-free pelt obtained using sodium aluminate. *ICAMS 2016: proceedings of the 6th international conference on advanced materials and systems, 20-22 October, 2016, Bucharest, Romania*; Bucharest: INCDTP-ICPI, pp. 323-327.
2. Bronco S, Castiello D, D'Elia G, Salvadori M, Seggiani M, Vitolo S. Oxidative unhairing with hydrogen peroxide: development of an industrial scale process for high-quality upper leather. *JALCA* 2005, **100**, 45-53.
3. Dettmer A, Cavalli E, Ayub M A Z, Gutterres M, Environmentally friendly hide unhairing: enzymatic hide processing for the replacement of sodium sulfide and deliming. *Journal of Cleaner Production* 2013, **47**, 11-18.
4. Gehring A G, Dudley R L, Mazenko C E, Marmer W N, Rapid oxidative dehairing with magnesium peroxide and potassium peroxymonosulfate. *JALCA* 2006, **101**, 324-329.
5. Gehring A G, Bailey D G, Dimaio G L, Dudley R L, Marmer W N, Mazenko C E, Rapid oxidative unhairing with alkaline calcium peroxide. JALCA 2003, 98, 216-223.

6. Golovteeva A A, Kutsidi D A, Sankin L B, *Laboratornyj praktikum po khimiyi i tekhnologiyi kozhy i mekha*, Legkaiya i Pischevaiya Prom. Moscow, 1982, 312 p.
7. Krawiecky C, Sabat J, Oksydatywne metody przygotowania skor do garbowania. Cz. 1. Proby wykorzystania chloru do odwlasania skor. *Przegland Skorzany* 1984, **39**, 198-200, 215.
8. Liu Y S, Yi C, Fan H J, Hu Z, Luo Z Y, Bi S, Environment friendly lime-free liming. *JSLTC* 2009, **93**, 56-60.
9. Morera J M, Bartoli E, Gavilanes, R M, Hide unhairing: achieving lower pollution loads, decreased wastewater toxicity and solid waste reduction. Journal of *Cleaner Production* 2016, **112**, 3040-3047.
10. Munz K H, Sonnleitner R, Application of soluble silicates in leather production. *JALCA* 2005, **100**, 66-75.
11. Patent USSR 767649, 1980, Method of determination of leather quality.
12. Saravanabhavan S, Thanikaivelan P, Rao J R, Nair B U, Silicate enhanced enzymatic dehairing: A new lime-sulfide-free process for cowhides. *Environment Science & Technology* 2005, **39**, 3776-3783.
13. Sirvaityte J, Beleska K, Valeika V, Lime Free Unhairing: Sodium Aluminate as an Alternative Towards a Cleaner Process, *JALCA* 2016, **111**, 406-412.
14. Sirvaityte J, Beleska K, Valeikiene V, Plavan V, Valeika V, Immunization action of sodium silicate on hair: Part 2 hair-save process based on lime substitution by sodium silicate. *JSLTC* 2015, **99**, 231-237.
15. Standard ISO 3380: 2002. Leather – Physical and mechanical tests – Determination of shrinkage temperature up to 100 degrees C.
16. Standard ISO 4045:2008. Leather – Chemical tests – Determination of pH.
17. Standard EN ISO 3376: 2003. Leather – Physical and mechanical tests – Determination of tensile strength and percentage extension.
18. Standard ISO 5398-2: 2009. Leather – Chemical determination of chromic oxide content – Part 2: Quantification by colorimetric determination.
19. Standard ISO 4048: 2008. Leather – Chemical tests – Determination of matter soluble in dichloromethane and free fatty acid content.
20. Standard EN ISO 4684: 2006. Leather – Chemical tests – Determination of volatile matter.
21. Standard ISO 15705:2002. Water quality – Determination of the chemical oxygen demand index (ST-COD) – Small-scale sealed-tube method.
22. Standard ISO 5815-1:2003. Water quality – Determination of biochemical oxygen demand after n days (BODn) – Part 1: Dilution and seeding method with allylthiourea addition.
23. Thanikaivelan P., Rao J R, Nair B U, Ramasami T, Approach towards zero discharge tanning: Exploration of NaOH based opening up method. *JALCA* 2001, **96**, 222-233.
24. Thorstensen T C, Dubost C, Studies on chemical unhairing systems. *JALCA* 1985, **80**, 47-53.
25. Valeika V, Balciuniene J, Beleska K, Valeikiene V, Lime-free unhairing: Part 3 Influence of unhairing method on chemical, physical and mechanical properties of pelt and leather. *JSLTC* 2000, **84**, 165-169.
26. Valeika V, Balciuniene J, Beleska K, Skrodenis A, Valeikiene V, Use of NaOH for unhairing hides and the influence of the addition of salts on the process and on the hide properties. *JSLTC* 1997, **81**, 165-169.

27. Valeika V, Beleska K, Valeikiene V, Kolodzeiskis V, An approach to cleaner production: from hair burning to hair saving using a lime-free unhairing system. *Journal of Cleaner Production* 2009, **17**, 214-221.
28. Valeika V, Sirvaityte J, Beleska K, Alaburdaite R, Valeikiene V, Immunization action of sodium silicate on hair. JSLTC 2015, **99**, 223-230.
29. Valeika V, Sirvaitytė J, Beleska K, Valeikiene V, Bacenaite L, Immunization of wool by aluminium salt. *Magic world of textiles: 7th international textile clothing & design conference, October 5-8, 2014, Dubrovnik, Croatia: book of proceedings*; Zagreb: University of Zagreb, pp. 695-699.
30. Xu W, Ha L F, Zhou L, Cleaner dehairing technology for goatskins: effects of hydrosulfide and peroxide on enzyme unhairing. Advanced *Materials Research* 2010, **113-116**, 1726-1731.
31. Zaides A, Mikhailov A, Pushenko O. Modiphitsirovanyi method opredeleniya oksiprolina, *Biokhimiya* 1964, **1**, 5-6.